Predictive Modelling of Energy Consumption in Melbourne by Using Energy Simulations and Passive Design Approaches in Residential Buildings.

Mina Ranjbaran

Thesis submitted for the fulfilment of the requirements for the degree of Ph.D.

Victoria University, Australia

Institute for Sustainable Industries and Liveable Cities

October 2025

Abstract

Due to the exponential increase in energy consumption within the residential building sector worldwide, there is a recognized need for targeted mechanisms to predict and optimize energy consumption in residential buildings. Accordingly, this research defines and investigates a predictive energy consumption model and optimizes geometric parameters of single-story residential buildings in Melbourne through energy performance simulation within a Performative Computational Architecture (PCA) framework. The main method of this research adopts a quantitative approach, involving coding based on the geometric parameters of residential buildings, simulation, modelling, and optimization within the Grasshopper programming environment in Rhino software. The study model focuses on common single-story residential buildings in Melbourne. Finally, based on linear and nonlinear regression testing, a predictive model for energy consumption, heating demand, and cooling demand of single-story residential buildings in Melbourne. is presented in six equations. Based on the findings, among architectural variables, building volume and area have the highest correlation with energy performance and are considered the most important architectural variables. Also, based on the findings, nonlinear models have a better fit and predict more than 97% of energy consumption changes of the single-story residential buildings in Melbourne based on the overall geometric characteristics of the building with a confidence factor of over 95%. Also, based on the findings, it is concluded that the square shape is the best plan shape for the single-story residential building in terms of energy performance. In addition, based on the findings, energy consumption per square meter decreases as the floor area increases and the height of the space decreases. It is concluded that the geometric characteristics of residential buildings influence building energy consumption by up to 34%. This could have a significant impact on global energy consumption. This highlights the need to consider the impact of geometric parameters in the development of urban planning and architectural regulations in Melbourne.

Keywords: Energy Consumption Simulation, Predictive Energy Consumption Model, Performative Computational Architecture, Energy Performance Optimization, Single-story Residential Buildings in Melbourne

Declaration of Authenticity

"I, Mina Ranjbaran, declare that the PhD thesis entitled Predictive Modelling of Energy Consumption in Residential Buildings in Melbourne by Using Energy Simulations and Passive Design Approach is no more than 85,000 words in length including quotes and exclusive of tables, figures, appendices, bibliography, references and footnotes. This thesis contains no material that has been submitted previously, in whole or in part, for the award of any other academic degree or diploma. Except where otherwise indicated, this thesis is my own work".

"I have conducted my research in alignment with the Australian Code for the Responsible Conduct of Research and Victoria University's Higher Degree by Research Policy and Procedures.

Signature: [redacted] Date:28/10/2025

Acknowledgements

I am deeply grateful to Professor Zora Vrcelj**,** Associate Professor Elmira Jamei**,** and Associate Professor Malindu Sandanayake for their invaluable guidance, support, and feedback throughout this research. I also extend my thanks to Victoria University for providing the resources and platform that made this work possible. Lastly, I acknowledge everyone who contributed through proofreading, editing, or other forms of support.

Declarations of Authenticity and Authorship Contribution in the Thesis with Publication Format

Contents

List of Abbreviations xiv
Chapter 1: Body of Thesis 2
1-1- Introduction 2
1-2- Problem Statement 3
1-3- Importance and Necessity of the Research 6
1-4- Research Objectives 7
1-5- Research Questions 7
1-6- Research Hypotheses 8
1-7- Scope of Research 9
1-8- Definition of Research Terms 10
Chapter 2: Literature Review 14
2-1- Introduction 14
2-2- Examination of Physical Factors Affecting Building Energy Performance 14
2-2-1 Building Form 15
2-2-2- Window-to-Wall Ratio 16
2-2-3- Building Materials 17
2-2-4- Window Type 19
2-2-5- Building Airtightness 20
2-2-6- Shading Devices 21
2-2-7- Azimuth 22
2-2-8- Orientation Angle of Buildings 24
2-2-9- Thermal Mass 27
2-2-10- Thermal Bridge 28
2-3- Examination of Factors Influencing the Relationship Between Physical Factors and Building Energy Performance 28
2.3.1 Environmental Conditions Surrounding the Building 29
2-3-2- Equipment and Facilities of the Building 30
2-3-3- Behavior of Building Occupants 31
2-4- Mechanisms of Energy Consumption in Buildings 32
2-4-1- Heating Requirements in Buildings 32
2-4-2- Lighting Requirements in Buildings 33
2-4-3- Ventilation Requirements in Buildings 34
2-4-4- Other Consumption Mechanisms 35
2-5. Energy Performance Simulation of Buildings 35
2-5.1 Calibration in Building Energy Simulation 37
2-5.1.1 Optimization-Based Calibration 38

2-6. Using Evolutionary Computation to Search for Solutions 39
2-6-1- Evolutionary Algorithms..... 42
2-7- Computational Performance Design Mechanism..... 43
2- 8. Overview of the Literature on Performance-based Computational Architecture 52
2-9. Conclusion..... 62
3-2- Research Tools..... 67
3-3- Detailed Explanation of the Research Method..... 69
3-3-1- Definition of the Generative Algorithm for the Reference Model..... 70
3-3-2- Research Variables..... 71
3-3-2-1- Scope of Variations in Spatial Layout Models for Simulation..... 71
3-3-2-2- Settings for Building Energy Performance Simulation 72
3-3-2-3- Description of the Study Area 73
3-3-2-4- Details of Materials Used in the Simulation..... 75
3-3-2-4-1- Description of Timber Framed Construction For simulation 75
3-3-2-5- Schedules and Loads Used in the Simulation..... 78
3-3-2-6- Validation of the Energy Simulation Model..... 79
3-3-3- Process of Modelling Simulation Data for the External Envelope of Residential buildings..... 86
3-3-3-1- Examination of Descriptive Statistics..... 86
3-3-3-2- Conducting the Correlation Test..... 87
3-3-3-3- Conducting the Regression Test 87
3-3-3-4- Process of Optimizing Energy Performance of Residential Building Envelopes..... 89
3-4- Conclusion..... 90
Chapter 4: Results..... 92
4-1- Introduction 92
4-2- Modelling Energy Performance of Residential buildings 92
4-2-1- Results of Correlation Analysis 98
4-2-2- Results of Curve Regression Testing 99
4-2-3 Linear Modeling of Building Energy Performance Relationships 145
4-2-4- Nonlinear Modeling of Building Energy Performance Relationships 157
4-3- Optimization of Energy Performance in Residential buildings..... 170
4-3-1: Best Responses for Optimizing Energy Performance in Residential buildings 177
4-4- Comparative Analysis of the Impact of Orientation Angle and Height on the Energy Performance of Residential buildings..... 182
4-5- Investigating the effect of the WWR on building energy performance 184
4-5 Summary..... 203
Chapter 5: Summary, Conclusion, Recommendations..... 206
5-1- Introduction 206

5-2- Analysis of the research results 206
5-2-1- Analysis of the results of energy performance modeling for residential buildings..... 206
5-2-2- Analysis of the Results of Energy Performance Optimization 212
5-2-2- Analysis of the optimal WWR at each building orientation angle..... 217
5-3- Discussion on Research Results 218
5-4- Examination of Research Hypotheses 221
5-5-Innovations of the Research 222
5-6-Strategic Approaches and Solutions..... 222
5-7-Final Conclusion 224
5-8-Research Limitations..... 226
5-9-Research Novelty 226
5-10-Research Contributions 229
References..... 232

Figures **Page**

Figure 1-1. Framework of Performative Computational Architecture **4**
Figure 1-2. Mechanism of Predictive Modelling for Energy Performance. **5**
Figure 1-3. Climatic Classification of Australia **9**

Figure 2-1: Law-Driven vs. Data-Driven Models **36**
Figure 2-2: Input and Output Data in Energy Performance Simulation **36**
Figure 2-3. Parametric-Algorithmic Process Based on the Perspective of Lazzeroni et al. **45**
Figure 2-4. The GD Based on the Perspective of Agkathidis **45**
Figure 2-5. The GD Based on the Perspective of Bohnacker et al. **46**
Figure 2-6. The GD based on Estkowski's perspective **47**
Figure 2-7. Performance-based PCA Framework **49**
Figure 2-8. The GD Based on the Autodesk Report **50**
Figure 2-9. The LCA Framework **51**
Figure 2-10. Frequency of Journals Reviewed in the Research Background **53**
Figure 2-11. Frequency of Various Scales and Frequency of Different Usages Reviewed **54**
Figure 2-12. Frequency of Use of Each Physical Factor in the Conducted Studies **55**
Figure 2-13. Shannon Entropy Coordinates Based on Weight and Normalized Frequency Axes **56**
Figure 2-14. Theoretical Framework of the Research **62**

Figure 3-1. Methodology Framework **65**
Figure 3-2. Staged Process Flow of Research Execution **66**
Figure 3-3. Research Tools **69**
Figure 3-4. A section of the process for constructing the generative algorithm model. **70**
Figure 3-5. GD Algorithm for Energy Performance Simulation in Grasshopper Environment **73**
Figure 3-6. Psychrometric Chart Based on the EnergyPlus Climate File for the City of Melbourne **74**
Figure 3-7. Wind and Solar Radiation Diagram Based on the EPW File for Melbourne **74**
Figure 3-8. Execution Details of the Foundation for Timber Framed Construction For simulation **75**
Figure 3-9. Detailed Execution of the Foundation for Timber Framed Structures For simulation **76**
Figure 3-10. Execution Details of Flat Roofs in Timber Framed Structure For simulation **77**
Figure 3-11. Sample Electricity Bills Collected from Residential buildings and Sample Gas Bills Collected from Residential Buildings **82**
Figure 3-12. Comparative Analysis of Actual and Simulated Energy Consumption per Square Meter for Selected Residential buildings. **83**
Figure 3-13. Comparative Analysis of Actual and Simulated Energy Consumption for Selected Residential buildings **83**

Figure 4-1. Results of Performance Objective Values and Standard Deviation of Responses in the Optimization Process **171**
Figure 4-2. Performance Objective Chart of All Responses **172**
Figure 4-3. Performance Objective Chart of All Responses **172**
Figure 4-4. Performance Objective Chart of Pareto Frontier Responses **173**
Figure 4-5. Performance Objective Chart of Pareto Frontier Responses **173**
Figure 4-6. Best Responses for Each Performance Objective Among All Optimization Responses **177**
Figure 4-7. Specifications of the Best Response Based on Average Useful Daylight **178**
Figure 4-8. Specifications of the Best Response Based on Cooling Demand per Square Meter **178**
Figure 4-9. Specifications of the Best Response Based on Heating Demand per Square Meter **179**
Figure 4-10. Diagram of Pareto Frontier Responses Classification via K-means Machine Learning **180**
Figure 4-11. Specifications of Classified Pareto Frontier Responses **182**
Figure 4-12. Comparative analysis of energy consumption based on the window-to-wall ratio for a 100 m² building with east–west dimensions of 7.07 m, north–south dimensions of 14.142 m. **185**
Figure 4-13. Analysis of the optimal window-to-wall ratio for a building with a floor area of 100 m², east–west dimensions of 7.07 m, north–south dimensions of 14.142 m, and an aspect ratio of 0.5 at various orientation angles. **186**
Figure 4-14. Comparative analysis of energy consumption based on the window-to-wall ratio for a 100 m² building with east–west and north–south dimensions of 10 m. **187**
Figure 4-15. Comparative analysis of the optimal window-to-wall ratio for a building with a floor area of 100 m², east–west dimensions of 10 m, north–south dimensions of 10 m, and an aspect ratio of 1 at various orientation angles. **188**

Figure 4-16. Comparative analysis of energy consumption based on the window-to-wall ratio for a 100 m² building with east–west dimensions of 14.142 m, north–south dimensions of 7.07 m **189**
Figure 4-17. Comparative analysis of the optimal window-to-wall ratio for a building with a floor area of 100 m², east–west dimensions of 7.07 m, north–south dimensions of 14.142 m, and an aspect ratio of 0.5 at various orientation angles. **190**
Figure 4-18. Comparative analysis of energy consumption based on the window-to-wall ratio for a 150 m² building with east–west dimensions of 8.66 m, north–south dimensions of 17.32 m **191**
Figure 4-19. Comparative analysis of the optimal window-to-wall ratio for a building with a floor area of 150 m², east–west dimensions of 8.66 m, north–south dimensions of 17.32 m, and an aspect ratio of 0.5 at various orientation angles. **192**
Figure 4-20. Comparative analysis of energy consumption based on the window-to-wall ratio for a 150 m² building with east–west and north–south dimensions of 12.247 m **193**
Figure 4-21. Comparative analysis of the optimal window-to-wall ratio for a building with a floor area of 150 m², east–west dimensions of 12.247 m, north–south dimensions of 12.247 m, and an aspect ratio of 1 at various orientation angles. **194**
Figure 4-22. Comparative analysis of energy consumption based on the window-to-wall ratio for a 150 m² building with east–west dimensions of 17.321 m, north–south dimensions of 8.66 m **195**
Figure 4-23. Comparative analysis of the optimal window-to-wall ratio for a building with a floor area of 150 m², east–west dimensions of 17.321 m, north–south dimensions of 8.66 m, and an aspect ratio of 2 at various orientation angles. **196**
Figure 4-24. Comparative analysis of energy consumption based on the WWR for a building with a floor area of 200 m², east–west dimensions of 10m, north–south dimensions of 20 m **197**
Figure 4-25. Comparative analysis of the optimal window-to-wall ratio for a building with a floor area of 200 m², east–west dimensions of 10 m, north–south dimensions of 20 m, and an aspect ratio of 0.5 at various orientation angles. **198**
Figure 4-26. Comparative analysis of energy consumption based on the WWR for a building with a floor area of 200 m², east–west dimensions of 14.14 m, north–south dimensions of 14.14 **199**
Figure 4-27. Comparative analysis of the optimal window-to-wall ratio for a building with a floor area of 200 m², east–west dimensions of 14.142 m, north–south dimensions of 14.142 m, and an aspect ratio of 1 at various orientation angles. **200**
Figure 4-28. Comparative analysis of energy consumption based on the WWR for a building with a floor area of 200 m², east–west dimensions of 20m, north–south dimensions of 10 m **201**
Figure 4-29. Comparative analysis of the optimal window-to-wall ratio for a building with a floor area of 200 m², east–west dimensions of 20 m, north–south dimensions of 10 m, and an aspect ratio of 2 at various orientation angles **202**

Figure 5-1. Analysis of the Impact of Floor Area on Energy Performance Based on Results **213**
Figure 5-2. Analysis of the Impact of Space Height on Energy Performance Based on Results **213**
Figure 5-3. Analysis of the Impact of Elongation on Energy Performance Based on Results **214**
Figure 5-4. Analysis of the Impact of orientation on Energy Performance Based on Results **214**
Figure 5-5. Analysis of the Impact of physical elements on Energy Performance Based on Results **215**
Figure 5-6. Analysis of the Impact of Height of Space and Orientation of Building on Energy and Daylighting Performance Based on Results **216**
Figure 5-7. Analysis of the Impact of Height of Space and Area of Building on Energy and Daylighting Performance Based on Results **216**
Figure 5-8. Comparative analysis Model of the optimal window-to-wall ratio **217**
Figure 5-9. Classification of Strategic Approaches and Design Solutions **223**
Figure 5-10. Variations in Geometric Characteristics of Residential buildings **228**

Tables **Page**

Table 1-1. Characteristics of the Climatic Classification of Australia **10**

Table 2-1: Frequency Values, Correlation with Publication Year of Studies, and Weights of Factors in Shannon Entropy Test **56**
Table 2-2: Recent Studies in the Field of Building Energy Consumption **57**

Table 3-1: Spatial layout Characteristics and References **66**
Table 3-2. The range of changes of the geometric variables of the reference model **72**
Table 3-3. Details of Timber Frame Foundation Execution For simulation **76**

Table 3-4. Execution Details of the External Wall of the Timber Framed Structure For simulation **77**
Table 3-5. Construction Details of the Exterior Wall in Timber Frame Structures For simulation **78**
Table 3-6. Occupancy Schedule Details Based on Various Standards **79**
Table 3-7. Selected Residential buildings in Different Areas of Melbourne for Simulation **80**
Table 3-8. Descriptive Statistics of Actual and Simulated Energy Consumption for Selected Residential buildings **84**
Table 3-9. Correlation Test Between Actual and Simulated Energy Consumption for Selected Residential buildings **84**
Table 3-10. NMBE and CVRMSE Report For model validation **84**
Table 3-11. Results of Sensitivity Analysis Based on the Correlation Test Between Physical Factors and Simulation Performance Objectives **85**
Table 3-12. States of the Building Model Under Simulation **86**
Table 3-13. Predefined Models and Formulas for Each Variable **88**
Table 3-14. Evolutionary Process Settings of Wallacei **89**

Table 4-1. Descriptive Statistics of the Architectural Factors for the Simulated Single-story residential buildings Models **92**
Table 4-2. Analysis of Descriptive Statistics of Energy Performance Results Based on All Simulations **93**
Table 4-3. Analysis of Descriptive Statistics of Energy Consumption Results Based on All Simulations **94**
Table 4-4. Analysis of Descriptive Statistics of Cooling Demand Results Based on All Simulations **95**
Table 4-5. Analysis of Descriptive Statistics of Heating Demand Results Based on All Simulations **96**
Table 4-6. Analysis of Descriptive Statistics of Daylight Results Based on All Simulations **97**
Table 4-7. Results of Correlation Test Between Architectural Factors and Performance Objectives **98**
Table 4-8: Results of Correlation Test Between Architectural Factors and Performance Objectives **99**
Table 4-9. Results of Curve Regression Between Energy Consumption per Square Meter and the East-West Dimension **100**
Table 4-10. Results of Curve Regression Between Cooling Demand per Square Meter and the East-West Dimension **101**
Table 4-11. Results of Curve Regression Between Heating Demand per Square Meter and the East-West Dimensions **101**
Table 4-12. Results of Curve Regression Between Energy Consumption and the East-West Dimensions **102**
Table 4-13. Results of Curve Regression Between Cooling Demand and the East-West Dimensions **102**
Table 4-14. Results of Curve Regression Between Heating Demand and the East-West Dimensions **103**
Table 4-15. Results of Curve Regression Between Lighting Demand and the East-West Dimensions **103**
Table 4-16. Results of Curve Regression Between Average UDI and the East-West Dimensions **104**
Table 4-17. Results of Curve Regression Between Average DA and the East-West Dimensions **104**
Table 4-18. Results of Curve Regression Between Energy Consumption per Square Meter and the North-South Dimensions **105**
Table 4-19. Results of Curve Regression Between Cooling Demand per Square Meter and the North-South Dimensions **105**
Table 4-20. Results of Curve Regression Between Heating Demand per Square Meter and the North-South Dimensions **106**
Table 4-21. Results of Curve Regression Between Energy Consumption and the North-South Dimensions **106**
Table 4-22. Results of Curve Regression Between Cooling Demand and the North-South Dimensions **107**
Table 4-23. Results of Curve Regression Between Heating Demand and the North-South Dimensions **107**
Table 4-24. Results of Curve Regression Between Lighting Demand and the North-South Dimensions **108**
Table 4-25. Results of Curve Regression Between Average UDI and the North-South Dimensions **108**
Table 4-26. Results of Curve Regression Between Average DA and the North-South Dimensions **109**
Table 4-27. Results of Curve Regression Between Energy Consumption per Square Meter and the Building Area **109**
Table 4-28. Results of Curve Regression Between Cooling Demand per Square Meter and the Building Area **110**

Table 4-29. Results of Curve Regression Between Heating Demand per Square Meter and the Building Area **110**
Table 4-30. Results of Curve Regression Between Energy Consumption and the Building Area **111**
Table 4-31. Results of Curve Regression Between Cooling Demand and the Building Area **111**
Table 4-32. Results of Curve Regression Between Heating Demand and the Building Area **112**
Table 4-33. Results of Curve Regression Between Lightng Demand and the Building Area **112**
Table 4-34. Results of Curve Regression Between Average UDI and the Building Area **113**
Table 4-35. Results of Curve Regression Between Average DA and the Building Area **113**
Table 4-36. Results of Curve Regression Between Energy Consumption per Square Meter and Building Height **114**
Table 4-37. Results of Curve Regression Between Cooling Demand per Square Meter and Building Height **114**
Table 4-38. Results of Curve Regression Regression Between Heating Demand per Square Meter and Building Height **115**
Table 4-39. Results of Curve Regression Between Energy Consumption and Building Height **115**
Table 4-40. Results of Curve Regression Between Cooling Demand and Building Height **116**
Table 4-41. Results of Curve Regression Between Heating Demand and Building Height **116**
Table 4-42. Results of Curve Regression Between Lighting Demand and Building Height **117**
Table 4-43. Results of Curve Regression Between Average UDI and Building Height **117**
Table 4-44. Results of Curve Regression Between Average DA and Building Height **118**
Table 4-45. Results of Curve Regression Between Energy Consumption per Square Meter and the Building Orientation **118**
Table 4-46. Results of Curve Regression Between Cooling Demand per Square Meter and the Building Orientation **119**
Table 4-47. Results of Curve Regression Between Heating Demand per Square Meter and the Building Orientation **119**
Table 4-48. Results of Curve Regression Regression Between Energy Consumption and the Building Orientation **120**
Table 4-49. Results of Curve Regression Between Cooling Demand and the Building Orientation **120**
Table 4-50. Results of Curve Regression Between Heating Demand and the Building Orientation **121**
Table 4-51. Results of Curve Regression Between Lighting Demand and the Building Orientation **121**
Table 4-52. Results of Curve Regression Between Average UDI and the Building Orientation **122**
Table 4-53. Results of Curve Regression Between Average DA and the Building Orientation **122**
Table 4-54. Results of Curve Regression Between Energy Consumption per Square Meter and the Building Volume **123**
Table 4-55. Results of Curve Regression Between Cooling Demand per Square Meter and the Building Volume **123**
Table 4-56. Results of Curve Regression Between Heating Demand per Square Meter and the Building Volume **124**
Table 4-57. Results of Curve Regression Between Energy Consumption and the Building Volume **124**
Table 4-58. Results of Curve Regression Between Cooling Demand and the Building Volume **125**
Table 4-59. Results of Curve Regression Between Heating Demand and the Building Volume **125**
Table 4-60. Results of Curve Regression Between Lighting Demand and the Building Volume **126**
Table 4-61. Results of Curve Regression Between Average UDI and the Building Volume **126**
Table 4-62. Results of Curve Regression Between Average DA and the Building Volume **127**
Table 4-63. Results of Curve Regression Between Energy Consumption per Square Meter and the WWR **127**
Table 4-64. Results of Curve Regression Between Cooling Demand per Square Meter and the WWR **128**
Table 4-65. Results of Curve Regression Between Heating Demand per Square Meter and the WWR **128**
Table 4-66. Results of Curve Regression Between Energy Consumption and the WWR **129**
Table 4-67. Results of Curve Regression Between Cooling Demand and the WWR **129**
Table 4-68. Results of Curve Regression Between Heating Demand and the WWR **130**
Table 4-69. Results of Curve Regression Between Lighting Demand and the WWR **130**
Table 4-70. Results of Curve Regression Between Average UDI and the WWR **131**
Table 4-71. Results of Curve Regression Between Average DA and the WWR **131**
Table 4-72. Results of Curve Regression Between Energy Consumption per Square Meter and the Width of the Window **132**
Table 4-73. Results of Curve Regression Between Cooling Demand per Square Meter and the Width of the Window **132**

Table 4-74. Results of Curve Regression Between Heating Demand per Square Meter and the Width of the Window **133**
Table 4-75. Results of Curve Regression Between Energy Consumption and the Width of the Window **133**
Table 4-76. Results of Curve Regression Between Cooling Demand and the Width of the Window **134**
Table 4-77. Results of Curve Regression Between Heating Demand and the Width of the Window **134**
Table 4-78. Results of Curve Regression Between Lighting Demand and the Width of the Window **135**
Table 4-79. Results of Curve Regression Between Average UDI and the Width of the Window **135**
Table 4-80. Results of Curve Regression Between Average DA and the Width of the Window **136**
Table 4-81. Results of Curve Regression Between Energy Consumption per Square Meter and the Height of the Window **136**
Table 4-82. Results of Curve Regression Between Cooling Demand per Square Meter and the Height of the Window **137**
Table 4-83. Results of Curve Regression Between Heating Demand per Square Meter and the Height of the Window **137**
Table 4-84. Results of Curve Regression Between Energy Consumption and the Height of the Window **138**
Table 4-85. Results of Curve Regression Between Cooling Demand and the Height of the Window **138**
Table 4-86. Results of Curve Regression Between Heating Demand and the Height of the Window **139**
Table 4-87. Results of Curve Regression Between Lighting Demand and the Height of the Window **139**
Table 4-88. Results of Curve Regression Between Average UDI and the Height of the Window **140**
Table 4-89. Results of Curve Regression Between Average DA and the Height of the Window **140**
Table 4-90. Results of Curve Regression Between Energy Consumption per Square Meter and the Area of the Window **141**
Table 4-91. Results of Curve Regression Between Cooling Demand per Square Meter and the Area of the Window **142**
Table 4-92. Results of Curve Regression Between Heating Demand per Square Meter and the Area of the Window **142**
Table 4-93. Results of Curve Regression Between Energy Consumption and the Area of the Window **143**
Table 4-94. Results of Curve Regression Between Cooling Demand and the Area of the Window **143**
Table 4-95. Results of Curve Regression Between Heating Demand and the Area of the Window **144**
Table 4-96. Results of Curve Regression Between Lighting Demand and the Area of the Window **144**
Table 4-97. Results of Curve Regression Between Average UDI and the Area of the Window **145**
Table 4-98. Results of Curve Regression Between Average DA and the Area of the Window **145**
Table 4-99. Results of Linear Regression Analysis between Spatial Factors and Global Energy Per Area **146**
Table 4-100. Results of Linear Regression Test Between Spatial Factors and Global Energy Per Area **147**
Table 4-101. Results of Linear Regression Test Between Spatial Factors and Cooling Energy Per Area **148**
Table 4-102. Results of Linear Regression Analysis Between Spatial Factors and Cooling Energy Per Area **148**
Table 4-103. Results of Linear Regression Test Between Spatial Factors and Heating Energy Per Area **149**
Table 4-104. Results of the Linear Regression Test between Spatial Factors and Heating Energy Per Area **149**
Table 4-105. Results of the Linear Regression Test Between Spatial Factors and Global Energy **150**
Table 4-106. Results of Linear Regression Test Between Spatial Factors and Global Energy **151**
Table 4-107. Results of Linear Regression Test Between Spatial Factors and Cooling Energy **151**
Table 4-108. Results of Linear Regression Analysis between Spatial Factors and Cooling Energy **152**
Table 4-109. Results of the Linear Regression Test Between Spatial Factors and Heating Energy **152**
Table 4-110. Results of the Linear Regression Test Between Spatial Factors and Heating Energy **153**
Table 4-111. Results of the Linear Regression Test Between Spatial Factors and Lighting Energy **154**
Table 4-112. Results of the Linear Regression Test Between Spatial Factors and Lighting Energy **154**
Table 4-113. Results of the linear regression test between spatial factors and UDI Average **155**
Table 4-114. Results of Linear Regression Test Between Physical Factors and UDI Average **155**
Table 4-115. Results of Linear Regression Test Between Spatial Factors and DA Average **156**
Table 4-116. Results of Linear Regression Analysis between Spatial Factors and DA Average **156**
Table 4-117. Results of Curvilinear Regression Tests **158**

Table 4-118. Results of Nonlinear Regression Test Between Spatial Factors and Global Energy Per Area **159**
Table 4-119. Results of Non-Linear Regression Test between Physical Factors and Global Energy Per Area **159**
Table 4-120. Results of Non-Linear Regression Test Between Spatial Factors and Performance Objectives of Simulation **160**
Table 4-121. Results of Non-linear Regression Tests Between Spatial Factors and Performance Objectives of Simulation **160**
Table 4-122. Results of Non-Linear Regression Test Between Spatial Factors and Performance Objectives of the Simulation **161**
Table 4-123. Results of Non-linear Regression Test Between Spatial Factors and Simulation Performance Objectives **162**
Table 4-124. Results of the Nonlinear Regression Test Between Physical Factors and Global Energy **163**
Table 4-125. Results of Non-Linear Regression Tests Between Physical Factors and Global Energy **163**
Table 4-126. Results of Nonlinear Regression Tests Between Physical Factors and Cooling Energy **164**
Table 4-127. Results of Nonlinear Regression Test Between Physical Factors and Cooling Energy **164**
Table 4-128. Results of the Nonlinear Regression Test Between Physical Factors and Heating Energy **165**
Table 4-129. Results of the Nonlinear Regression Test Between Physical Factors and Heating Energy **166**
Table 4-130. Results of the Nonlinear Regression Test Between Spatial Factors and Lighting Energy **166**
Table 4-131. Results of the Nonlinear Regression Test Between Physical Factors and Lighting Energy **167**
Table 4-132. Results of the Nonlinear Regression Test Between Physical Factors and UDI Average **168**
Table 4-133. Results of the Nonlinear Regression Test Between Physical Factors and UDI Average **168**
Table 4-134. Results of the Linear Regression Test Between Physical Factors and DA Average **169**
Table 4-135. Results of the Nonlinear Regression Test Between Physical Factors and DA Average **169**
Table 4-136. Stepwise Breakdown of Genes in Spatial layout Models for Optimization Process **171**
Table 4-137. Specifications of Pareto Frontier Responses **174**
Table 4-138. Descriptive Statistics of Pareto Frontier Response Specifications **175**
Table 4-139. Specifications of Pareto Frontier Response **175**
Table 4-140. Specifications of Pareto Frontier Responses **176**
Table 4-141. Descriptive Statistics of Pareto Frontier Response Specifications **176**
Table 4-142. Specifications of Classified Pareto Frontier Responses **180**
Table 4-143. Specifications of Classified Pareto Frontier Responses **181**
Table 4-144 Energy Performance Based on Variations in Orientation Angle Across Different Areas with a Height of 3 Meters for Spaces **183**
Table 4-145. Energy Performance Based on Variations in Space Height Across Different Areas with an Orientation Angle of 0 Degrees **184**

Table 5-1: Linear and Nonlinear Equations for Energy Performance Objectives of the Study **210**
Table 5-2: Classification of Strategic Approaches and Design Solutions **223**
Table 5-3. Research Limitations **226**

List of Abbreviations

PCA	Performative Computational Architecture
GD	Generative Design
PBD	Performance-Based Design
GSL	Generative Design of Spatial Layouts
EPO	Energy Performance Optimization
G-EPO	Generating Spatial Layouts with Optimal Energy Performance
BES	Building Energy Simulation
BEP	Building Energy Performance
AI	Artificial Intelligence
UDI	Useful Daylight Illuminance
DA	Daylight autonomy
DF	Daylight Factor
GA	Genetic Algorithm
PSO	Particle Swarm Optimization
EA	Evolutionary Algorithm
MOEA	Multi-Objective Evolutionary Algorithms
SPEA-II	Strength Pareto Evolutionary Algorithm II
PESA	Pareto Envelope-Based Selection Algorithm
NSGA-II	Non-dominated Sorting Genetic Algorithm II
IEC	Interactive Evolutionary Computation
LCA	Life Cycle Assessment
IEA	International Energy Agency
IEA-EBC	International Energy Agency on Energy in Buildings and Communities
BCA	Building Code of Australia
HVAC	Heating, Ventilation, and Air Conditioning
ECMs	Energy Conservation Measures
WWR	Window-to-Wall Ratio

Chapter 1

Body of Thesis

Chapter 1: Body of Thesis

1-1- Introduction

Housing design, as the most fundamental living space for humans and the environment where people spend most of their time, holds significant importance. The rapid expansion of the building sector has led to an increase in global energy consumption (Chong et al., 2021). Due to the limitations of energy resources, development should proceed alongside energy consumption efficiency solutions (Abdul Hakim, 2011). The building sector is recognized as the largest energy consumer, accounting for a substantial percentage of global energy use, particularly in major cities (Masoso & Grobler, 2010).

Based on conducted research, one-third of total energy in most countries pertains to the building sector (Chong et al., 2021), and a major portion of energy consumption within buildings is related to residential buildings in urban areas (International Energy Agency, 2022). The United Nations Environment Programme (UNEP) also reports that 30 to 40 percent of the world's energy is consumed by buildings (Bakar et al., 2015). If this trend continues, the building sector's share of energy consumption alone may eventually match the combined shares of the industrial and transportation sectors (Jiye & Liang, 2010). Although this could be perceived as a threat, it presents a significant opportunity for sustainable energy planning within the building sector.

Consequently, optimizing building energy efficiency is essential for sustainable energy management (Jamaludin et al., 2011). Energy efficiency plays a crucial role in controlling energy consumption, reducing costs, preserving the environment, and maintaining environmental comfort in buildings (Parameshwaran et al., 2012). With the current increase in global energy consumption, the main concern extends beyond how to produce the required energy to identifying ways to improve energy efficiency and make better use of sustainable energy sources (Bakar et al., 2015). To this end, various approaches have been proposed in building energy analysis methods. The architectural design process plays a critical role in achieving low-energy consumption in buildings; therefore, analyzing building energy performance within the design process can be highly significant. Accordingly, this study examines building energy performance throughout the building design process.

1-2- Problem Statement

As mentioned, research indicates that one-third of total energy in most countries is associated with the building sector (Zhang et al., 2022; Chong et al., 2021). With global population growth and the resulting rise in residential construction, housing can be identified as one of the most significant sectors influencing global energy consumption. In this regard, a review of the literature reveals that one of the most influential factors affecting the energy performance of residential buildings is physical factors (Ataman & Dino, 2022; Cao et al., 2020). In this study, the physical factors of single-story residential buildings in Melbourne are defined based on the layout of the building's exterior shell. Studies have shown that spatial layout can significantly impact a building's energy performance, including heating, cooling, lighting, and ventilation requirements. In the context of building energy performance, the use of simulation mechanisms in the design process can be highly beneficial. However, the use of simulation software has not been common among designers in recent years (Kanters et al., 2014). The reasons for this include the complexity of using simulation programs, the specialization of interpreting the resulting information, converting the results into design, and the length of the simulation process.

Performative Computational Architecture (PCA), however, provides an effective solution to address all these concerns. Performative Computational Architecture employs a computer algorithm (Singh & Gu, 2012) that allows for easy examination of energy performance variations by modifying the building's geometric parameters. The proposed framework, termed "Performative computational architecture," consists of three main stages: Form Generation, Performance Evaluation, and Optimization, as illustrated in the figure 1-1. The mechanism of Performative Computational Architecture provides an effective response for utilizing energy performance simulation in the design process of spatial layout. This mechanism employs a parametric computer algorithm in the design process aimed at improving building performance (Ekici et al., 2019). In this study, the Performative Computational Architecture process is utilized within the framework of Generative Design of Spatial Layouts (GSL) (Attia et al., 2013). This framework, offers an opportunity to (1) automate the generation of a large set of spatial layouts for the external shell of single-story residential buildings (2) evaluate their energy performance (3) and optimize the best responses. This process is carried out within a reasonable time frame based on parametric

and algorithmic rules. Overall, this mechanism has the capability to optimize single-story residential buildings spatial layouts across largely contradictory performance objectives.

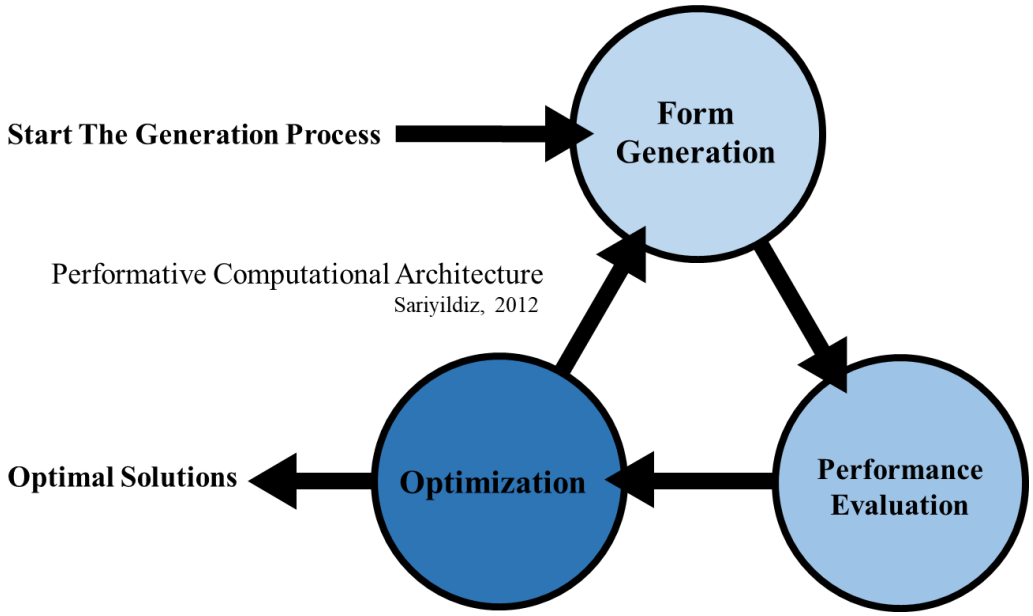

Figure 1-1. Framework of Performative Computational Architecture (Sariyildiz, 2012)

In this approach, the Grasshopper programming environment is used for coding. Furthermore, in the subsequent process of automatically generating spatial layouts with optimal energy performance (G-EPO), energy performance evaluation is considered. In this research, energy performance is simulated based on total energy consumption, heating demands, cooling demands, and useful daylight factor within the Grasshopper programming environment and by Ladybug Tools plugin.

Following this process, two cycles of Performative Computational Architecture are defined for the study, including a modelling cycle and an optimization cycle. In the modelling cycle, the Colibri tool is utilized to define a comprehensive set of design responses and the energy performance results for each layout, and the results obtained are modelled using the algorithm. Additionally, in the optimization cycle, the Non-dominated Sorting Genetic Algorithm II (NSGA-II) is used within the Wallacei plugin to optimize energy performance. Ultimately, this study presents models for predicting the energy performance of single-story residential buildings in Melbourne based on the spatial layout parameters.

Furthermore, the spatial layout parameters of single-story residential buildings are determined and prioritized based on optimal energy performance. Accordingly, this research

employs the Grasshopper tool and the Ladybug Tools plugin for the Performative Computational Architecture of single-story residential building's external shell based on its geometric variables in Melbourne. To achieve accurate energy performance prediction, predictive modelling is conducted using nonlinear regression tests in SPSS on the collected data. In conclusion, this study provides the predictive equations for energy performance of single-story residential buildings in Melbourne (Figure 1-2).

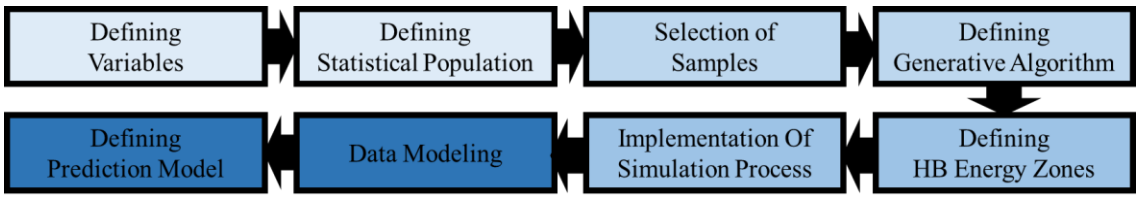

Figure 1-2. Mechanism of Predictive Modelling for Energy Performance.

The mechanism of predictive modelling for energy performance provides an effective response for utilizing energy performance simulation in the design process of spatial layout. Accordingly, this research encompasses twelve sections, including selecting design variables, defining the statistical population, selecting sample models, defining energy zones and energy simulation settings, executing the simulation process, analysing simulation data, conducting the modelling process, defining algorithms and optimization settings, carrying out the optimization process, analysing the data obtained from optimization, executing the modelling process based on optimization data, and conducting a comparative review of the data obtained from the simulation and optimization processes. As mentioned, in this study, Melbourne in Australia is chosen as the design territory, with single-story residential building, a common model in Melbourne, selected for simulation. The reason for choosing Melbourne is due to the increasing development of construction processes in this city in recent years. Also, this study was conducted on single-storey residential buildings. Single-storey residential buildings are the most common residential buildings in Melbourne. Therefore, the study of these buildings can be helpful in the environmental sustainability of Melbourne. Also, based on the literature, given that the impact of the general characteristics of the building on the energy performance and daylight of the building is much greater than other characteristics, in this study, in order to achieve a set of standards, only the general characteristics of the building are considered. Adding other characteristics to this study reduces the accuracy of achieving the overall characteristics. Accordingly, other characteristics are considered as fixed control variables. Ultimately, it is anticipated that this

research will present an organized mechanism for designing residential buildings in Melbourne.

1-3- Importance and Necessity of the Research

According to the International Energy Agency (IEA) report, residential and commercial buildings worldwide accounted for over 31% of final energy consumption in 2020 (Chong et al., 2021). In OECD countries, energy consumption is 32%, while in the United States, it is 31%, and in Portugal, it is 26% (International Energy Agency, 2011). When analyzed based on end-use, heating and cooling account for 55% of energy use in residential buildings (International Energy Agency, 2013). Therefore, designing energy-efficient buildings is key to minimizing the expected growth rate of energy consumption in residential buildings (Gouveia et al., 2012), highlighting the necessity for achieving energy-efficient architectural solutions.

Using performance simulation in the design process to estimate how buildings behave can help improve their energy efficiency. However, the use of such simulators is still not a common practice in architectural design. Architects typically rely on their past experiences or rule-based approaches (Ramezani et al., 2025; Kanters et al., 2014). Researchers have worked on the usability of graphical interfaces and the development of optimization techniques to enhance the design solutions of buildings. However, such approaches focus on final design stages, while significant decisions affecting a building's thermal performance are made in the early stages. Therefore, it is essential to define a method for energy evaluation in the early design phases.

In this regard, the performative computational architecture approach at the spatial layout and programming stages can provide an appropriate response to this issue. The aim of this research is to optimize the spatial layout of residential buildings based on building energy performance (BEP), which is currently receiving significant attention due to the global energy crisis and the importance of architectural impact on it (Coakley et al., 2014). Although it is anticipated that building energy performance (BEP) will be significantly influenced by the geometric factors of architectural space, these factors are rarely considered in discussions related to energy-efficient building design. Hence, the significance of this research in optimizing the geometric factors of residential buildings based on the energy performance of residential buildings is affirmed.

1-4- Research Objectives

In this research, a performative computational architecture model will be utilized to develop a generative algorithm for residential building based on its geometric factors, aimed at optimizing energy performance. To this end, the objectives of this research are presented in two sections: the main objective and sub-objectives. Accordingly, the main objective of this research, based on the stated problem, is as follows:

To identify and analyse the predictive model of energy performance of typical single-story residential buildings in Melbourne based on geometric parameters through performative computational architecture model.

The sub-objectives of this research are as follows:

1. Clarification of the most significant geometric parameters of residential buildings based on energy performance.
2. Optimizing the specifications of single-storey residential buildings based on building energy performance in Melbourne and determining energy efficiency and daylight performance.
3. Provide a set of standards and recommendations for the energy performance efficiency of typical single-storey residential buildings in Melbourne.

Additionally, broader objectives such as global energy consumption efficiency and achieving sustainable housing solutions at urban and regional scales will also be considered in this research.

1-5- Research Questions

The architectural design process involves a continually evolving trial-and-error approach to design solutions for buildings. Architects expect the energy performance of new buildings to align with past building experiences or regulatory measures; however, this approach is prone to failure. Since architects typically work on a single design solution that evolves through each design stage to reach the final building design, other potential design solutions that might perform better are often overlooked. Therefore, a mechanism for generating, evaluating, and comparing alternative design solutions to achieve the best outcomes is crucial (Attia et al., 2012; Papamichael & Pal, 2002). Thus, the research questions are

presented in two main sections: primary and secondary. Based on the above, the main research question is as follows:

How can the predictive model of energy performance of typical single-story residential buildings in Melbourne based on geometric parameters be developed, and to what extent can this model predict and optimize energy performance?

The secondary questions are as follows:

1. What are the geometric parameters of residential buildings that affect energy performance, and how are their impacts prioritized?
2. What are the optimal specifications of residential buildings based on building energy and daylight performance and to what extent can these specifications improve energy and daylight performance?
3. What architectural strategies are there for the geometric parameters of typical single-storey residential buildings in Melbourne to improve their energy and daylight performance?

Based on the above questions, this research considers the performance-based design (PBD) approach (Ekici et al., 2019) as the main focus, with the foundation of the research built on the framework of "Performative computational architecture" (PCD). Accordingly, the hypotheses of the research will be presented next.

1-6- Research Hypotheses

Based on the aforementioned points, this research aims to examine and optimize the spatial layout of the external envelope of residential buildings based on energy performance using the proposed framework by Sariyildiz (2012), known as Performative Computational Architecture (PCA). Accordingly, the hypotheses of the current research are presented in two main and secondary sections, aligned with the research objectives. The main hypothesis of the research is as follows:

The predictive model of the impact of geometric parameters of typical single-story residential buildings in Melbourne can significantly predict and optimize energy performance.

The secondary hypotheses of the research are as follows:

1. This research identifies the geometric parameters of residential buildings that affect energy performance and prioritizes them based on energy performance.
2. The optimal specifications for the geometric parameters of residential buildings are determined based on the energy performance of the building according to the Performative Computational Architecture model.
3. Architectural strategies for the geometric parameters of typical single-story residential buildings in Melbourne are identified to improve their energy performance based on the Performative Computational Architecture model.

Additionally, it can be stated that the initial hypothesis of this research is the use of the proposed Performative Computational Architecture mechanism by Sariyildiz (2012) to achieve the research objectives.

1-7- Scope of Research

This research examines the climate of the city of Melbourne in Australia. Australia is located in the Southern Hemisphere and has diverse climatic conditions. Its climatic regions consist of several different climatic classifications (Figure 1-3; Table 1-1). Köppen defines various climate classifications for Australia, while the Building Code of Australia (BCA) identifies eight main climatic zones: tropical, subtropical, grassland, desert, warm temperate, temperate, cool temperate, and mountainous.

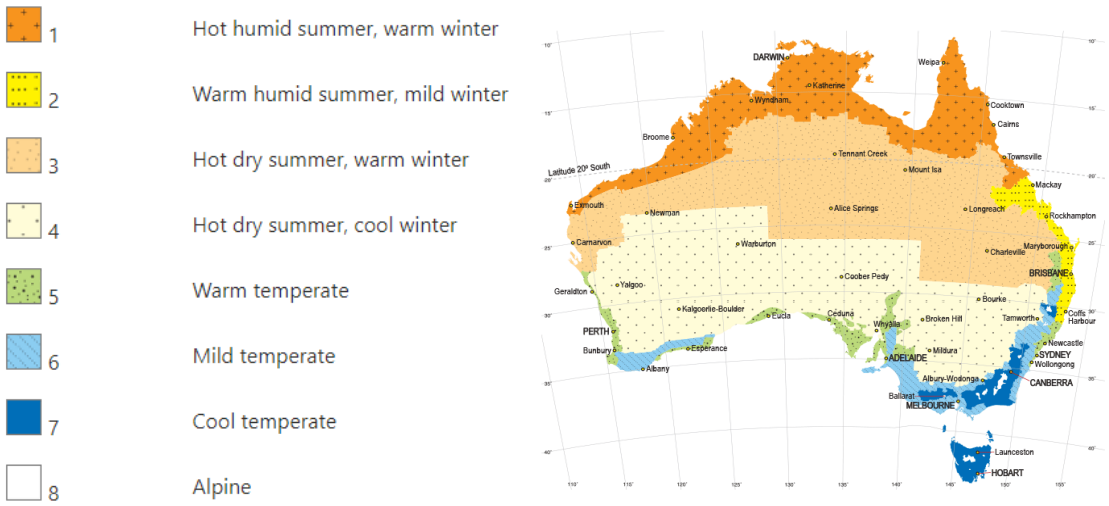

Figure 1-3. Climatic Classification of Australia

In this study, one of the eight major climatic regions defined by the Building Code of Australia (BCA), specifically the city of Melbourne, is considered for optimizing energy needs through passive energy designs.

Table 1-1. Characteristics of the Climatic Classification of Australia

Zone	Name	Climate in summer	Climate in winter	Energy consumption	Example Location
1	Tropical	Hot high humidity	warm	Cooling	Darwin
2	Subtropical	Very hot high humidity	Mild	Cooling	Brisbane
3	Grassland	Hot, dry	warm	Heating, Cooling	Alice Spring
4	Desert	Hot ,dry	Cool	Heating, Cooling	Griffith
5	Warm Temperate	Hot	Mild	Heating, Cooling	Sydney, Perth
6	Mild Temperate	Warm	Cold	Heating	Melbourne
7	Cool Temperate	Hot, dry	Cold, dry	Heating, Cooling	Canberra
8	Alpine	Mild	Cold	Heating	Perisher, Smiggins

The table below outlines the key characteristics of each of the eight climatic zones. Melbourne, the capital of Victoria and the second most populous city in Australia (the most populous city in urban areas), has a temperate oceanic climate (Köppen climate classification) and is well-known for its variable weather conditions. This variability is primarily attributed to Melbourne's geographical location. The temperature difference is most pronounced during the spring and summer seasons, which can lead to the formation of strong cold fronts. These cold fronts can lead to various severe weather conditions, ranging from storms to thunderstorms and heavy hail, as well as minor temperature drops and heavy rainfall. Generally, the city experiences low humidity during the summer.

1-8- Definition of Research Terms

As mentioned, this research focuses on the writing and application of a generative design algorithm within the context of performative computational architecture to produce spatial layouts of typical single-story residential buildingss aimed at optimizing energy performance. Accordingly, the specialized terms used in this research are defined as follows:

- **Predictive Modelling**: This mechanism is a method for generating predictions based on the performance of a system through the evaluation of a set of inputs and outputs derived from a series of specified characteristics and constraints set by the designer. The results can be defined in the form of mathematical equations (Chen et al., 2022; Himeur et al., 2021; Wei et al., 2018).
- **Performative Computational Architecture**: This concept focuses on a performance-based design (PBD) framework, introduced by Sariyildiz (2012) at the Delft

University of Technology to enhance the design process. The framework of performative computational architecture consists of three main stages: form generation, performance evaluation, and optimization, demonstrating a repeatable design cycle mechanism aimed at achieving optimal design responses based on specific performance criteria.

- **Parametric Design**: Parametric design is defined as the design of a subject based on dimensions and characteristics expressed in the form of parameters (Moretti, 1971). Kalay (1989) also defines parametric design as the formulation, calculation, and representation of relationships between a group of variables in the form of a series of parameters that change automatically.
- **Building Energy Simulation**: This concept refers to a mechanism for predicting rule-based energy performance in buildings. It utilizes a well-defined set of rules to forecast the energy behaviour of a complex system (Coakley et al., 2014).

The concepts presented in this section are the most significant specialized terms relevant to this research. Additional concepts will be introduced throughout the thesis. The keywords defined above will suffice for locating related articles in the main field of this study. Based on the aforementioned information, residential buildings account for a significant portion of final energy consumption worldwide. Therefore, optimizing building design for energy performance is essential for minimizing energy consumption rates in residential buildings. In this context, the use of simulation mechanisms in the energy performance assessment of buildings is highly significant. However, the use of simulation software has not been widespread among designers in recent years due to various reasons, including the complexity of using dynamic simulation programs, such as correctly constructing simulation models, interpreting results, making design decisions based on those results, user-unfriendly interfaces, lengthy simulation processes in architectural design, and compatibility issues with common computer-aided design software.

However, the mechanism of Performative Computational Architecture (PCA) can provide a framework based on a computational algorithm that allows for the easy examination of energy performance changes by altering the geometric variables of the building. According to the points mentioned, this research aims to present a performative computational architecture model that defines a design problem concerning the external shell of housing. It seeks to conduct an extensive search across various common residential buildings and, subsequently, determine the best spatial layouts in terms of energy performance through the

evaluation and optimization of the obtained responses. This mechanism also enables the development of a model for predicting energy performance based on assessments of the final inputs and outputs.

Accordingly, the research questions, objectives, and hypotheses have been defined in two main and sub-sections correspondingly. Additionally, based on the objectives of this research, the overall methodology adopts a quantitative approach, involving coding, energy performance simulation, optimization, and modelling based on the results obtained. In alignment with these objectives, the second chapter will review the relevant literature.

Chapter 2

Literature Review

Chapter 2: Literature Review

2-1- Introduction

This chapter reviews the literature relevant to the research topic. As mentioned in Chapter One, the objective of this research is to investigate the impact of geometric factors of a typical single-story residence in Melbourne, Australia, on energy performance. This will be achieved by defining a performative computational architecture model aimed at identifying optimal solutions based on energy performance goals. Various factors influence energy performance, among which geometric factors are a primary category. This chapter first addresses the literature concerning factors that impact energy performance. Following this, the performative computational architecture process utilized in this research is introduced. The chapter also examines theoretical foundations related to the study, and, finally, evaluates studies related to the field of this doctoral dissertation. At the end of this chapter, the variables of this research will be delineated.

2-2- Examination of Physical Factors Affecting Building Energy Performance

The physical factors of buildings constitute the primary focus of this research, encompassing a wide range of characteristics related to buildings and construction (Chen et al., 2020). This examination mainly centers on the most prevalent factors, such as building shape, orientation, wall insulation, window glazing, window-to-wall ratio (WWR), insulation materials, and optimal insulation thickness. According to the studies reviewed, physical factors can significantly influence a building's energy performance (Rodrigues et al., 2014). The most basic effect of physical factors on energy performance is that varying building dimensions accommodate different occupant densities (Du et al., 2020). Additionally, spatial layout impacts occupant behavior, and variations in space occupancy directly affect environmental comfort. Buildings possess diverse properties and characteristics that impact energy consumption, identified and defined through various terms in the literature. Tsanas and Xifara (2012) use the term "variable," while Li et al. (2019) refer to "form." Geyer and Singaravel (2018) use "component," and Ciulla et al. (2019) employ "forms and characteristics." Meanwhile, Seyedzadeh et al. (2019) use the term "feature." Building characteristics can be categorized into physical and non-physical elements. The following sections will explore the key physical factors in buildings that impact energy consumption.

2-2-1 Building Form

Significant efforts have been made to identify the impact of building form on energy loads. Research has been conducted based on diverse parameters. Ourghi et al. (2007) proposed a simple analysis method to predict the effect of building form on annual cooling and total energy consumption for an air-conditioned office building. Simulations were conducted for four locations—Rome, Tunis, Cairo, and Gabes—indicating a strong interdependence between annual energy consumption and various building features such as form, window size, and glazing type. Caruso and Kämpf (2015) analyzed optimal three-dimensional building forms that minimize energy consumption from solar radiation using an evolutionary algorithm. The results suggest that compact forms with orientation towards a specific direction in the sky, following a self-shading concept, are optimal and site-dependent.

Additionally, Depecker et al. (2001) suggested that in cold climates, the heating load is directly proportional to the shape coefficient, which they define as the surface-to-volume ratio. AlAnzi et al. (2009) introduced an analytical method to estimate the impact of building form on the energy efficiency of air-conditioned office buildings in Kuwait. This analysis considered multiple building forms, including rectangular, L-shape, U-shape, T-shape, cross-shape, and H-shape. A study by Gomez-Mejia et al. (2007) in Tehran demonstrated that building form orientation can save up to 105% of a building's annual energy, highlighting the importance of assessing orientation as a factor of form affecting energy consumption.

Hachem et al. (2011) examined building form and found that the number of shaded facades and the shading-to-shaded-facade ratio significantly affect solar radiation on non-convex forms. This study was based on residential buildings in cold climates and examined seven forms, including square, rectangular, trapezoidal, L, U, H, and T. In research on single-family homes across five locations in the United States, Bichiou and Krarti (2011) identified building form, window-to-wall ratio, and orientation as critical parameters for optimization. Using three optimization algorithms, they were able to reduce energy consumption by 10–25% depending on the house type, climate, and life-cycle cost.

For naturally ventilated residential buildings in Singapore, Wang et al. (2007) examined optimal thermal comfort by adjusting thermal transmittance, window-to-wall ratio, orientation, and shading device length. Mirrahimi et al. (2016) studied the impact of building

form in Malaysia's tropical climate, also evaluating other factors such as external walls, roof, glazing, and natural ventilation. The primary goals were to improve thermal performance and overall energy and lighting consumption in high-rise residential buildings. In Argentina, Bre et al. (2016) conducted an energy optimization study on a typical residential building, where some rooms were mechanically ventilated, while others relied on natural ventilation. The results underscored solar absorption of exterior walls, thermal transmittance, orientation, and window area as significant factors for cooling load reduction in naturally ventilated spaces.

Oral and Yilmaz (2002; 2003) developed a method for determining building form to minimize thermal load. Additionally, Marks (1997) studied optimal wall length ratios, angles, and glazing form parameters for multi-story office buildings in Australia. This study was expanded by Jedrzejuk and Marks (2002), who proposed a multi-criteria energy consumption optimization method based on building form and layout.

2-2-2- Window-to-Wall Ratio

The building envelope significantly impacts energy consumption by separating conditioned interior spaces from the external environment. This includes windows, exterior walls, and the roof, which affect heat gain and heat loss processes (Marino et al., 2012). Among these elements, the window-to-wall ratio (WWR) is one of the most critical aspects of the building envelope, substantially influencing a building's energy efficiency (Rana et al., 2022). Solar heat gain through windows harnesses renewable energy sources like sunlight, reducing heating loads in winter. However, windows, with their lower thermal insulation, also contribute significantly to indoor heat loss (Hesaraki, 2017). In summer, windows facilitate solar heat gain from the outside, increasing the cooling load of air conditioning systems. An increase in window size, and consequently WWR, raises cooling loads in summer-dominant areas (Rana et al., 2022). Gelesz and Reith (2015) found that a fully glazed facade could account for up to 45% of a building's cooling load, while Pathirana et al. (2019) reported that increasing WWR could raise solar heat gain from 20% to 50%.

In Saudi Arabia, Alwetaishi and Balabel (2017) conducted a study on educational buildings to determine the optimal WWR under various climatic conditions, recommending a 10% WWR for hot, humid climates. Goia (2016) suggested an optimal WWR range of 30–45% for the general European climate. Marino et al. (2017) found that a WWR of 32% with low

thermal transmittance glazing of 1.87 W/m²K optimized energy performance in Italy. Lee et al. (2013) proposed that window sizes should be minimized on all orientations except the north, with an optimal WWR of 25% in Asian climates. Feng et al. (2017) examined different WWRs for various orientations in Shenyang's severe cold climate, recommending an energy-efficient WWR of 10–15% for the east and 10–22.5% for the south. Sedigh Ziabari et al. (2019) demonstrated that the highest energy consumption occurs when WWR exceeds 20% on the west side, but with ventilation, a 25% WWR performs best on the north facade, and 20–30% is optimal for the south and east sides. In Pakistan, Masood et al. (2014) found that increasing WWR beyond 20% impacts heat gain and heat loss in all directions. Ahsan (2009) in Bangladesh showed that larger window areas significantly reduce electricity consumption with a wall thickness of 125mm and window glazing of 5mm at an opening rate up to 50%.

Alwetaishi et al. (2017) also conducted research to determine the optimal WWR for educational buildings in diverse climates, recommending a 10% WWR for hot, humid regions. Gomez-Mejia et al. (2007) highlighted WWR's role in influencing building orientation decisions. Bichiou and Krarti (2011) optimized single-family homes in the U.S., focusing on WWR, building form, and orientation, reducing energy consumption by 10–25%. Wang et al. (2007) found that a 24% WWR optimized energy consumption in Singapore.

Additionally, Mangkuto et al. (2016) conducted a simulation study on tropical buildings to evaluate the effects of WWR, window orientation, and wall reflectance on lighting energy consumption and daylight metrics. The optimal solution from Pareto optimization suggested a 30% WWR, 0.8 wall reflectance, and south orientation as optimal for design. This literature suggests that optimal WWR varies depending on a building's climatic context, with no universal guideline for all locations (Rana et al., 2022). The WWR design evolves with solar radiation intensity, influenced by latitude, longitude, and the region's solar path (Tong et al., 2019).

2-2-3- Building Materials

Building materials significantly impact energy consumption (Yüksek, 2015), as energy use in buildings can be reduced by altering material properties such as thermal mass, insulation, and heat transfer coefficient. Efficient building materials can be the most effective means of

saving energy (Usta & Zengin, 2021), as they reduce fuel consumption and increase thermal comfort by minimizing heat loss in buildings (Bolattürk, 2008; Chwieduk, 2000). Many researchers have highlighted the importance of energy-efficient building materials (Tronchin & Fabbri, 2008; Su et al., 2016).

Thermal mass, as a property of materials, allows buildings to store heat against temperature fluctuations (Sharaf, 2020). For example, a large thermal mass in the insulated section of a home can mitigate daily temperature swings when outdoor temperatures fluctuate throughout the day. Thermal mass absorbs thermal energy when the ambient temperature exceeds that of the mass and releases it when the surroundings are cooler, reaching thermal equilibrium (Brambilla et al., 2018).

Building materials and elements such as walls, roofs, floors, windows, doors, and ventilation systems play a crucial role in the heat exchange process between the building's interior and exterior. For instance, walls and roofs together account for 60% of heat leakage in buildings lacking proper thermal insulation. Without adequate insulation, heat loss increases through other building elements. Failure to control heat exchange between the building and its external environment results in increased energy consumption to maintain suitable indoor temperatures for occupants (Sadineni et al., 2011). Ignoring the thermal mass properties of materials and sufficient thermal insulation leads to higher energy consumption in buildings (DEFRA, 2016).

Building elements such as walls, roofs, floors, windows, doors, and ventilation systems significantly impact heat equalization between the building interior and exterior. For example, Sharaf's study (Sharaf, 2020) indicates that uninsulated walls and roofs together contribute to 60% of heat leakage in buildings. Sharaf's research explores the role of thermal mass in buildings to achieve thermal comfort within lower cooling and heating loads and reduced energy consumption. If not adequately insulated, increased heat loss occurs through other building elements. Uncontrolled heat exchange between a building and its external environment leads to higher energy usage to provide suitable indoor temperatures for users (Zhang et al., 2019).

Several studies have evaluated the impact of the heat transfer coefficient variable on building energy performance. Findings from Wang et al. (2007) in Singapore suggest that the heat transfer coefficient for façade materials on the north, south, west, and east sides should be

less than 2.5 W/m²K. Research by Al-Tarhuni et al. (2019) also examined energy consumption in the U.S. Midwest based on wall area, wall heat transfer coefficient, window area, and window heat transfer coefficient, assessing 972 samples. Other studies, including Chen & Yang (2017), Ciulla et al. (2019), Amico et al. (2019), and Geyer & Singaravel (2018), have evaluated the influence of materials on energy consumption.

2-2-4- Window Type

Conventional windows are crucial elements that allow sunlight to enter buildings. In these windows, the solar heat gain depends on the type of glass used, window area, and building orientation (Ateeque et al., 2017). Numerous studies have examined the impact of windows on energy consumption, as they significantly influence energy consumption compared to other building envelope elements (Abdelrady et al., 2021; Ragab Abdel Radi, 2020). Hee et al. (2015) identified several criteria for the optimal selection of glass, including thermal properties, optical properties, window size, window orientation, occupancy area, and costs. Yoon et al. (2013) conducted a foundational study on energy performance characteristics based on glass performance during the development of office buildings. Cesari et al. (2018) studied the effects of different window sizes and types of glass on energy needs in hospital patient rooms to determine energy savings using larger apertures and to identify the most effective types of glass. Additionally, Seyedzadeh et al. (2019) investigated glass characteristics, including distribution and area, to assess cooling and heating loads in the Athens region of Greece.

The heat transfer coefficient of glass is a determinant factor in the selection of glass types and has been analyzed in several studies. A poor heat transfer coefficient for glass leads to reduced conductive heat loss and increased energy consumption. Re Cecconi et al. (2019) examined a school in Lombardy, Italy, based on the heat transfer coefficient of glass alongside the heat transfer coefficients of walls and roofs, studying 1,632 samples. Various studies, including those by Al-Tarhuni et al. (2019), Amico et al. (2019), and Ciulla et al. (2019), have also evaluated the heat transfer coefficient of glass.

Other studies have explored the use of nanomaterials in exterior windows due to their thermal and visible light transmission properties (Ragab & Abdelrady, 2020; Leskovar & Premrov, 2011). Leskovar and Premrov (2011) investigated an architectural design method to create an ideal ratio of glazed areas in prefabricated wooden frame buildings concerning

energy efficiency, focusing particularly on south-facing glazed surfaces. Abdelrady et al. (2021) also examined the impact of nano-gel glass on the energy consumption of residential buildings in New Aswan, Egypt. Moreover, various types of windows with active shading systems can reduce the amount of solar radiation entering buildings. Thus, based on these systems, the thermal performance of buildings can be significantly improved (Jelle, 2013). These active shading systems can be classified into smart glass and kinetic shading devices (Jalil & Roza, 2019). Smart chromatic glass can be divided into various categories, including electrochromic (EC), gasochromic (GC), thermochromic (TC), and photochromic (PC) glass (Nageib et al., 2020).

Electrochromic glass is one of the modern smart systems that are electrically activated (Ye et al., 2019). According to Zhao et al. (2019), electrochromic glass can be controlled by sunlight, temperature, and thermal load or any user-defined parameters. Gasochromic glass has a simpler configuration than electrochromic glass (Nageib et al., 2020). The materials for gasochromic glass can be coated directly onto a clear glass or plastic substrate without the need for expensive transparent conductive layers. Based on research by Mirzaei et al. (2019), gasochromic glass is suitable for large glass building facades due to its simple configuration and low implementation costs. Thermochromic glass can automatically adjust its spectral response properties according to temperature changes (Granqvist et al., 2014). Thermochromic glass alters its thermal properties by transitioning and reflecting at a critical temperature when its crystalline structure changes beyond a specific ambient temperature (Runqi et al., 2018). At lower temperatures, thermochromic glass allows solar radiation to enter, while at higher temperatures, it reflects sunlight (Cui et al., 2018). Additionally, photochromic glass changes color based on the intensity of incoming light or the spectral distribution of light (Helmy & de Alaniz, 2015). Photochromic materials change their optical properties when exposed to UV sunlight and revert to their original properties in the dark. Overall, photochromic materials act as energy absorbers (Casini, 2016). Many studies (Myunghwan et al., 2019; Aste et al., 2018) have examined the materials used in smart glass.

2-2-5- Building Airtightness

Airtightness of the building envelope or uncontrolled exchange of air between the interior and exterior is a key variable in energy consumption and thermal comfort (Domínguez-Amarillo et al., 2019). The method commonly accepted by the scientific community for assessing airtightness is the blower door test. Numerous studies on air leakage in single-

family homes have been conducted in Northern Europe (Gillott et al., 2016; Caillou et al., 2010) and the United States (Chan et al., 2012; Chan et al., 2013) over the past three decades. Additionally, in the last ten years, Spain has emerged as a research area for this topic in Southern Europe (Fernández-Agüera et al., 2011; Tiberio & Branchi, 2013).

Overall, a review of the literature reveals that most articles examining energy consumption related to infiltration report conditions in Northern Europe (Spiekman et al., 2010). The study by Feijó-Muñoz et al. (2019) was conducted in Spain under temperate and continental climates, focusing on the impact of airtightness on energy consumption. In another study, Alves et al. (2014) evaluated the effect of infiltrations on energy consumption using a simplified model. Meiss and Feijó-Muñoz (2014) analyzed 13 residential buildings in Northern Spain to investigate the influence of airtightness on energy consumption. According to the literature (Bekö et al., 2011; Wall, 2006; Pinto et al., 2011), research on building airtightness in developed countries has started earlier. Studies on airtightness in China have also gained attention (Chen et al., 2012; Sun et al., 2011).

2-2-6- Shading Devices

Thermal and visual comfort inside a building varies depending on exposure to direct sunlight during the day and night, as well as across seasons. Innovative daylighting shading devices can effectively enhance interior comfort and control energy consumption (Proietti et al., 2011; Sdringola et al., 2014). Numerous studies have been conducted on the use and evaluation of external and internal shading systems. Kim et al. (2012) performed an experimental configuration simulation and energy analysis of several internal and external shading devices for apartment buildings in South Korea, demonstrating that external shading devices provided a significantly higher percentage of energy savings for cooling compared to internal devices. Yun et al. (2014) proposed a lighting and shading control strategy. Freewan (2014) analyzed various parameters of an office building concerning visual comfort and energy consumption, examining the impact of several types of shading devices on air temperature control and light levels in offices located in hot climate regions, finding that all shading devices improved the thermal and visual environment of the offices.

Several simulation studies have been conducted by Huang et al. (2014) to evaluate the performance of different commonly used window designs in predominantly cooling climates, indicating that the comprehensive performance of preset assumptions is better than

internal shades. Atzeri et al. (2014) compared the performance of external and internal shading devices concerning thermal and visual comfort in an open-plan office located in Rome, showing that while the use of shades always improves thermal comfort, energy consumption could increase as a result of specific building configurations. Babaizadeh et al. (2015) compared five common shading configurations in five climate zones defined by ASHRAE standards, ultimately providing a reference set of guidelines for decision-making regarding the design of shading systems in various facilities. Kirimtat et al. (2016) conducted a review of different types of shading devices used in various building types and climatic regions.

Some studies have discussed the use of dynamic shading facades, specifically highlighting how such devices can potentially impact heating and cooling energy consumptions and lighting energy needs in a building (Marszal et al., 2011; Sartori et al., 2012). Extensive research has been conducted to evaluate the effects of dynamic shading devices on energy consumption. In earlier studies, heating and energy performance were assessed when a building was equipped with roller shades, horizontal shading devices, vertical shading devices, and Venetian blinds (Lee et al., 2016). Tzempelikos et al. (2013) compared the thermal and lighting energy performance differences of a facade depending on various shading control strategies, such as solar radiation, lighting, and glare. This study indicated that a maximum difference of 50% in the annual lighting energy required for a facade where roller shades were installed could occur depending on shading device control strategies. Other studies (Montier et al., 2013; Van Den Wymelenberg, 2012) proposed methods to divide the movements of a shading device into several stages at equal intervals to describe changes in position with the performance of a shading device. In Montier et al. (2013), the position changes of three shading devices—namely sliding panels, vertical folding panels, and horizontal folding panels—were divided into four stages. Kim (2013) proposed a method for extracting shading coordinates at the facade level, utilizing sun vectors, shading device position coordinates, and window position coordinates. Additionally, Feito et al. (1995) introduced a method for examining shading in a two-dimensional framework. The study conducted by Murta (2016) proposed a General Polygon Clipper (GPC).

2-2-7- Azimuth

Due to issues related to the use of non-renewable energy sources, there has always been a need for sustainable and non-polluting alternative energy sources, which has led to extensive

research in this area (Kamanga et al., 2014). Solar energy, due to its availability, is a highly popular renewable energy source (Božiková et al., 2021). Based on presented facts, it is evident that solar energy can be converted into electrical and thermal energy with positive and economic effects. Today, one of the primary reasons for utilizing solar mechanisms and systems is their ecological benefits and sustainability (Sadati et al., 2015). Kalogirou (2004) observed that solar energy provides one of the best solutions to the problem of climate change. The amount of solar radiation received depends on geographical latitude, the day of the year, the tilt or slope angle, the azimuth angle of the surface, the time of day, and the angle of incident radiation (Xu et al., 2017; Jafarkazemi & Saadabadi, 2013). One of the most crucial factors that can be controlled to maximize the amount of received irradiance is the azimuth angle of the surface (Antonanzas et al., 2018).

Many researchers (Hussein et al., 2004; Rowlands et al., 2011; Salih, 2017; Yadav, 2013) have presented findings indicating that for any location on Earth with different radiation characteristics, an optimal tilt angle can be determined to achieve the best solar energy reception. The received energy is highest when solar radiation is incident perpendicular to the surface (Yadav, 2013). A case study focused on determining the optimal tilt angle for photovoltaic cells for each month in Nigeria confirmed its variability throughout the year. The performance of a photovoltaic cell is also influenced by the azimuth angle. The impact of various orientations of horizontal and vertical solar panels on the integration of solar energy into low-voltage distribution networks was identified by Laveyne et al. (2020). Mehleri et al. (2010) provided results for the optimal tilt angle and azimuth orientation for solar energy reception to maximize solar irradiance for a specific time period. In particular, the effect of azimuth angle on energy production in photovoltaic cells was studied and empirically evaluated (Dhimish & Silvestre, 2019). Overall, in the field of azimuth angle, most studies have discussed optimal tilt angles for the best performance, design, and simulation of solar energy systems. There are also several studies conducted to find the best performing geographic areas in terms of solar energy reception, while others compare different locations (Hafez et al., 2017).

Optimizing the tilt angle for solar energy reception based on azimuth angle has been studied for various locations in European countries, including Turkey (Bakirci, 2012; Ertekin et al., 2008), Romania (Stanciu et al., 2016), Austria and Germany (Hartner et al., 2015), Italy (Calabr, 2013), Greece (Mehleri et al., 2010), Cyprus (Ibrahim, 1995), Spain (De Miguel et

al., 1995), as well as for Middle Eastern countries like Oman (Jafari & Javaran, 2012), the United Arab Emirates (Jafarkazemi & Saadabadi, 2013), Saudi Arabia (Tamimi & Sowayan, 2012; Benghanem, 2011), Egypt (Elminir, 2006), Jordan (Alatarawneh et al., 2016; Shariah et al., 2002), and Syria (Shariah, 2002). In Asian countries such as Pakistan (Khahro et al., 2015), Thailand (Krishna et al., 2015), Indonesia (Handoyo et al., 2013), China (Shen et al., 2018; Li et al., 2007), Taiwan (Chang, 2010), India (Jamil Ahmad & Tiwari, 2009; Agarwal et al., 2012), Japan (Hiraoka et al., 2003), and Bangladesh (Ghosh et al., 2010), as well as in the Americas, such as Canada (Siraki & Pillay, 2012) and the United States (Lave & Kleissl, 2011; Gong & Kulkarni, 2005). All the mentioned studies indicate that the tilt angle and changes in azimuth angle have a significant impact on the amount of solar energy received and, consequently, on energy consumption. From a theoretical perspective, mathematical models and methods exist for calculating and comparing the best solar reception angles based on monthly diffuse radiation and actual monthly diffuse radiation (Tang & Wu, 2004). The operational parameters of photovoltaic modules have also been modeled and discussed in the literature (Nguyen & Nguyen, 2015). The relationship between energy production and energy consumption in irrigation networks was also investigated by Pardo et al. (2018).

From a practical perspective, an optimal technique to enhance solar reception on a surface is the use of solar trackers (Poulek et al., 2016; Mishra & Thakur, 2016). Active solar trackers follow the sun's path and optimize the position of the solar surface. Tracking systems are used to maximize the daily solar energy received by photovoltaic modules (Hailu & Fung, 2019). Solar trackers consist of mechanical components that ensure the rotation of solar modules; therefore, one of the disadvantages of solar trackers is the mechanical failure of their parts and the more challenging maintenance compared to stationary solar panels. Trackers are slightly more expensive, require energy to operate, and may not always be usable due to specific installation conditions.

2-2-8- Orientation Angle of Buildings

Morrissey et al. (2001) examined the topic of orientation concerning the energy consumption of buildings, recommending a southern orientation for buildings located in the Northern Hemisphere. This orientation can maximize heat and solar radiation. Most design guidelines suggest that the longest wall sections should face south (Morrissey et al., 2001). For optimal performance of passive solar panels, Littlefair (2001) suggested that the best orientation for buildings is 20 to 30 degrees toward the south. Gupta and Ralegaonkar (2004) developed a

model for related calculations, rotating the building from 0 to 180 degrees and applying varying shape values to estimate the received solar radiation. This method can be used to find the optimal orientation angle for receiving minimal solar radiation in summer and maximum solar radiation in winter. The authors concluded that the optimal orientation is generally achieved when the longest wall sections are oriented toward the north and south, meaning the building has an east-west elongation.

Most previous studies believed that the shape of the building is the most important factor in determining its optimal orientation. However, optimal solutions may vary under different conditions. For instance, Aksoy and Inalli (2006) examined the relationship between the optimal orientation of buildings and their shape with three shape coefficient values (0.5, 1, and 2). According to their numerical analyses, square-shaped buildings (shape coefficient = 1) have more advantages compared to the other two buildings without any insulation. For rectangular buildings with shape coefficients of 2 and 0.5, the optimal solutions dictate that the azimuth angles of the buildings should be 0 degrees and 80 degrees, respectively. Florides et al. (2002) evaluated the most efficient energy orientations for a square building in terms of minimizing heating demand. The optimal orientation for a building is to face the four cardinal directions. In contrast, for a rectangular building, the best orientation is for the smallest wall section to face east, with the building elongated in an east-west direction, to minimize heating requirements.

However, considering only the shape of the building cannot guarantee its optimal orientation, as the orientation variable can depend on many factors. For example, the glass-to-wall ratio and relative compactness are significantly important for optimizing energy performance based on building orientation. Some studies even indicated that the glazing ratio is a more critical parameter than building shape and relative compactness in determining building orientation (Fallahtafti & Mahdavinejad, 2015). To reduce the heating demand of a building, both the relative compactness and large glazing ratio should be taken into account (Pessenlehner & Mahdavi, 2013).

Some studies have focused on additional determinants of building orientation. Building size has been proposed as an important consideration in the design of passive solar residential buildings (Morrissey et al., 2011). Morrissey et al. (2011) found that smaller buildings are less sensitive to changes in orientation. In other words, higher design standards for smaller buildings can be more easily applied across various directions, resulting in relatively lower

associated costs. Abanda and Byers (2016) suggested that the life cycle of a building should be considered when assessing the impacts of orientation for smaller buildings. Based on their simulations, the most cost-effective orientation is +180 degrees from the baseline, which could lead to annual energy savings of £878 over a 30-year lifespan.

Morrissey et al. (2001) explored the topic of orientation regarding energy consumption in buildings, recommending a southern orientation for buildings located in the Northern Hemisphere, as this orientation can maximize heat and solar radiation. Most design guidelines suggest that the longest wall sections should face south (Morrissey et al., 2001). For optimal performance of passive solar panels, Littlefair (2001) suggested that the best orientation for buildings is 20 to 30 degrees toward the south. Gupta and Ralegaonkar (2004) developed a model for relevant calculations, rotating the building from 0 to 180 degrees and applying varying shape values to estimate the received solar radiation. This method can be used to find the optimal orientation angle for receiving minimal solar radiation in summer and maximum solar radiation in winter. The authors concluded that the optimal orientation is generally achieved when the longest wall sections are oriented north and south, meaning the building is elongated in an east-west direction.

Most previous studies have asserted that the shape of the building is the most critical factor in determining its optimal orientation. However, optimal solutions may vary under different conditions. For instance, Aksoy and Inalli (2006) examined the relationship between the optimal orientation of buildings and their shape using three shape coefficient values (0.5, 1, and 2). According to their numerical analyses, square-shaped buildings (shape coefficient = 1) provide more advantages compared to the other two buildings without any insulation. For rectangular buildings with shape coefficients of 2 and 0.5, the optimal solutions indicate that the azimuth angles of the buildings should be 0 degrees and 80 degrees, respectively. Florides et al. (2002) evaluated the most efficient energy orientations for square buildings in terms of minimizing heating demand. The optimal orientation for a building is to face the four cardinal directions. In contrast, for rectangular buildings, the best orientation is for the smallest wall section to face east, with the building elongated in an east-west direction, to minimize heating requirements.

However, considering only the shape of the building cannot guarantee its optimal orientation, as the orientation variable can depend on many factors. For example, the glass-to-wall ratio and relative compactness are significantly important for optimizing energy

performance based on building orientation. Some studies even indicate that the glazing ratio is a more critical parameter than the shape of the building and relative compactness in determining building orientation (Fallahtafti & Mahdavinejad, 2015). To reduce a building's heating demand, both a high relative compactness ratio and glazing should be considered (Pessenlehner & Mahdavi, 2013).

Several studies have focused on other determinants of building orientation. Building size has been suggested as an important consideration in the design of passive solar residential buildings (Morrissey et al., 2011). Morrissey et al. (2011) found that smaller buildings are less sensitive to changes in orientation. In other words, higher design standards can be more easily applied across various directions for smaller buildings, resulting in relatively lower associated costs. Abanda and Byers (2016) proposed that the life cycle of a building should be considered when assessing the effects of orientation for smaller buildings. According to their simulations, the most cost-effective orientation is +180 degrees from the baseline, which could lead to annual energy savings of £878 over a 30-year lifespan.

2-2-9- Thermal Mass

One of the physical factors influencing the energy performance of a building is its thermal mass. The thermal mass of the materials used in a building determines the ability of the building to store thermal energy (Sharaf, 2020). Thermal mass, in turn, can have a significant impact on the indoor temperature, electrical requirements, and occupant comfort. (Reilly & Kinnane, 2017). Thermal mass is important for heating and cooling applications for buildings that are continuously and sustainably active. For the thermal mass of a building, three components can be defined: structural elements, air volume, and other objects. In this regard, several studies have been conducted to understand the impact of thermal mass on buildings in a more structured manner.

Aste et al. (Aste et al., 2015) conducted a parametric study for a number of wall types for heating and cooling applications. In this regard, their study was limited to the climate of Milan, Italy. Asan (Asan, 2006), conducted a study on the effect of wall materials and thickness on the delay time and reduction factor for a wide range of homogeneous walls. Few studies have investigated the different effects of placing insulation and thermal storage layers in a wall, usually relying on 1D studies and controlling wall thickness (Kossecka &

Kosny, 2002). Some research has also investigated the effect of thermal mass on energy performance.

2-2-10- Thermal Bridge

Part of the heating load comes from heat loss through thermal bridges of the building envelope, which can account for up to 30% of the total energy consumption of an apartment building in winter (Zhang et al., 2022; Brás et al., 2014). In general, apartment buildings have a great potential to reduce energy consumption by improving the effects of thermal bridges. Accordingly, many researchers have focused their attention on the construction details in the field of thermal bridges. In general, thermal bridges are created by high thermal conductivity materials in the insulation structures of buildings, which leads to a significant increase in heat flow through the wall (Theodosiou et al., 2021). As a result, thermal bridges increase excess heat loss in winter and heat gain in summer (Capozzoli et al., 2013). Also, heat loss due to thermal bridges in winter leads to a decrease in indoor temperature and an increase in condensation (Alhawari & Mukhopadhyaya, 2018). In general, in a building, windows, doors, and joints are weak areas that can form thermal bridges (Zhang et al., 2022; Asdrubali et al., 2012). An effective solution to reduce heat loss due to thermal bridges is to improve the thermal resistance of the locations where thermal bridges are formed (Garrido et al., 2018). To prevent heat loss due to thermal bridges, the first step is to apply more insulation to the building envelope (Zhang et al., 2022). In general, various studies (Theodosiou et al., 2021; Alhawari & Mukhopadhyaya, 2018) explained that a well-insulated building structure can prevent thermal bridges. In general, two categories of external and internal systems for building insulation affect thermal bridges (Zhang et al., 2022). Generally, the external insulation system performs better than the internal insulation system under the influence of thermal bridges (Brás et al., 2014).

2-3- Examination of Factors Influencing the Relationship Between Physical Factors and Building Energy Performance

A diverse set of factors influences the relationship between physical factors and building energy performance. In fact, building energy performance is affected by a complex interaction of various elements. A review of research related to the impact of physical factors on energy performance shows that the physical characteristics of a building can affect energy

performance in multiple aspects. Accordingly, the influence of physical factors on Building Energy Performance (BEP) can be examined alongside three general factors:

2.3.1 Environmental Conditions Surrounding the Building

This section examines the impacts of climatic conditions on building energy consumption, including outdoor air temperature, relative humidity, solar radiation, and wind speed. Outdoor air temperature is considered the most significant environmental factor for determining building energy consumption. Previous studies have shown that heating and cooling periods are based on degree days and outdoor air temperature (Liu et al., 2017). Lok et al. (2005) recorded long-term climate data for five cities in China, which represent five main climates: cold, cold with cold winters and hot summers, temperate winters with hot summers, and warm summers. Among the climatic factors examined, outdoor air temperature demonstrates significant effects on the thermal demands of buildings during the design phase and energy consumption during the operational phase.

Relative humidity also has a crucial impact on air conditioning systems during the cooling period. Air conditioning systems are influenced by outdoor air temperature and relative humidity (Liu et al., 2017; Neto et al., 2008). Santamouris et al. (2001) demonstrated that the heat island effect reduces the efficiency of HVAC systems by approximately 25%. Vakiloroaya and Madadnia (2013) stated that the efficiency of cooling towers increases when relative humidity is below 40 percent. Solar radiation also affects the cooling demand of buildings, particularly in subtropical and tropical conditions. The heat generated from solar radiation can be harnessed to produce electricity for buildings (Liu et al., 2017; Lok et al., 2005). Chwieduk and Bogdanska (2004) concluded that buildings can maximize the benefits of solar radiation throughout the year when the azimuth angle of the surface is approximately 15 degrees. An angle range between -15 degrees and +45 degrees also indicates good energy performance for buildings, which is beneficial for the installation of solar panels. This directly influences the daylighting and lighting requirements of buildings.

Wind speed has been identified as having the least significant impact on building energy compared to other meteorological factors based on relevant numerical analyses (Liu et al., 2017; Li et al., 2014). Buildings equipped with central air conditioning are always maintained at a positive pressure, resulting in a higher influx of fresh air compared to the air being exhausted. Therefore, the heat gain from infiltration is minimal. However, the nature

of ventilation design through a building can be significantly affected by wind direction and speed (Santamouris et al., 2001). A reduction in heating demand has been observed under changing climatic conditions. For instance, in a cold climate, a study of residential buildings indicated that heating energy will decrease by approximately 25-30% over the next century (Nik & Kalagasidis, 2013). Previous studies have noted that climatic changes during the twentieth century have had a greater impact on heating energy needs than on cooling energy requirements (Xiang & Tian, 2013).

2-3-2- Equipment and Facilities of the Building

In general, a variety of equipment affects the energy performance and daylighting of a building. Cooling, heating, and air conditioning systems, intelligent control systems, lighting equipment, and other electrical devices are the primary subjects in this section. The selection and efficiency of air conditioning systems play a crucial role in energy consumption. High-efficiency heating and cooling equipment, coupled with well-designed distribution systems, contribute to energy savings. Research by Socolow et al. (2011) examines the potential for improving energy efficiency in cooling, heating, and air conditioning systems. Additionally, advanced control systems, including programmable thermostats and building automation, optimize cooling, heating, and air conditioning performance based on occupancy, weather conditions, and time of day. Haves and Kim (2001) also provide insights into the application of advanced control strategies for cooling, heating, and air conditioning systems. The selection of lighting technologies such as LEDs (Light Emitting Diodes) and CFLs (Compact Fluorescent Lamps) helps save energy. Furthermore, effective daylighting strategies, combined with responsive lighting controls, enhance energy efficiency. The book "Advanced Lighting Controls" by Rubinstein et al. (2007) provides comprehensive information on lighting control strategies for energy savings.

For various types of control systems for heating, cooling, ventilation, and lighting, diverse spatial characteristics are necessary. For instance, individual control is more suitable for cellular office structures than for open-plan offices, as demonstrated in two studies by Shahzad et al. (2017a; 2017b). Different types of digital controls lead to varying energy performance outcomes. Moreover, solar energy and natural ventilation indicators can be utilized as control metrics; for example, the availability of solar energy for lighting control (Haq et al., 2014) and air quality and thermal comfort for ventilation system control (Schulze & Eicker, 2013). By employing dynamic control based on available solar energy and natural

ventilation, the effects of spatial layout on Building Energy Performance (BEP) are enhanced (Du et al., 2020).

2-3-3- Behavior of Building Occupants

The behavior of occupants, including awareness of energy consumption and active participation in energy-saving practices, is crucial. Understanding the complex dynamics between energy efficiency in residential buildings and occupant behavior is fundamental for promoting sustainable practices, reducing environmental impacts, and optimizing energy use. This introduction aims to provide a comprehensive overview of the existing dimensions in this intricate relationship, utilizing a diverse array of scientific literature to examine key insights and emerging trends. Behavioral theories and frameworks serve as essential foundations for conceptualizing and investigating these dynamics. Social cognitive theories, such as the Theory of Planned Behavior (Ajzen, 1991) and the Norm Activation Model (Schwartz, 1977), offer valuable insights into the cognitive processes and socio-cultural influences that affect individuals' energy-related behaviors.

As people are the primary energy consumers and spend considerable time inside residential buildings, occupants passively influence the energy balance of buildings through their mere presence (Harputlugil et al., 2019). They are also responsible for the consumption, emissions, and waste produced, utilizing energy in buildings through heating, ventilation, and air conditioning (HVAC) systems, cooling, lighting, electrical loads/appliances, and domestic hot water services for various consumption reasons. Understanding and predicting occupant behavior can greatly aid in reducing energy consumption in residential buildings. However, measuring and modeling occupant behavior in building research is challenging, even though it is recognized as a key factor in building energy consumption. Moreover, occupants do not form homogeneous groups, nor do they respond based on specific logic. This variability makes predicting the relationship between occupant behavior and energy consumption particularly difficult.

Different functions in architecture require diverse spatial characteristics, and various spatial layouts enable the accommodation of different occupant densities. For instance, an open-plan office allows for higher occupant density compared to a cellular office layout (Hedge, 1982; Musau & Steemers, 2008). Different residential densities create varying requirements for comfort objectives, such as ventilation needs (Du et al., 2020). Additionally, different

spatial characteristics influence occupant behavior (Goldstein et al., 2011), which in turn affects comfort provision needs. This variation directly affects the building energy performance (BEP).

2-4- Mechanisms of Energy Consumption in Buildings

Building service systems are the primary energy consumers within a structure. Significant efforts have been made by researchers and industry practitioners to develop various advanced technologies aimed at reducing energy consumption in buildings while also improving energy efficiency in building service systems (Chen et al., 2020). To achieve optimal energy consumption in a building, it is essential to evaluate the architectural impact on each of these mechanisms, both separately and in an interconnected manner. Accordingly, the discussion will first focus on examining the mechanisms of energy consumption.

2-4-1- Heating Requirements in Buildings

In recent years, cooling and heating demands have received significant attention from researchers. This is due to the increasing intensity of energy consumption and related environmental concerns; as the shape, orientation, space, and components of a building represent fundamental characteristics for building design that must be considered in energy efficiency optimization studies (Plörer et al., 2021). Energy consumption for heating buildings depends on various factors, the most important of which are thermal insulation, air-tightness of the external heating envelope, thermal mass of the building, heating method, and thermal efficiency. To determine cooling and heating requirements, various computational methods are utilized, including three main sets: engineering methods, artificial intelligence, and hybrid approaches. The engineering method employs a transparent process based on solving physical equations to describe the energy behavior of buildings. The artificial intelligence (AI) method primarily relies on statistical time series analysis and machine learning algorithms to access and predict building energy consumption. The hybrid method combines the two aforementioned approaches.

The general calculation method uses simplified relationships to describe the final energy consumption in a building, based on the assumption that the thermal load of the building is proportional to the temperature difference between the heated space and its surroundings at

a given external temperature (Szul, 2021). In this formula, the instantaneous thermal load of the building at a specified temperature is calculated in kilowatts based on the building's heating thermal load design, the design indoor temperature, the design outdoor temperature, and the instantaneous outdoor temperature. Additionally, the theoretical value of the heat transferred from the building to the environment over the entire heating season is derived from the results obtained from the above relationship.

2-4-2- Lighting Requirements in Buildings

Lighting is one of the primary energy consumers in buildings (Amasyali and El-Gohary, 2018). Optimizing the lighting system of buildings during the early design stages is a fundamental step toward achieving high-performance buildings. Various methods have been employed to simulate building lighting, including lighting energy, daylight, and daylight factors (Plörer et al., 2021). Design lighting standards and guidelines have been introduced in many countries to enhance energy efficiency while promoting the visual comfort and safety of occupants. Therefore, the design lighting level in buildings considers factors such as the predominant age of occupants, primary activities, work speed, and precision levels (Dubois, 2003).

The performance of daylight in a building is typically assessed using metrics such as Daylight Factor (DF), Daylight Availability (DA), and Useful Daylight Illuminance (UDI). The Daylight Factor (DF) is defined as the ratio of internal illuminance to external horizontal illuminance under overcast sky conditions, according to the International Commission on Illumination (CIE) (Bian Y and Ma, 2017). Daylight Availability (DA) is defined as the percentage of occupied hours in a year during which a specific point meets a minimum specified daylight illuminance level. Nationally recommended standards for specific visual tasks are often used as thresholds for daylight autonomy (DA) since most standards are based on minimum illuminance levels (Pellegrino et al., 2017). Useful Daylight Illuminance (UDI) is defined as the percentage of annual occupied time during which a given workspace is within a specific range of daylight illuminance, varying from 100 to 2000 lux (Li & Lou, 2017). Lighting requirements are utilized to define standards and guidelines for building design, as they are independent of the light source. Daylight can be considered the most direct and purest approach to evaluating daylight in buildings, whereas the aforementioned daylight metrics represent an indirect and computation-based approach (Kruisselbrink et al., 2018). Lighting Power Density (LPD) is a tool commonly used to estimate energy savings

from lighting in buildings and is expressed as watts of lighting per square meter of floor area. Reducing lighting power density, which correlates with lower energy consumption, can be achieved through efficient lighting optimization, daylight control switches, and occupancy sensor controls (Wang, 2009). Different layouts introduce varying levels of daylight into the building.

2-4-3- Ventilation Requirements in Buildings

Air conditioning accounts for approximately 40% of the total energy consumption in a commercial building (Yang et al., 2016). Various advanced technologies have been developed and implemented for air conditioning systems to reduce energy consumption, including variable air volume systems, variable speed pumps or fans, ground-coupled heating, ventilation, and air conditioning (HVAC) systems, thermal storage systems, heat recovery systems, ejector systems, chilled beam systems, and evaporative cooling systems (Chen et al., 2020). Variable air volume pumps and variable speed pumps are currently the most popular and advanced HVAC technologies (Yang & Ting, 2000; Ardehali & Smith, 1996).

Internal temperature regulation or the recirculation of fresh air when the building is unoccupied can also impact the building's ventilation (Yousefi et al., 2017). Natural ventilation has also been regarded as an effective measure for improving thermal comfort and reducing energy consumption (Wang et al., 2013). Furthermore, various openings are combined to distribute fresh air throughout the room. For instance, higher occupancy performance can be positioned near a facade with wind catchers, while areas requiring less ventilation, such as storage rooms or utility areas, can be located close to the back facade sheltered from the wind.

A study by Zhao et al. (2019) indicates that altering the shape of internal corridor partitions can achieve a higher average airflow velocity, increasing by up to 33%, and airflow can form more rapidly within the building. Additionally, modifying the location and dimensions of buffer spaces, such as courtyards (Luo et al., 2018), solar chimneys (Asadi & Fakhari, 2016), atriums (Moosavi & Mahyuddin, 2014), and skylights (Lomas, 2007), can significantly alter natural ventilation in buildings. For example, results show that optimally designing courtyards can save approximately 19% of the cooling load in summer and about 22% of the heating load in winter (Luo et al., 2018).

2-4-4- Other Consumption Mechanisms

Other service systems in modern buildings include hot water supply, lighting, and electrical appliances. Advanced technologies have primarily been employed to provide thermal energy or electricity for buildings to achieve sustainable development. Hot water systems and lighting are the second main energy consumers in buildings. Hot water accounts for 10 to 40% of total energy consumption in residential and commercial sectors (Bohdanowicz & Martinac, 2007). This necessitates their consideration in energy consumption calculations.

2-5. Energy Performance Simulation of Buildings

In Section Two, the computational design performance is assessed according to the performance objectives. Given the objectives of this research, the evaluation is based on energy performance simulation. Building energy simulation (BES) can generally be defined as a physics-based mathematical model that allows for the precise calculation of a building's energy performance and the thermal comfort of its occupants, influenced by various inputs such as weather, building geometry, internal loads, HVAC systems, operational schedules, and specific simulation parameters. Initially intended for use during the design phase, building energy simulation is increasingly employed throughout the building's lifecycle (Hensen & Lamberts, 2019).

Over the past four decades, building energy simulation programs have been designed and developed. In 1971, during a period when energy simulation programs were first created, the United States Postal Service funded the development of a computer simulation program to analyze the energy consumption of postal facilities across the United States (USPS, 1971), often referred to as the Postal Service Program. This building energy simulation program was initially designed for building simulation, calculating hourly cooling and heating loads, HVAC system performance, and energy consumption of facilities while being capable of performing hourly economic analysis (USPS, 1971; Haberl & Cho, 2004). Lokmanhekim (1971) described the program's main structure, which includes four main subprograms executed sequentially: (1) load calculation, (2) thermal load design, (3) systems simulation, and (4) economic analysis.

Building energy simulation (BES), as utilized in building design, can generally be categorized as a law-driven mechanism for predicting behavior, employing a well-defined

set of rules to forecast the behavior of a complex system (Coakley et al., 2014). Based on the simulation results, correlations and other statistical tests can be performed on the data, which will be discussed later depending on the quantity and quality of results.

To understand building energy simulation, it is essential to comprehend scientific models in general. According to Saltelli et al. (2008), models can be either diagnostic or prognostic. Diagnostic models are used to identify the nature or cause of certain phenomena, aiming to gain a better understanding of the laws governing a specific system. Conversely, prognostic models are employed to predict the behavior of a system based on a defined set of governing laws (Figure 2-1). Furthermore, according to Saltelli et al. (2008), models can be law-driven or data-driven. Law-driven models apply a set of governing laws (such as gravity, heat/mass transfer, etc.) to predict the system's behavior based on the system's characteristics and conditions (Figure 2-1).

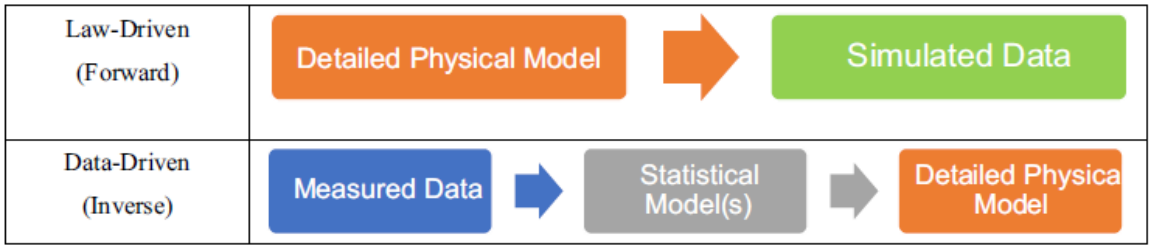

Figure 2-1: Law-Driven vs. Data-Driven Models (Saltelli et al., 2008)

Data-driven models (or inverse models) operate in a reverse approach and utilize the behaviour of the system as a predictor of its characteristics (Figure 2-1). Therefore, data-driven models can be employed to describe a system with minimal adjustable inputs (Young et al., 1996). In contrast, law-driven models are often over-parameterized; they require additional inputs to support the existing data.

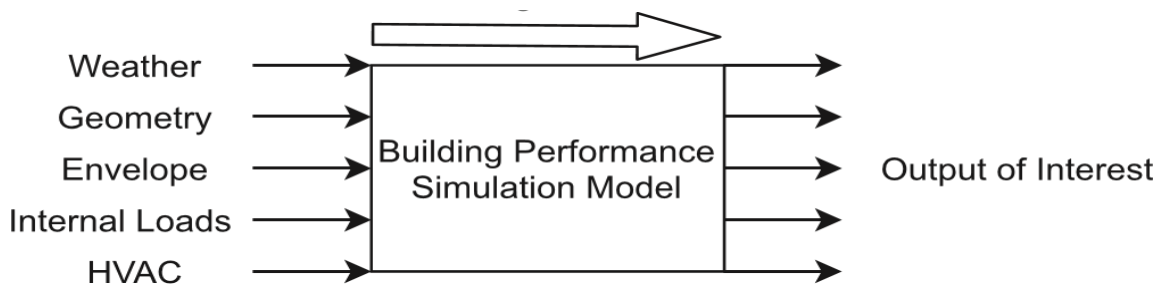

Figure 2-2: Input and Output Data in Energy Performance Simulation (Chen et al., 2020)

However, the advantage of law-driven models is that they can provide modelling of system behaviour based on a set of predetermined uncontrolled conditions, whereas data-driven models require prior data to model behaviour. A simple comparison of law-driven and data-driven models is presented in the figure. As shown in the image, five data groups, including climate, geometry, envelope specifications, internal loads, and HVAC data, are input into the energy performance simulation engine (Figure 2-2).

2-5.1 Calibration in Building Energy Simulation

However, there are increasing concerns regarding model validity in the construction industry, as significant discrepancies between simulated and measured energy consumption become more apparent with the rapid deployment of smart energy meters. For instance, Turner et al. (2008) analysed 121 buildings under the LEED standard and found that measured energy consumption could be between 0.5 and 2.75 times the predicted energy consumption. Mantesi et al. (2018) demonstrated that default settings and methods for modelling thermal mass could lead to a divergence of up to 26 percent in simulation predictions.

Previous studies (Menezes et al., 2012; De Wit & Augenbroe, 2002) have observed that the main reasons for discrepancies between predicted and actual energy performance arise from: (a) uncertainty in specifications due to assumptions stemming from a lack of information; (b) model inadequacies resulting from the simplification and abstraction of real physical building systems; (c) operational uncertainty due to a lack of feedback on the actual use and operation of buildings; and (d) scenario uncertainty arising from the specification of model conditions such as climate conditions and building occupancy (Chong et al., 2021). Consequently, model calibration is often performed to better align simulation predictions with actual observations and to enhance the model's validity for forecasting. While calibration is not essential for building energy simulation research, it is increasingly important for establishing model credibility. Annex 53 of the International Energy Agency on Energy in Buildings and Communities (IEA-EBC) also reports the significance of developing and applying model calibration and uncertainty analysis for energy simulation (Yoshino et al., 2017).

The common rationale for calibrating building energy simulation is to make predictions with greater confidence. Although forecasts may be incorrect, they can still be valuable. Trucano

et al. (2006) list examples of such forecasts that are relevant to building energy simulation, including simulating an experiment without prior knowledge of its outcomes or before its execution. For instance, resilience analysis compares the cost-effectiveness of various energy conservation measures (ECMs) (Chong et al., 2021).

Calibration, validation, and verification are often used in the existing literature to demonstrate consistency between model predictions and actual observations, which can be misleading since they are not synonymous. The semantics of the terms calibration, validation, and verification have sparked philosophical discussions due to the contradictory perspective that models are representations of reality and are therefore, by definition, not accurate (Oreskes et al., 1994). Consequently, there are arguments that simulation models can never be validated but can only improve through discrediting (Konikow & Bredehoeft, 1992). Nevertheless, Building Energy Simulation (BES) models are typically developed for practical purposes such as architectural design, HVAC design and operation, resilience analysis, building operational optimization, urban energy efficiency analysis, and more. Thus, from the perspective of computational simulation and engineering, the notion of validation is not to prove the truth of a scientific theory; rather, it is to assess and quantify whether the model is acceptable for its intended purpose.

2-5-1-1 Optimization-Based Calibration

Genetic Algorithm (GA) (Bandera & Ruiz, 2017; Zuhaib et al., 2019), Particle Swarm Optimization (PSO) (Andrade-Cabrera et al., 2017; Ferrara et al., 2018), and Hooke-Jeeves (HJ) algorithm (Li et al., 2018; Carlon et al., 2016) are the most widely used algorithms for optimization-based calibration. Both Genetic Algorithms and Particle Swarm Optimization belong to the class of evolutionary algorithms, which are population-based with a metaheuristic characteristic. Specifically, the Non-Dominated Sorting Genetic Algorithm II (NSGA-II) is extensively employed for optimization-based calibration of building energy simulation models (Martínez et al., 2020) due to its ability to achieve superior solutions and convergence compared to other evolutionary algorithms (Deb et al., 2002). Particle Swarm Optimization, introduced by Kennedy and Eberhart (Kennedy, R. Eberhart, 1995), optimizes through swarm intelligence, drawing inspiration from the social behavior of creatures in groups, such as flocks of birds or schools of fish. Finally, the Hooke-Jeeves algorithm (Hooke & Jeeves, 1961) belongs to the family of Generalized Pattern Search (GPS) algorithms and has gained popularity in building energy simulation because the number of

function evaluations increases linearly with the number of design parameters (Wetter et al., 2001). A common characteristic of Genetic Algorithms, Particle Swarm Optimization, and Hooke-Jeeves is that all are gradient-free. Therefore, they are suitable for optimization frameworks that minimize a cost function requiring evaluation by an external building energy simulation program. Furthermore, population-based metaheuristic algorithms like Genetic Algorithms and Particle Swarm Optimization initiate optimization with a population of randomly distributed points to reduce the risk of converging to local minima. However, identifying falling positions away from the Pareto-optimal frontier can be challenging, making it difficult to define a stopping criterion. Although energy guidelines (ASHRAE, Guideline 14; EVO; US DOE) are often used to determine threshold criteria for accuracy, it has been demonstrated that these stopping criteria are not suitable for optimization-based calibration (Martínez et al., 2020).

2-6. Using Evolutionary Computation to Search for Solutions

In the third section on performative computational architecture, an optimization algorithm must be employed for optimization purposes. Generally, optimization algorithms are computational search methods that are often inspired by nature. In this section, optimization algorithms are utilized to optimize the generated designs in performative computational architecture. Optimization algorithms are applied to problems with complex calculations. Over the past few decades, nature has inspired the creation of a relatively large number of powerful optimization algorithms. A common feature of all these algorithms is their derivation from biological and molecular systems to solve complex optimization problems (Marzbani, 2014). Among the capabilities of these algorithms are:

1. The ability to effectively search very large spaces
2. The ability to escape local optima
3. Significant searches within limited timeframes
4. Very low computational cost
5. No requirement for the derivative of the objective function
6. Simple mathematics despite the complexity of the problem

A common characteristic of all these algorithms is their inspiration from biological and molecular systems to address complex optimization issues (Ekici et al., 2019). These algorithms possess capabilities such as effective searching in very large spaces, the ability

to escape local optima, significant searches within limited timeframes, very low computational costs, and straightforward mathematics despite the complexity of the problem (Michalewicz & Fogel, 2013). In this research, evolutionary computation will be employed for optimization.

Evolutionary computation has become one of the focal approaches for designers in the realm of artificial intelligence in architectural design. In the 1950s, Arthur Samuel posed the question of how computers could solve problems without explicit programming, leading to the birth of evolutionary computation. Evolutionary computation is rooted in Darwinian evolution and is based on the iterative modeling of natural structures, simulating evolution to generate systems that adapt to their environment similarly to natural selection (Pena et al., 2021). It encompasses four types of algorithms generally referred to as evolutionary algorithms: Genetic Algorithms (GAs) (Holland, 1992), Evolution Strategies (Rechenberg, 1965), Evolutionary Programming (Fogel et al., 1966), and Genetic Programming (Koza, 1992). In the context of design, evolutionary search has been widely used for optimizing existing designs (Holland, 1992). This understanding stems from the recognition that evolutionary-based algorithms are among the most flexible, efficient, and powerful search algorithms known (Goldberg, 1989; Beasley et al., 1993).

Regarding conceptual design, Goldberg (Goldberg, 1991) proposed an ideal framework that includes four components: the problem to be solved, the individual solving it, one or more designs, and a means to compare them (genetic algorithm), along with the limitations of a human designer's performance using recombination and selection processes. The use of computational tools in producing architectural designs necessitates the application of parametric relationships, self-organizing processes, and algorithms to create designs with limited human interaction (Pazos, 2017).

Sutherland (Sutherland, 1964) suggested creating a set of rules using parametric relationships and algorithms that evolve the original design through the manual manipulation of its parameters by the user, leading to results that the designer may not necessarily expect. Dunn (Dunn, 2012) added that parametric design allows for the definition of relationships between elements or groups of elements and the assignment of values or expressions to organize and control those definitions. Furthermore, Davis (Davis, 2013) demonstrated that the geometry of a design also changes with parameter adjustments. In other words, a parametric design establishes connections and relationships among all

design elements, such that when one is modified, the others adjust accordingly, typically through the automatic alteration of parameters or associated values, much like a system of equations. A drawback of this design approach is the extensive time spent developing parametric codes. This cost has led to the latest approaches utilizing generative algorithms that leverage computer analytical potential to address inherent human limitations (Marcos, 2010).

In 2013, Moreno and Carrillo (Moreno-De-Luca & Carrillo, 2013) established a set of commonly used multi-objective optimization techniques that are applied not only as optimization models in structural and architectural design but also as an essential component of the design methodology for creating high-performance, efficient, creative, and aesthetically pleasing architectural items. The authors proposed a combination of structural design, bioclimatic considerations, green building principles, acoustics, and lighting into an integrated and morphogenetic optimization approach. They argue that such a methodology results in comprehensive design solutions with optimal performance and significantly reduced costs.

Dutta and Sarthak (Dutta & Sarthak, 2011) reviewed the literature related to the application of evolutionary computation approaches for architectural spatial planning, highlighting the utility of these methods in undefined problems with varying constraint scopes. They noted that evolutionary computational approaches excel at finding solutions that prioritize specific criteria. In many cases, rather than seeking a correct and complete solution, the best compromise is pursued. Dutta and Sarthak (2011) concluded that there is a demand for tools that can assist in spatial layout planning and optimization, although most of these approaches are still in research phases and have not yet been integrated into commercial products.

In general, traditional genetic algorithms identify appropriate fitness criteria and then automatically search for optimal solutions, while interactive approaches utilize user input as subjective evaluation criteria. The development of user-friendly design environments, visual interfaces, providing parametric variables, skill visualization, and performance feedback has strongly supported the growth of this approach (Lin & Gerber, 2014). Ultimately, Interactive Evolutionary Computation (IEC) is an optimization method based on human subjective evaluation that incorporates evolutionary computation (EC) in system optimization. This technique replaces the adjustment function with a human user (Tagaki, 2014).

2-6-1- Evolutionary Algorithms

Evolutionary Algorithms (EAs) are stochastic optimization methods based on Darwinian evolutionary theory. These algorithms operate with a set of alternative solutions that evolve according to the principles of natural selection, meaning these solutions compete with one another based on processes modeled after evolutionary theory, resulting in the emergence of the most suitable responses (Trompoukis et al., 2012). The Genetic Algorithm (GA) is one of the most widely used evolutionary algorithms, utilized in this research. Developed by Holland in the 1970s, the GA is inspired by Darwin's Theory of Natural Selection and Mendel's Theory of Genetics. The Genetic Algorithm is a fully parallel, stochastic, adaptive optimization algorithm based on the concepts of natural selection and survival of the fittest (Holland, 1975). Genetic algorithms begin with a randomly generated population of solutions to the problem and evolve new solutions using operators for objective evaluation, selection, crossover, and mutation, transitioning from one solution to another.

Generally, in genetic algorithms, solutions are represented not by their original variables but by a code. Typically, a solution is represented by a string of bits, known as a chromosome. The complexity of Multi-Objective Evolutionary Algorithms (MOEAs) arises from the competitive relationship among each objective function; that is, when one objective function achieves better results, the optimization results for the others may not be valid. Consequently, the optimal solution is often not a single solution but a set of optimal solutions that do not dominate one another; that is, they are not mutually exclusive. This phenomenon is particularly prevalent in architectural problems with conflicting objectives, such as thermal comfort versus energy consumption. The Multi-Objective Evolutionary Algorithm (MOEA) employs the Pareto principle to achieve a set of optimal solutions.

In recent years, many Multi-Objective Evolutionary Algorithms (MOEAs) have been proposed, such as the Non-dominated Sorting Genetic Algorithm II (NSGA-II) (Sadeghi et al., 2014; Ding et al., 2018). The Strength Pareto Evolutionary Algorithm 2 (SPEA-2) (Salgueiro et al., 2016; Zhao et al., 2016; Gong et al., 2014; Liefooghe et al., 2011) and the Pareto Archived Evolution Strategy (PARES) (Yi et al., 2016; Knowles et al., 2014; Aguirre et al., 2010) have shown promising results in solving multi-objective optimization problems. One type of Multi-Objective Evolutionary Algorithm (MOEA) is the Strength Pareto Evolutionary Algorithm 2 (SPEA2) (Xi & Don, 2019), designed and presented by Zitzler et al. (Zitzler et al., 2001). This algorithm provides a multi-objective framework for genetic

algorithms. Improvements in this algorithm, through the selection of criteria and population enhancement, have led to its high efficiency in architectural research. Therefore, due to its advantageous accessibility, it is utilized as the search engine in this study.

The Strength Pareto Evolutionary Algorithm 2 (SPEA-2) demonstrates good convergence and diversity performance, outperforming the original Strength Pareto Evolutionary Algorithm (SPEA) and compares favorably with the Pareto Envelope-Based Selection Algorithm (PESA) and the Non-dominated Sorting Genetic Algorithm II (NSGA-II) across various problems (Zitzler et al., 2001). In all test cases conducted, SPEA-2 has shown significant improvements over its predecessor, SPEA, as it achieves better results across all considered problems.

Both the Strength Pareto Evolutionary Algorithm 2 (SPEA-2) and the Non-dominated Sorting Genetic Algorithm II (NSGA-II) exhibit very similar behaviors across different problems. In some cases, NSGA-II achieves a broader scope and thus demonstrates superior performance, while SPEA-2 provides a better distribution of solutions, particularly as the number of objectives increases. The Pareto Envelope-Based Selection Algorithm (PESA) also tends to test external solutions for specific functions. For many problems, PESA appears to converge more rapidly initially, likely due to its high degree of implicit elitism.

Both the Non-dominated Sorting Genetic Algorithm II (NSGA-II) and the Strength Pareto Evolutionary Algorithm 2 (SPEA-2), which also allows dominant individuals to maintain a minimum archive size, seem to leverage this increased diversity during the subsequent stages of the program's execution, where they have broader distributions and thus better performance metrics (Zitzler et al., 2001). In general, a common criticism of all Multi-Objective Evolutionary Algorithms (MOEAs) is their slow convergence speed (Liu & Zhang, 2019). This algorithm begins with a random population of solutions and, during a specified cycle, archives non-dominated solutions based on the combination and mutation of solutions.

2-7- Computational Performance Design Mechanism

The design process requires an increasing awareness to achieve desired outcomes (Ekici, 2019) and is a multi-faceted problem (Magnier & Haghighat, 2010) that unfolds in an iterative format (Cobb et al., 2003). This has led to a heightened focus on the use of

computer-based computational systems in design (Du et al., 2020), as these systems allow for the design to be amendable and revisable from the beginning of the process in a repeatable manner (Sonta et al., 2021). With technological advancements and the availability of hardware and software, the use of computers in architectural design, both in research centers and in the industry, has increased, and this trend continues. The utilization of computers in design mechanisms such as parametric design (Gerber, 2007) and algorithmic design (Terzidis, 2006) is increasingly developing within the architectural and interdisciplinary design processes.

Gero (1985) identifies three influential events concerning the use of computers in architectural design: space configuration planning, exemplified by the spatial planning of the Sader and Clark hospital in the years 1963 and 1964 (Souder JJ, Clark, 1963, 1964); computer graphics in the representation and manipulation of virtual models for buildings, such as in the publication of Sutherland's Sketchpad system in 1963 (Sutherland, 1963); and notes on the synthesis of form by Alexander (1964). With technological advancements and the availability of hardware and software, the use of computers in architectural design has grown both in research centers and in industry, and this trend continues. Currently, the use of computers in parametric design (Gerber, 2007) and generative and algorithmic design (Terzidis, 2006) is increasingly being developed within the architectural and interdisciplinary design processes.

Various programs for optimization in architectural design exist, which can be accompanied by building performance assessment tools, seeking near-optimal design options to achieve efficient building designs. Accordingly, there have been various approaches to utilizing computers in design computations, and some of the most notable ones will be discussed in this context. One of the approaches to utilizing computers in design is Generative Design (GD), which was introduced by Mitchell in the late 1970s (Mitchell, 1975). The Cambridge Dictionary defines "Generative" as “the capacity to produce or create something.” Some authors describe Generative Design (GD) as a design process that employs evolutionary techniques to generate solutions (Fischer and Herr, 2001; Frazer et al., 2002; Zhang and Xu, 2018). However, others do not limit Generative Design (GD) to evolutionary processes; rather, they consider it a design approach based on algorithmic or rule-based processes that produce multiple, diverse, and potentially complex solutions (Bernal et al., 2015; Humppi and Osterlund, 2016).

This research presents Generative Design (GD) systems as tools capable of producing potential solutions for specific problems. Over the next two decades, the literature rarely addressed Generative Design (GD). At the beginning of the 21st century, Fischer and Herr (2001) defined Generative Design (GD) as a design approach in which the designer does not directly interact with materials and products during the design process; instead, the interaction occurs through a generative system. According to Herr (2002), a generative system refers to computer-aided production systems employed by architects to find solutions to unique architectural design problems.

In this context, Lazzeroni et al. (2009) define Generative Design as a cyclical process based on a simple abstract idea applied through a rule or algorithm (Figure 2-3). This algorithm is then translated into source codes that generate a series of outputs through the computer. The output allows the designer to enhance the algorithm and source codes through a feedback loop. This is a repeatable activity based on the exchange of feedback between the designer and the design system.

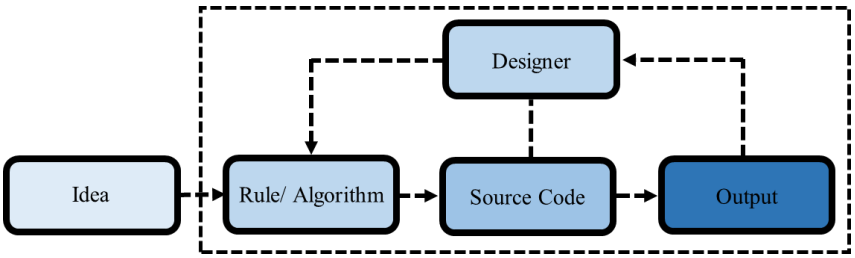

Figure 2-3. Parametric-Algorithmic Process Based on the Perspective of Lazzeroni et al. (2009)

According to Agkathidis (2016), the process of form generation in generative design is based on three fundamental phases: analysis, genetics, and metamorphosis, aimed at producing architectural proposals (Figure 2-4).

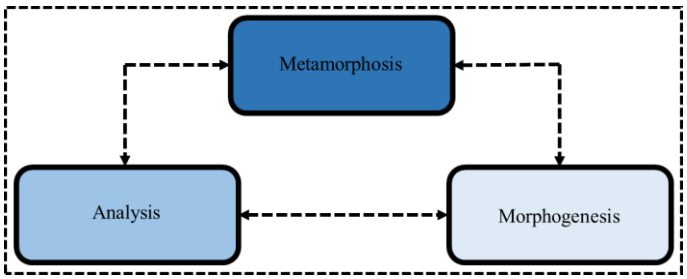

Figure 2-4. The GD Based on the Perspective of Agkathidis (2016)

This is a nonlinear design process in the form of a continuous cycle that allows all design phases to reinforce each other, ultimately leading to the most comprehensive possible design solutions. The three main phases of generative design according to Agkathidis (2016) are as follows:

- **Analysis:** This phase focuses on gathering information regarding various aspects such as context, planning, materials, performance, and structure.
- **Configuration Genealogy:** This phase involves producing abstract prototypes based on spatial principles and organization, including unit aggregation, surface continuity, volume, façade, and algorithmic textures.
- **Morphogenesis:** This phase transforms an initial abstract design into the final architecture through two approaches: directly arriving at the final solution and generating a set of solutions with different organizations.

Bohnacker et al. (2009) interpret Lazzeroni et al.'s (2009) view on the parametric-algorithmic process as follows: this process utilizes computational energy as a source of creative search energy, empowering human designers to explore a significantly larger number of possible designs under adjustable constraints (Sivam Kirish, 2013). This study also employs the term "generative design" to introduce the process (Figure 2-5).

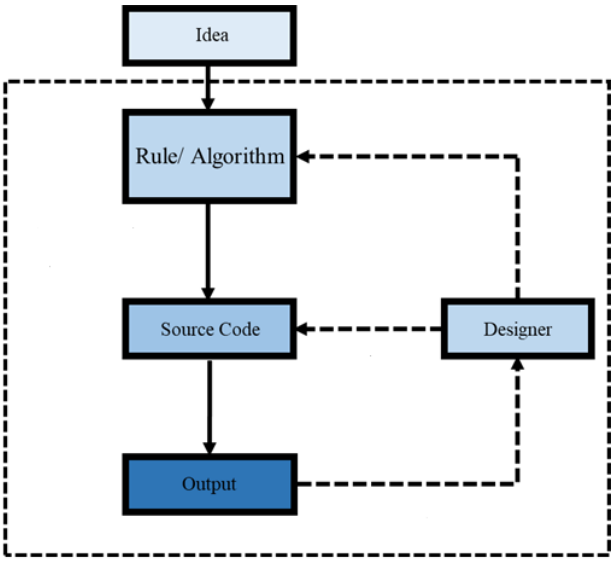

Figure 2-5. The GD Based on the Perspective of Bohnacker et al. (2009)

Additionally, according to Estkowski (2013), the generative design process is based on two mechanisms: adaptation and iteration. A generative design system must encompass both.

The adaptation phase is a goal-oriented mechanism in which the building model (solution) is modified to achieve design objectives (environment). The adaptation process can be automated within the generative design system (Figure 2-6). Design objectives are defined by a user, and the adaptation-based algorithm must create a building model. In fact, depending on the constraints set by the designer for the algorithm, the system automatically provides compatible responses. On the other hand, the iterative process is a method for reaching a solution or optimizing less than a knowledge-acquisition process regarding the design state. The generative design process is cyclically repeated until optimal responses are achieved. This cycle can be observed in the illustration.

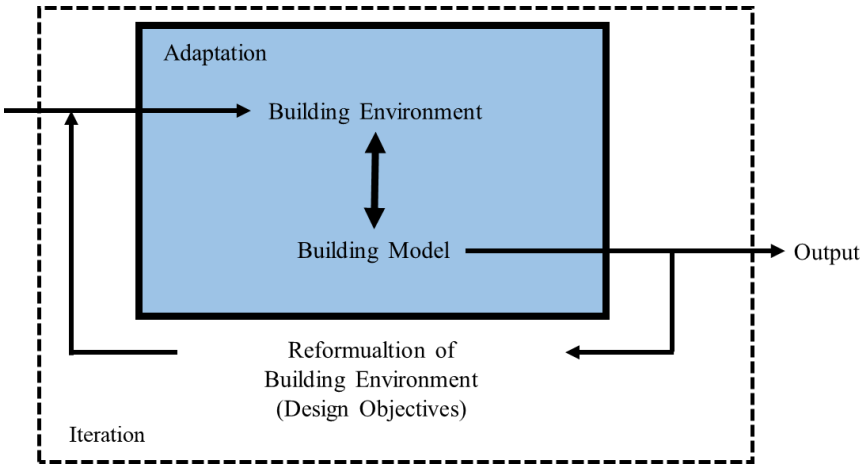

Figure 2-6. The GD based on the Perspective of Estkowski (2013)

In a design process, a mental building model undergoes a series of transformations to achieve design objectives. Each design problem begins with the effort to achieve a balance between two entities, including the desired form and its context (Alexander, 1970). Similarly, in a generative design system, evaluating a building model determines the suitability of a specific model to the building environment. Specifically, this can be done by comparing each feature of the building model with the corresponding feature in the building's environment.

Frazer et al. (2002) describe generative design (GD) as the use of computer virtual space in a manner similar to evolutionary processes in nature. Likewise, Krause (2003) defines generative design (GD) as systems that can independently develop, transform, or design architectural structures, objects, or spaces. According to Caldas (2008), these systems are evolution-based and search the design space for solutions that meet functional requirements.

McCormack et al. (2004) define generative design (GD) as exploring the generation of forms and complex patterns from a simple specification. Research by Malkawi (2005), Chase (2005), Shea et al. (2005), Fasoulaki (2008), Oxman (2006; 2008), Puusepp (2011), Larsen (2012), Karzel & Matcha (2009), Granadeiro et al. (2013), Garber (2014), and Roggema & Nikolay (2015) offers similar definitions.

Zee & Vrie (2008) go further, stating that generative design (GD) can find solutions to complex problems that are difficult to solve using traditional problem-solving methods. According to Bernal et al. (2015), generative design (GD) provides potentially creative outcomes because each new combination of parameters presents an opportunity to explore the emergence of new properties or affordances from the resulting combination. According to Chaszar and Joyce (2016), generative design (GD) addresses problems requiring speed, accuracy, complexity, and enhanced creativity by utilizing computational power, as it increases the number and range of design variations that include desirable random solutions—unexpected outcomes that positively influence the design process. Abrishami et al. (2014) describe generative design (GD) as the use of a computer-based computational system to produce design problem solutions at a nearly independent level. Bukhari (2011) restricts the domain of generative design (GD) to the use of algorithms to produce a multitude of different solutions from a given set of design goals and constraints, proposing this concept as a type of algorithmic design (AD). Similarly, Humppi & Osterlund (2016) define generative design (GD) as design using algorithmic logic and generative processes.

Generative design (GD) is employed under various structures. One of its intelligent structures, which is currently of great interest to designers, is the performance-based design (PBD) approach (Ekici et al., 2019). This approach has become an essential method for achieving objectives. It predicts the performance of a design based on design variables. The performance-based design approach evaluates design alternatives with better performance by altering design variables and observing the results (Wei et al., 2014). Kolarevic (2003) emphasizes the importance of performance-based design (PBD) as a guiding design principle. Among the various possible methods, this research focuses on a specific performance-based design (PBD) framework presented by Sariyildiz (2012) at the Delft University of Technology's Faculty of Architecture to enhance the design process. The proposed framework is termed "Performance-based Computational Architecture" (PCA) (Figure 2-7). The framework of Performance-based Computational Architecture (PCA)

consists of three main stages: form generation, performance evaluation, and optimization, as illustrated in Figure 2-7.

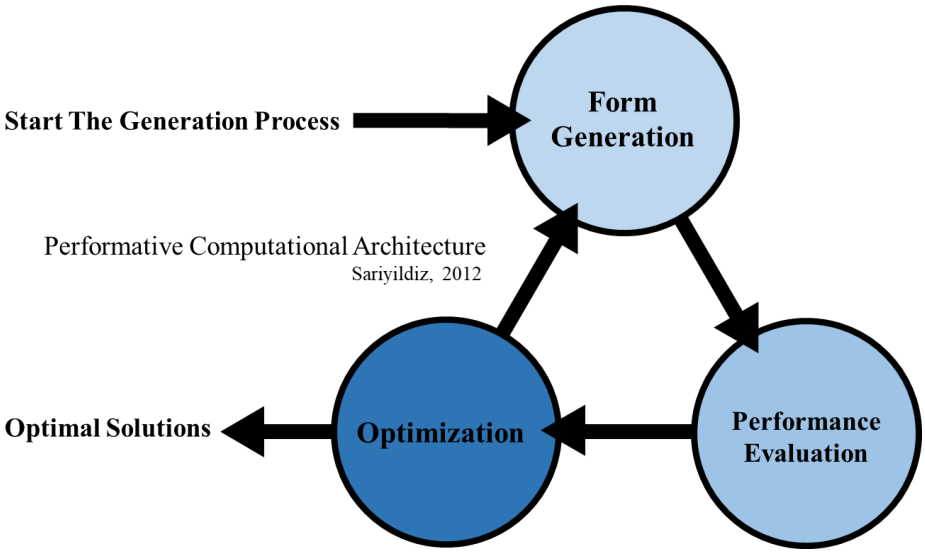

Figure 2-7. Performance-based PCA Framework (Sariyildiz, 2012)

Therefore, the main issue of this research should be introduced in these three sections, which will be discussed further. The primary goal of Performance-based Computational Architecture (PCA) is to identify the optimal geometry that achieves performance-related objectives during the conceptual design phase. The PCA framework consists of three main stages: form generation, performance evaluation, and optimization (Ekici et al., 2019). Similar to Sariyildiz's model (Sariyildiz, 2012), Autodesk's 2017 report (Villaggi & Nagy, 2017) on Generative Design (GD) integrates Performance-based Computational Architecture through the use of innovative search algorithms with the design process to discover new and highly efficient results within the design system. This structure is composed of three main components:

1. The generative model's geometry, which defines the design space of possible responses.
2. A set of actions and criteria that describe the objectives of the design problem.
3. An innovative search algorithm, such as a genetic algorithm, which can explore diverse, efficient design options within the design space based on the stated objectives (Villaggi & Nagy, 2017).

As seen, Autodesk's Generative Design (GD) is very similar to the Performance-based Computational Architecture (PCA) framework introduced by Sariyildiz (Sariyildiz, 2012). In fact, according to this report, Generative Design (GD) belongs to a larger ecosystem that is complemented by pre-GD and post-GD phases.

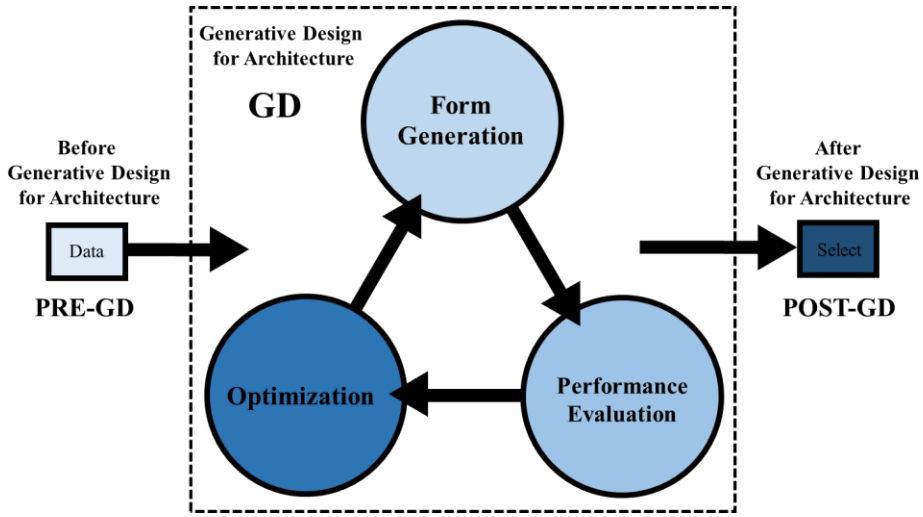

Figure 2-8. The GD Based on the Autodesk Report (Villaggi & Nagy, 2017)

In this process, the three components of generation, evaluation, and evolution are identified as the main parts of generative design, distinguished by three colors. In this report (Villaggi & Nagy, 2017), the three phases of the ecosystem are described as follows:

- **Pre-Generative Design Phase**: This phase is related to stakeholders and involves collecting unique and significant data about the project, which includes the following sections:

    1. Information Gathering: Requirements and Constraints
    2. Goal Formulation

- **Generative Design Phase**: This phase consists of three main components:

    1. Generation: A generative model that can describe a broad design space of possible solutions.
    2. Evaluation: An evaluation component that includes the specific design objectives.
    3. Intervention: A metaheuristic search algorithm that can navigate the design space and generate better and better design solutions.

- **Post-Generative Design Phase**: This phase highlights the critical role of the human component. In this section, the designer can utilize spatial design tools to explore design options and assess the quality of each.

    1. Selection: Direct inspection by the designer of options, along with key stakeholders, to select the best designs.
    2. Refinement: Making necessary modifications to the design and improving it (Villaggi & Nagy, 2017).

Additionally, Kiss and Szalay (Kiss & Szalay, 2020) present a similar structure under the title of Life Cycle Assessment (LCA) framework in five sections. The main objective of Kiss and Szalay's research (Kiss & Szalay, 2020) is to create a framework for the automatic optimization of the life cycle in a design (Figure 2-9). Precise calculations must be made at each stage of the life cycle. In this research, the three sections of generation, evaluation, and optimization can also be clearly observed. In this cycle, the generation and optimization components remain constant; however, the evaluation component is introduced in the form of two sections: computation and result evaluation. Furthermore, a section titled "Source Data" is introduced as a pre-generation phase, which focuses on collecting prerequisite data.

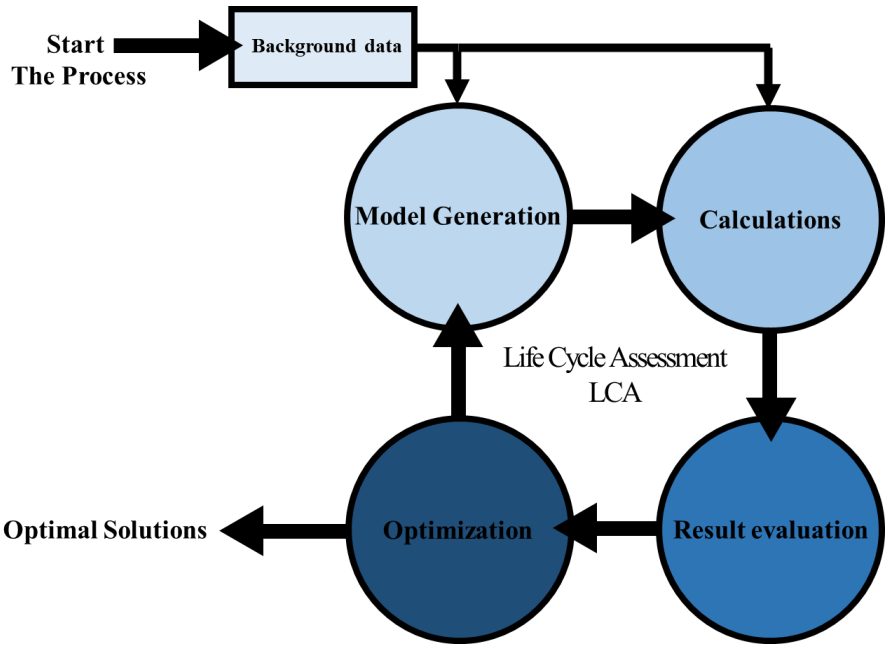

Figure 2-9. The LCA Framework (Kiss & Szalay, 2020)

In the structure of Performance-based Computational Architecture (PCA), the form generation section involves a repeatable process based on design parameters and constraints, referred to as Parametric Design (PD). In the second section, namely performance evaluation, the process involves Building Energy Simulation (BES), focusing on the thermal performance of the building. In this section, the forms generated in the context of thermal performance are evaluated, and ultimately, in the last section, optimization is performed based on evolutionary algorithms.

2- 8. Overview of the Literature on Performance-based Computational Architecture

The research methodology of this study follows a quantitative-qualitative and holistic approach based on the literature in the field of energy architecture. Given the research objective, which is a comprehensive analysis of approaches, methods, and physical factors in energy consumption prediction models, the methodology involves content analysis of documents, focusing on research studies of building energy consumption prediction models with an emphasis on three approaches: White Box, Black Box, and Gray Box, from around 2002 to 2023. Sampling was conducted purposefully using a snowball structure, where each identified article relevant to the topic led to further searches based on its references, continuing until theoretical saturation was reached; that is, sampling continued until no new data were added with the inclusion of additional samples.

In general, mechanisms for predicting building energy consumption are only feasible based on changes in the physical factors of the building. Therefore, in reviewing the literature, only studies that include architectural physical changes have been considered, avoiding an absolute engineering approach. Numerous articles were reviewed across a wide range of thematic areas by considering the framework of energy consumption prediction models. To identify related research, a set of keywords was used, including Building Design, Architecture Design, Energy Optimization, Energy Simulation, Energy Performance Simulation, Energy Consumption, and Energy Consumption Prediction. Databases such as Google Scholar, Science Direct, Scopus, and Thomson Reuters were utilized for this search. In the initial search, over 2,000 research articles were obtained from the mentioned databases. The preliminary screening of the articles was conducted based on topic, abstract, and keywords. This extensive search resulted in a collection of relevant articles that met the following criteria:

- The research must definitively employ one of the White Box, Black Box, or Gray Box approaches.
- The study must address at least one of the topics related to total energy consumption, lighting demands, cooling demands, heating demands, and daylighting.
- The article must clearly discuss architectural physical factors.
- The article must be published in a reputable journal.

Subsequently, secondary screening was conducted based on the findings and results of the research. Ultimately, the final studies under review were categorized and coded based on content analysis. A total of 119 studies were reviewed; as shown in the chart, all the reviewed studies are published in journals indexed in the Scopus database. Additionally, 99 out of the 119 studies are published in journals indexed in Thomson Reuters (Figure 2-10). The articles obtained cover the period from 2002 to 2023. The categorizations performed in the content analysis were shared with ten experts in energy and architecture to ensure validity and received their approval.

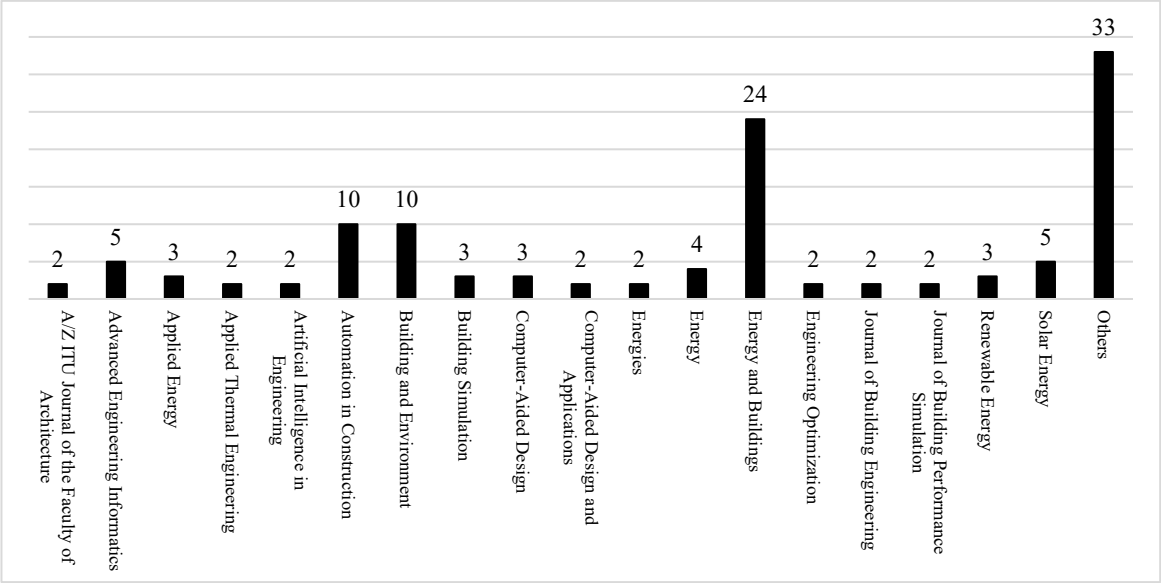

Figure 2-10. Frequency of Journals Reviewed in the Research Background

The year of publication, physical factors, energy objective functions, general research topics, energy consumption prediction approaches, and prediction methods were subjected to content analysis. Ultimately, the data obtained from the studies were coded and then subjected to descriptive statistics, correlation tests, and Shannon entropy analysis. To conduct the correlation tests, all data were coded and organized into a matrix format. The

year of publication was used as a variable alongside physical factors, energy factors under review, and research topics in the tests. To ensure the validity of the research process and the accuracy of the results, the data and findings were reviewed by ten statistics experts and received their approval.

Based on the findings, 119 studies were content analysed qualitatively. The findings were shared with ten energy and architecture specialists to verify their validity. Accordingly, the studies were categorized into three main topics: form, skin, and configuration. Among these, 31 studies focused on building configuration, 38 on building shape and form, and 70 on building skin. It is noteworthy that some studies targeted two topics simultaneously. The findings indicate that a significant portion of the research focused on building skin. Additionally, an examination of the scales and target usages across different studies was conducted (Figure 2-11). Regarding the scales of the studies, the highest frequency was related to mid-rise buildings, with 66 studies addressing mid-rise buildings, 24 studies examining single spaces (e.g., a room), and 10 studies focusing on high-rise buildings (see Chart 2). Furthermore, 11 studies were conducted at the urban scale. The analysis of target usages in the studies showed that the office and residential sectors, with 31 and 34 studies respectively, accounted for the highest number of research studies, which seems reasonable given the share of these two usages in construction.

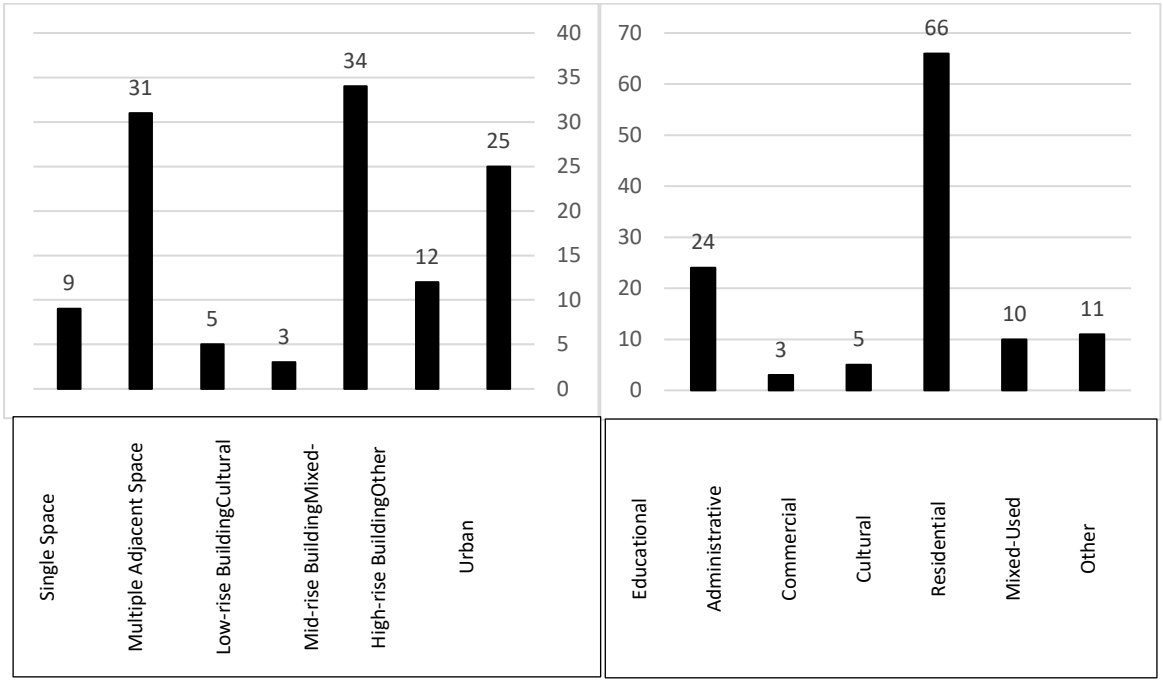

Figure 2-11. Frequency of Various Scales and Frequency of Different Usages Reviewed in the Studies Analyzed

However, after examining the general topics of energy consumption prediction, the selected studies were analyzed based on form-finding factors through content analysis. As observed, among the 119 studies reviewed, 17 physical factors were extracted, and their descriptive and analytical statistics are presented below (Figure 2-12).

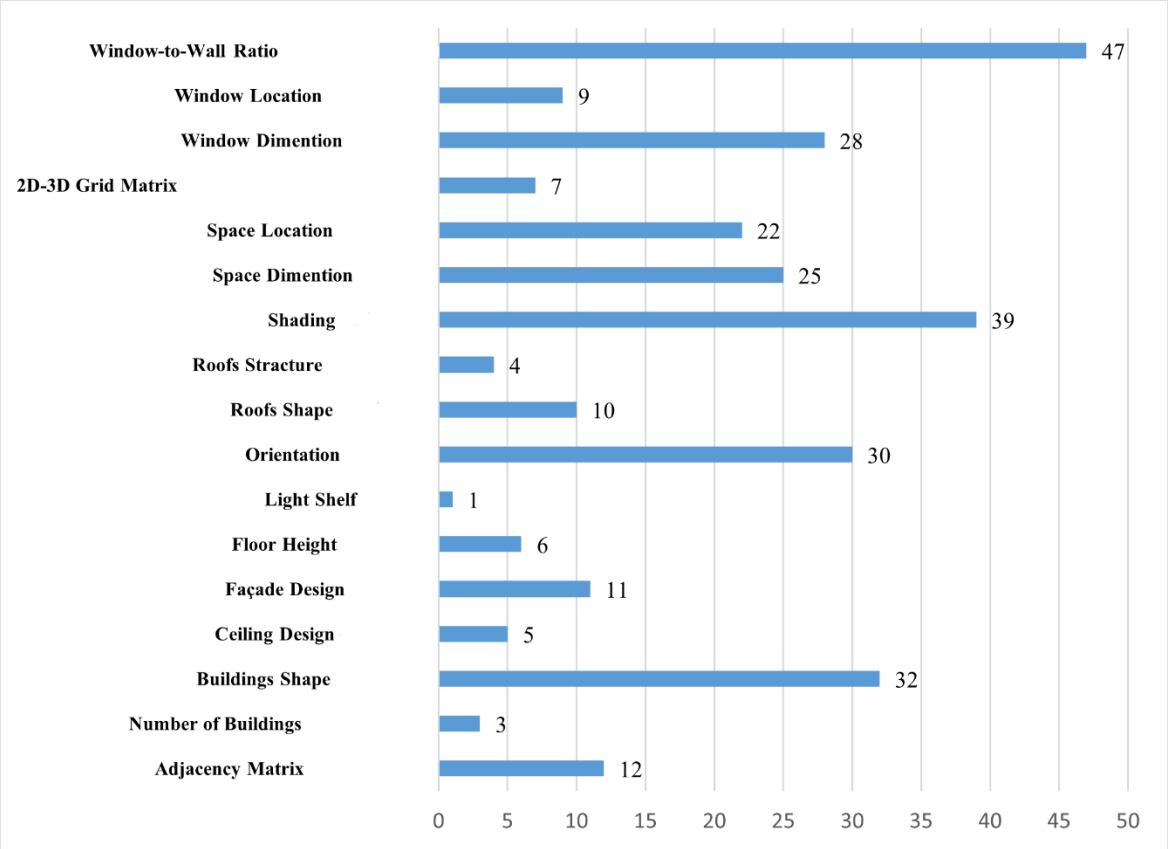

Figure 2-12. Frequency of Use of Each Physical Factor in the Conducted Studies

The extraction process was conducted qualitatively, and the findings were reviewed and validated by ten energy and architecture specialists to ensure their validity. According to the chart, the highest frequency corresponds to the window-to-wall ratio and shading. This is because these two factors have been selected as variables in various studies across all three topics: form, skin, and configuration. Conversely, the lowest frequency relates to daylighting and the number of buildings, which were mentioned 1 and 3 times, respectively.

To prioritize the physical factors and determine the degree of importance for each, Shannon entropy was applied to the data from the selected studies among the 119 reviewed (see Table 1). This test elucidates the three variables: weight, frequency of each form-finding factor. As seen in the table, among the 17 identified factors, daylighting and roof structure have the

highest normalized weights of 0.095 and 0.092, respectively, while shading and the WWR have the lowest normalized weights of 0.024 and 0.026, respectively (Table 2-1).

Table 2-1: Frequency Values, Correlation with Publication Year of Studies, and Weights of Factors in Shannon Entropy Test

	Window-to-Wall Ratio	Window Location	Window Dimention	Grid Matrix	Space Location	Space Dimention	Shading	Roofs Structure	Roofs Shape	Orientation	Light Shelf	Floor Height	Façade Design	Ceiling Design	Buildings Shape	Number of Buildings	Adjacency Matrix
Code in Diagram	**17**	**16**	**15**	**14**	**13**	**12**	**11**	**10**	**9**	**8**	**7**	**6**	**5**	**4**	**3**	**2**	**1**
Weight of Factors	**0.026**	**0.065**	**0.036**	**0.068**	**0.040**	**0.045**	**0.024**	**0.092**	**0.051**	**0.029**	**0.095**	**0.080**	**0.049**	**0.068**	**0.033**	**0.071**	**0.059**
Frequency of Factors	**0.165**	**0.017**	**0.098**	**0.026**	**0.066**	**0.058**	**0.160**	**0.017**	**0.040**	**0.116**	**0.004**	**0.008**	**0.049**	**0.017**	**0.111**	**0.013**	**0.026**

To conduct a more detailed examination of the results from the Shannon entropy test, the weight-frequency coordinates chart has been analyzed. Based on the results, the Shannon entropy chart has been plotted according to the two axes of weight and normalized frequency (Figure 2-13).

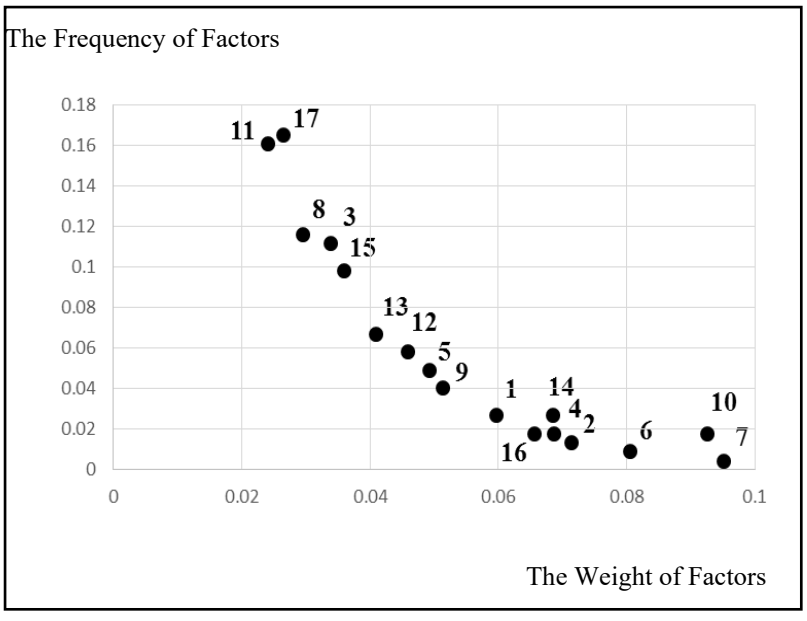

1	Adjacency Matrix
2	Number of Buildings
3	Building Shape
4	Ceiling Design
5	Facade Design
6	Floor Height
7	Light Shelf
8	Orientation
9	Roof Shape
10	Roof Structure
11	Shading
12	Space Dimensions
13	Space Location
14	Grid Matrix
15	Window Dimensions
16	Window Location
17	Window-to-Wall Ratio

Figure 2-13. Shannon Entropy Coordinates Based on Weight and Normalized Frequency Axes

Based on the chart, it can be observed that the roof structure, daylighting, and floor height have received less attention but are of greater importance for further investigation.

Conversely, the window-to-wall ratio, shading, and orientation appear to be of lesser importance yet have been more frequently addressed.

Furthermore, to conduct a more detailed examination of recent studies, a content analysis has been performed focusing on energy consumption (Table 2-2). Related studies have been categorized based on simulation design position, building type, functional objectives, architectural variables under consideration, number of simulation samples, and prediction methods, as shown in the table.

Table 2-2: Recent Studies in the Field of Building Energy Consumption

Reference	Location	Building type	Functional purpose	Architectural variables	Dimension of samples	Prediction method
Tran et al., 2020	Ho chi minh Vietnam	Residential	cooling load heating load	wall area Relative compression surface area Roof area Total height orientation glass area Glass distribution	768	ENMIM
Le et al., 2019	Vietnam	Prototype model	Heating load	wall area Height Roof area glass area Glass distribution Relative compression orientation	837	PSO-XGBoost XGBoost SVM RF GP CART
Al-Tarhuni et al., 2019	Midwest America	Residential	Energy consumption	wall area Wall heat transfer coefficient glass area Glass heat transfer coefficient	973	RF ANN
Al-Rakhami et al., 2019	Athens Greece	Residential	cooling load heating load	Height Relative compression wall area surface area Roof area Glass distribution glass area orientation	768	XGBoost
Chen & Yang, 2017	Hong Kong Los Angles	Residential	cooling load energy consumption lighting load	Wall heat transfer coefficient Glass heat transfer coefficient orientation Window-to-floor ratio	unspecified	MLR MARS SVM
Ciulla & Amico, 2019	Termoli Cortina *Sestriere*	Non-residential	cooling load heating load	Surface area to volume ratio	1560	MLR

			energy consumption			
Ciulla et al., 2019	Germany England Spain Belgium Italy France Sweden	Non-residential	Heating load	Surface area to volume ratio wall area Wall heat transfer coefficient Glass heat transfer coefficient Glass orientation	2184	ANN
Amico et al., 2019	Italy	Non-residential	Heating load	Surface area to volume ratio Wall heat transfer coefficient Heat transfer coefficient of glass wall area Glass orientation	1560	ANN
Dong et al., 2017	China	Office	energy consumption consumption cost	Aspect ratio Window-to-wall ratio Number of floors Wall insulation thickness orientation	500 groups	BP-ANN
Gao et al., 2019	unspecified	Residential	cooling load heating load	wall area Relative compression Area Roof area total height orientation glass area Glass distribution	768	EN GPR LMSR MLR MPR MLP RBFR SMOR XNV Lazy K-star Lazy LWL Function XNV RDT AMT DPC RF
Geyer & Singaravel, 2018	Unspecified	High-rise office complex	cooling load heating load	Wall heat transfer coefficient Glass heat transfer coefficient Roof heat transfer coefficient length width Window-to-wall ratio orientation	800	Static ML Dynamic ML (LSTM)
Re Cecconi et al., 2019	Lombardy Italy	School	Energy consumption	Wall heat transfer coefficient Glass heat transfer coefficient Roof heat transfer coefficient	1632	ANN with GIS K-means
Tien Bui et al., 2019	Unspecified	residential	cooling load heating load	wall area	768	ANN GA-ANN

				Relative compression Surface area Roof area total height orientation glass area Glass distribution		ICA-ANN
Kumar et al., 2018	California	Residential	cooling load heating load	wall area Relative compression surface area Roof area total height orientation glass area Glass distribution	768	ELM OSELM B-ELM
Le et al., 2019	Unspecified	Unspecified	Heating load	wall area Relative compression surface area Roof area total height orientation glass area Glass distribution	837	GA-ANN PSO-ANN ICA-ANN ABC-ANN
Li et al., 2019	Beijing Shanghai	Prototype model	cooling load heating load lighting load	length width Height Window-to-wall ratio Number of rooms Number of floors	243 173980	MCD MSHD
Moayedi et al., 2019	unspecified	Residential	Heating load	Relative compression surface area wall area Roof area total height orientation glass area Glass distribution	768	LLWL AMT RF ENet MLPr RBFr
Naji et al., 2016	Istanbul Türkiye	Residential	Energy consumption	Wall heat transfer coefficient wall thickness	180	ELM ANN GP
Navarro-Gonzalez & Villacampa, 2019	Alicante Spain	Residential	cooling load heating load	wall area Relative compression surface area Roof area total height orientation glass area Glass distribution	768	Octahedric regression IRLS RF
Ngo, 2019	Taiwan	office	Cooling load	Wall heat transfer coefficient Glass heat transfer coefficient Number of floors Aspect ratio Window-to-wall ratio floor area Height	243	ANNs SVR CART LR

Nilashi et al., 2017	Yerevan	Residential	cooling load heating load	wall area Relative compression surface area Roof area total height orientation glass area Glass distribution	768	SVR ANFIS ANN CART MLR EMARS PCA-ANFIS EM-PCA-ANFIS
Papadopoulos et al., 2018	Unspecified	Public building	cooling load heating load	wall area Relative compression surface area Roof area total height orientation glass area Glass distribution	unspecified	GBRT RF ET SVR+ANN GPA
Roy et al., 2020	Athens Greece	Residential	cooling load heating load	wall area Relative compression Surface wall area Roof area orientation total height glass area Glass distribution	768	DNN GBM GPR MPMR GP LR ANN RBF Net SVM
Sadeghi et al., 2020	Athens Greece	Residential	cooling load heating load	wall area Relative compression surface area Roof area orientation total height glass area Glass distribution	768	DNN with SA
Sangireddy et al.,2019	Jaipur Hyderabad	office	Energy consumption	Heat transfer coefficient of glass Orientation Window-to-wall ratio Aspect ratio	99000 100000 0	Linear Ridge Lasso Bayesian Ridge RANSAC Theil Sen Huber kNN SVR DT
Roy et al., 2018	Unspecified	Unspecified	cooling load heating load	wall area Relative compression surface area Roof area Total height orientation glass area Glass distribution	768	MARS ELM MARS-ELM GP LR ANN RBFN
Seyedzadeh et al., 2019	Athens Greece	residential Office	cooling load heating load	wall area Relative compression Surface wall area Roof area Total height orientation glass area Glass distribution	768	SVM RF NN GP GBRT XGBoost
Sharif, & Hammad, 2019	Montreal Canada	Unspecified	Energy consumption	Wall heat transfer coefficient	463	ANN

				Roof heat transfer coefficient Window-to-wall ratio		
Singaravel et al., 2018	Brussels Belgium	office	cooling load heating load	Wall heat transfer coefficient Glass heat transfer coefficient Roof heat transfer coefficient length width Window-to-wall ratio orientation	9600	ANN LSTM 2-layer Deep LSTM 3-layer Deep LSTM
Tian et al., 2017	Harbin China	office	electrical charge heating load	Aspect ratio Window-to-wall ratio floor number Floor area orientation	1200	ANN Ordinary linear model MARS Bag MARS SVM RF GP
Ascione et al., 2017	Naples Italy		cooling load heating load Hours of discomfort	Wall heat transfer coefficient Roof heat transfer coefficient Orientation floor area form ratio Height Window-to-wall ratio Window-to-floor area ratio wall thickness roof thickness	500 1000	ANN
Bui et al., 2019	Istanbul Türkiye	Residential	energy consumption cooling load	Insulation viscosity number Insulation thickness of wall type Relative compression surface area wall area Roof area Total height orientation glass area Glass distribution	180 768	ELM ANN GP EFA-ANN IRLS RF Ensemble model SAFCA-SVR
Zhou et al., 2020	Unspecified	Residential	cooling load heating load	Relative compression surface area wall area Roof area total height orientation glass area Glass distribution	768	MLP ABC-MLP PSO-ELM

Based on the findings in the table, it can be concluded that although numerous factors influence energy consumption in various types of buildings, the envelope and characteristics

of the building are of greater priority during the design phase. The building envelope plays the most significant role in heat transfer and, consequently, energy consumption; therefore, attention must be paid to this aspect for potential energy savings. Additionally, glass, as one of the important parameters of the building envelope, holds significant importance. Based on the results of the literature review, the impact of general building characteristics, including the overall dimensions of the infrastructure and the overall characteristics of the shell, on the energy performance and daylighting of the building is much greater than other building characteristics. Accordingly, this study considers the study on the general characteristics of the residential building and considers other characteristics as control variables.

2-9. Conclusion

Based on the literature review conducted, it can be concluded that the dimensions and proportions of space, along with orientation, are the most critical physical factors in optimizing energy performance and should be emphasized. To this end, it is essential to evaluate the specifications of single-story residential buildings through field observations.

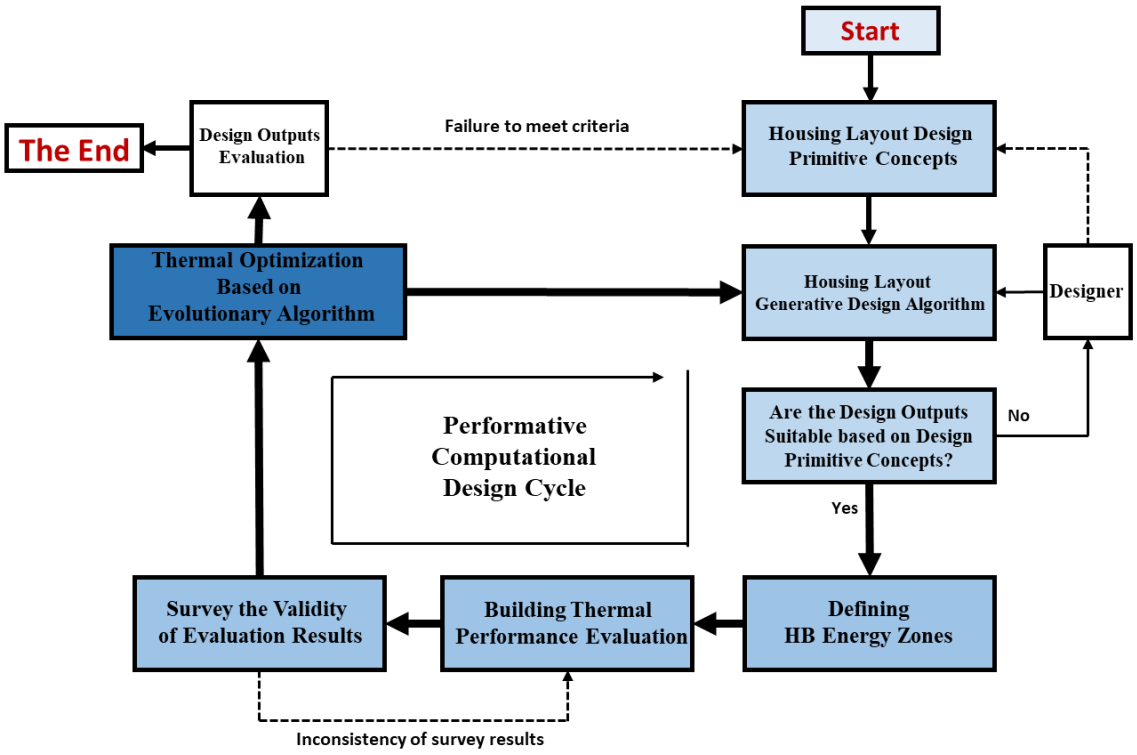

Figure 2-14. Theoretical Framework of the Research

According to the literature, the theoretical framework of this research based on Performance-Based Computational Architecture is presented as follows (Figure 2-14). This framework utilizes evolutionary computations in its processes. Based on the model, initially, the geometric parameters of the residential building are determined according to the relevant literature, which has been validated by experts. Based on these parameters, the performative computational architecture algorithm is defined to optimize energy performance. The cycle present in the theoretical framework is repeated multiple times to enable the research algorithm to reach the optimal spatial layouts based on the conducted adjustments. Subsequently, based on the findings of the algorithm, the research can progress to the stage of modeling energy performance. Additionally, based on the results of the algorithm, it is possible to define the geometric specifications that exhibit optimal energy performance.

Based on the results obtained from the literature, this study investigates the energy and daylight performance of common single-storey residential buildings in Melbourne. The reason for choosing Melbourne is the increasing development of construction processes in this city in recent years without high standards in general building specifications. In this study, due to the uncontrollable effect of building type on energy and daylight performance, it is necessary to control this variable. Accordingly, and considering that single-storey residential buildings are the most common residential buildings in Melbourne, its investigation has been considered and it is found that this issue can be important in the environmental sustainability of Melbourne. Also, considering that the results showed that the effect of general building characteristics on the energy and daylight performance of the building is much greater than other characteristics, in this study, only general building characteristics have been considered to achieve a set of standards.

Chapter 3:

Methodology

Chapter 3: Methodology

3-1-Introduction

The method of this research involves a quantitative approach, utilizing coding, simulation, and optimization within the programming environment of Grasshopper in Rhino software (Figure 3-1). Additionally, the spatial layout results obtained from the coding process have been statistically evaluated and modelled.

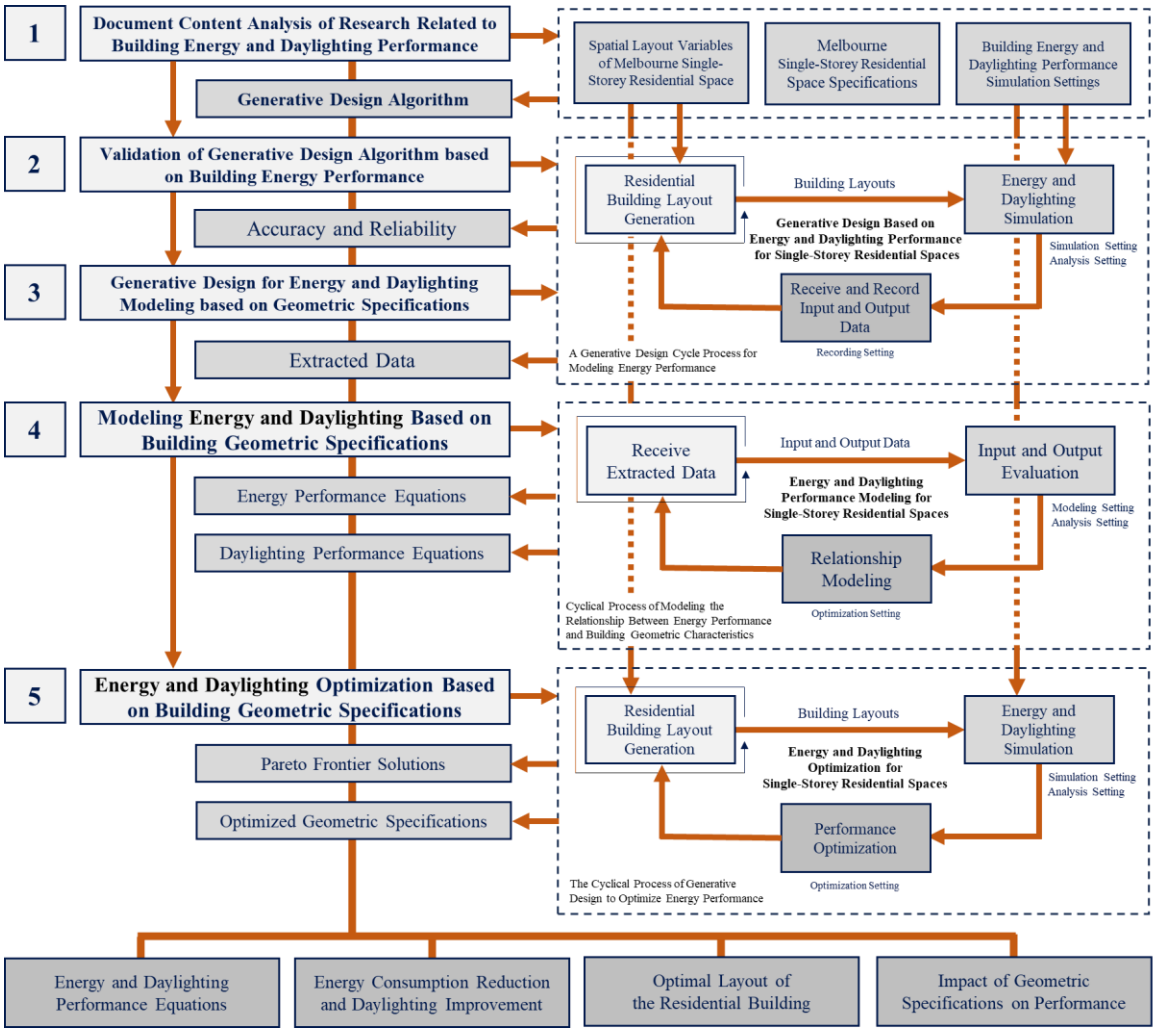

Figure 3-1. Methodology Framework

The target space for this study is a typical single-story residential building in Melbourne, Australia (Figure 3-2). For this purpose, the physical variables of residential buildings were first derived through a documentary content analysis of the literature review (Table 3-1). Following this, the external form characteristics of the residential building were optimized based on energy and daylighting performance. In this context, an algorithm for simulating

the performance of single-story residential buildings, based on their external form characteristics, was developed. Subsequently, using the prepared algorithm, the process of modeling and optimizing the building based on energy and daylighting performance was conducted.

Table 3-1: Spatial layout Characteristics and References

Spatial layout Characteristics	References
Eest-West Dimention	Dong et al., 2017; Ciulla & Amico, 2019; Geyer & Singaravel, 2018
North-South Dimention	Ciulla & Amico, 2019; Tien Bui et al., 2019; Geyer & Singaravel, 2018
Height of Building	Le et al., 2019; Al-Rakhami et al., 2019
Area of Building	Gao et al., 2019; Al-Rakhami et al., 2019
Volume of Building	Dong et al., 2017; Ciulla & Amico, 2019
North-South Direction	Chen & Yang, 2017; Dong et al., 2017; Gao et al., 2019
Window to Area Ratio	Geyer & Singaravel, 2018; Dong et al., 2017; Al-Tarhuni et al., 2019
Window Dimentions	Tran et al., 2020; Le et al., 2019; Al-Tarhuni et al., 2019

The primary tools for data collection in this research are the Grasshopper programming environment in Rhino, the Python programming environment in Grasshopper, as well as the Ladybug Tools plugin and the Wallacei plugin. The tools used for data analysis are the Wallacei plugin and SPSS software.

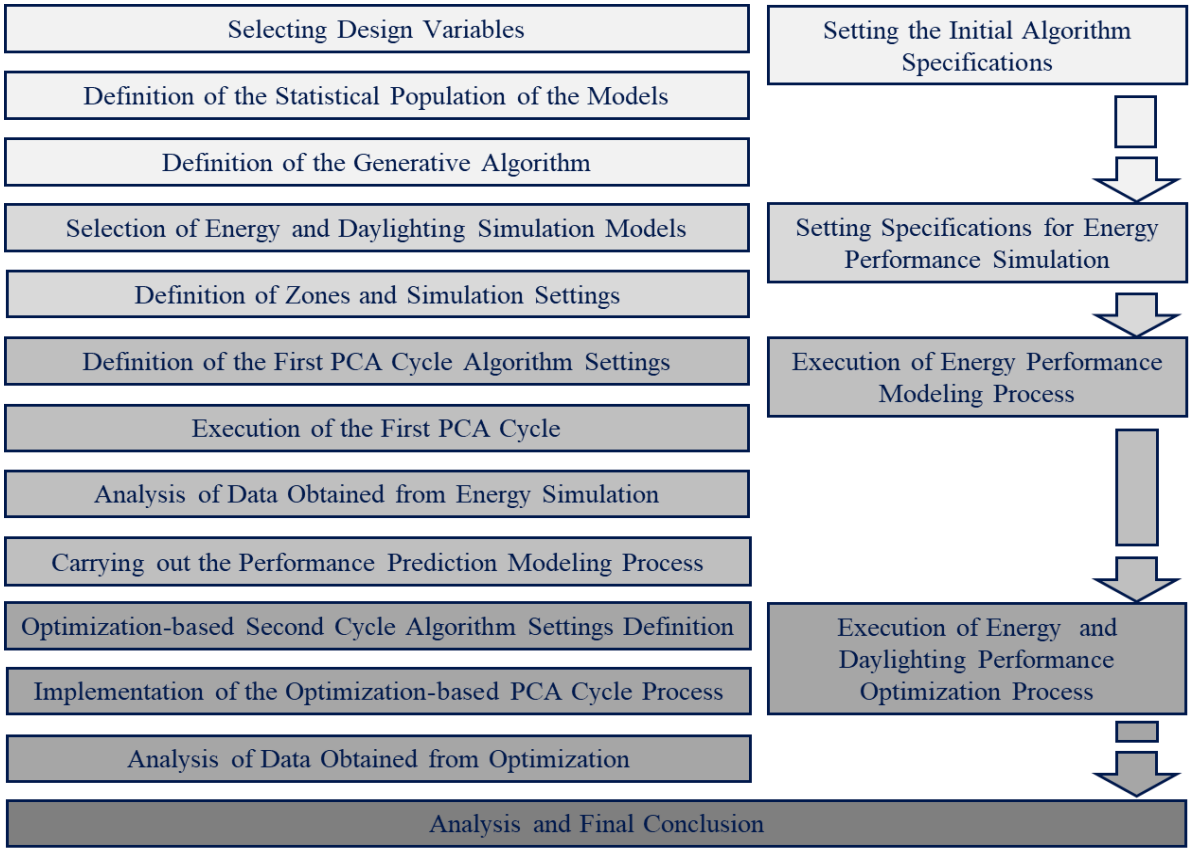

Figure 3-2. Staged Process Flow of Research Execution

Simulation and Evaluation of Building Thermal Performance based on spatial layout characteristics during the early design stages can help determine the best strategies for sustainable design and reduce building energy consumption. However, the use of thermal analysis software is still not widespread in architectural design, with architects typically relying on past experiences or conventional empirical methods (Kanters et al., 2014). The reasons for this include the complexity of using simulation programs and interpreting their results, the long time required for architectural design processes due to iterative simulations, and issues of incompatibility with common CAD (Computer-Aided Design) and BIM (Building Information Modeling) software (Attia et al., 2012). Additionally, the geometric complexity of spaces presents a wide range of possible design responses. A recent international survey conducted by the International Energy Agency (IEA) (IEA-SHC Task 41) highlighted the need to develop tools that meet the requirements of different design phases and support the comparison of alternative competing designs (Kanters et al., 2014). Thus, the need for dynamic computer-based methods becomes essential when exploring a wide design solution space during the early design stages.

Using performative computational architecture (PCA), as proposed by Sariyildiz (2012), can generate a diverse set of responses based on the spatial layout coding of single-story residential buildingss. By leveraging the Grasshopper programming environment, design responses can be generated quickly based on the initial configuration specifications. Additionally, by incorporating evolutionary algorithms into the performative computational architecture process, a wide variety of design solutions can be produced, evaluated, and optimized based on energy performance. In this regard, the Ladybug Tools plugin facilitates the use of the EnergyPlus engine for dynamic energy assessments. Furthermore, the NSGA-II non-dominated sorting genetic algorithm in the Wallacei plugin, integrated with Grasshopper, can achieve optimal convergence toward a global optimum in the design environment.

3-2- Research Tools

This research generally encompasses four categories of tools: modeling, simulation, optimization, and analysis and modelling (Figure 3-3). Considering the capabilities of the Grasshopper platform in parametric design, all tools have been defined on the Rhino software platform to the greatest extent possible.

Modeling Tools: The modeling tool for this research is the Rhino software along with the Grasshopper platform. Based on the geometric specifications of the simulation sample models, the models are defined parametrically in the Grasshopper platform to facilitate rapid changes. The Grasshopper tool was utilized for addressing the first research question, specifically for defining the geometric parameters of residential buildings and generating the resulting plans. In this context, architectural variables were initially derived based on the literature review. Subsequently, through coding in the Grasshopper environment, building models were prepared for simulation. Accordingly, an algorithm was implemented within the Grasshopper environment to input the geometric specifications of the building models and output the generated building models.

Energy Performance Simulation Tools: In the energy performance simulation section, two tools, Honeybee and Ladybug, are used in the new and updated Ladybug Tools (1.6) on the Grasshopper platform. Ladybug allows users to visualize and analyze weather data within Grasshopper (Grasshopper 3D). This includes charts such as solar paths, wind roses, psychrometric charts, and so on, as well as geometric studies like radiation analysis, shadow studies, and visibility analysis. Honeybee connects Grasshopper (Grasshopper 3D) to reputable simulation engines, including EnergyPlus and OpenStudio, for building energy, HVAC systems, and thermal comfort, as well as Radiance for daylight and glare simulation.

The Ladybug Tools were employed to address the second research question and to perform energy performance simulations for the generated models. In this context, the energy performance simulation settings were defined at the end of the building generation algorithm using Ladybug Tools. This setup allows the input of the building model and outputs the energy consumption and daylighting performance of the building at the conclusion of the algorithm.

Optimization Tools: In the optimization section, Wallacei is used as needed within the Grasshopper software to implement the optimization process. Wallacei is a component in Grasshopper designed for multi-objective evolutionary optimization. It enables simultaneous exploration of multiple objectives, generating a range of optimal solutions between the extremes of each objective. This component utilizes the Pareto principle in its design to address multiple objectives.

The Wallacei tool is utilized to address the third research question and is integrated at the end of the energy performance simulation algorithm. This tool takes the specifications of the building models as input genes and the energy consumption and daylighting performance as output objectives. Ultimately, it provides a set of optimized solutions, which are defined based on the Pareto front.

Data Analysis and Modeling Tools: Additionally, for the analysis and modeling of the simulated data, two software programs, Excel and SPSS, are utilized. Data is categorized and arranged in Excel, and analyzed in SPSS. Descriptive tests, Pearson correlation, curve regression, linear regression, and nonlinear regression are conducted on the data. Ultimately, based on the regression test results, optimal energy performance models are defined.

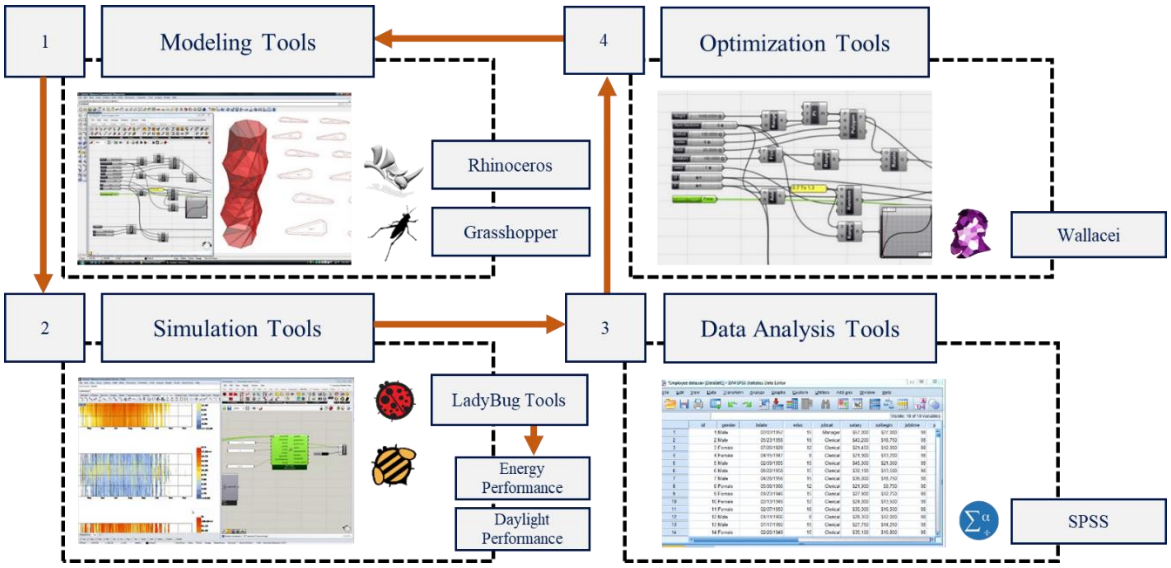

Figure 3-3. Research Tools

The SPSS tool is also employed to address the third research question and is used independently after collecting the simulated data. This tool takes the specifications of the building models as input genes and the energy consumption and daylighting performance as output objectives. Ultimately, it provides regression equations for energy performance.

3-3- Detailed Explanation of the Research Method

In this section, the complete research method is explained in detail. Based on the conducted reviews, the research methodology can be presented in four main sections, as shown in the diagram. These four sections include: setting initial specifications, setting simulation specifications, the modelling process, and the optimization process.

The twelve stages of the research methodology include: (1) Selecting design variables, (2) Defining the Specifications of the Models for Simulation, (3) Coding the generative design algorithm, (4) Selecting building models for energy simulation, (5) Defining energy zones and setting energy simulation parameters, (6) Defining the first performative computational cycle algorithm, (7) Executing the first computational cycle, (8) Analyzing the data obtained from energy simulations, (9) Conducting the modeling process to develop energy performance prediction models, (10) Defining and configuring the optimization cycle algorithms, (11) Executing the optimization computational cycles, and (12) Analyzing the data obtained from the optimization process.

3-3-1- Definition of the Generative Algorithm for the Reference Model

In this section of the research, a quantitative approach is taken to model and simulate energy performance (Figure 3-4). To this end, the geometric factors influencing the building's energy consumption are introduced into the parametric modelling process for simulation based on documentary content analysis and field surveys. The reference model, for the purpose of simulation, is defined as a rectangular-shaped residential building without internal walls. The geometric specifications of this reference model, including the length of the north-south side, the length of the east-west side, the building height, and the building's orientation relative to the north-south axis, are parametrically configured.

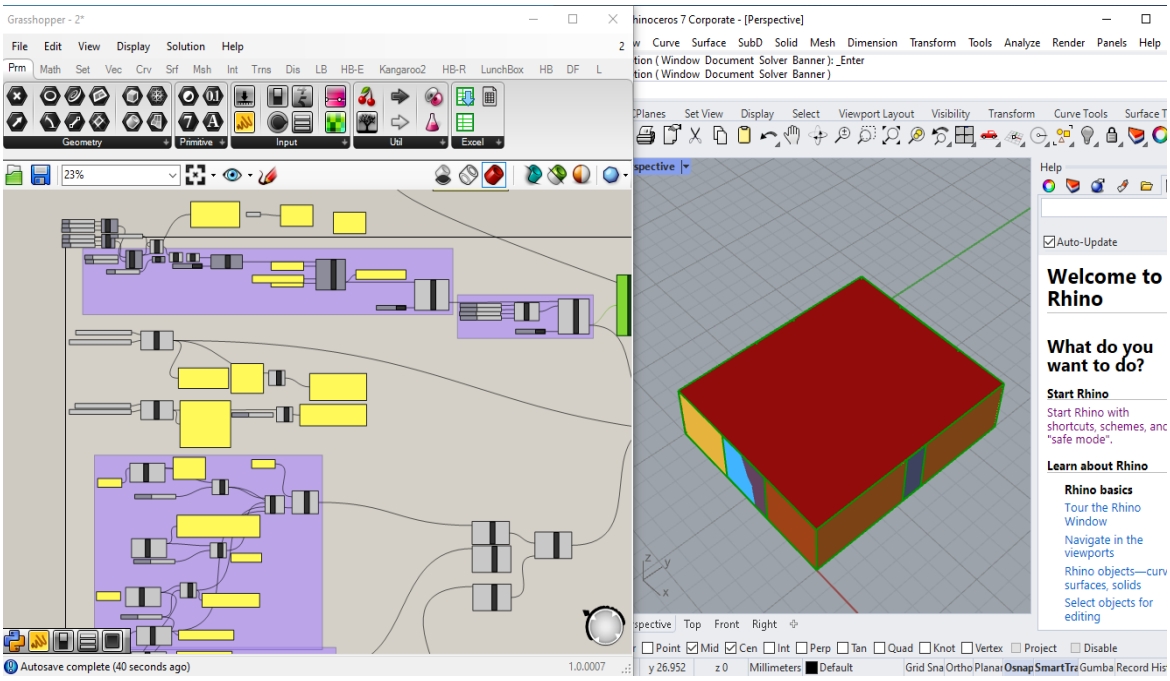

Figure 3-4. A section of the process for constructing the generative algorithm model.

The generative algorithm for simulating the energy performance of the residential building is defined in the Grasshopper programming environment within Rhinoceros software. Based on the investigations (which investigations- field work or literature review), the longitudinal dimensions of the residential building, the height of the residential building, and the orientation angle of the residential building are included as predictor variables in the algorithm. Additionally, variables such as material types, mechanical equipment, and other influential factors like the window-to-wall ratio are defined as control variables in the algorithm. Subsequently, based on the conducted surveys of the area and document studies, the inputs for the generated generative algorithm have been segmented. Finally, the settings for energy performance simulation in the generative algorithm of the external shell of the single-story residential buildings have been defined.

3-3-2- Research Variables

This section discusses the research variables. In general, the independent variables in this study include the geometric specifications of the reference model, such as the length of the north-south side, the length of the east-west side, the building height, and the building's orientation relative to the north-south axis. Additionally, the materials of the building envelope, window-to-wall ratio, window opening ratio, scheduling, input loads, and heating, cooling, and lighting equipment are set as control variables. Furthermore, based on the resulting model specifications, the window width, window height, window area, residential building area, and building volume are derived as mediating variables. The dependent variables of the study include energy consumption, energy consumption per square meter, cooling demand, cooling demand per square meter, heating demand, heating demand per square meter, useful daylight illuminance, and daylight autonomy index. In the simulation, thermal bridge is defined as a control variable based on the R-value and U-value of the materials used in the walls and floors.

3-3-2-1- Scope of Variations in Spatial Layout Models for Simulation

In the following, based on field studies and document analysis, the range of variations in spatial layout models for energy performance simulation has been determined. As mentioned, considering the complexities of spatial layout and the diversity of possible responses for a single-story residential building, these factors have been taken into account. Additionally, in all cases examined, windows are defined only on the northern sides. The

window-to-wall ratio is set as a controlled variable on the northern facade, based on the National Construction Code of Australia (NCC, 2022), considering 10% of the floor area.

Table 3-2. The range of changes of the geometric variables of the reference model

	Number of Floors Building	Dimensions of the North-South Side	Dimensions of the East-West Side	Height of the Units	Building Orientation
Minimum	**1**	**8**	**8**	**2.6**	**-45**
Maximum	**9**	**22**	**22**	**4**	**45**

In this section of the research, the external shell is considered rectangular, reflecting the common form of most land parcels in the area. To define its dimensional range, two dimensions—east-west and north-south—are specified. Accordingly, the dimensions of the east-west side and the north-south side are defined to range from 8 to 22 meters, covering buildings with an area between 64 to 484 square meters (Table 3-2).

These dimensions are assumed to encompass all proportions of buildings ranging from 80 to 200 square meters, which represent the predominant area in Melbourne. Additionally, to assess the impact of interior space height on energy performance, the height of interior spaces has been considered to range from 2.6 to 4 meters, ensuring a comprehensive coverage of possible heights for residential buildings in the city. Furthermore, to investigate the influence of building orientation on energy performance, the primary axis of the initial building is assumed to be aligned along the north-south axis, with orientations ranging from -45 to +45 degrees relative to this axis. Based on the presented range, a set of inputs for the algorithm has been defined.

3-3-2-2- Settings for Building Energy Performance Simulation

In this research, several energy performance simulation processes are presented within the framework of performative computational architecture (Figure 3-5). In this context, the open-source tool Ladybug Tools is utilized in the Grasshopper programming environment. This tool connects the Grasshopper environment to EnergyPlus, Radiance, Daysim, and OpenStudio for energy consumption and lighting simulations (Pandit, 2016).

To conduct the energy performance simulation, four groups of building specifications must be defined: the geometry and envelope of the building, the thermal properties of materials, the settings for cooling, heating, and air conditioning equipment, and the behavioral

characteristics of the occupants. In this study, the specifications for materials, equipment, and occupant behaviour are defined as fixed control variables.

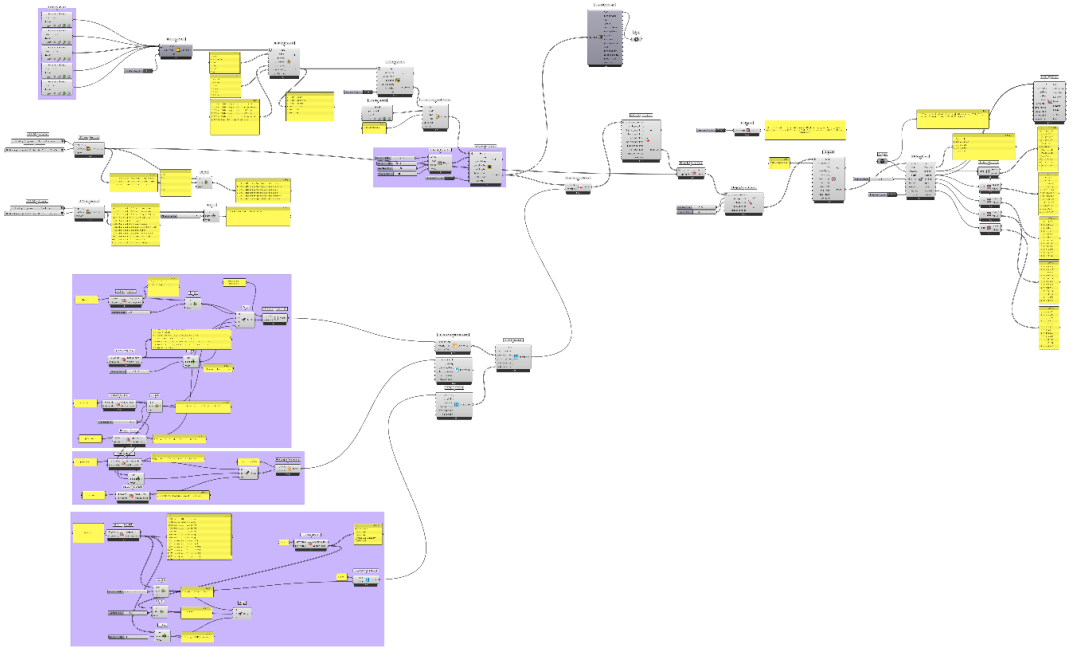

Figure 3-5. GD Algorithm for Energy Performance Simulation in Grasshopper Environment

The energy performance simulation process is based on nine performance objectives, which include total energy consumption of the residential building, energy consumption per square meter, heating demand of the residential building, heating demand per square meter, cooling demand of the residential building, cooling demand per square meter, lighting demand of the residential building, useful daylight illuminance, and daylight autonomy index.

3-3-2-3- Description of the Study Area

This study examines the climate of Melbourne in Australia. Australia, located in the Southern Hemisphere, exhibits diverse climatic conditions. Its climatic zones consist of several different classifications. Köppen defines various climatic classifications for Australia, while the Building Code of Australia (BCA) delineates eight main climatic regions: tropical, subtropical, grassland, desert, warm temperate, mild temperate, cool temperate, and mountainous.

Melbourne, the capital of the state of Victoria and the second most populous city in Australia (the most populous city in urban areas), has a temperate oceanic climate (Köppen climate

classification Cfb) and is well known for its variable weather conditions. This is primarily due to Melbourne's geographical location.

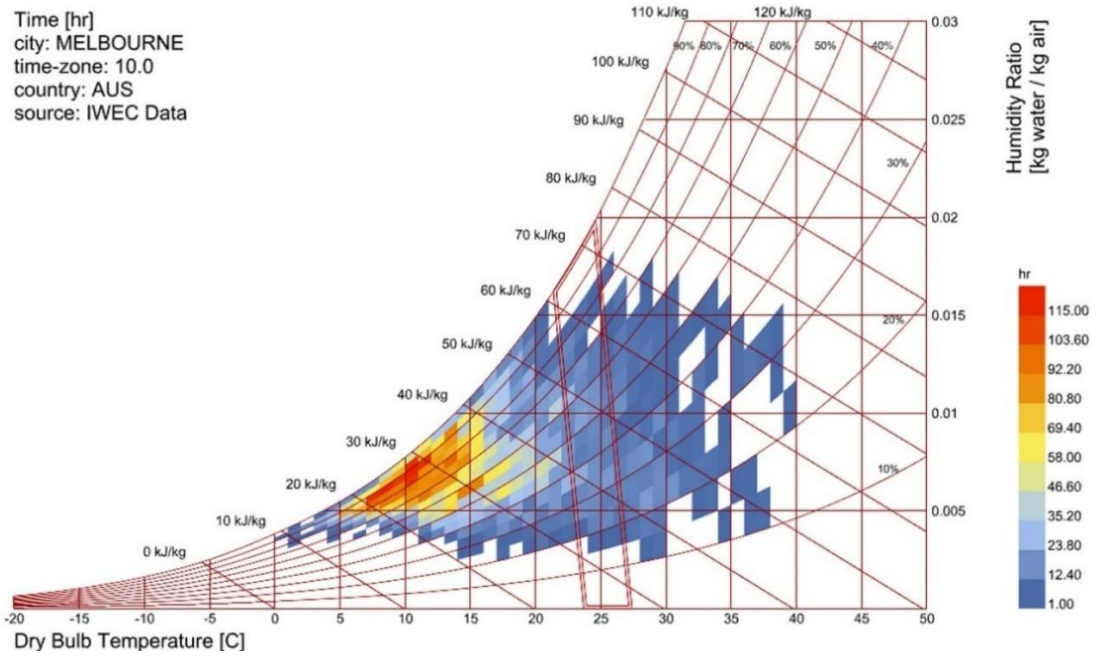

Figure 3-6. Psychrometric Chart Based on the EnergyPlus Climate File for the City of Melbourne

In this study, one of the most significant climatic regions of the eight, namely the city of Melbourne as defined by the Building Code of Australia (BCA), is considered for optimizing energy needs through passive energy design.

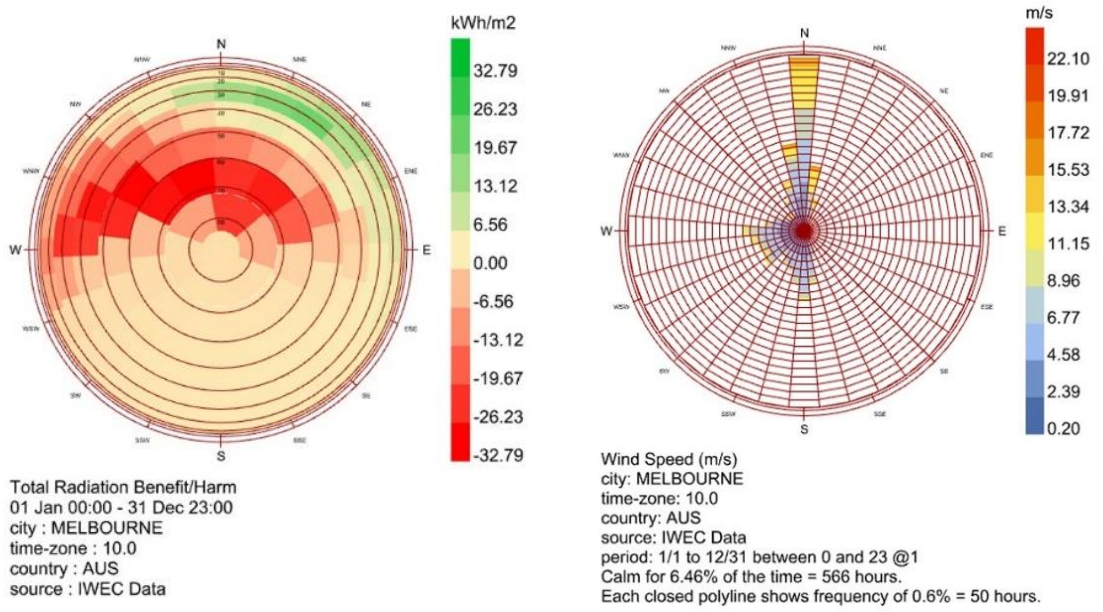

Figure 3-7. Wind and Solar Radiation Diagram Based on the EPW File for Melbourne

Temperature differences in the spring and summer are more pronounced, which can lead to the formation of strong cold weather fronts. These cold fronts can result in various severe weather conditions, ranging from storms and thunderstorms to heavy hail, minor temperature drops, and intense rainfall. Generally, the city experiences low humidity during the summer. Based on the above, the climatic data for the city of Melbourne has been obtained from the EnergyPlus climate files (EPW) for simulation purposes (Energy Plus, 2020). The psychrometric chart based on the EnergyPlus climate file for the city of Melbourne is illustrated in the figure 3-6 and 3-7.

3-3-2-4- Details of Materials Used in the Simulation

In this research, to carry out the energy simulation process based on the reference model of single-storey residential buildings in the city of Melbourne, Australia, a timber-framed construction has been utilized after extensive reviews and consultations with architectural experts. Based on field surveys, timber frame construction is the most common structure for single-storey residential buildings in Melbourne. Following an examination of the Green Star standards (GreenStar, 2021) and the National Construction Code of Australia (NCC, 2022), no precise execution details for timber-framed construction of single-storey residential buildings in Melbourne have been provided. Therefore, the evaluation and simulation of the structure in this study have been based on reputable construction companies specializing in timber-framed construction (MBC Timber Frame UK Ltd, 2026).

3-3-2-4-1- Description of Timber Framed Construction For simulation

After extensive reviews, the construction details for the simulation have been selected from the execution specifications of MBC Timber Framed Construction, which operates in the design and construction of energy-efficient timber frame homes and passive energy homes.

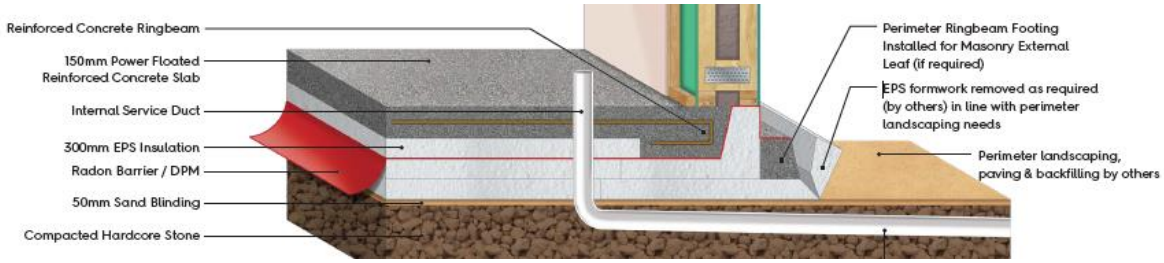

Figure 3-8. Execution Details of the Foundation for Timber Framed Construction For simulation (MBC Timber Frame UK Ltd, 2026)

In accordance with the reference model for this study, a single-storey building with a flat roof has been considered. The construction details and information for each component are provided as follows. In the first image, the execution details of the MBC Timber Framed foundations are presented. These execution details are based on MBC standards, which include an Oriented Strand Board (OSB) layer added on top of the concrete foundation surface (Figure 3-8; Table 3-3).

Table 3-3. Details of Timber Frame Foundation Execution For simulation (MBC Timber Frame UK Ltd, 2026)

Material	Thickness	Conductivity	Density	Specific Heat	Roughness	Ref
Compacted Hardcore Stone	800mm	0.85W/m-K	1500 Kg/m3	1000 J/Kg-K	R	MSZ EN, 2008
Blinding Sand	50mm	2W/m-K	2200Kg/m3	1180J/Kg-K	M R	MSZ EN, 2008
Expanded Polystyrene	200mm	0.036W/m-K	18Kg/m3	1250J/Kg-K	M S	Kumar et al., 2020
Polyethylene (Radon Barrier)	0.1mm	0.5W/m-K	980Kg/m3	1800J/Kg-K	M R	MSZ EN, 2008
Expanded Polystyrene	100mm	0.036W/m-K	18Kg/m3	1250J/Kg-K	M S	Kumar et al., 2020
Reinforced Concrete 1pSteel	150mm	2.3W/m-K	2300Kg/m3	1000J/Kg-K	M R	MSZ EN, 2008
Oriented Strand Board (OSB)	11mm	0.13W/m-K	650Kg/m3	1700J/Kg-K	M R	MSZ EN, 2008

In the reference building simulated, these details are utilized in the form of ground-attached floors. According to the simulation conducted in LadyBug Tools (LadyBug Tools 1.6), the R-Value of the ground-attached floor in the SI standard is 9.45 m²K/W, and the U-Factor in the SI standard is 0.104 W/m²K (Figure 3-9; Table 3-4).

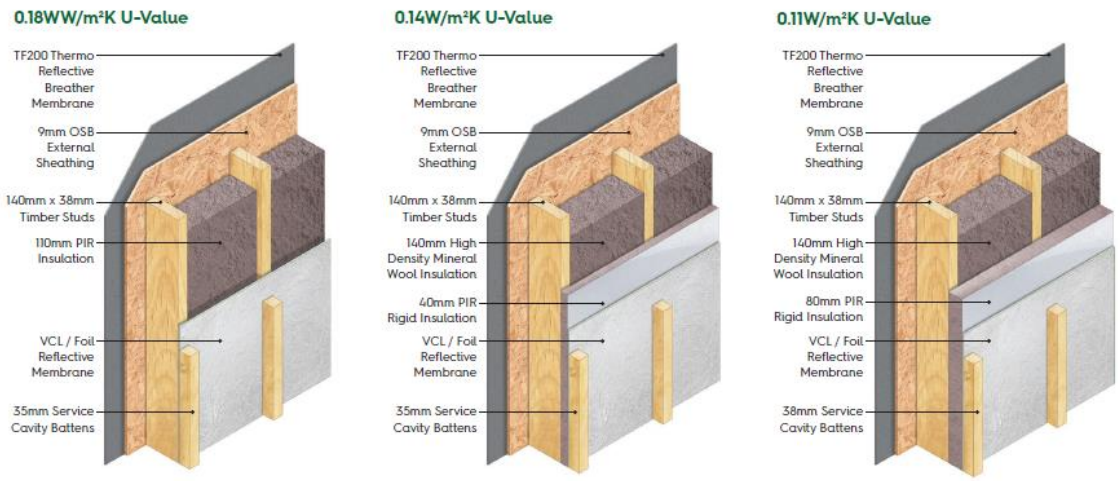

Figure 3-9. Detailed Execution of the Foundation for Timber Framed Structures For simulation (MBC Timber Frame UK Ltd, 2026)

These values largely align with the standards provided by the MBC Timber Framed construction group. In the second image, the detailed execution of the external walls of MBC

Timber Framed structures is presented. According to MBC standards, plasterboard is used on the interior surface, while polyurethane is applied on the exterior surface.

Table 3-4. Execution Details of the External Wall of the Timber Framed Structure For simulation (MBC Timber Frame UK Ltd, 2026)

Material	Thickness	Conductivity	Density	Specific Heat	Roughness	Ref
Polyurethane (Radon Barrier)	0.1mm	0.25W/m-K	1200Kg/m3	1800J/Kg-K	M R	MSZ EN, 2008
Oriented Strand Board (OSB)	12.5mm	0.13W/m-K	650Kg/m3	1700J/Kg-K	M R	MSZ EN, 2008
Cellulose Insulation	300mm	0.039W/m-K	50Kg/m3	1400J/Kg-K	S	Schiavoni et al., 2016
Oriented Strand Board (OSB)	12.5mm	0.13W/m-K	650Kg/m3	1700J/Kg-K	M R	MSZ EN, 2008
Polyethylene (Radon Barrier)	0.1mm	0.5W/m-K	980Kg/m3	1800J/Kg-K	M R	MSZ EN, 2008
Wall air space	-	-	-	-	-	ASHRAE, 2022
PlasterBoard	15mm	0.13W/m-K	650Kg/m3	1700J/Kg-K	M R	MSZ EN, 2008

In the reference building simulated, these details were used in the form of external walls on all four sides of the building. Based on the simulation conducted, the R-Value of the external wall is 7.95 m²·K/W in SI units (Figure 3-9; Table 3-4).

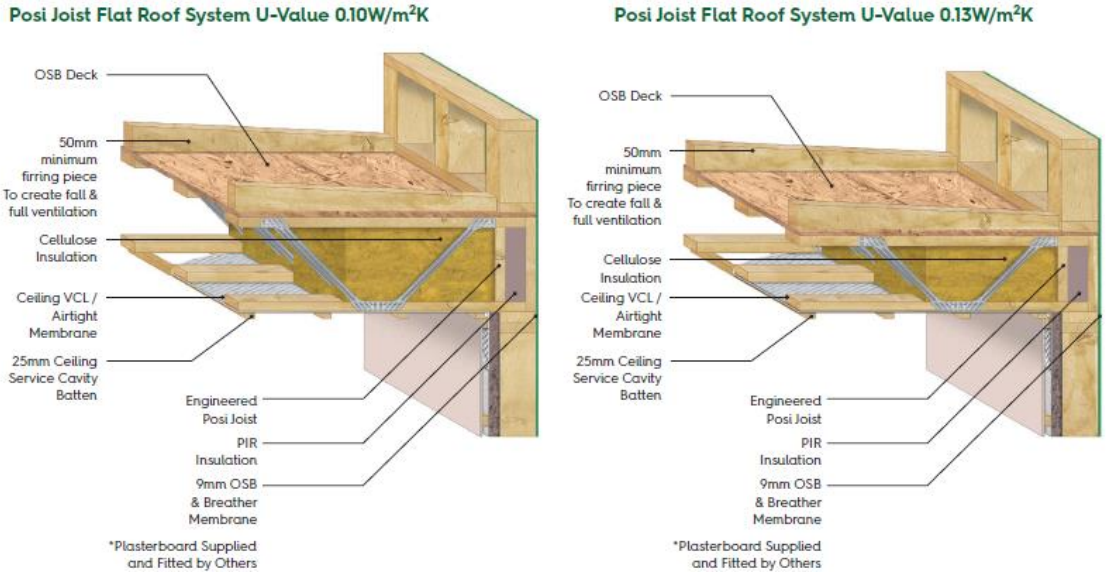

Figure 3-10. Execution Details of Flat Roofs in Timber Framed Structure For simulation (MBC Timber Frame UK Ltd, 2026)

In this simulation, the U-Factor was determined to be 0.123 W/m²·K in SI units, which largely aligns with the standards set by MBC Timber Framed Construction.In the third

image, the execution details of flat roofs in the MBC Timber Framed system are presented. In this section, based on MBC standards, OBC was used for the exterior surface and plasterboard for the interior surface. In the simulated reference building, these materials were utilized in the external roofing components. According to the simulation, the R-value of the external roofs, in compliance with SI standards, is 10.93 m²K/W (10.939487 m²K/W).

Table 3-5. Construction Details of the Exterior Wall in Timber Frame Structures For simulation (MBC Timber Frame UK Ltd, 2026)

Material	Thickness	Conductivity	Density	Specific Heat	Roughness	Ref
Oriented Strand Board (OSB)	11mm	0.13W/m-K	650Kg/m3	1700J/Kg-K	M R	MSZ EN, 2008
Cellulose Insulation	421mm	0.039W/m-K	50Kg/m3	1400J/Kg-K	S	Schiavoni et al., 2016
PlasterBoard	15mm	0.13W/m-K	650Kg/m3	1700J/Kg-K	M R	MSZ EN, 2008

In this simulation, the U-Factor, according to SI standards, was determined to be 0.090 W/m²K (0.090064 W/m²K), which closely aligns with the standard provided by the MBC Timber Framed Building Group. Based on this, the material information required for simulating energy performance was defined as a control variable in the algorithm using LadyBug Tools 1.6 (Figure 3-10; Table 3-5).

3-3-2-5- Schedules and Loads Used in the Simulation

To define the building's occupancy schedule, one can use the scheduling standards from recognized Australian sources. This section briefly reviews the occupancy schedules from ASHRAE 90.1 (2019), Green Star (2021), and the National Construction Code (NCC 2022) of Australia. Based on the results of the comparative analysis shown in the table, this study intends to use the National Construction Code of Australia (NCC, 2022).

In this regard, the total values of bedrooms and living rooms in the National Construction Code of Australia (NCC, 2022) have been used together. Due to the lack of a complete physical program in the NCC standard, the ASHRAE standard has been used to adjust other physical program indicators. The physical schedule is defined according to ASHRAE 90.1-2019, and based on the existing standards, the physical schedule of a mid-rise apartment (MidriseApartment::Apartment) has been considered. In order to ensure the intended settings, the information has been provided to and verified by experts in the field of building

energy performance. Also, it should be noted that since the physical program and simulation loads are considered as control variables, they will not have a large impact on the results.

Table 3-6. Occupancy Schedule Details Based on Various Standards

	00:00-01:00	01:00-02:00	02:00-03:00	03:00-04:00	04:00-05:00	05:00-06:00	06:00-07:00	07:00-08:00	08:00-09:00	09:00-10:00	10:00-11:00	11:00-12:00	12:00-13:00	13:00-14:00	14:00-15:00	15:00-16:00	16:00-17:00	17:00-18:00	18:00-19:00	19:00-20:00	20:00-21:00	21:00-22:00	22:00-23:00	23:00-24:00
ASHRAE 2019; Midrise Apartment; All Days	1	1	1	1	1	1	1	0.85	0.39	0.25	0.25	0.25	0.25	0.25	0.25	0.25	0.3	0.52	0.87	0.87	0.87	1	1	1
NCC 2022; C1 Building; Rooms; Weekdays	0	0	0	0	0	0	0.3	0.3	1	1	0.5	0.5	0.5	0.5	0.5	0.5	1	1	1	1	1	0.3	0.3	0
NCC 2022; C1 Building; Bedrooms; All Days	1	1	1	1	1	1	0.5	0.5	0.5	0	0	0	0	0	0	0	0	0	0.5	0.5	0.5	1	1	1
NCC 2022; C1 Building; Sum of 2; Weekdays	1	1	1	1	1	1	0.8	0.8	1.5	1	0.5	0.5	0.5	0.5	0.5	0.5	1	1	1	1	1	1	1	1
NCC 2022; C1 Building; Rooms; Weekends	0	0	0	0	0	0	0.3	0.3	0.3	1	1	1	1	0.5	0.5	0.5	0.5	0.5	1	1	1	1	0.3	0
NCC 2022; C1 Building; Bedrooms; All Days	1	1	1	1	1	1	0.5	0.5	0.5	0	0	0	0	0	0	0	0	0	0.5	0.5	0.5	1	1	1
NCC 2022; C1 Building; Sum of 2; Weekends	1	1	1	1	1	1	0.8	0.8	0.8	1	1	1	1	0.5	0.5	0.5	0.5	0.5	1	1	1	1	1	1
Green Star 2021; RMUnit; Living Space; All Days	0	0	0	0	0	0	0	1	1	0.5	0.5	0.5	0.5	0.5	0.5	0.5	0.5	0.75	0.75	0.75	0.75	0.75	0	0
Green Star 2021; RMUnit; Bedroom; All Days	1	1	1	1	1	1	1	0	0	0	0	0	0	0	0	0	0	0	0	0	0	0	1	1
Green Star 2021 RMUnit; Sum of 2; All Days	1	1	1	1	1	1	1	1	1	0.5	0.5	0.5	0.5	0.5	0.5	0.5	0.5	0.75	0.75	0.75	0.75	0.75	1	1

Additionally, according to ASHRAE 90.1-2019, the cooling and heating set points are set at 24.4°C and 21.7°C, respectively.

3-3-2-6- Validation of the Energy Simulation Model

In the following, in the section on building energy performance simulation, a calibration mechanism based on real energy consumption values has been used to assess the validity of the model. The algorithm uses an ideal heating system. Therefore, in the validation phase, only the total electricity and gas consumption was compared. However, for more accurate validation, several different indicators were used, including the median of the data, Pearson correlation, NMBE, and CVRMSE.

Additionally, to enhance the validity, specifications for locally used and common building materials, as well as a residential scheduling program based on a field survey of the residents, have been employed. Furthermore, to assess the reliability of the model, sensitivity analysis using Pearson correlation testing has been applied. The process of reliability and validity in the research will be explained in the following sections. Model calibration is often used to better align simulation predictions with real observations and to increase the model's credibility for future predictions. Although calibration is not essential for building energy simulation studies, it has become increasingly important for establishing model validity (Yoshino et al., 2017). In this regard, for the validation of the simulation process in this

research, 16 residential buildings from various areas of Melbourne city, with different sizes, were selected. Their details and specifications are shown in the table below. Sampling in this section was purposeful, with an effort to include a comprehensive range of dimensions relevant to the research in the selection of residential buildings. Additionally, buildings with construction materials consistent with the simulation algorithm used in the research were chosen. Accordingly, electricity and gas consumption data for all selected residential buildings were collected based on monthly bills over a one-year period. Below is a sample of the bills (Figure 3-11).

Table 3-7. Selected Residential buildings in Different Areas of Melbourne for Simulation

Code	Area of Building	NS-D	EW-D	Direction	S-WWR	N-WWR	E-WWR	W-WWR	Number of Residents	Annual Energy Demnad
1	144.5	8.5	17	-45	0.6	0.45	0	0	5	21979.57
2	96	12	8	5	0	0.4	0	0	2	22906.3333
3	225	12.5	18	0	0.7	0	0	0.2	4	38285.97626
4	152.25	14.5	10.5	8	0.6	0.2	0	0	3	36267.90408
5	195	12	16.25	5	0.6	0.45	0	0	6	27149.60198
6	219.8	14	15.7	7	0.65	0.35	0	0	4	37944.38618
7	96	12	8	12	0.4	0.2	0	0	3	20246.9311
8	156	12	13	5	0.7	0	0	0	4	32111.39628
9	227.5	13	17.5	5	0.7	0.3	0	0.3	4	37951.58728
10	188.5	13	14.5	0	0.7	0.25	0	0	3	32910.28682
11	91	13	7	5	0	0.4	0	0	3	20373.43964
12	160	16	10	8	0.6	0	0.3	0	4	34208.88388
13	88	11	8	12	0.55	0.45	0	0	3	22111.76342
14	162.5	12.5	13	5	0.7	0	0	0	5	35312.95532
15	225	12.5	18	0	0.7	0	0	0.25	3	39447.76432
16	203.5	11	18.5	10	0.4	0.4	0	0	4	26433.32246

To conduct a comparative analysis of the energy consumption of residential buildings with the energy needs simulated, it is necessary to examine both variables based on a common unit. Therefore, it is required to calculate the energy consumption of the residential buildings in the selected buildings in kilowatt-hours, sum them up, and compare them with the simulation results. In Australia, electricity bills for buildings are presented in kilowatt-hours, while gas bills are provided in megajoules. For this reason, in order to carry out the comparative analysis, it is first necessary to convert the gas consumption of the residential buildings from megajoules to energy consumption in kilowatt-hours. For this purpose, according to studies conducted, the following formula is used to convert gas consumption to energy consumption in kilowatt-hours:

$$EC\ (KWH) = GC(MJ) \times 0.27777777777778$$

Additionally, the occupancy load of all selected residential buildings has been extracted. The simulation process was then carried out based on the external boundary specifications of the 16 selected residential buildings, and for each unit, energy consumption was simulated using the defined generative design algorithms. The results of this process are presented in the next chapter to validate the simulation's accuracy. In each section, after completing the simulation process, the data is encoded based on energy consumption in kilowatt-hours and energy consumption per square meter in both actual and simulated forms. Then, the validation of the simulation process is performed through both descriptive statistics and correlation testing. In the descriptive statistics section, the difference between simulated and actual energy consumption is evaluated at two levels: kilowatt-hours and kilowatt-hours per square meter. Additionally, the percentage difference relative to total energy consumption is also used in the descriptive analysis. This test demonstrates that the energy performance simulation is accurate in reflecting the actual energy performance. Although, given the diverse lifestyles of the residents, a high level of accuracy cannot always be achieved, a difference of less than 30 percent is considered acceptable, taking into account the impact of resident behavior. In this context, using descriptive statistics such as median, standard deviation, minimum, and maximum values can help improve the precision of the descriptive evaluation. If the difference is less than 30 percent in all the statistics, this indicates a high level of simulation accuracy, considering the diversity of residents' lifestyles.

Next, Pearson correlation testing is used between actual and simulated energy consumption at two levels: kilowatt-hours and kilowatt-hours per square meter. This test can show the accuracy of the simulation in capturing variations in energy consumption. The use of this measure provides a better evaluation of the simulation's accuracy in energy performance, as it controls for the lifestyle of the residents to a large extent, considering the study of 16 different residential buildings in various areas of Melbourne (Table 3-7). In this test, the significance level and the correlation coefficient are examined. If the significance level is close to zero and less than 0.05, and the correlation coefficient is higher than 0.7, this indicates a strong and direct relationship between actual and simulated energy performance.

Additionally, to assess the reliability of the energy performance simulation, sensitivity analysis is used on the data. Sensitivity analysis in energy performance simulation studies the impact of the building's physical factors on the results of the simulation. Accordingly, all correlation and regression tests performed on the energy performance results contribute to the assessment of the reliability of the simulation.

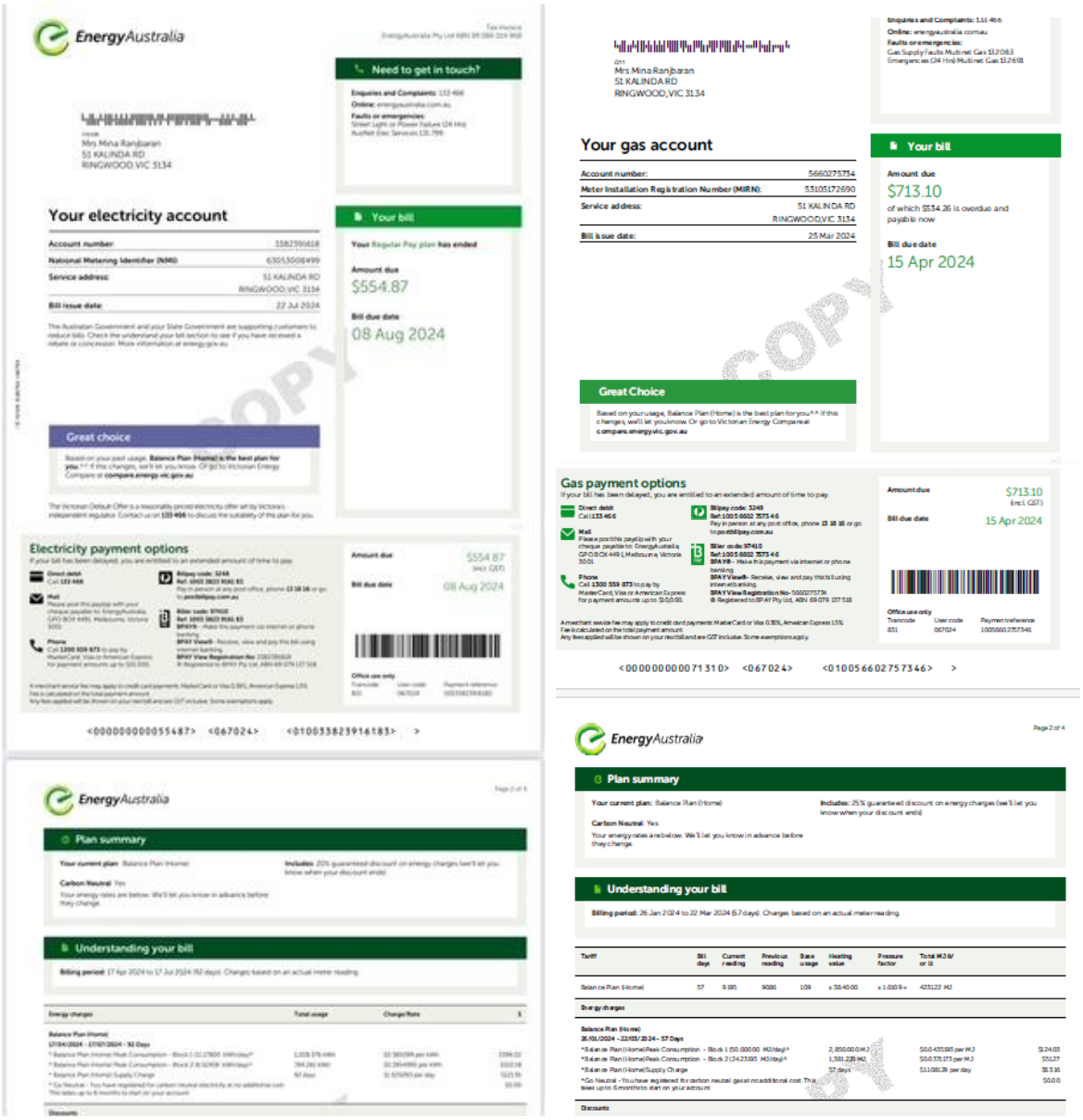

Figure 3-11. Sample Electricity Bills Collected from Residential buildings and Sample Gas Bills Collected from Residential Buildings

Specifically, after obtaining each energy performance simulation algorithm in this research, a pilot simulation was conducted. Then, Pearson correlation testing was applied between the physical factors and the energy performance results of the models. In this section, based on the results, if the significance level is close to zero and less than 0.05, and the correlation coefficient of some physical variables is higher than 0.7, the reliability of the energy performance simulation results for that section is confirmed.

After preparing the model, the validation of the generative design model for the building envelope was performed by comparing the simulation predictions with real observations. In

this assessment, the average difference between actual and simulated total energy consumption was found to be approximately -841 kilowatt-hours.

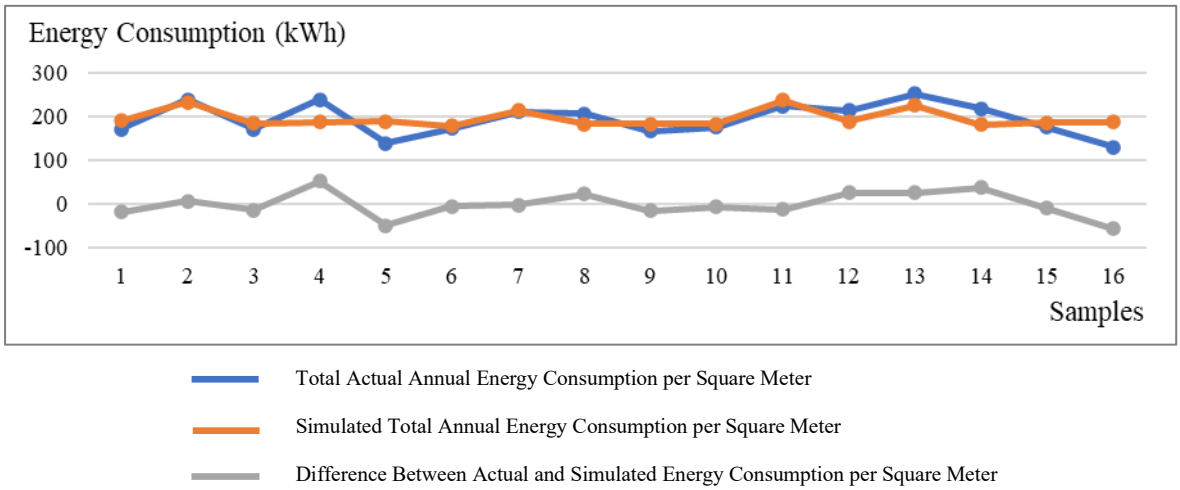

Figure 3-12. Comparative Analysis of Actual and Simulated Energy Consumption per Square Meter for Selected Residential buildings (Figure 3-12; Table 3-10).

Additionally, the average difference in actual and simulated energy consumption per square meter was found to be -1.475 kilowatt-hours.

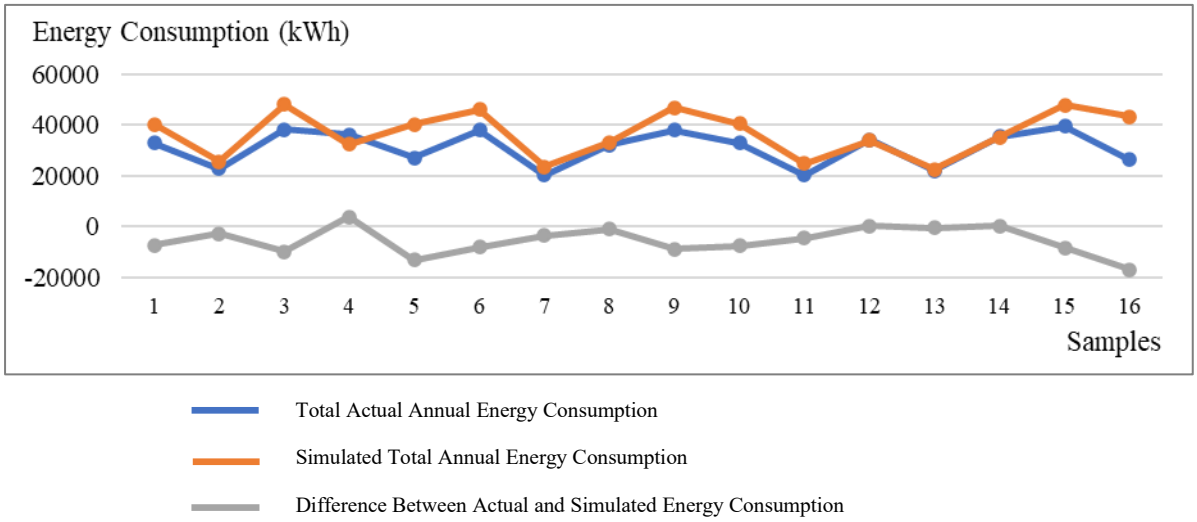

Figure 3-13. Comparative Analysis of Actual and Simulated Energy Consumption for Selected Residential buildings

Accordingly, the average percentage difference between actual and simulated energy consumption relative to the actual energy consumption was found to be -3.3%. The findings are presented in two graphs. An analysis of the bills related to the three responses showed that two of the responses correspond to residential buildings whose energy performance was significantly lower than the energy consumption standard in Melbourne. In the third case,

the bills indicate an increase in energy consumption for this unit. The reason for this can be traced to the lifestyle of the residents. To investigate further, outlier data was removed by excluding three responses with very high standard deviations. A correlation test between actual and simulated energy consumption was then conducted (Table 3-8).

Table 3-8. Descriptive Statistics of Actual and Simulated Energy Consumption for Selected Residential buildings

	Number	Minimum	Maximum	Median	Standard Deviation
Total Actual Annual Energy Consumption	16	20246.931	39447.764	31030.177	6804.765
Total Actual Annual Energy Consumption per Square Meter	16	129.893	251.270	193.7140	36.155
Simulated Total Annual Energy Consumption	16	19813.263	41713.396	31871.584	7881.621
Difference Between Actual and Simulated Energy Consumption	16	-11656.789	7844.276	-841.407	5130.941
Simulated Total Annual Energy Consumption per Square Meter	16	178.040	236.300	195.189	19.533
Difference Between Actual and Simulated Energy Consumption per Square Meter	16	-57.281	51.522	-1.475	29.123
Percentage Difference Compared to Total Actual Energy Consumption	16	-44%	21.6%	-3.3%	17.3%

In this test, a significance level of less than 0.05 and a correlation coefficient higher than 0.75 were obtained, which is highly favorable and confirms the validity of the simulation process (Table 3-9).

Table 3-9. Correlation Test Between Actual and Simulated Energy Consumption for Selected Residential buildings

		Simulated Total Annual Energy Consumption	Simulated Total Annual Energy Consumption per Square Meter
Total Actual Annual Energy Consumption	Pearson Correlation	.932**	-.915**
	Sig. (2-tailed)	.000	.000
	N	13	13
Total Actual Annual Energy Consumption per Square Meter	Pearson Correlation	-.915**	.760**
	Sig. (2-tailed)	.000	.003
	N	13	13

**. Correlation is significant at the 0.01 level (2-tailed).

*. Correlation is significant at the 0.05 level (2-tailed).

For model validation, the two statistical indicators NMBE and CVRMSE were evaluated based on both total energy consumption and energy use per square meter (Table 3-10).

Table 3-10. NMBE and CVRMSE Report For model validation

	Energy Consumption	Energy Consumption per Area
NMBE	2.3042681%	2.3763401%
CVRMSE	3.1074381%	3.1965%

The results showed an NMBE below 5% and a CVRMSE below 15%, which are within the acceptable limits defined by ASHRAE standards, thereby confirming the model's reliability.

Future work may involve validation with an independent set of units to strengthen the model's generalizability in broader contexts. Additionally, to conduct a sensitivity analysis, 200 models were randomly selected and simulated based on the energy performance simulation algorithm for the building envelope of the research. Then, a Pearson correlation test was performed between the model inputs and outputs, the results of which are presented in the table 3-11.

Table 3-11. Results of Sensitivity Analysis Based on the Correlation Test Between Physical Factors and Simulation Performance Objectives

		Total Energy Consumption per Residential building	Energy Consumption per Square Meter of Residential building	Cooling Demand per Residential building	Cooling Demand per Square Meter of Residential building	Heating Demand per Residential building	Heating Demand per Square Meter of Residential building
Number of Floors	Pearson Correlation	-.368**	-.506**	-.255**	-.174*	-.642**	-.604**
	Sig. (2-tailed)	.000	.000	.000	.014	.000	.000
Dimensions of the East-West Side	Pearson Correlation	.808**	-.415**	.891**	-.317**	.493**	-.404**
	Sig. (2-tailed)	.000	.000	.000	.000	.000	.000
Dimensions of the North-South Side	Pearson Correlation	.597**	-.448**	.505**	-.799**	.437**	-.196**
	Sig. (2-tailed)	.000	.000	.000	.000	.000	.006
Orientation	Pearson Correlation	.111	-.089	.100	-.118	.098	-.061
	Sig. (2-tailed)	.119	.208	.160	.096	.166	.392
Height of the Building Units	Pearson Correlation	.179*	.281**	.239**	.356**	.216**	.200**
	Sig. (2-tailed)	.011	.000	.001	.000	.002	.005
Floor Area of the Building	Pearson Correlation	.937**	-.528**	.945**	-.645**	.616**	-.387**
	Sig. (2-tailed)	.000	.000	.000	.000	.000	.000
Building Volume	Pearson Correlation	.291**	-.640**	.409**	-.455**	-.132	-.641**
	Sig. (2-tailed)	.000	.000	.000	.000	.062	.000
Width of the South Window	Pearson Correlation	.793**	-.436**	.870**	-.343**	.475**	-.419**
	Sig. (2-tailed)	.000	.000	.000	.000	.000	.000
Height of the South Window	Pearson Correlation	.179*	.281**	.239**	.356**	.216**	.200**
	Sig. (2-tailed)	.011	.000	.001	.000	.002	.005
Width of the North Window	Pearson Correlation	.757**	-.462**	.825**	-.380**	.439**	-.436**
	Sig. (2-tailed)	.000	.000	.000	.000	.000	.000
Height of the North Window	Pearson Correlation	.179*	.281**	.239**	.356**	.216**	.200**
	Sig. (2-tailed)	.011	.000	.001	.000	.002	.005
Number of Samples		200	200	200	200	200	200

**. Correlation is significant at the 0.01 level (2-tailed).
*. Correlation is significant at the 0.05 level (2-tailed).

As shown in the table, each of the energy performance parameters has a relatively favourable correlation with the spatial layout configuration variable, and the reliability is confirmed. A more detailed examination of the subject is conducted based on correlation and regression tests, considering all the simulations performed.

3-3-3- Process of Modelling Simulation Data for the External Envelope of Residential buildings

After the complete definition of the algorithm through the **Colibri cycle**, the simulation process was conducted. For this purpose, the cycle was incrementally structured based on the limited variations in the geometric specifications of the residential buildings, as shown in the table 3-12.

Table 3-12. States of the Building Model Under Simulation

Variable	States	Number of States
X dim of Residential building	8; 10; 12; 14; 16; 18; 20; 22 meters	8
Y dim of Residential building	8; 10; 12; 14; 16; 18; 20; 22 meters	8
Z dim of Residential building	2.6; 2.8; 3; 3.2; 3.4; 3.6, 3.8; 4 meters	8
Angle Relative to the Y Axis	45; 30; 15; 0; -15; -30; -45 Degrees	7

After simulating the final sample models, the data was categorized based on the climatic characteristics of Melbourne for a single-story building, using spatial data that included the building's length, width, orientation, footprint area, aspect ratio (length to width), and volume, as well as energy data such as the total energy consumption of the model building, heating demand, cooling demand, daylighting requirements, and daylight illumination levels, all organized in Excel. This data was examined and evaluated in two formats. The evaluations were conducted in three sections: descriptive statistics, Pearson correlation tests, and regression analysis. Initially, the descriptive statistics of the spatial layout factors of the external envelope of the single-story residential buildings and energy performance were qualitatively and quantitatively analysed. Ultimately, the relationship between each of the spatial layout factors and the energy performance indicators was assessed through Pearson correlation testing. Following the correlation test results, a nonlinear regression test was conducted for each of the spatial layout factors and energy performance indicators. Additionally, to model energy performance based on the set of spatial layout factors, both linear and nonlinear regression tests were performed for each energy performance indicator and across all spatial layout factors of the external envelope, and the results were evaluated.

3-3-3-1- Examination of Descriptive Statistics

Descriptive statistics are evaluated in two sections: spatial data and energy performance data. In this context, the mean, median, standard deviation, variance, minimum, and maximum values for each parameter are analyzed. Additionally, all performance objectives based on the relevant models are plotted on a chart for qualitative analysis.

3-3-3-2- Conducting the Correlation Test

Initially, the correlation test between the geometric parameters and energy performance results is conducted on a one-to-one basis to identify significant relationships. The correlation coefficient is a statistical tool used to determine the type and degree of the relationship between one quantitative variable and another. The correlation coefficient is one of the criteria used to assess the correlation between two variables. It indicates both the strength of the relationship and the type of relationship (positive or negative). This coefficient ranges from 1 to -1, and if there is no relationship between the two variables, it equals zero.

In this analysis, the Pearson correlation test is used based on the variables. The Pearson correlation test is a parametric method applicable to data with a normal distribution or a large number of data points. Significance is reported only for these tests because, according to Amrhein et al. (2019), the significance coefficient does not necessarily indicate whether the data is significant or not; it merely provides a report that can assist in this assessment. Given the presence of 6 geometric parameters and 5 performance objectives, a total of 30 correlation tests are conducted.

3-3-3-3- Conducting the Regression Test

Subsequently, the regression test is performed on the data. Regression analysis in statistical models is a statistical process used to estimate relationships between variables. This method encompasses various techniques for modeling and analyzing specific and unique variables, focusing on the relationship between the dependent variable and one or more independent variables. Regression analysis particularly aids in understanding how the value of the dependent variable changes with the alteration of each independent variable while keeping other independent variables constant.

Based on regression tests, mathematical models can be defined between independent and dependent variables that predict the dependent variable based on independent variables, with a specified error margin. In this research, three regression tests—curvilinear, linear, and nonlinear—are conducted between the mentioned geometric parameters and simulated performance objectives. Initially, curvilinear regression tests are conducted between the variables on a one-to-one basis, followed by linear and nonlinear regression tests based on the presumed relationships. In the regression test process, the curvilinear regression test is

first performed between the variables one at a time. Curvilinear regression evaluates the relationship between two variables based on predefined models and predicts which model fits the data best. In this study, all 11 possible models are included in the curvilinear regression test conducted using SPSS software (Table 3-13).

Table 3-13. Predefined Models and Formulas for Each Variable

Model	Formula: X is the dependent variable and Y is the independent variable
Linear	$Y = a + bX$
Logarithmic	$Y = a + (b \times lnX)$
Inverse	$Y = a + (b / X)$
Quadratic	$Y = a + (b_1 \times X) + (b_2 \times X^2)$
Cubic	$Y = a + (b_1 \times X) + (b_2 \times X^2) + (b_3 \times X^3)$
Compound	$Y = a(b1^X)$
Power	$lnY = lna + (b_1 \times lnX)$ or $Y = aX^{b1}$
S	$Y = 1 / (1 + e^{-X})$
Growth	$Y = e^{a+b_1 x}$
Exponential	$Y = ae^{b_1 x}$
Logistic	$Y = 1 / (1/u + ab_1^X)$; Maximum Limit: u

Then, based on the results obtained from curvilinear regression, linear and nonlinear regression tests are performed, assuming that the established significant relationships are linear and nonlinear. The findings from this section can define the predictive model of the relationships under investigation. To achieve the relationships and models of the research, this section initially considers the probable relationships between the architectural and energy variables. Linear regression, also known as ordinary least squares regression, is one of the regression analysis methods. Regression is a type of statistical model used to predict one variable based on one or more other variables.

Linear regression is a method of regression analysis in which a type of linear predictor function describes the effect of the dependent variable on independent variables. The final answer is obtained according to the following formula, where A is the dependent variable influenced by 5 independent variables Bi.

$$A = a + (b_1 B_1) + (b_2 B_2) + (b_3 B_3) + (b_4 B_4) + (b_5 B_5)$$

The final answer will be the sum of the products plus a constant value, which is also derived in the estimation process. The simplest type of linear regression is simple linear regression, which, unlike multiple linear regression, has only one independent variable. Another type of

linear regression is multivariate linear regression, where instead of predicting one dependent variable, multiple dependent variables are predicted.

Subsequently, the nonlinear regression test is conducted based on the results obtained from curvilinear regression. In this test, for each relationship between the independent and dependent variables, a relationship obtained in the curvilinear regression is defined. Finally, the results of linear and nonlinear regression are compared, and the more optimal models are selected.

3-3-3-4- Process of Optimizing Energy Performance of Residential Building Envelopes

In the following, based on the generative design algorithm for the external configuration of residential buildings defined in the previous section, the optimization of the characteristics of the external envelope configuration is carried out quantitatively. This optimization focuses on energy performance through the Non-Dominated Sorting Genetic Algorithm II (NSGA-II). The performance objectives for the optimization process include cooling demand per square meter, heating demand per square meter, and daylight factor.

The optimization in this section is conducted using the Wallacei tool. To achieve this, a comprehensive optimization process is first performed with the discretization steps used in the previous section. In this optimization, considering the broadness of the response environment, a population of 30 and 100 generations are specified. The spatial layout factors considered in this section are the longitudinal dimensions of the residential building, orientation, and height of the unit. The discretization in this phase is defined with greater frequency compared to the modeling process, due to the use of evolutionary algorithms.

Table 3-14. Evolutionary Process Settings of Wallacei

	Crossover Probability	Mutation Probability	Crossover Distribution Index	Mutation Distribution Index	Distribution Mode
Amount	**0.9**	1 divided by the number of genes	**20**	**20**	**1**

In all genetic algorithms with Non-Dominated Sorting (NSGA-II), identical evolutionary process settings have been defined based on the designers' recommendations, as shown in the table. Accordingly, the crossover probability is set at 0.9, and the mutation probability is defined as one divided by the number of genes in the optimization process (Table 3-14).

3-4- Conclusion

Based on the discussions, this research method clearly adopts a quantitative approach rooted in performative computational architecture. The primary methodologies utilized in this study include coding, energy performance simulation, and optimization of geometric variables for residential buildings based on energy performance, all within the programming environment of Grasshopper in Rhino, specifically for residential applications. Furthermore, the configurations obtained from coding have undergone statistical evaluation.

This research focuses on single-story residential buildings commonly found in Melbourne. Overall, the methodology is structured into twelve sections, encompassing the selection of design variables, definition of the statistical population of the models under study, formulation of the generative design algorithm, selection of energy simulation sample models, definition of energy zones and energy simulation settings, establishment of the first computational performance cycle algorithm, execution of the initial computational cycle process, analysis of the data obtained from energy simulation, modeling processes aimed at developing predictive models for energy performance, definition of the optimization algorithm and settings for the optimization cycles, execution of the computational optimization processes, and analysis of the data obtained from the defined optimization.

Chapter 4:

Results

Chapter 4: Results

4-1- Introduction

This study aims to optimize the geometric characteristics of single-story residential buildings in Melbourne based on Building Energy Performance (BEP) using the Performative Computational Architecture (PCA) framework and a quantitative approach. The findings of this research are derived from coding, energy performance simulation, and optimization of residential building based on energy performance. As outlined in the previous chapter, the results are presented in two main sections: the results of the energy performance modeling of the building envelope and the optimization of the energy performance of the building envelope.

4-2- Modelling Energy Performance of Residential buildings

In this section of the research, a dynamic simulation process using parametric modelling of the building envelope has been conducted with a quantitative approach. The simulation focuses on single-story buildings with northern daylighting and a window-to-wall ratio of 10% on the northern facade. Additionally, as detailed in the research methodology, the execution and thermal specifics of timber-framed construction have been considered as the building system in the simulation.

Table 4-1. Descriptive Statistics of the Architectural Factors for the Simulated Single-story residential buildings Models

Architectural Factors	Number	Minimum	Maximum	Median	Standard Deviation	Variance
Dimensions of the North-South Side	3584	8	22	15.00	4.583	21.006
Dimensions of the East-West Side	3584	8	22	15.00	4.583	21.006
Building Floor Area	3584	64	484	225.00	99.467	9893.761
Building Height	3584	2.6	4.0	3.300	.4583	.210
Building Orientation	3584	-45	45	.00	30.004	900.251
Building Volume	3584	166.4	1936.0	742.500	347.0662	120454.959
Window-to-North Wall Ratio	3584	.200	.846	.463	.1575	.025
Width of the North Window	3584	3.577	20.237	10.062	3.578	12.804
Height of the North Window	3584	1.442	2.966	2.192	.380	.145
Area of the North Window	3584	6.399	48.400	22.500	9.946	98.938

To assess the impact of spatial factors on the energy consumption of single-story residential buildings, various dimensions have been analysed, including the north-south and east-west dimensions of the building, unit heights, and building orientation, based on the climatic conditions of Melbourne, Australia. A descriptive statistical summary of all simulation scenarios is presented in the table 4-1 and 4-2.

The simulation of the energy performance of residential buildings has focused on total energy consumption, energy consumption per square meter, heating demand, heating demand per square meter, cooling demand, and cooling demand per square meter. Based on the generative models, the variables of building area, building volume, as well as the width, height, and area of the northern windows and the window-to-wall ratio of the northern façade are provided in the output and have been utilized in the modeling process.

Table 4-2. Analysis of Descriptive Statistics of Energy Performance Results Based on All Simulations

	Number	Minimum	Maximum	Median	Standard Deviation	Variance
Total Energy Consumption	3584	10298.622	73836.993	34152.410	13570.975	184171387.380
Energy Consumption per Square Meter	3584	133.713	204.342	155.371	11.755	138.193
Cooling Demand	3584	1257.221	10098.598	4505.171	1984.396	3937830.975
Cooling Demand per Square Meter	3584	19.405	21.130	20.045	.493	.244
Heating Demand	3584	2883.683	17180.031	8001.600	2505.516	6277615.095
Heating Demand per Square Meter	3584	17.950	87.125	39.123	11.662	136.005
Lighting Demand	3584	271.560	2053.674	954.704	422.052	178128.687
Average Useful daylight illuminance	3584	37.276	82.384	68.687	10.502	110.298
Average Daylight autonomy Index	3584	28.830	75.391	47.929	9.307	86.638

The descriptive data of the input and output parameters of the research's generative algorithm, including minimum, maximum, median, standard deviation, and variance, are presented in the table. In this simulation, all research scheduling programs, except for the occupancy schedule, are defined based on the ASHRAE 90.1 2019 standard, specifically the Midrise Apartment schedule and its Apartment subgroup. The occupancy schedule is also based on the findings of this research, using the Australian National Construction Code (NCC, 2022). The energy performance simulation algorithm is connected to the Colibri algorithm, and all samples have been simulated. Accordingly, within the established steps, a total of 3,584 single-story residential buildings morphology samples has been energy-simulated based on the climatic conditions of Melbourne, Australia. The energy consumption simulation results in the Colibri plugin have been organized and saved as an SPSS file. Initially, the descriptive statistics of the energy performance results, based on all simulations conducted, have been reviewed. According to the 3,584 simulated samples, the minimum energy consumption per square meter, 133.713 kWh/m², corresponds to a single-story residential building with dimensions of 22 by 22 meters, oriented at 15 degrees, and a residential building height of 2.6 meters. Additionally, the minimum total energy consumption, 10,298.62 kWh, is associated with a building measuring 8 by 8 meters, with an orientation of 0 degrees and a residential building height of 2.6 meters. The maximum total energy consumption was 73,836.99 kWh, corresponding to a building with dimensions of 22 by 22 meters, oriented at -45 degrees, and a residential building height of 4 meters.

Furthermore, the maximum energy consumption per square meter was 204.342 kWh/m², which is associated with a building measuring 8 by 8 meters, oriented at -45 degrees, and a residential building height of 4 meters. The descriptive statistics of energy consumption results, based on all simulations conducted, for the minimum and maximum energy consumption per square meter and total energy consumption, are presented in the table 4-3.

Table 4-3. Analysis of Descriptive Statistics of Energy Consumption Results Based on All Simulations

Performance Objective	Target	East-West Dimension	North-South Dimension	Building Area	Building Height	Orientation Angle	Building Volume	Window-to-Wall Ratio	North Window Width	North Window Height	North Window Area	Performance Target Value
Total Energy Consumption	Minimum Value	8	8	64	2.6	0	166.4	0.307	4.437	1.442	6.400	10298.62
		8	8	64	2.6	15	166.4	0.307	4.437	1.442	6.400	10303.41
		8	8	64	2.6	-15	166.4	0.307	4.437	1.442	6.400	10358.4
	Maximum Value	22	22	484	4	-45	1936	0.55	16.315	2.966	48.399	73836.99
		22	22	484	4	-30	1936	0.55	16.315	2.966	48.399	72893.01
		22	22	484	4	45	1936	0.55	16.315	2.966	48.399	72876.44
Energy Consumption per square meter	Minimum Value	22	22	484	2.6	15	1258.4	0.846	20.237	2.391	48.4	133.7131
		22	22	484	2.6	0	1258.4	0.846	20.237	2.391	48.4	133.7142
		20	22	440	2.6	0	1144	0.846	18.397	2.391	44	134.3503
	Maximum Value	8	8	64	4	-45	256	0.2	3.577	1.788	6.399	204.342
		8	8	64	4	45	256	0.2	3.577	1.788	6.399	202.5209
		8	8	64	4	-30	256	0.2	3.577	1.788	6.399	201.837

The minimum cooling demand per square meter is 19.4 kWh, corresponding to a building with an east-west dimension of 16 meters and a north-south dimension of 22 meters, with a height of 2.8 meters and an orientation angle of 15 degrees. The maximum cooling demand per square meter is 19.4 kWh, associated with a building with an east-west dimension of 22 meters and a north-south dimension of 8 meters, with a height of 2.6 meters and an orientation angle of -45 degrees. The minimum total cooling demand is 1,257.22 kWh, corresponding to a building with an east-west dimension of 8 meters and a north-south dimension of 8 meters, with a height of 2.8 meters and an orientation angle of 0 degrees. The maximum cooling demand per square meter is 10,096.6 kWh/m², associated with a building with an east-west dimension of 22 meters and a north-south dimension of 22 meters, with a height of 3.2 meters and an orientation angle of -45 degrees. The descriptive statistics of cooling demand results, based on all simulations conducted, for the minimum and

maximum cooling demand per square meter and total cooling demand, are presented in the table 4-4.

Table 4-4. Analysis of Descriptive Statistics of Cooling Demand Results Based on All Simulations

Performance Objective	Target	East-West Dimension	North-South Dimension	Building Area	Building Height	Orientation Angle	Building Volume	Window-to-Wall Ratio	North Window Width	North Window Height	North Window Area	Performance Target Value
Total Cooling Demand	Minimum Value	8	8	64	2.8	0	179.2	0.285	4.276	1.496	6.4	1257.222
		8	8	64	2.6	15	166.4	0.307	4.437	1.442	6.400	1257.246
		8	8	64	2.8	15	179.2	0.285	4.276	1.496	6.4	1257.419
	Maximum Value	22	22	484	3.2	-45	1548.8	0.6875	18.241	2.653	48.4	10098.6
		22	22	484	3.8	-45	1839.2	0.578	16.739	2.891	48.399	10096.81
		22	22	484	2.6	-45	1258.4	0.846	20.237	2.391	48.4	10095.55
Cooling Demand per Square Meter	Minimum Value	16	22	352	2.8	15	985.6	0.785	14.182	2.481	35.2	19.405
		14	22	308	2.6	15	800.8	0.846	12.878	2.391	30.8	19.407
		18	22	396	2.8	15	1108.8	0.785	15.955	2.481	39.600	19.412
	Maximum Value	22	8	176	2.6	-45	457.6	0.307	12.203	1.442	17.600	21.130
		20	8	160	2.6	-45	416	0.307	11.094	1.442	16.000	21.124
		22	8	176	3.2	-45	563.2	0.25	11	1.6	17.6	21.120

The minimum heating demand per square meter is 17.95 kWh/m², associated with a building with an east-west dimension of 22 meters and a north-south dimension of 22 meters, with a height of 2.6 meters and an orientation angle of 0 degrees. The maximum heating demand per square meter is 87.125 kWh/m², corresponding to a building with an east-west dimension of 8 meters and a north-south dimension of 8 meters, with a height of 4 meters and an orientation angle of -45 degrees. The minimum total heating demand is 2,884.684 kWh, related to a building with an east-west dimension of 8 meters and a north-south dimension of 8 meters, with a height of 2.6 meters and an orientation angle of 0 degrees. The maximum total heating demand is 17,180.03 kWh, associated with a building with an east-west dimension of 22 meters and a north-south dimension of 22 meters, with a height of 4 meters and an orientation angle of -45 degrees. The descriptive statistics of heating demand results, based on all simulations conducted, for the minimum and maximum heating demand per square meter and total heating demand, are presented in the table 4-5.

Additionally, an analysis of lighting demand indicates a clear dependence on the unit area. Accordingly, the minimum lighting demand is associated with a building measuring 8 meters by 8 meters, while the maximum lighting demand is associated with a building

measuring 22 meters by 22 meters. To further investigate lighting demand, two indices, the Useful daylight illuminance and the Daylight autonomy Index, are also considered.

Table 4-5. Analysis of Descriptive Statistics of Heating Demand Results Based on All Simulations

Performance Objective	Target	East-West Dimension	North-South Dimension	Building Area	Building Height	Orientation Angle	Building Volume	Window-to-Wall Ratio	North Window Width	North Window Height	North Window Area	Performance Target Value
Total Heating Demand	Minimum Value	8	8	64	2.6	0	166.4	0.307	4.4376	1.442	6.400	2883.684
		8	8	64	2.6	15	166.4	0.307	4.437	1.442	6.400	2889.18
		8	8	64	2.6	-15	166.4	0.307	4.4376	1.442	6.400	2915.96
	Maximum Value	22	22	484	4	-45	1936	0.55	16.315	2.966	48.399	17180.03
		22	22	484	4	45	1936	0.55	16.315	2.966	48.399	16747.76
		22	22	484	4	-30	1936	0.55	16.315	2.966	48.399	16427.77
Heating Demand per square Meter	Minimum Value	22	22	484	2.6	0	1258.4	0.846	20.237	2.391	48.4	17.950
		22	22	484	2.6	15	1258.4	0.846	20.237	2.391	48.4	18.079
		22	22	484	2.6	-15	1258.4	0.846	20.237	2.391	48.4	18.269
	Maximum Value	8	8	64	4	-45	256	0.2	3.577	1.788	6.399	87.125
		8	8	64	4	45	256	0.2	3.577	1.788	6.399	86.006
		8	8	64	4	-30	256	0.2	3.577	1.788	6.399	85.042

The minimum average Useful daylight illuminance is associated with a building with an east-west dimension of 8 meters and a north-south dimension of 22 meters, with a height of 2.6 meters and an orientation angle of -15 degrees. Conversely, the maximum average Useful daylight illuminance is linked to a building with an east-west dimension of 8 meters and a north-south dimension of 8 meters, with a height of 4 meters and an orientation angle of -45 degrees. Additionally, the maximum average Daylight autonomy Index is associated with the same building dimensions (8 meters by 8 meters), height (4 meters), and orientation angle (-45 degrees). The minimum average Daylight autonomy Index is associated with a building with an east-west dimension of 8 meters and a north-south dimension of 22 meters, with a height of 2.6 meters and an orientation angle of -15 degrees.

Based on the findings, alterations in the architectural features of the buildings studied can lead to changes of up to 63,538 kWh in the total annual energy consumption of the residential buildings, which is a significant amount. According to this section's findings, variations in building geometrical factors in Melbourne can alter residential energy consumption by up to 86%. Additionally, changes in the architectural features of the buildings studied can result in a variation of up to 71 kWh per square meter in the total annual energy consumption of

the residential buildings, which is also notable. These findings suggest that changes in building geometrical factors in Melbourne can affect residential energy consumption by up to 34% (Table 4-6).

Table 4-6. Analysis of Descriptive Statistics of Daylight Results Based on All Simulations

Performance Objective	Target Objective	East-West Side Dimensions	North-South Side Dimensions	Building Area	Building Height	Orientation Angle	Building Volume	Window-to-Wall Ratio	North Window Width	North Window Height	North Window Area	Targeted Performance Level
Daylight Useful Index	Minimum Value	8	22	176	2.6	-15	457.6	0.846	7.358	2.391	17.6	37.276
		8	22	176	2.6	0	457.6	0.846	7.358	2.391	17.6	37.3
		8	22	176	2.6	-45	457.6	0.846	7.358	2.391	17.6	37.427
	Maximum Value	8	8	64	4	-45	256	0.2	3.577	1.788	6.399	82.384
		8	8	64	3.8	-45	243.2	0.210	3.670	1.743	6.400	81.872
		8	8	64	4	-30	256	0.2	3.577	1.788	6.399	81.720
Daylight autonomy Index	Minimum Value	8	22	176	2.6	-45	457.6	0.846	7.358	2.391	17.6	28.830
		8	22	176	2.6	-30	457.6	0.846	7.358	2.391	17.6	29.478
		8	22	176	2.6	-15	457.6	0.846	7.358	2.391	17.6	29.880
	Maximum Value	10	8	80	4	30	320	0.2	4.472	1.788	7.999	75.391
		10	8	80	4	15	320	0.2	4.472	1.788	7.999	75.203
		10	8	80	4	0	320	0.2	4.472	1.788	7.999	75.014

The changes in the architectural features studied in this research result in a variation of approximately 8,841 kWh and 87% in the cooling demand of the residential buildings. These changes can also lead to approximately 2 kWh per square meter and a 9% variation in cooling demand per square meter. Furthermore, the alterations in architectural features lead to about 70 kWh per square meter and an 86% change in heating demand per square meter of the residential building. Additionally, the changes result in a variation of 14,297 kWh and 83% in total heating demand. In terms of daylight performance, the architectural changes lead to a variation of 45 units and 52% in the average Useful daylight illuminance. The average Daylight autonomy Index also shows a variation of approximately 47 units and 62%. These figures underscore the significant impact of building geometrical factors on energy performance, which is crucial for urban planning and the formulation of city planning and architectural regulations.

4-2-1- Results of Correlation Analysis

Initially, correlation analysis is performed on the data pairwise to identify significant relationships (Table 4-7; 4-8). The correlation coefficient is a statistical tool used to determine the type and degree of the relationship between two quantitative variables. The correlation coefficient is one of the criteria used to assess the correlation between two variables. It indicates both the strength and the type (positive or negative) of the relationship. This coefficient ranges from -1 to 1, with a value of 0 indicating no relationship between the two variables. In this context, Pearson's correlation test is utilized based on the variables.

Table 4-7. Results of Correlation Test Between Architectural Factors and Performance Objectives

		Global Energy Per Area	Cooling Energy Per Area	Heating Energy Per Area	Lighting Energy Per Area	Global Energy	Cooling Energy	Heating Energy	Lighting Energy	UDI Average	DA Average
EW Side Dimention	Pearson Correlation	-.498**	.004	-.503**	.b	.690**	.694**	.548**	.691**	.281**	.103**
	Sig. (2-tailed)	.000	.805	.000	.	.000	.000	.000	.000	.000	.000
	N	3584	3584	3584	3584	3584	3584	3584	3584	3584	3584
NS Side Dimention	Pearson Correlation	-.506**	-.154**	-.504**	.b	.689**	.686**	.547**	.691**	-.743**	-.787**
	Sig. (2-tailed)	.000	.000	.000	.	.000	.000	.000	.000	.000	.000
	N	3584	3584	3584	3584	3584	3584	3584	3584	3584	3584
Area of Building	Pearson Correlation	-.690**	-.103**	-.691**	.b	.993**	.998**	.768**	1.000**	-.255**	-.446**
	Sig. (2-tailed)	.000	.000	.000	.	.000	.000	.000	.000	.000	.000
	N	3584	3584	3584	3584	3584	3584	3584	3584	3584	3584
Height of Building	Pearson Correlation	.636**	.021	.640**	.b	.112**	.001	.606**	.000	.376**	.536**
	Sig. (2-tailed)	.000	.209	.000	.	.000	.947	.000	1.000	.000	.000
	N	3584	3584	3584	3584	3584	3584	3584	3584	3584	3584
NS Direction towards the North	Pearson Correlation	-.060**	-.754**	-.028	.b	-.012	-.043**	-.028	.000	.042*	.105**
	Sig. (2-tailed)	.000	.000	.093	.	.490	.009	.092	1.000	.011	.000
	N	3584	3584	3584	3584	3584	3584	3584	3584	3584	3584
Volume of Building	Pearson Correlation	-.481**	-.092**	-.481**	.b	.976**	.944**	.924**	.946**	-.113**	-.271**
	Sig. (2-tailed)	.000	.000	.000	.	.000	.000	.000	.000	.000	.000
	N	3584	3584	3584	3584	3584	3584	3584	3584	3584	3584

**. Correlation is significant at the 0.01 level (2-tailed).

*. Correlation is significant at the 0.05 level (2-tailed).

b. Cannot be computed because at least one of the variables is constant.

Pearson Correlation is a parametric method used for data that follows a normal distribution or when the sample size is large. In these tests, only significance is reported. According to Amrhein et al. (2019), the significance coefficient alone does not necessarily indicate the meaningfulness of the data; it is simply a report that can assist in this assessment. Based on the simulation results, Pearson correlation tests are conducted between architectural factors

and performance objectives. The results are presented in the table. The tables provided examine the correlation between general architectural characteristics of residential buildings with energy performance objectives and window specifications of residential buildings with energy performance objectives.

Table 4-8: Results of Correlation Test Between Architectural Factors and Performance Objectives

		Global Energy Per Area	Cooling Energy Per Area	Heating Energy Per Area	Lighting Energy Per Area	Global Energy	Cooling Energy	Heating Energy	Lighting Energy	UDI Average	DA Average
WWR of North Facade	Pearson Correlation	-.706**	-.148**	-.705**	.b	.571**	.617**	.228**	.622**	-.853**	-.915**
	Sig. (2-tailed)	.000	.000	.000	.	.000	.000	.000	.000	.000	.000
	N	3584	3584	3584	3584	3584	3584	3584	3584	3584	3584
Width of Window	Pearson Correlation	-.772**	-.069**	-.775**	.b	.901**	.930**	.592**	.930**	-.121**	-.351**
	Sig. (2-tailed)	.000	.000	.000	.	.000	.000	.000	.000	.000	.000
	N	3584	3584	3584	3584	3584	3584	3584	3584	3584	3584
Height of Window	Pearson Correlation	-.222**	-.133**	-.218**	.b	.673**	.625**	.747**	.629**	-.498**	-.515**
	Sig. (2-tailed)	.000	.000	.000	.	.000	.000	.000	.000	.000	.000
	N	3584	3584	3584	3584	3584	3584	3584	3584	3584	3584
Area of Window	Pearson Correlation	-.690**	-.103**	-.691**	.b	.993**	.998**	.768**	1.000**	-.255**	-.446**
	Sig. (2-tailed)	.000	.000	.000	.	.000	.000	.000	.000	.000	.000
	N	3584	3584	3584	3584	3584	3584	3584	3584	3584	3584

**. Correlation is significant at the 0.01 level (2-tailed).

*. Correlation is significant at the 0.05 level (2-tailed).

b. Cannot be computed because at least one of the variables is constant.

According to the correlation test findings, the highest correlation between performance objectives and architectural factors is observed in the relationship between the floor area and energy consumption, as well as cooling demand, with correlation coefficients of 0.993 and 0.998, respectively. Among window specifications, the highest correlation is found in the window area with energy consumption and cooling demand per square meter, with correlation coefficients of 0.993 and 0.998, respectively. Following these factors, the next highest correlations are related to the building volume with total energy consumption, cooling demand, heating demand, and lighting demand.

4-2-2- Results of Curve Regression Testing

Subsequently, regression tests are conducted on the data based on the significant relationships identified through correlation results. Regression testing is a method used to identify new software defects or regressions in active and inactive areas of the system after

making changes such as optimizations, patches, or configuration modifications. Initially, curve regression tests are performed between variables on a pairwise basis. This process forms the basis for the modeling sought in the research. Curve Regression evaluates the relationship between two variables based on predefined model types and predicts which model best fits the data.

In this study, all 11 possible models in SPSS software were tested using curve regression. The predefined models are listed in the table below. Based on the results from curve regression, both linear and nonlinear regression tests are conducted assuming the relationships are significant. Thus, in this section, the curve regression test for architectural factors and performance objectives is conducted pairwise.

In this section, the relationship between energy consumption per square meter and the east-west dimension is examined. According to the findings from the curve regression test, the highest F-statistic is related to the inverse relationship, and the highest R-squared value corresponds to the **inverse and cubic model**. Thus, the relationship between the two variables is identified as an inverse equation. Based on the results of the regression test, a moderate relationship is detected between the two variables (Table 4-9).

Table 4-9. Results of Curve Regression Between Energy Consumption per Square Meter and the East-West Dimension

Model formula	Model Results		Model Diagram
	R Square	F	
Linear	.248	1183.731	
Logarithmic	.266	1299.209	
Inverse	.274	1349.307	
Quadratic	.272	668.175	
Cubic	.274	449.523	
Compound	.251	1198.244	
Power	.267	1306.497	
S	.273	1347.402	
Growth	.251	1198.244	
Exponential	.251	1198.244	
Logistic	.251	1198.244	

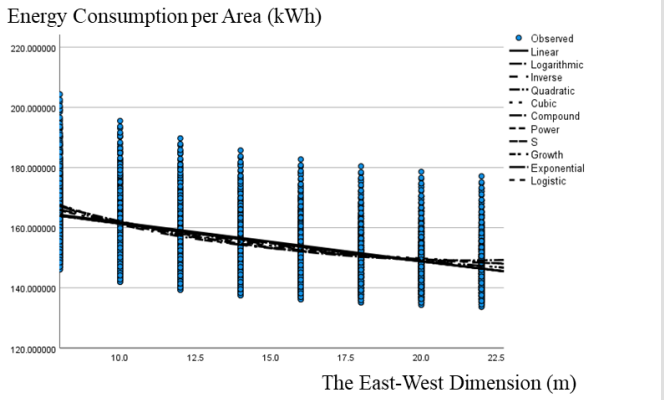

Dependent Variable: Global Energy Per Area
The independent variable is EW Side Dimention.

In this section, the relationship between cooling demand per square meter and the east-west dimension is examined (Table 4-10). Based on the findings from the curve regression test, the highest F-statistic is associated with the linear relationship, and the R-squared values for all relationships are close to zero. Consequently, the relationship between the two variables

is identified as a **linear equation** with a prediction accuracy close to zero. Based on the results of the curve regression test, a weak relationship is detected between the two variables.

Table 4-10. Results of Curve Regression Between Cooling Demand per Square Meter and the East-West Dimension

Model formula	Model Results		Model Diagram
	R Square	F	
Linear	.000	.061	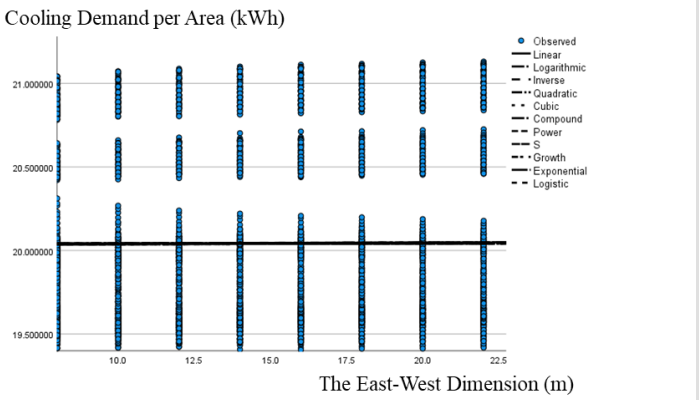
Logarithmic	.000	.053	
Inverse	.000	.043	
Quadratic	.000	.034	
Cubic	.000	.024	
Compound	.000	.051	
Power	.000	.043	
S	.000	.034	
Growth	.000	.051	
Exponential	.000	.051	
Logistic	.000	.051	

Dependent Variable: Cooling Energy Per Area

The independent variable is EW Side Dimention.

In this section, the relationship between heating demand per square meter and the east-west dimensions of the east-west side has been examined. Based on the findings from the curvature regression test, the highest F-statistic was related to the inverse relationship, and the highest R-squared value was associated with the inverse and cubic relationship. Therefore, the relationship between the two variables is identified as an **inverse equation**. In addition, based on the results of the regression test, a moderate and direct relationship is detected between the two variables. The R-squared values in this test were less than 0.3 in all equations (Table 4-11).

Table 4-11. Results of Curve Regression Between Heating Demand per Square Meter and the East-West Dimensions

Model formula	Model Results		Model Diagram
	R Square	F	
Linear	.253	1210.327	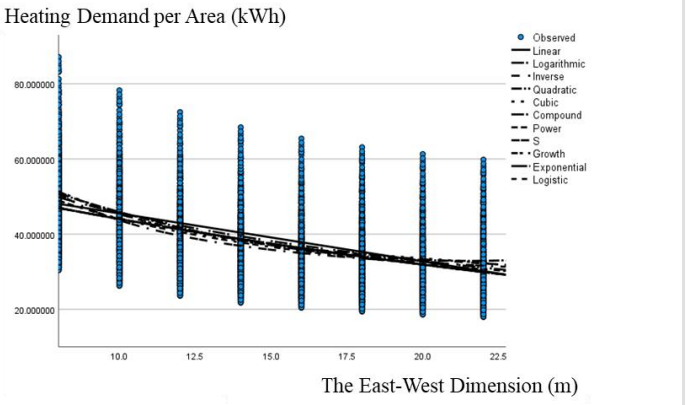
Logarithmic	.271	1328.999	
Inverse	.278	1380.440	
Quadratic	.276	683.561	
Cubic	.278	459.890	
Compound	.256	1232.956	
Power	.269	1318.458	
S	.271	1332.352	
Growth	.256	1232.956	
Exponential	.256	1232.956	
Logistic	.256	1232.956	

Dependent Variable: Heating Energy Per Area

The independent variable is EW Side Dimention.

In this section, the relationship between energy consumption and the dimensions of the east-west side has been examined. Based on the findings from the curvature regression test, the highest F-statistic was associated with the power model, and the highest R-squared value was also related to the **power model**. Therefore, the relationship between the two variables is identified as a power equation (Table 4-12).

Table 4-12. Results of Curve Regression Between Energy Consumption and the East-West Dimensions

Model formula	Model Results		Model Diagram
	R Square	F	
Linear	.476	3254.433	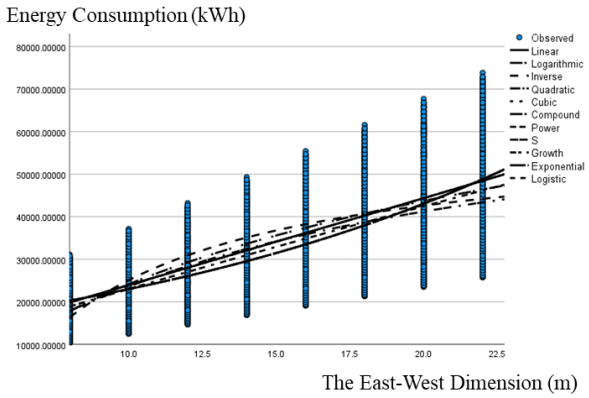
Logarithmic	.466	3124.989	
Inverse	.437	2779.530	
Quadratic	.476	1626.784	
Cubic	.476	1084.221	
Compound	.486	3391.163	
Power	.494	3492.495	
S	.480	3312.655	
Growth	.486	3391.163	
Exponential	.486	3391.163	
Logistic	.486	3391.163	

Dependent Variable: Global Energy
The independent variable is EW Side Dimention.

In this section, the relationship between cooling demand and the dimensions of the east-west side has been examined. Based on the findings from the curvature regression test, the highest F-statistic was associated with the power relationship, and the highest R-squared value was also related to the power relationship. Therefore, the relationship between the two variables is identified as a **power equation**. In addition, based on the results of the regression test, a moderate and direct relationship is detected between the two variables (Table 4-13).

Table 4-13. Results of Curve Regression Between Cooling Demand and the East-West Dimensions

Model formula	Model Results		Model Diagram
	R Square	F	
Linear	.482	3327.065	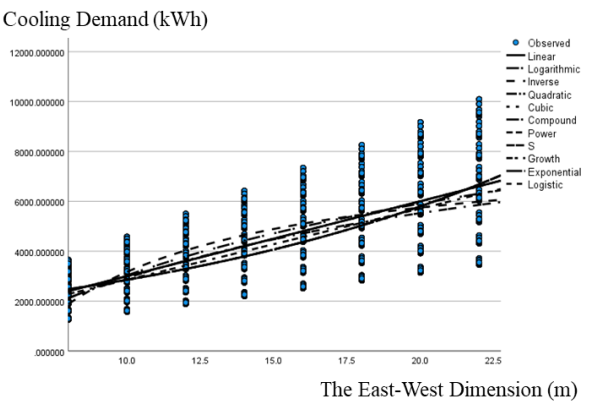
Logarithmic	.472	3197.858	
Inverse	.443	2844.908	
Quadratic	.482	1663.068	
Cubic	.482	1108.403	
Compound	.494	3501.243	
Power	.505	3648.565	
S	.494	3496.481	
Growth	.494	3501.243	
Exponential	.494	3501.243	
Logistic	.494	3501.243	

Dependent Variable: Cooling Energy
The independent variable is EW Side Dimention.

In this section, the relationship between heating demand and the dimensions of the east-west side has been examined. Based on the findings from the curvature regression test, the highest F-statistic and the highest R-squared value were associated with the composite, logistic, and growth relationships. Therefore, the relationship between the two variables is identified as a **compound equation**. In addition, based on the results of the regression test, a moderate and direct relationship is detected between the two variables (Table 4-14).

Table 4-14. Results of Curve Regression Between Heating Demand and the East-West Dimensions

Model formula	Model Results		Model Diagram
	R Square	F	
Linear	.300	1535.963	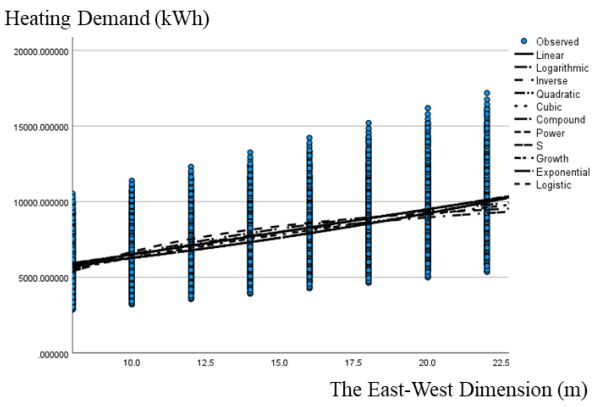
Logarithmic	.292	1480.187	
Inverse	.273	1344.298	
Quadratic	.300	768.121	
Cubic	.300	511.952	
Compound	.308	1597.293	
Power	.307	1588.840	
S	.293	1486.877	
Growth	.308	1597.293	
Exponential	.308	1597.293	
Logistic	.308	1597.293	

Dependent Variable: Heating Energy
The independent variable is EW Side Dimention.

In this section, the relationship between lighting demand and the dimensions of the east-west side has been examined (Table 4-15). Based on the findings from the curvature regression test, the highest F-statistic and the highest R-squared value were associated with the **power model**. Therefore, the relationship between the two variables is identified as a power equation.

Table 4-15. Results of Curve Regression Between Lighting Demand and the East-West Dimensions

Model formula	Model Results		Model Diagram
	R Square	F	
Linear	.478	3276.220	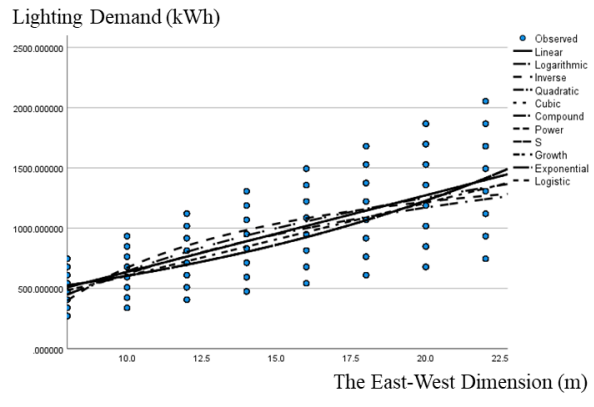
Logarithmic	.468	3150.188	
Inverse	.439	2804.943	
Quadratic	.478	1637.652	
Cubic	.478	1091.463	
Compound	.490	3438.308	
Power	.500	3582.000	
S	.489	3434.370	
Growth	.490	3438.308	
Exponential	.490	3438.308	
Logistic	.490	3438.308	

Dependent Variable: Lighting Energy
The independent variable is EW Side Dimention.

In this section, the relationship between the average useful daylight and the dimensions of the east-west side has been examined. Based on the findings from the curvature regression test, the highest F-statistic and the highest R-squared value were associated with the **S-curve model**. Therefore, the relationship between the two variables is identified as an S-curve equation (Table 4-16).

Table 4-16. Results of Curve Regression Between Average UDI and the East-West Dimensions

Model formula	Model Results		Model Diagram
	R Square	F	
Linear	.079	306.704	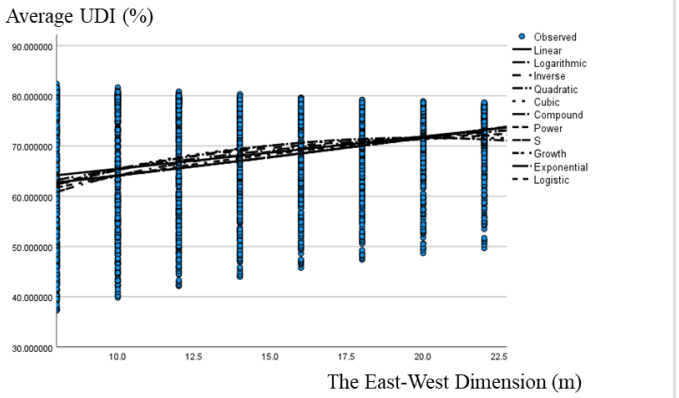
Logarithmic	.087	341.003	
Inverse	.092	361.082	
Quadratic	.092	182.293	
Cubic	.093	122.045	
Compound	.090	354.309	
Power	.099	394.349	
S	.105	418.013	
Growth	.090	354.309	
Exponential	.090	354.309	
Logistic	.090	354.309	

Dependent Variable: UDI Average
The independent variable is EW Side Dimention.

In this section, the relationship between the average daylight autonomy and the dimensions of the east-west side has been examined. Based on the findings from the curvature regression test, the highest F-statistic and the highest R-squared value were associated with the S-curve relationship. Therefore, the relationship between the two variables is identified as an **S-curve equation**. Based on the results of the curve regression test, a weak relationship is detected between the two variables (Table 4-17).

Table 4-17. Results of Curve Regression Between Average DA and the East-West Dimensions

Model formula	Model Results		Model Diagram
	R Square	F	
Linear	.011	38.614	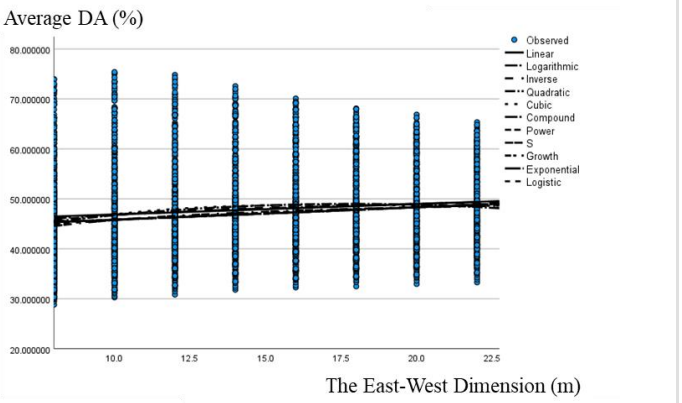
Logarithmic	.013	46.284	
Inverse	.015	52.723	
Quadratic	.016	28.948	
Cubic	.016	19.837	
Compound	.016	58.989	
Power	.019	68.663	
S	.021	76.185	
Growth	.016	58.989	
Exponential	.016	58.989	
Logistic	.016	58.989	

Dependent Variable: DA Average
The independent variable is EW Side Dimention.

In this section, the relationship between energy consumption per square meter and the dimensions of the north-south side has been examined. Based on the findings, the highest F-statistic was associated with the inverse equation, and the highest R-squared value was related to the inverse, **S-curve, and cubic model**. Therefore, the relationship between the two variables is identified as an S-curve equation (Table 4-18).

Table 4-18. Results of Curve Regression Between Energy Consumption per Square Meter and the North-South Dimensions

Model formula	Model Results		Model Diagram
	R Square	F	
Linear	.257	1235.818	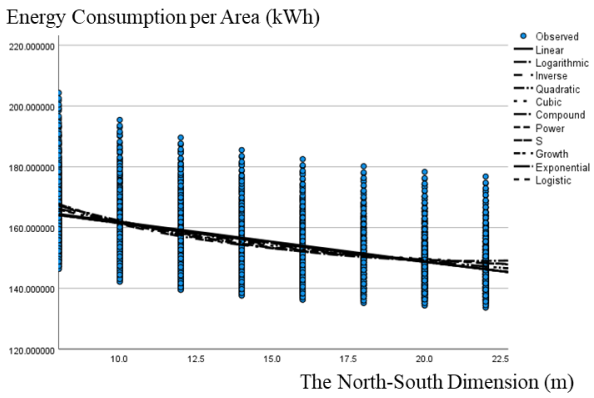
Logarithmic	.275	1356.021	
Inverse	.282	1407.084	
Quadratic	.280	696.766	
Cubic	.282	468.695	
Compound	.259	1251.762	
Power	.276	1364.240	
S	.282	1405.434	
Growth	.259	1251.762	
Exponential	.259	1251.762	
Logistic	.259	1251.762	

Dependent Variable: Global Energy Per Area
The independent variable is NS Side Dimention.

In this section, the relationship between cooling demand per square meter and the dimensions of the north-south side has been examined. Based on the findings from the curvature regression test, the highest F-statistic and the highest R-squared value were associated with the **power model**. Therefore, the relationship between the two variables is identified as a power equation (Table 4-19).

Table 4-19. Results of Curve Regression Between Cooling Demand per Square Meter and the North-South Dimensions

Model formula	Model Results		Model Diagram
	R Square	F	
Linear	.024	87.347	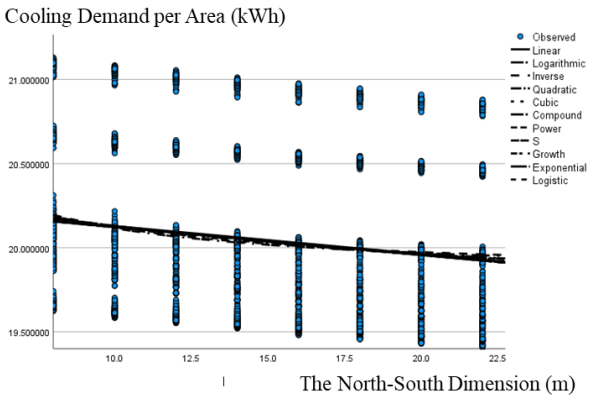
Logarithmic	.024	88.225	
Inverse	.023	85.330	
Quadratic	.024	44.161	
Cubic	.024	29.436	
Compound	.024	88.847	
Power	.024	89.705	
S	.024	86.727	
Growth	.024	88.847	
Exponential	.024	88.847	
Logistic	.024	88.847	

Dependent Variable: Cooling Energy Per Area
The independent variable is NS Side Dimention.

In this section, the relationship between heating demand per square meter and the dimensions of the north-south side has been examined. Based on the findings from the curvature regression test, the highest F-statistic was associated with the inverse equation, and the highest R-squared value was related to the **inverse and cubic model**. Therefore, the relationship between the two variables is identified as an S-curve equation (Table 4-20).

Table 4-20. Results of Curve Regression Between Heating Demand per Square Meter and the North-South Dimensions

Model formula	Model Results		Model Diagram
	R Square	F	
Linear	.254	1219.653	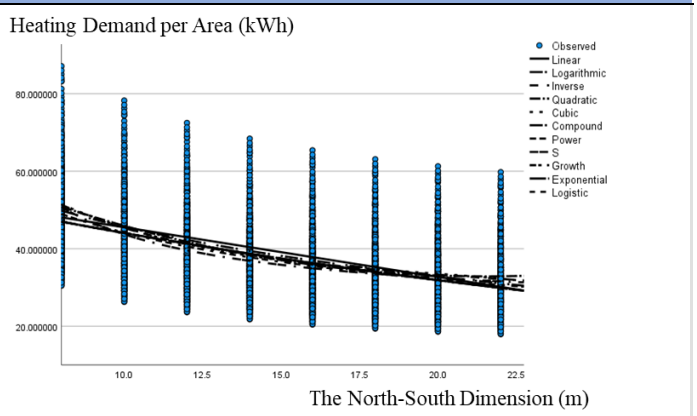
Logarithmic	.272	1339.219	
Inverse	.280	1390.890	
Quadratic	.278	688.720	
Cubic	.280	463.358	
Compound	.258	1242.773	
Power	.271	1328.747	
S	.273	1342.387	
Growth	.258	1242.773	
Exponential	.258	1242.773	
Logistic	.258	1242.773	

Dependent Variable: Heating Energy Per Area
The independent variable is NS Side Dimention.

In this section, the relationship between energy consumption and the north-south dimensions has been examined. Based on the findings from the curvature regression test, the highest F-statistic and the highest R-squared value were associated with the **power model**. Therefore, the relationship between the two variables is identified as a power equation (Table 4-21).

Table 4-21. Results of Curve Regression Between Energy Consumption and the North-South Dimensions

Model formula	Model Results		Model Diagram
	R Square	F	
Linear	.474	3229.571	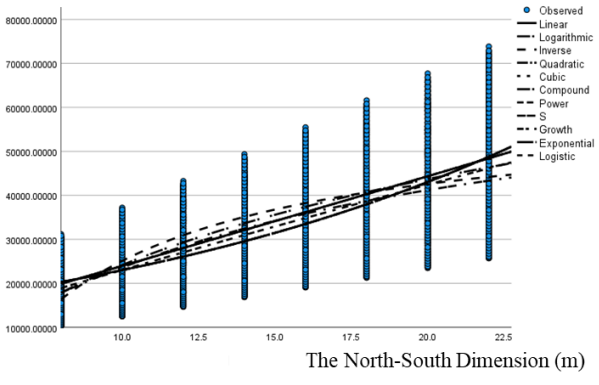
Logarithmic	.464	3102.207	
Inverse	.435	2760.858	
Quadratic	.474	1614.351	
Cubic	.474	1075.934	
Compound	.484	3363.377	
Power	.492	3463.717	
S	.478	3286.286	
Growth	.484	3363.377	
Exponential	.484	3363.377	
Logistic	.484	3363.377	

Dependent Variable: Global Energy
The independent variable is NS Side Dimention.

In this section, the relationship between cooling demand and the dimensions of the north-south side has been examined. Based on the findings, the highest F-statistic and the highest R-squared value were associated with the **power model**. Therefore, the relationship between the two variables is identified as a power equation (Table 4-22).

Table 4-22. Results of Curve Regression Between Cooling Demand and the North-South Dimensions

Model formula	Model Results		Model Diagram
	R Square	F	
Linear	.471	3186.127	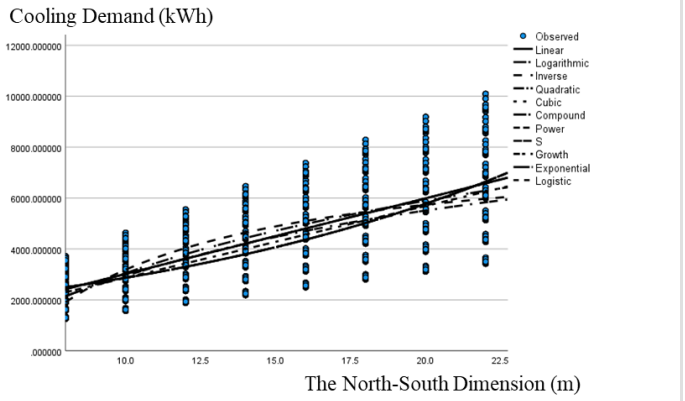
Logarithmic	.461	3068.543	
Inverse	.433	2738.869	
Quadratic	.471	1592.632	
Cubic	.471	1061.458	
Compound	.483	3339.989	
Power	.493	3478.452	
S	.482	3337.962	
Growth	.483	3339.989	
Exponential	.483	3339.989	
Logistic	.483	3339.989	

Dependent Variable: Cooling Energy
The independent variable is NS Side Dimention.

In this section, the relationship between heating demand and the dimensions of the north-south side has been examined. Based on the findings from the curvature regression test, the highest F-statistic and the highest R-squared value were associated with the **compound, growth, and logistic relationships**. Therefore, the relationship between the two variables is identified as a composite equation (Table 4-23).

Table 4-23. Results of Curve Regression Between Heating Demand and the North-South Dimensions

Model formula	Model Results		Model Diagram
	R Square	F	
Linear	.299	1525.434	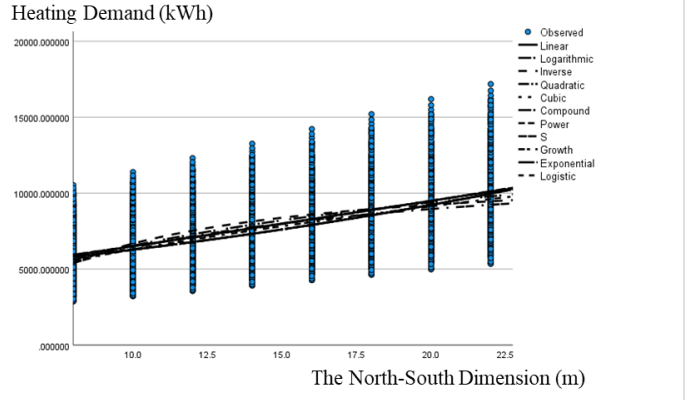
Logarithmic	.291	1470.368	
Inverse	.272	1335.809	
Quadratic	.299	762.841	
Cubic	.299	508.433	
Compound	.307	1585.942	
Power	.306	1577.694	
S	.292	1476.763	
Growth	.307	1585.942	
Exponential	.307	1585.942	
Logistic	.307	1585.942	

Dependent Variable: Heating Energy
The independent variable is NS Side Dimention.

In this section, the relationship between lighting demand and the dimensions of the north-south side has been examined. Based on the findings, the highest F-statistic and the highest R-squared value were associated with the **S-curve model**. Therefore, the relationship between the two variables is identified as an S-curve equation (Table 4-24).

Table 4-24. Results of Curve Regression Between Lighting Demand and the North-South Dimensions

Model formula	Model Results		Model Diagram
	R Square	F	
Linear	.478	3276.220	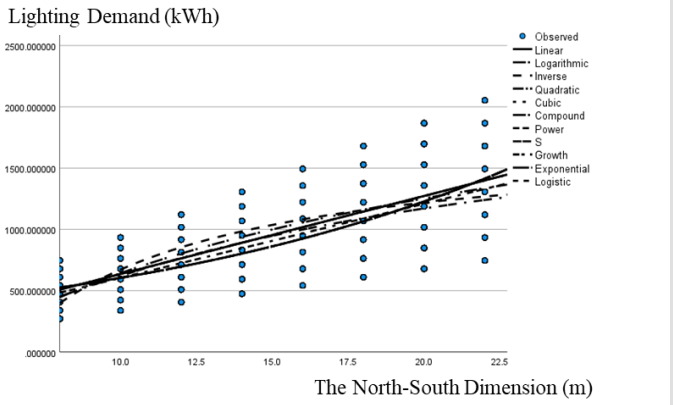
Logarithmic	.468	3150.188	
Inverse	.439	2804.943	
Quadratic	.478	1637.652	
Cubic	.478	1091.463	
Compound	.490	3438.308	
Power	.500	3582.000	
S	.489	3434.370	
Growth	.490	3438.308	
Exponential	.490	3438.308	
Logistic	.490	3438.308	

Dependent Variable: Lighting Energy
The independent variable is NS Side Dimention.

In this section, the relationship between the average useful daylight and the dimensions of the north-south side has been examined. Based on the findings, the highest F-statistic was associated with the linear equation, and the highest R-squared value was related to the **linear and cubic model**. Therefore, given the low F-statistic for the cubic curve, the relationship between the two variables is identified as a linear equation (Table 4-25).

Table 4-25. Results of Curve Regression Between Average UDI and the North-South Dimensions

Model formula	Model Results		Model Diagram
	R Square	F	
Linear	.552	4414.648	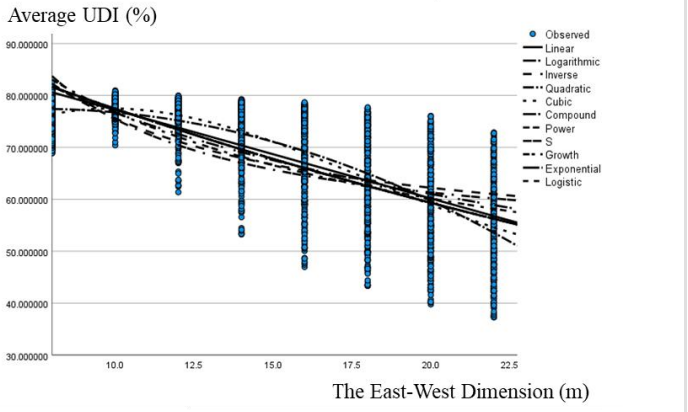
Logarithmic	.497	3542.411	
Inverse	.425	2643.318	
Quadratic	.592	2599.460	
Cubic	.599	1781.013	
Compound	.523	3932.268	
Power	.468	3146.812	
S	.396	2353.217	
Growth	.523	3932.268	
Exponential	.523	3932.268	
Logistic	.523	3932.268	

Dependent Variable: UDI Average
The independent variable is NS Side Dimention.

In this section, the relationship between the average daylight autonomy and the dimensions of the north-south side has been examined. Based on the findings, the highest F-statistic was associated with the logarithmic equation, and the highest R-squared value was related to the **power, quadratic and cubic curves**. Therefore, the relationship between the two variables is identified as a logarithmic equation (Table 4-26).

Table 4-26. Results of Curve Regression Between Average DA and the North-South Dimensions

Model formula	Model Results		Model Diagram
	R Square	F	
Linear	.619	5816.968	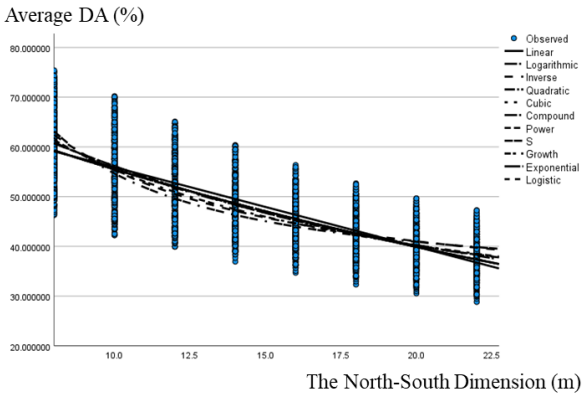
Logarithmic	.631	6124.337	
Inverse	.616	5741.854	
Quadratic	.632	3068.417	
Cubic	.632	2045.042	
Compound	.630	6090.054	
Power	.631	6113.149	
S	.605	5476.278	
Growth	.630	6090.054	
Exponential	.630	6090.054	
Logistic	.630	6090.054	

Dependent Variable: DA Average
The independent variable is NS Side Dimention.

In this section, the relationship between energy consumption per square meter and the building area has been examined. Based on the findings from the curvature regression test, the highest F-statistic was associated with the power equation, and the highest R-squared value was related to the **cubic and power relationship**. Therefore, based on the R-squared value of the power equation, the relationship between the two variables is identified as a power equation (Table 4-27).

Table 4-27. Results of Curve Regression Between Energy Consumption per Square Meter and the Building Area

Model formula	Model Results		Model Diagram
	R Square	F	
Linear	.476	3249.412	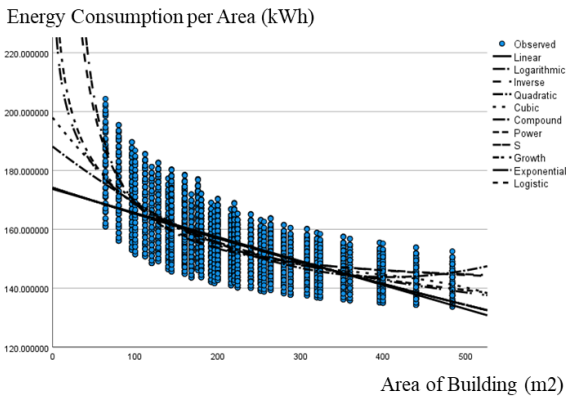
Logarithmic	.541	4217.512	
Inverse	.533	4085.119	
Quadratic	.539	2093.510	
Cubic	.546	1436.752	
Compound	.486	3384.299	
Power	.543	4256.749	
S	.525	3958.873	
Growth	.486	3384.299	
Exponential	.486	3384.299	
Logistic	.486	3384.299	

Dependent Variable: Global Energy Per Area
The independent variable is Area of Building.

In this section, the relationship between cooling demand per square meter and the building's floor area has been examined. Based on the findings from the curvature regression test, the highest F-statistic and the highest R-squared value were associated with the **power model**. Therefore, based on the overall findings, the relationship between the two variables is identified as a power equation (Table 4-28).

Table 4-28. Results of Curve Regression Between Cooling Demand per Square Meter and the Building Area

Model formula	Model Results		Model Diagram
	R Square	F	
Linear	.011	38.707	
Logarithmic	.011	41.411	
Inverse	.011	38.412	
Quadratic	.011	20.481	
Cubic	.011	13.769	
Compound	.011	39.555	
Power	.012	42.334	
S	.011	39.284	
Growth	.011	39.555	
Exponential	.011	39.555	
Logistic	.011	39.555	

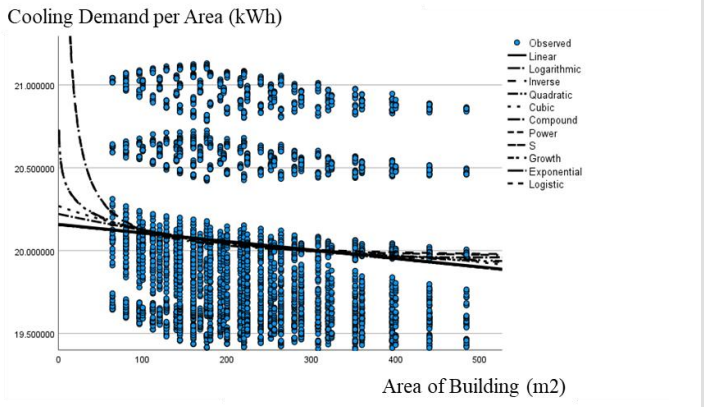

Dependent Variable: Cooling Energy Per Area
The independent variable is Area of Building.

In this section, the relationship between heating demand per square meter and the building area has been examined. Based on the findings, the highest F-statistic was associated with the logarithmic equation, and the highest R-squared value was related to the **cubic and logarithmic model**. Based on the R-squared value and the F-statistic, the relationship between the two variables is identified as a logarithmic equation (Table 4-29).

Table 4-29. Results of Curve Regression Between Heating Demand per Square Meter and the Building Area

Model formula	Model Results		Model Diagram
	R Square	F	
Linear	.477	3270.088	
Logarithmic	.543	4251.744	
Inverse	.535	4120.903	
Quadratic	.541	2111.010	
Cubic	.548	1449.057	
Compound	.505	3657.594	
Power	.540	4198.635	
S	.496	3528.545	
Growth	.505	3657.594	
Exponential	.505	3657.594	
Logistic	.505	3657.594	

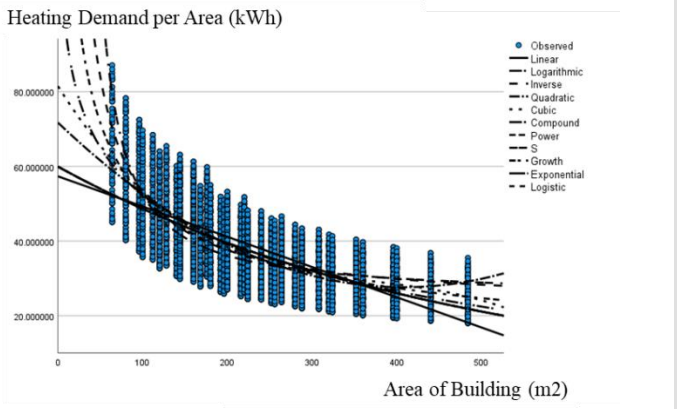

Dependent Variable: Heating Energy Per Area
The independent variable is Area of Building.

In this section, the relationship between energy consumption and the building area has been examined. Based on the findings from the curvature regression test, the highest F-statistic was associated with the linear equation, and the highest R-squared value was related to the **linear, quadratic, and cubic model**. Therefore, the relationship between the two variables is identified as a linear equation. In addition, based on the results of the regression test, a strong and direct relationship is detected between the two variables (Table 4-30).

Table 4-30. Results of Curve Regression Between Energy Consumption and the Building Area

Model formula	Model Results		Model Diagram
	R Square	F	
Linear	.986	245360.528	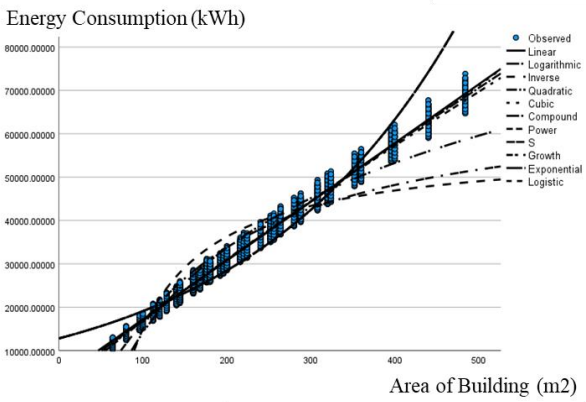
Logarithmic	.930	47618.202	
Inverse	.750	10758.711	
Quadratic	.986	124346.303	
Cubic	.986	83204.317	
Compound	.928	45869.876	
Power	.985	239744.693	
S	.905	34066.049	
Growth	.928	45869.876	
Exponential	.928	45869.876	
Logistic	.928	45869.876	

Dependent Variable: Global Energy
The independent variable is Area of Building.

In this section, the relationship between cooling demand and the building's floor area has been examined. Based on the findings from the curvature regression test, the highest F-statistic and the highest R-squared value were associated with the **power relationship**. Given all the results, it can be concluded that the relationship between the two variables is identified as a power equation (Table 4-31).

Table 4-31. Results of Curve Regression Between Cooling Demand and the Building Area

Model formula	Model Results		Model Diagram
	R Square	F	
Linear	.996	955625.147	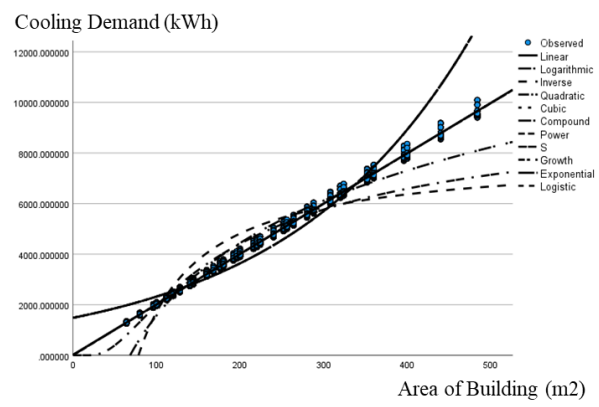
Logarithmic	.933	49912.160	
Inverse	.746	10504.489	
Quadratic	.996	477937.133	
Cubic	.996	318537.809	
Compound	.933	50100.781	
Power	.997	1291578.066	
S	.921	42000.537	
Growth	.933	50100.781	
Exponential	.933	50100.781	
Logistic	.933	50100.781	

Dependent Variable: Cooling Energy
The independent variable is Area of Building.

In this section, the relationship between heating demand and the building's floor area has been examined. Based on the findings, overall, the highest F-statistic and the highest R-squared value were associated with the **power relationship**. Therefore, according to the results of the curvature regression test, the relationship between the two variables is identified as a power equation. In addition, based on the results of the regression test, a moderate and direct relationship is detected between the two variables (Table 4-32).

Table 4-32. Results of Curve Regression Between Heating Demand and the Building Area

Model formula	Model Results		Model Diagram
	R Square	F	
Linear	.589	5138.023	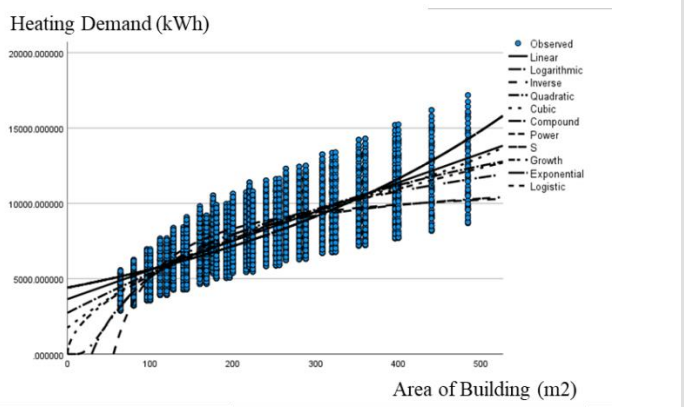
Logarithmic	.583	5016.701	
Inverse	.498	3555.302	
Quadratic	.595	2627.689	
Cubic	.596	1763.109	
Compound	.574	4816.935	
Power	.613	5674.794	
S	.569	4724.550	
Growth	.574	4816.935	
Exponential	.574	4816.935	
Logistic	.574	4816.935	

Dependent Variable: Heating Energy

The independent variable is Area of Building.

In this section, the relationship between lighting demand and the building's floor area has been examined. Based on the findings from the curvature regression test, the highest F-statistic and the highest R-squared value were associated with the **linear relationship** between the two variables. Therefore, according to the results, the relationship between the two variables is identified as a linear equation (Table 4-33).

Table 4-33. Results of Curve Regression Between Lightng Demand and the Building Area

Model formula	Model Results		Model Diagram
	R Square	F	
Linear	1.000	460911253292599740.000	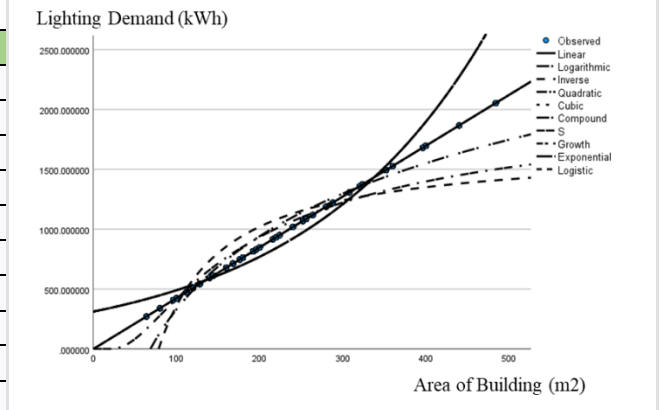
Logarithmic	.936	52263.311	
Inverse	.747	10597.661	
Quadratic	1.000	230391289508782144.000	
Cubic	1.000	153551301580921568.000	
Compound	.936	52263.311	
Power	.	.	
S	.924	43549.410	
Growth	.936	52263.311	
Exponential	.936	52263.311	
Logistic	.936	52263.311	

Dependent Variable: Lighting Energy

The independent variable is Area of Building.

In this section, the relationship between the average useful daylight and the building area has been examined. Based on the findings from the curvature regression test, the highest F-statistic was associated with the inverse equation, and the highest R-squared value was related to the cubic model. Therefore, the relationship between the two variables is identified as an **inverse equation**. Based on the results of the curve regression test, a weak relationship is detected between the two variables (Table 4-34).

Table 4-34. Results of Curve Regression Between Average UDI and the Building Area

Model formula	Model Results		Model Diagram
	R Square	F	
Linear	.065	248.758	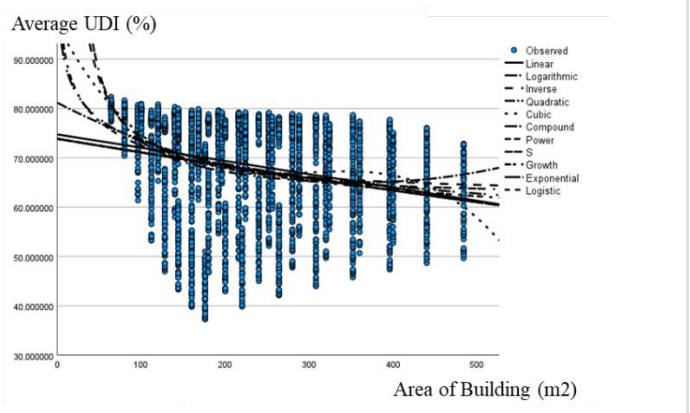
Logarithmic	.084	329.238	
Inverse	.098	389.941	
Quadratic	.081	157.002	
Cubic	.104	138.800	
Compound	.051	191.318	
Power	.068	261.588	
S	.082	318.723	
Growth	.051	191.318	
Exponential	.051	191.318	
Logistic	.051	191.318	

Dependent Variable: UDI Average
The independent variable is Area of Building.

In this section, the relationship between the average daylight autonomy and the building area has been examined. Based on the findings from the curvature regression test, the highest F-statistic was associated with the inverse equation, and the highest R-squared value was related to the **inverse, quadratic, and cubic model**. Therefore, the relationship between the two variables is identified as an inverse equation (Table 4-35).

Table 4-35. Results of Curve Regression Between Average DA and the Building Area

Model formula	Model Results		Model Diagram
	R Square	F	
Linear	.199	890.749	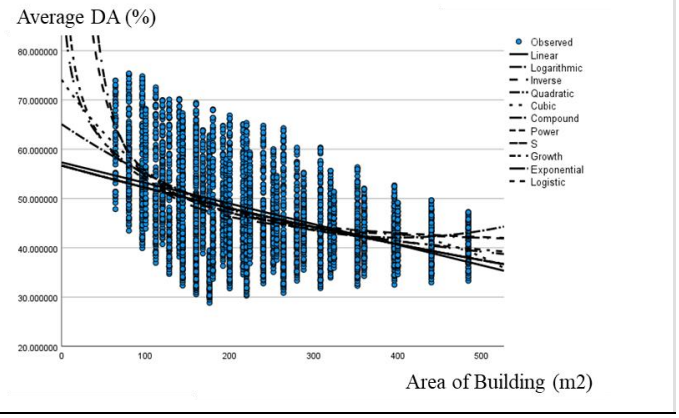
Logarithmic	.232	1082.941	
Inverse	.238	1116.587	
Quadratic	.228	529.441	
Cubic	.238	372.720	
Compound	.187	822.402	
Power	.216	985.550	
S	.219	1004.211	
Growth	.187	822.402	
Exponential	.187	822.402	
Logistic	.187	822.402	

Dependent Variable: DA Average
The independent variable is Area of Building.

In this section, the relationship between energy consumption per square meter and building height has been examined. Based on the findings from the curvature regression test, the highest F-statistic and the highest R-squared value were associated with the compoond, growth, and logistic equations. Therefore, the relationship between the two variables is identified as a **compound equation** (Table 4-36).

Table 4-36. Results of Curve Regression Between Energy Consumption per Square Meter and Building Height

Model formula	Model Results		Model Diagram
	R Square	F	
Linear	.404	2432.011	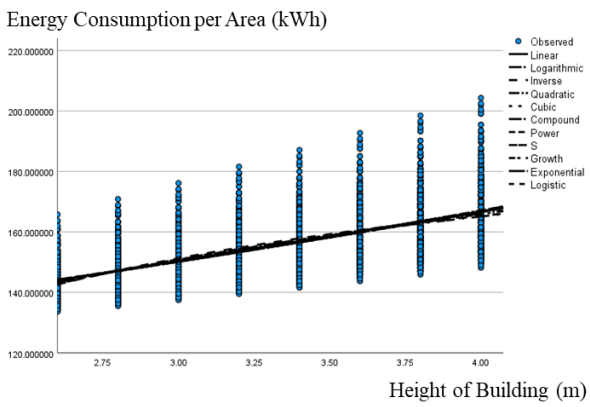
Logarithmic	.401	2402.804	
Inverse	.396	2344.197	
Quadratic	.405	1217.248	
Cubic	.405	1217.248	
Compound	.415	2539.575	
Power	.413	2519.675	
S	.408	2467.881	
Growth	.415	2539.575	
Exponential	.415	2539.575	
Logistic	.415	2539.575	

Dependent Variable: Global Energy Per Area
The independent variable is Height of Building.

In this section, the relationship between cooling demand per square meter and building height has been examined. Based on the findings from the curvature regression test, the highest F-statistic was associated with the composite, growth, and logistic equations, while the R-squared values for all equations were zero. Therefore, the relationship between the two variables is identified as a **compound equation** (Table 4-37).

Table 4-37. Results of Curve Regression Between Cooling Demand per Square Meter and Building Height

Model formula	Model Results		Model Diagram
	R Square	F	
Linear	.000	1.580	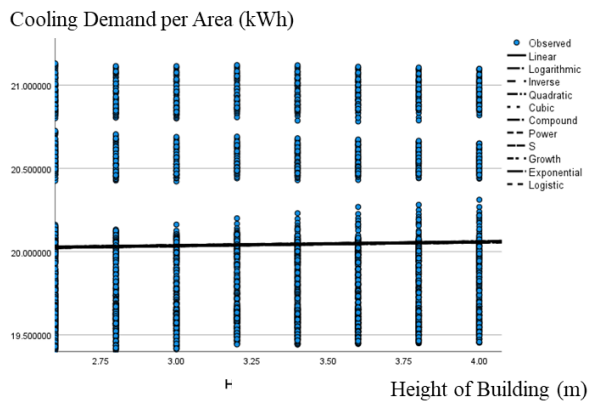
Logarithmic	.000	1.551	
Inverse	.000	1.505	
Quadratic	.000	.797	
Cubic	.000	.797	
Compound	.000	1.643	
Power	.000	1.613	
S	.000	1.566	
Growth	.000	1.643	
Exponential	.000	1.643	
Logistic	.000	1.643	

Dependent Variable: Cooling Energy Per Area
The independent variable is Height of Building.

In this section, the relationship between heating demand per square meter and building height has been examined. Based on the findings the highest R-squared value were associated with the power relationship. Therefore, the relationship between the two variables is identified as a **power equation**. In addition, based on the results of the regression test, a moderate and direct relationship is detected between the two variables. The R-squared values in this test were less than 0.45 in all equations (Table 4-38).

Table 4-38. Results of Curve Regression Regression Between Heating Demand per Square Meter and Building Height

Model formula	Model Results		Model Diagram
	R Square	F	
Linear	.410	2486.685	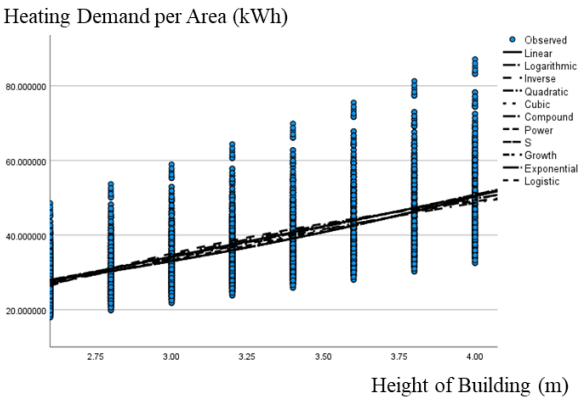
Logarithmic	.407	2456.619	
Inverse	.401	2396.255	
Quadratic	.410	1244.617	
Cubic	.410	1244.617	
Compound	.441	2820.626	
Power	.442	2836.511	
S	.440	2813.997	
Growth	.441	2820.626	
Exponential	.441	2820.626	
Logistic	.441	2820.626	

Dependent Variable: Heating Energy Per Area
The independent variable is Height of Building.

In this section, the relationship between total building energy consumption and building height has been examined. Based on the findings from the curvature regression test, the highest F-statistic and the highest R-squared value were associated with the compound, growth, and logistic equations. Therefore, the relationship between the two variables is identified as a **compound equation** (Table 4-39).

Table 4-39. Results of Curve Regression Between Energy Consumption and Building Height

Model formula	Model Results		Model Diagram
	R Square	F	
Linear	.013	45.600	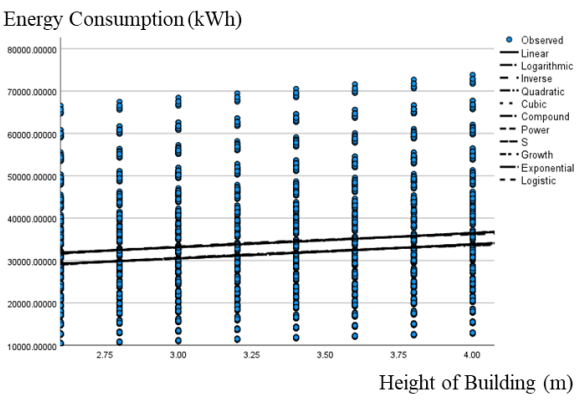
Logarithmic	.012	45.264	
Inverse	.012	44.584	
Quadratic	.013	22.813	
Cubic	.013	22.813	
Compound	.013	48.520	
Power	.013	48.294	
S	.013	47.699	
Growth	.013	48.520	
Exponential	.013	48.520	
Logistic	.013	48.520	

Dependent Variable: Global Energy
The independent variable is Height of Building.

In this section, the relationship between cooling demand and building height is examined. Based on the findings of, the highest F-statistic values are associated with the **power, compound, growth, and logistic equations**, and the R-squared value obtained is close to zero. Accordingly, the relationship between the two variables can be selected from among these equations, although the prediction accuracy is close to zero (Table 4-40).

Table 4-40. Results of Curve Regression Between Cooling Demand and Building Height

Model formula	Model Results		Model Diagram
	R Square	F	
Linear	.000	.004	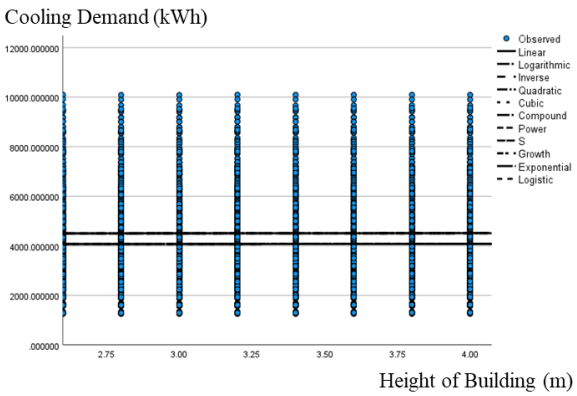
Logarithmic	.000	.004	
Inverse	.000	.004	
Quadratic	.000	.002	
Cubic	.000	.002	
Compound	.000	.005	
Power	.000	.005	
S	.000	.004	
Growth	.000	.005	
Exponential	.000	.005	
Logistic	.000	.005	

Dependent Variable: Cooling Energy
The independent variable is Height of Building.

In this section, the relationship between the total heating demand of the building and its height is examined. Based on the findings of the curvilinear regression test, the highest F-statistic and R-squared values correspond to the power relationship. Accordingly, the relationship between the two variables—total building heating demand and building height—is identified as a **power equation** (Table 4-41).

Table 4-41. Results of Curve Regression Between Heating Demand and Building Height

Model formula	Model Results		Model Diagram
	R Square	F	
Linear	.368	2083.170	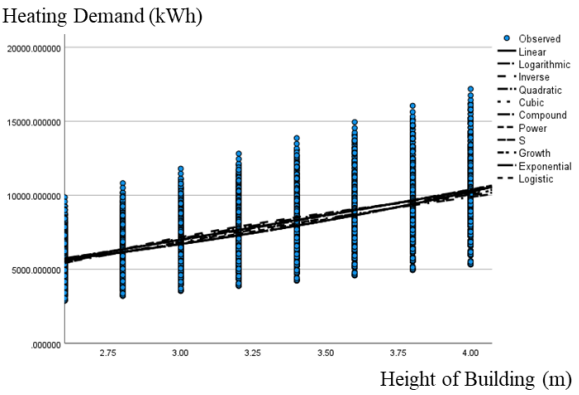
Logarithmic	.365	2059.309	
Inverse	.360	2011.641	
Quadratic	.368	1042.639	
Cubic	.368	1042.639	
Compound	.370	2106.332	
Power	.371	2116.863	
S	.370	2101.932	
Growth	.370	2106.332	
Exponential	.370	2106.332	
Logistic	.370	2106.332	

Dependent Variable: Heating Energy
The independent variable is Height of Building.

In this section, the relationship between lighting demand and building height is examined. According to the findings of the curvilinear regression test, both the F-statistic value and the R-squared value are zero. Therefore, no relationship is identified between the two variables. It is suggested to input the data into both linear and nonlinear regression models for further testing. Based on the results of the curve regression test, a weak relationship is detected between the two variables (Table 4-42).

Table 4-42. Results of Curve Regression Between Lighting Demand and Building Height

Model formula	Model Results		Model Diagram
	R Square	F	
Linear	.000	.000	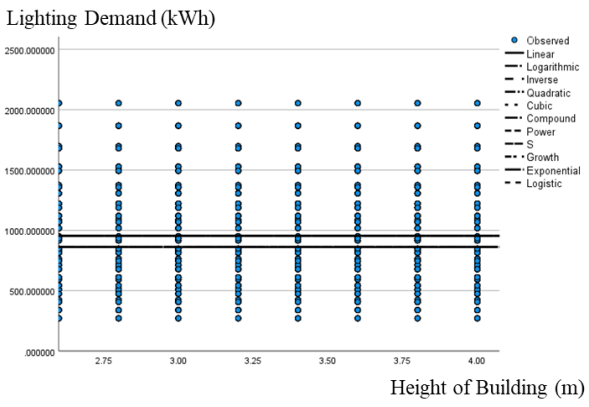
Logarithmic	.000	.000	
Inverse	.000	.000	
Quadratic	.000	.000	
Cubic	.000	.000	
Compound	.000	.000	
Power	.000	.000	
S	.000	.000	
Growth	.000	.000	
Exponential	.000	.000	
Logistic	.000	.000	

Dependent Variable: Lighting Energy
The independent variable is Height of Building.

In this section, the relationship between the average useful daylight and building height is examined. Based on the findings of the curvilinear regression test, the highest F-statistic value is associated with the inverse equation, and the highest R-squared value corresponds to the inverse, quadratic, and cubic relationships. Therefore, the relationship between the two variables is identified as an **inverse equation** (Table 4-43).

Table 4-43. Results of Curve Regression Between Average UDI and Building Height

Model formula	Model Results		Model Diagram
	R Square	F	
Linear	.141	590.133	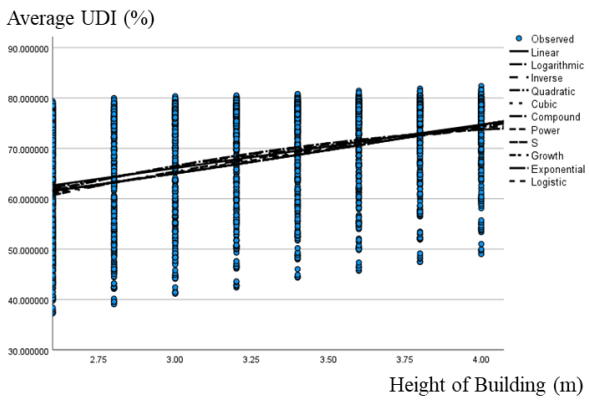
Logarithmic	.144	601.749	
Inverse	.145	608.198	
Quadratic	.145	304.524	
Cubic	.145	304.524	
Compound	.140	581.943	
Power	.143	595.322	
S	.144	603.670	
Growth	.140	581.943	
Exponential	.140	581.943	
Logistic	.140	581.943	

Dependent Variable: UDI Average
The independent variable is Height of Building.

In this section, the relationship between the average daylight autonomy and building height is examined. Based on the findings of the curvilinear regression test, the highest F-statistic and the highest R-squared value are associated with the S-curve relationship. Therefore, the relationship between the two variables, average daylight autonomy and building height, is identified as an **S-curve equation** (Table 4-44).

Table 4-44. Results of Curve Regression Between Average DA and Building Height

Model formula	Model Results		Model Diagram
	R Square	F	
Linear	.287	1443.634	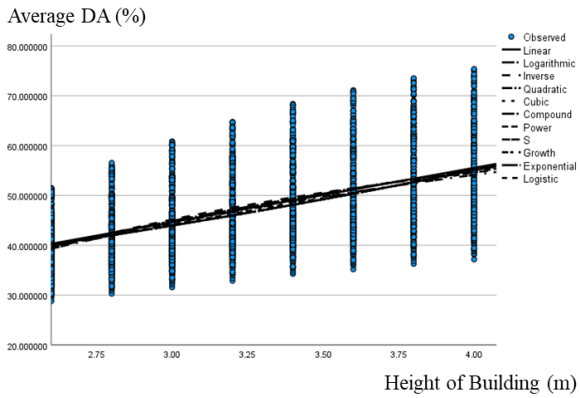
Logarithmic	.288	1449.483	
Inverse	.287	1439.829	
Quadratic	.288	724.628	
Cubic	.288	724.632	
Compound	.296	1506.187	
Power	.298	1523.499	
S	.299	1524.419	
Growth	.296	1506.187	
Exponential	.296	1506.187	
Logistic	.296	1506.187	

Dependent Variable: DA Average

The independent variable is Height of Building.

In this section, the relationship between energy consumption per square meter and the building orientation relative to the north is examined. Based on the findings, the highest F-statistic value is associated with the quadratic equation, and the highest R-squared value corresponds to the quadratic and cubic relationships. The relationship between the two variables is identified as a **quadratic equation** (Table 4-45).

Table 4-45. Results of Curve Regression Between Energy Consumption per Square Meter and the Building Orientation

Model formula	Model Results		Model Diagram
	R Square	F	
Linear	.004	12.747	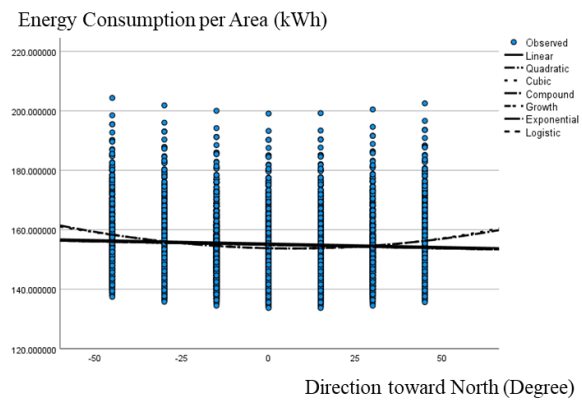
Logarithmic	.	.	
Inverse	.	.	
Quadratic	.017	30.424	
Cubic	.017	20.309	
Compound	.004	13.255	
Power	.	.	
S	.	.	
Growth	.004	13.255	
Exponential	.004	13.255	
Logistic	.004	13.255	

Dependent Variable: Global Energy Per Area

The independent variable is NS Direction towards the North.

a. The independent variable (NS Direction towards the North) contains non-positive values. The minimum value is -45. The Logarithmic and Power models cannot be calculated.

Also, the relationship between cooling demand per square meter and building orientation relative to the north is examined. The highest F-statistic value is associated with the quadratic equation, while the highest R-squared value corresponds to the cubic relationship. Thus the relationship is generally identified as a **quadratic equation** (Table 4-46).

Table 4-46. Results of Curve Regression Between Cooling Demand per Square Meter and the Building Orientation

Model formula	Model Results		Model Diagram
	R Square	F	
Linear	.569	4724.747	
Logarithmic	.	.	
Inverse	.	.	
Quadratic	.938	27028.788	
Cubic	.944	20008.010	
Compound	.566	4667.150	
Power	.	.	
S	.	.	
Growth	.566	4667.150	
Exponential	.566	4667.150	
Logistic	.566	4667.150	

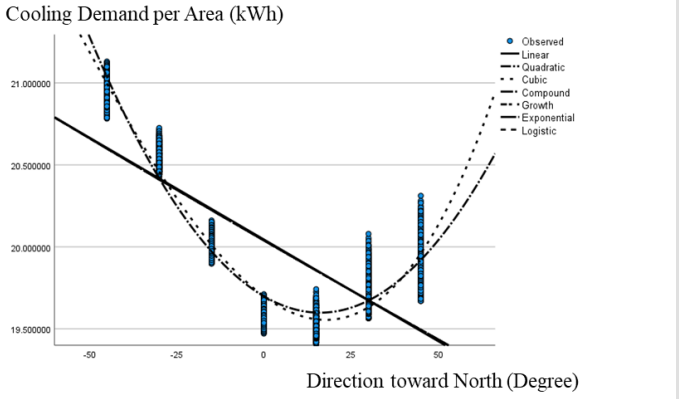

Dependent Variable: Cooling Energy Per Area

The independent variable is NS Direction towards the North.

a. The independent variable (NS Direction towards the North) contains non-positive values. The minimum value is -45. The Logarithmic and Power models cannot be calculated.

Also, the relationship between heating demand per square meter and building orientation relative to the north is examined. The highest F-statistic value is associated with the quadratic equation, while the highest R-squared value corresponds to both the quadratic and cubic relationships and the relationship is identified as a **quadratic equation** (Table 4-47).

Table 4-47. Results of Curve Regression Between Heating Demand per Square Meter and the Building Orientation

Model formula	Model Results		Model Diagram
	R Square	F	
Linear	.001	2.827	
Logarithmic	.	.	
Inverse	.	.	
Quadratic	.009	16.030	
Cubic	.009	10.688	
Compound	.001	3.066	
Power	.	.	
S	.	.	
Growth	.001	3.066	
Exponential	.001	3.066	
Logistic	.001	3.066	

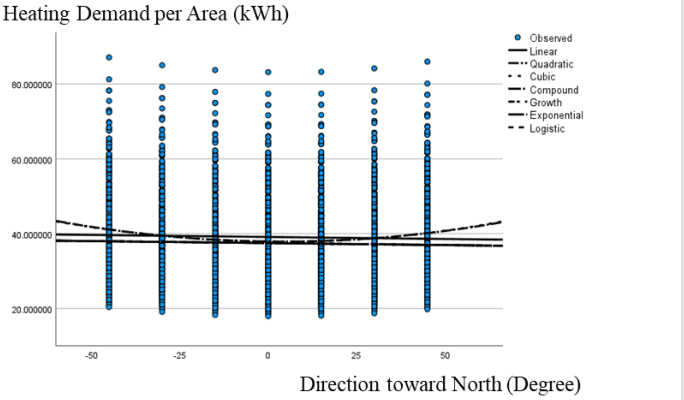

Dependent Variable: Heating Energy Per Area

The independent variable is NS Direction towards the North.

a. The independent variable (NS Direction towards the North) contains non-positive values. The minimum value is -45. The Logarithmic and Power models cannot be calculated.

In this section, the relationship between energy consumption and building orientation relative to the north is examined. According to the findings, the highest F-statistic value and the highest R-squared value are associated with the **quadratic relationship**. Therefore, the relationship between the two variables is identified as a quadratic equation (Table 4-48).

Table 4-48. Results of Curve Regression Regression Between Energy Consumption and the Building Orientation

Model formula	Model Results		Model Diagram
	R Square	F	
Linear	.000	.477	
Logarithmic	.	.	
Inverse	.	.	
Quadratic	.001	1.078	
Cubic	.001	.719	
Compound	.000	.425	
Power	.	.	
S	.	.	
Growth	.000	.425	
Exponential	.000	.425	
Logistic	.000	.425	

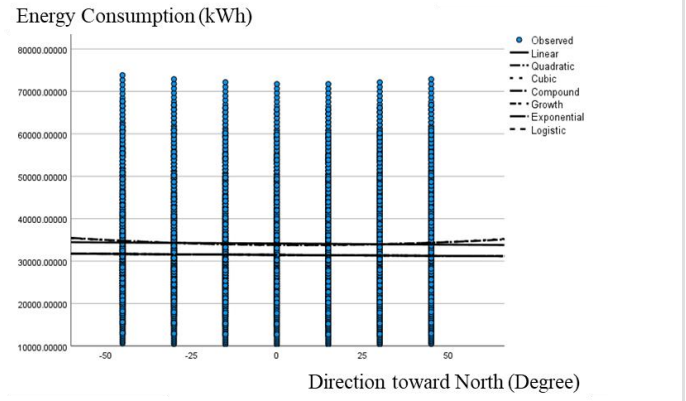

Dependent Variable: Global Energy

The independent variable is NS Direction towards the North.

a. The independent variable (NS Direction towards the North) contains non-positive values. The minimum value is -45. The Logarithmic and Power models cannot be calculated.

In this section, the relationship between cooling demand and orientation is examined. Based on the findings of the curvilinear regression test, the relationship between the two variables is identified as a **linear equation**. Based on the results of the curve regression test, a weak relationship is detected between the two variables (Table 4-49).

Table 4-49. Results of Curve Regression Between Cooling Demand and the Building Orientation

Model formula	Model Results		Model Diagram
	R Square	F	
Linear	.002	6.774	
Logarithmic	.	.	
Inverse	.	.	
Quadratic	.003	5.343	
Cubic	.003	3.584	
Compound	.002	5.680	
Power	.	.	
S	.	.	
Growth	.002	5.680	
Exponential	.002	5.680	
Logistic	.002	5.680	

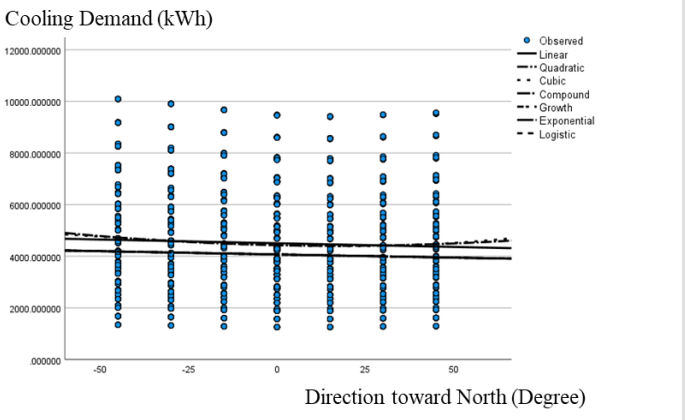

Dependent Variable: Cooling Energy

The independent variable is NS Direction towards the North.

a. The independent variable (NS Direction towards the North) contains non-positive values. The minimum value is -45. The Logarithmic and Power models cannot be calculated.

Also, the relationship between heating demand and building orientation relative to the north is examined. According to the findings, the highest F-statistic value is associated with the quadratic equation, and the highest R-squared value corresponds to both the quadratic and cubic relationships and the relationship is identified as a **quadratic equation** (Table 4-50).

Table 4-50. Results of Curve Regression Between Heating Demand and the Building Orientation

Model formula	Model Results		Model Diagram
	R Square	F	
Linear	.001	2.832	
Logarithmic	.	.	
Inverse	.	.	
Quadratic	.009	16.424	
Cubic	.009	10.950	
Compound	.001	2.576	
Power	.	.	
S	.	.	
Growth	.001	2.576	
Exponential	.001	2.576	
Logistic	.001	2.576	

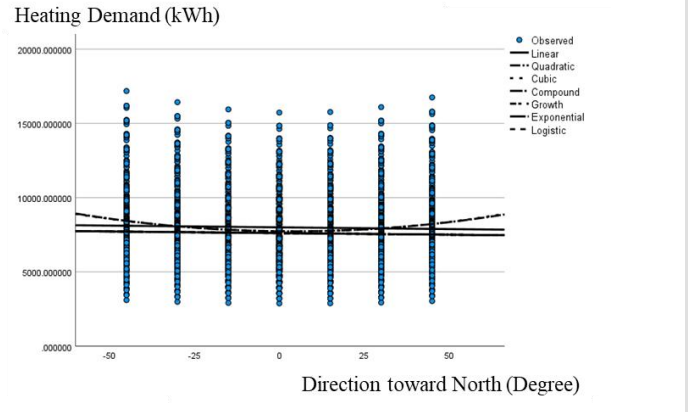

Dependent Variable: Heating Energy

The independent variable is NS Direction towards the North.

a. The independent variable (NS Direction towards the North) contains non-positive values. The minimum value is -45. The Logarithmic and Power models cannot be calculated.

b. The independent variable (NS Direction towards the North) contains values of zero. The Inverse and S models cannot be calculated.

In this section, the relationship between lighting demand and building orientation relative to the north is examined. According to the findings, both the F-statistic value and the R-squared value are close to zero. Based on the results of the curve regression test, a weak relationship is detected between the two variables (Table 4-51).

Table 4-51. Results of Curve Regression Between Lighting Demand and the Building Orientation

Model formula	Model Results		Model Diagram
	R Square	F	
Linear	.000	.000	
Logarithmic	.	.	
Inverse	.	.	
Quadratic	.000	.000	
Cubic	.000	.000	
Compound	.000	.000	
Power	.	.	
S	.	.	
Growth	.000	.000	
Exponential	.000	.000	
Logistic	.000	.000	

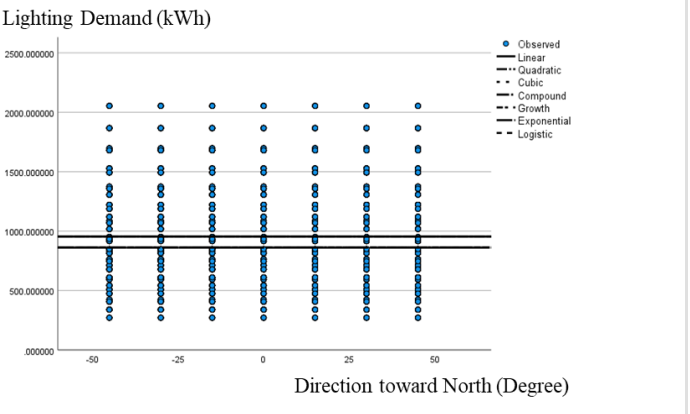

Dependent Variable: Lighting Energy

The independent variable is NS Direction towards the North.

a. The independent variable (NS Direction towards the North) contains non-positive values. The minimum value is -45. The Logarithmic and Power models cannot be calculated.

Also, the relationship between the average useful daylight and building orientation relative to the north is examined. According to the findings, the highest F-statistic value is associated with the linear equation, and the R-squared value remains constant across all relationships. Thus, the relationship of the two variables is identified as a **linear equation** (Table 4-52).

Table 4-52. Results of Curve Regression Between Average UDI and the Building Orientation

Model formula	Model Results		Model Diagram
	R Square	F	
Linear	.002	6.441	
Logarithmic	.	.	
Inverse	.	.	
Quadratic	.002	3.236	
Cubic	.002	2.161	
Compound	.002	5.941	
Power	.	.	
S	.	.	
Growth	.002	5.941	
Exponential	.002	5.941	
Logistic	.002	5.941	

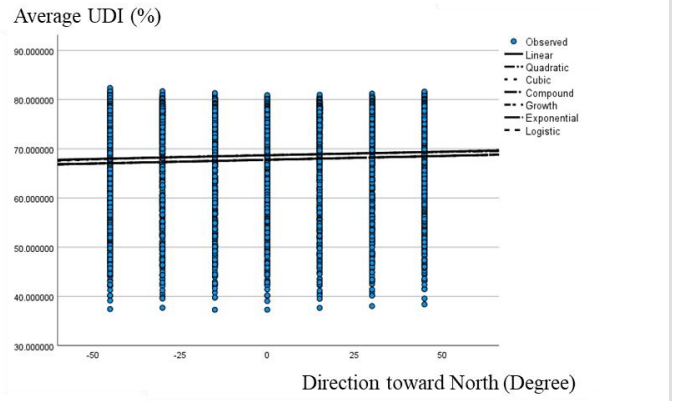

Dependent Variable: UDI Average

The independent variable is NS Direction towards the North.

a. The independent variable (NS Direction towards the North) contains non-positive values. The minimum value is -45. The Logarithmic and Power models cannot be calculated.

In this section, the relationship between the average daylight autonomy and building orientation relative to the north is examined. Based on the values of the two statistics, the relationship between the two variables is identified as a **compound equation**. Based on the results of the curve regression test, a weak relationship is detected between the two variables (Table 4-53).

Table 4-53. Results of Curve Regression Between Average DA and the Building Orientation

Model formula	Model Results		Model Diagram
	R Square	F	
Linear	.011	40.311	
Logarithmic	.	.	
Inverse	.	.	
Quadratic	.014	24.523	
Cubic	.014	16.349	
Compound	.011	41.382	
Power	.	.	
S	.	.	
Growth	.011	41.382	
Exponential	.011	41.382	
Logistic	.011	41.382	

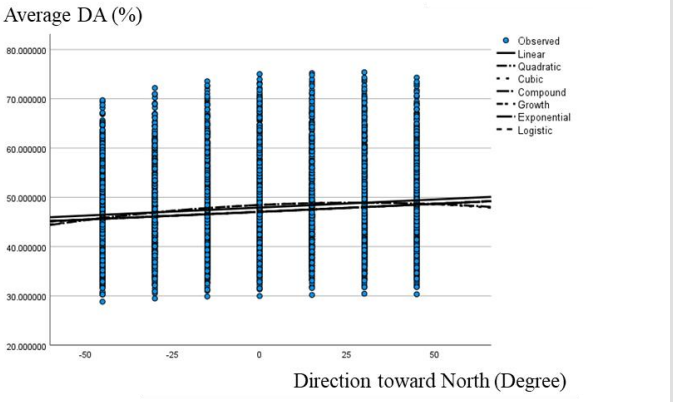

Dependent Variable: DA Average

The independent variable is NS Direction towards the North.

a. The independent variable (NS Direction towards the North) contains non-positive values. The minimum value is -45. The Logarithmic and Power models cannot be calculated.

In this section, the relationship between energy consumption per square meter and building volume is examined. According to the findings of the curvilinear regression test, the highest F-statistic value is associated with the logarithmic equation, while the highest R-squared value corresponds to the cubic curve relationship. Based on the values of the statistics, the relationship between the two variables is identified as a **logarithmic equation** (Table 4-54).

Table 4-54. Results of Curve Regression Between Energy Consumption per Square Meter and the Building Volume

Model formula	Model Results		Model Diagram
	R Square	F	
Linear	.232	1080.231	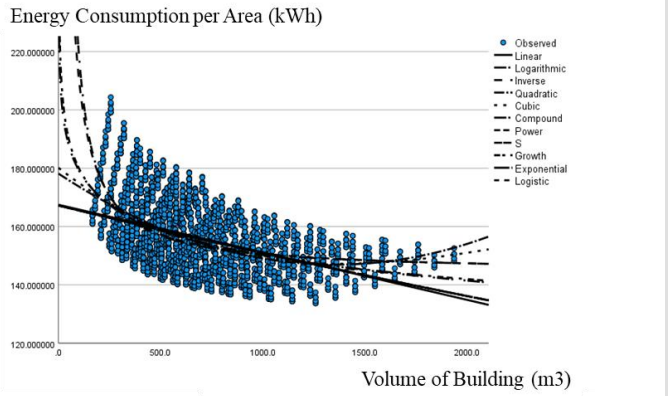
Logarithmic	.270	1324.909	
Inverse	.257	1238.507	
Quadratic	.278	689.844	
Cubic	.279	460.846	
Compound	.232	1082.558	
Power	.269	1317.142	
S	.254	1219.553	
Growth	.232	1082.558	
Exponential	.232	1082.558	
Logistic	.232	1082.558	

Dependent Variable: Global Energy Per Area
The independent variable is Volume of Building.

In this section, the relationship between cooling demand per square meter and building volume is examined. According to the findings of the curvilinear regression test, the highest F-statistic value and the highest R-squared value are associated with the power relationship. Therefore, the relationship between the two variables is identified as a **power equation**. Based on the results, a weak relationship is detected between the two variables (Table 4-55).

Table 4-55. Results of Curve Regression Between Cooling Demand per Square Meter and the Building Volume

Model formula	Model Results		Model Diagram
	R Square	F	
Linear	.008	30.494	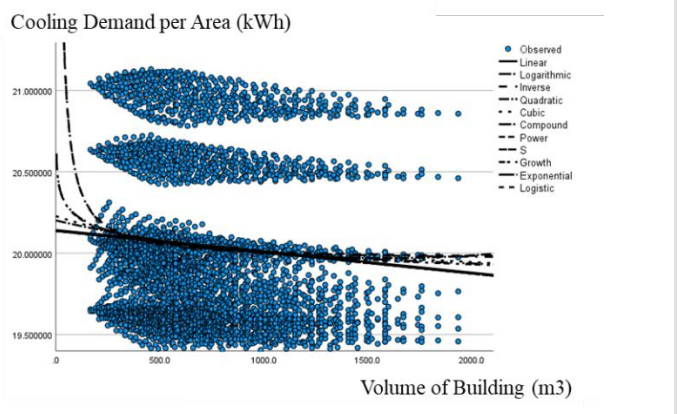
Logarithmic	.009	33.498	
Inverse	.008	30.645	
Quadratic	.009	16.695	
Cubic	.009	11.185	
Compound	.009	31.129	
Power	.009	34.204	
S	.009	31.299	
Growth	.009	31.129	
Exponential	.009	31.129	
Logistic	.009	31.129	

Dependent Variable: Cooling Energy Per Area
The independent variable is Volume of Building.

In this section, the relationship between heating demand per square meter and building volume is examined. According to the findings of the curvilinear regression test, the highest F-statistic value is associated with the logarithmic equation, while the highest R-squared value corresponds to the cubic curve relationship. Based on the values of the statistics, the relationship between the two variables is identified as a **logarithmic equation** (Table 4-56).

Table 4-56. Results of Curve Regression Between Heating Demand per Square Meter and the Building Volume

Model formula	Model Results		Model Diagram
	R Square	F	
Linear	.232	1080.026	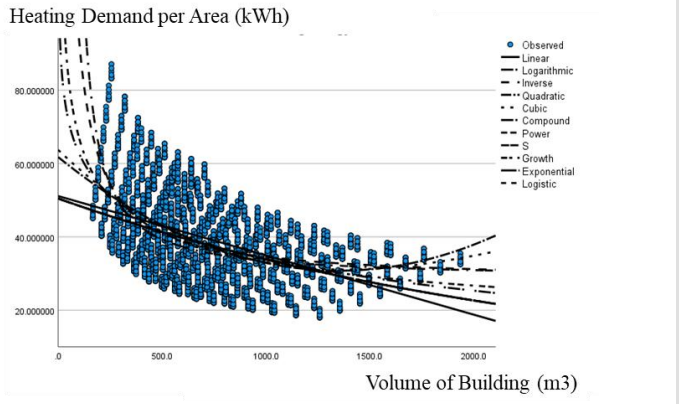
Logarithmic	.270	1325.511	
Inverse	.257	1239.559	
Quadratic	.278	690.515	
Cubic	.279	461.282	
Compound	.227	1049.605	
Power	.260	1258.207	
S	.242	1142.640	
Growth	.227	1049.605	
Exponential	.227	1049.605	
Logistic	.227	1049.605	

Dependent Variable: Heating Energy Per Area
The independent variable is Volume of Building.

In this section, the relationship between energy consumption and building volume is examined. According to the findings, the highest F-statistic value and the highest R-squared value are associated with the power relationship. Therefore, the relationship between the two variables is identified as a **power equation**. In addition, based on the results of the regression test, a strong and direct relationship is detected between the two variables. The R-squared values in this test were more than 0.7 in all equations (Table 4-57).

Table 4-57. Results of Curve Regression Between Energy Consumption and the Building Volume

Model formula	Model Results		Model Diagram
	R Square	F	
Linear	.952	70770.586	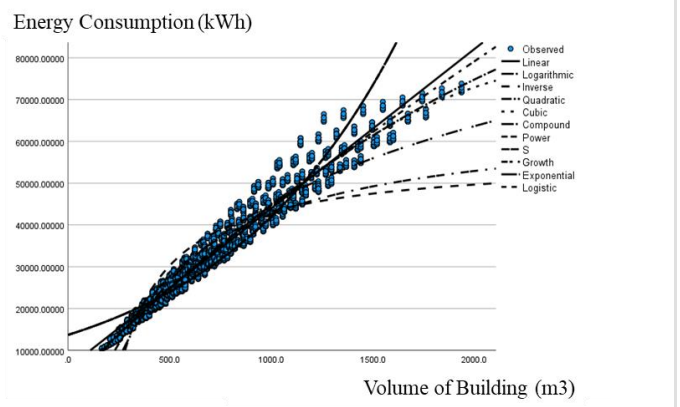
Logarithmic	.913	37364.449	
Inverse	.727	9525.905	
Quadratic	.957	39722.302	
Cubic	.957	26559.347	
Compound	.889	28605.125	
Power	.967	104717.925	
S	.884	27397.199	
Growth	.889	28605.125	
Exponential	.889	28605.125	
Logistic	.889	28605.125	

Dependent Variable: Global Energy
The independent variable is Volume of Building.

In this section, the relationship between cooling demand and building volume is examined. According to the findings, the highest F-statistic value and the highest R-squared value are associated with the power relationship. Therefore, the relationship between the two variables is identified as a **power equation**. In addition, based on the results of the regression test, a strong and direct relationship is detected between the two variables. The R-squared values in this test were more than 0.67 in all equations (Table 4-58).

Table 4-58. Results of Curve Regression Between Cooling Demand and the Building Volume

Model formula	Model Results		Model Diagram
	R Square	F	
Linear	.892	29541.462	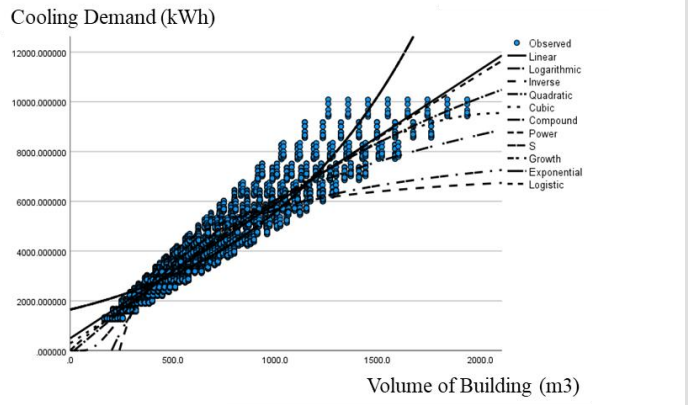
Logarithmic	.855	21109.166	
Inverse	.678	7549.260	
Quadratic	.898	15677.851	
Cubic	.898	10535.933	
Compound	.835	18175.363	
Power	.914	37942.227	
S	.838	18541.999	
Growth	.835	18175.363	
Exponential	.835	18175.363	
Logistic	.835	18175.363	

Dependent Variable: Cooling Energy
The independent variable is Volume of Building.

In this section, the relationship between heating demand and building volume is examined. According to the findings, the highest F-statistic value and the highest R-squared value are associated with the power model. Therefore, the relationship between heating demand and building volume is identified as a **power equation** (Table 4-59).

Table 4-59. Results of Curve Regression Between Heating Demand and the Building Volume

Model formula	Model Results		Model Diagram
	R Square	F	
Linear	.854	21022.403	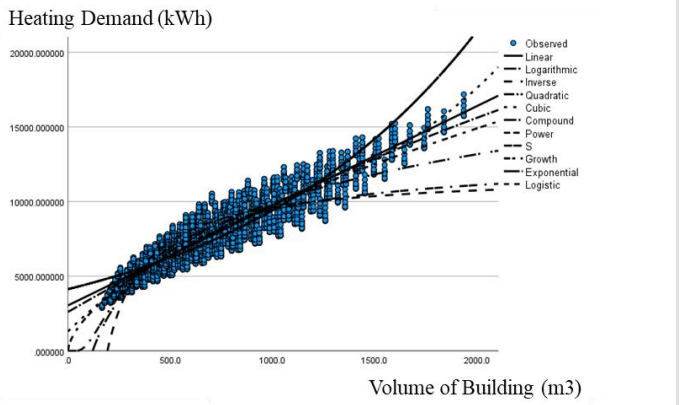
Logarithmic	.822	16487.116	
Inverse	.668	7211.598	
Quadratic	.856	10654.676	
Cubic	.861	7365.808	
Compound	.803	14601.389	
Power	.858	21626.398	
S	.781	12790.046	
Growth	.803	14601.389	
Exponential	.803	14601.389	
Logistic	.803	14601.389	

Dependent Variable: Heating Energy
The independent variable is Volume of Building.

Also, the relationship between lighting demand and building volume is examined. According to the findings, the highest F-statistic value and the highest R-squared value are associated with the power model. Therefore, the relationship between lighting demand and building volume is identified as a **power equation** (Table 4-60).

Table 4-60. Results of Curve Regression Between Lighting Demand and the Building Volume

Model formula	Model Results		Model Diagram
	R Square	F	
Linear	.894	30360.167	
Logarithmic	.857	21452.159	
Inverse	.679	7587.674	
Quadratic	.900	16112.827	
Cubic	.901	10833.627	
Compound	.837	18406.288	
Power	.916	38882.106	
S	.840	18782.941	
Growth	.837	18406.288	
Exponential	.837	18406.288	
Logistic	.837	18406.288	

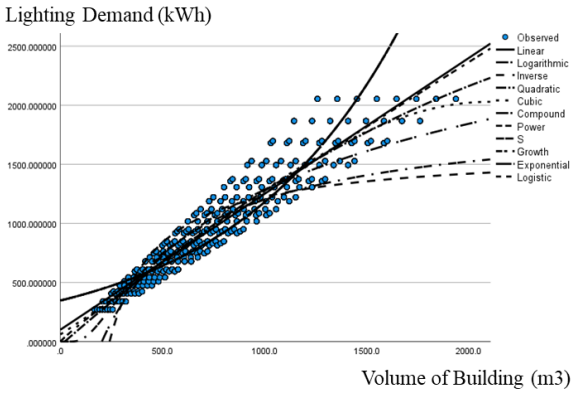

Dependent Variable: Lighting Energy
The independent variable is Volume of Building.

In this section, the relationship between average useful daylight and building volume is examined. According to the findings of the curvilinear regression test, the highest F-statistic value is associated with the inverse equation, while the highest R-squared value corresponds to the cubic curve relationship. Based on the overall statistical measures, the relationship between the two variables is identified as an **inverse equation**. In addition, based on the results of the regression test, a weak relationship is detected between the two variables. The R-squared values in this test were less than 0.13 in all equations (Table 4-61).

Table 4-61. Results of Curve Regression Between Average UDI and the Building Volume

Model formula	Model Results		Model Diagram
	R Square	F	
Linear	.013	46.085	
Logarithmic	.028	103.372	
Inverse	.045	167.119	
Quadratic	.047	89.187	
Cubic	.057	71.993	
Compound	.007	26.235	
Power	.020	71.602	
S	.035	128.393	
Growth	.007	26.235	
Exponential	.007	26.235	
Logistic	.007	26.235	

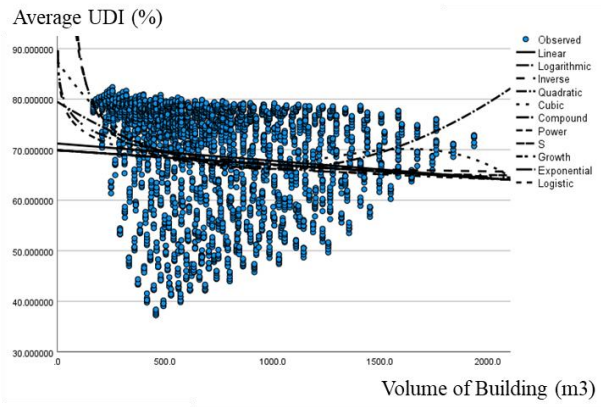

Dependent Variable: UDI Average
The independent variable is Volume of Building.

In this section, the relationship between average daylight autonomy and building volume is examined. According to the findings of the curvilinear regression test, the highest F-statistic value is associated with the inverse equation, while the highest R-squared value corresponds to the cubic curve relationship. Based on the overall statistical measures, the relationship between the two variables is identified as an **inverse equation** (Table 4-62).

Table 4-62. Results of Curve Regression Between Average DA and the Building Volume

Model formula	Model Results		Model Diagram
	R Square	F	
Linear	.074	284.684	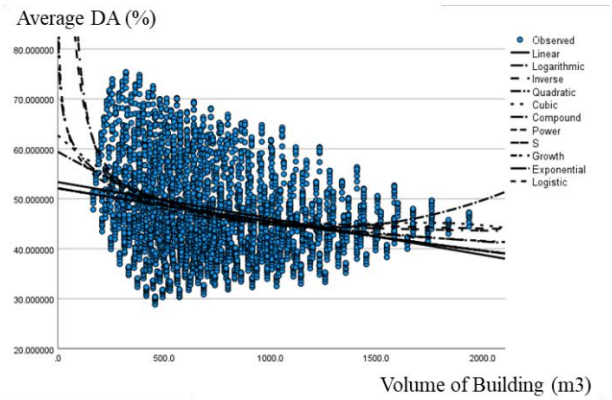
Logarithmic	.093	367.811	
Inverse	.096	381.783	
Quadratic	.098	193.882	
Cubic	.100	132.202	
Compound	.062	237.798	
Power	.082	318.692	
S	.087	343.014	
Growth	.062	237.798	
Exponential	.062	237.798	
Logistic	.062	237.798	

Dependent Variable: DA Average
The independent variable is Volume of Building.

In this section, the relationship between energy consumption per square meter and the window-to-wall ratio is examined. According to the findings of the curvilinear regression test, the highest F-statistic value and the highest R-squared value are associated with the S-curve relationship. Therefore, the relationship between the two variables is identified as an **S-curve equation** (Table 4-63).

Table 4-63. Results of Curve Regression Between Energy Consumption per Square Meter and the WWR

Model formula	Model Results		Model Diagram
	R Square	F	
Linear	.498	3557.362	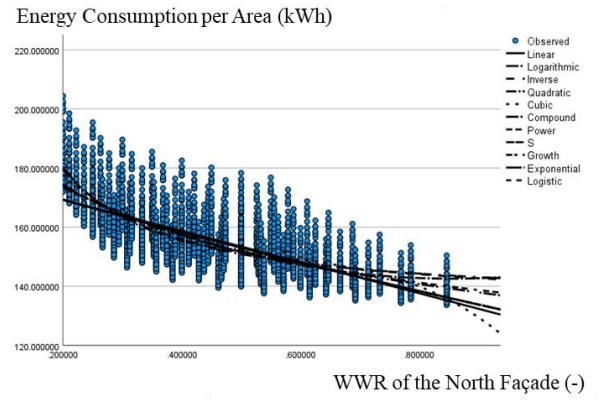
Logarithmic	.535	4122.061	
Inverse	.544	4271.560	
Quadratic	.526	1988.855	
Cubic	.546	1436.179	
Compound	.511	3748.479	
Power	.542	4235.536	
S	.543	4259.711	
Growth	.511	3748.479	
Exponential	.511	3748.479	
Logistic	.511	3748.479	

Dependent Variable: Global Energy Per Area
The independent variable is WWR of North Facade.

In this section, the relationship between cooling demand per square meter and the window-to-wall ratio is examined. According to the findings of the curvilinear regression test, the highest F-statistic value and the highest R-squared value are associated with the power relationship. Therefore, the relationship between cooling demand per square meter and the window-to-wall ratio is identified as a **power equation**. In addition, based on the results of the regression test, a weak relationship is detected between the two variables (Table 4-64).

Table 4-64. Results of Curve Regression Between Cooling Demand per Square Meter and the WWR

Model formula	Model Results		Model Diagram
	R Square	F	
Linear	.022	79.957	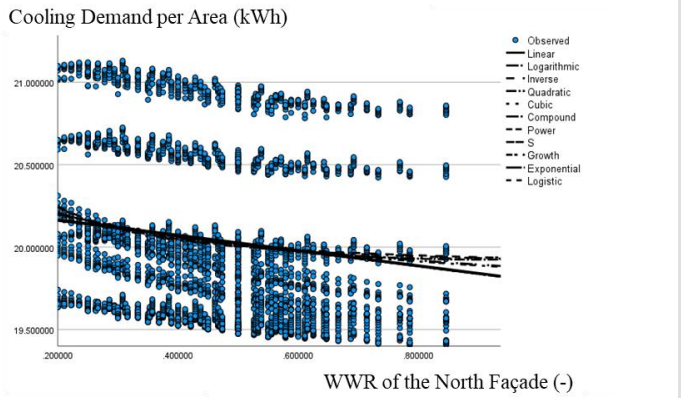
Logarithmic	.023	83.213	
Inverse	.022	79.946	
Quadratic	.023	41.804	
Cubic	.023	27.868	
Compound	.022	81.443	
Power	.023	84.718	
S	.022	81.355	
Growth	.022	81.443	
Exponential	.022	81.443	
Logistic	.022	81.443	

Dependent Variable: Cooling Energy Per Area
The independent variable is WWR of North Facade.

In this section, the relationship between heating demand per square meter and the window-to-wall ratio is examined. According to the findings of the curvilinear regression test, the highest F-statistic value and the highest R-squared value are associated with the power relationship. Therefore, the relationship between heating demand per square meter and the window-to-wall ratio is identified as a **power equation** (Table 4-65).

Table 4-65. Results of Curve Regression Between Heating Demand per Square Meter and the WWR

Model formula	Model Results		Model Diagram
	R Square	F	
Linear	.497	3545.269	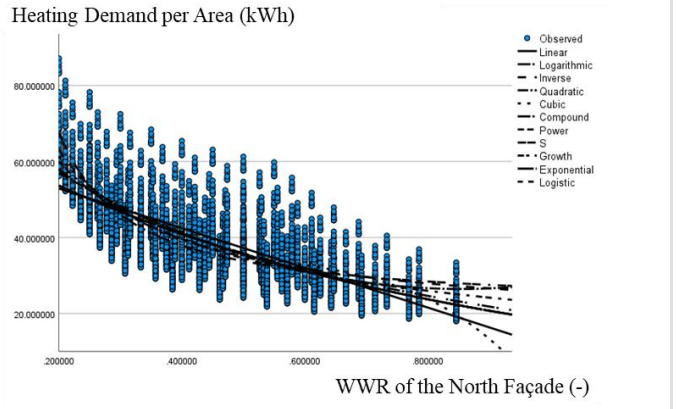
Logarithmic	.534	4109.443	
Inverse	.543	4262.693	
Quadratic	.525	1982.112	
Cubic	.546	1433.298	
Compound	.537	4162.386	
Power	.548	4341.267	
S	.528	4012.279	
Growth	.537	4162.386	
Exponential	.537	4162.386	
Logistic	.537	4162.386	

Dependent Variable: Heating Energy Per Area
The independent variable is WWR of North Facade.

In this section, the relationship between energy consumption and the window-to-wall ratio is examined. According to the findings of the curvilinear regression test, the highest F-statistic value and the highest R-squared value are associated with the power relationship. Therefore, the relationship between energy consumption and the window-to-wall ratio is identified as a **power equation**. In addition, based on the results of the regression test, a moderate and direct relationship is detected between the two variables (Table 4-66).

Table 4-66. Results of Curve Regression Between Energy Consumption and the WWR

Model formula	Model Results		Model Diagram
	R Square	F	
Linear	.326	1729.148	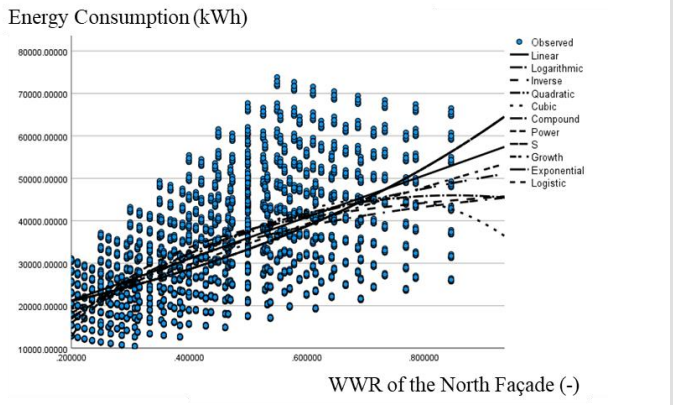
Logarithmic	.339	1834.406	
Inverse	.322	1703.434	
Quadratic	.344	940.159	
Cubic	.348	635.988	
Compound	.336	1812.520	
Power	.359	2002.365	
S	.350	1930.467	
Growth	.336	1812.520	
Exponential	.336	1812.520	
Logistic	.336	1812.520	

Dependent Variable: Global Energy
The independent variable is WWR of North Facade.

In this section, the relationship between cooling demand and the window-to-wall ratio is examined. According to the findings of the curvilinear regression test, the highest F-statistic value and the highest R-squared value are associated with the power relationship. Therefore, the relationship between cooling demand and the window-to-wall ratio is identified as a **power equation** (Table 4-67).

Table 4-67. Results of Curve Regression Between Cooling Demand and the WWR

Model formula	Model Results		Model Diagram
	R Square	F	
Linear	.380	2196.511	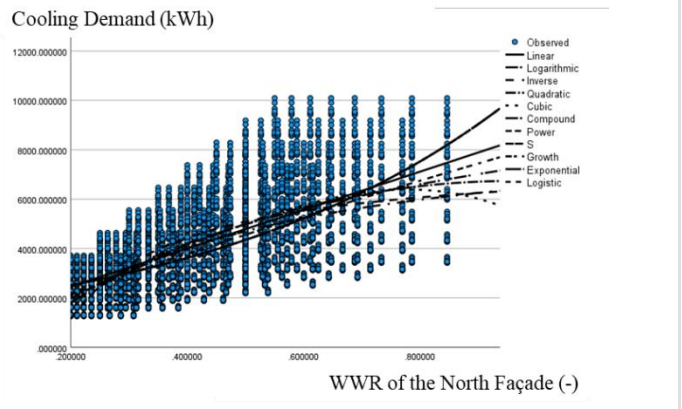
Logarithmic	.389	2281.168	
Inverse	.366	2071.019	
Quadratic	.393	1159.115	
Cubic	.395	778.737	
Compound	.390	2287.005	
Power	.415	2545.743	
S	.408	2466.576	
Growth	.390	2287.005	
Exponential	.390	2287.005	
Logistic	.390	2287.005	

Dependent Variable: Cooling Energy
The independent variable is WWR of North Facade.

In this section, the relationship between heating demand and the window-to-wall ratio is examined. According to the findings of the curvilinear regression test, the highest F-statistic value and the highest R-squared value are associated with the S-curve relationship. Therefore, the relationship between heating demand and the window-to-wall ratio is identified as an **S-curve equation**. In addition, based on the results of the regression test, a weak relationship is detected between the two variables (Table 4-68).

Table 4-68. Results of Curve Regression Between Heating Demand and the WWR

Model formula	Model Results		Model Diagram
	R Square	F	
Linear	.052	196.828	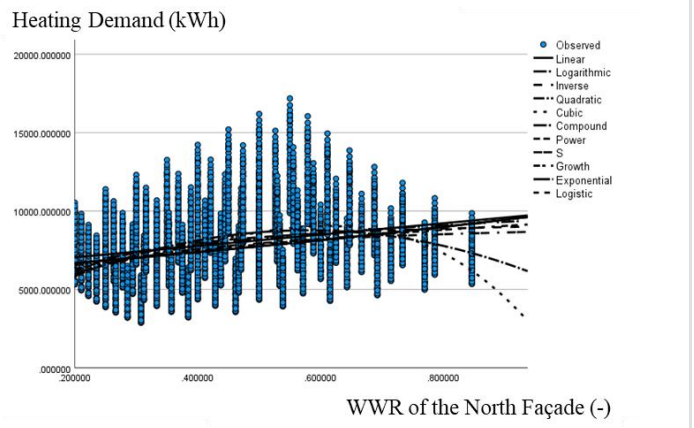
Logarithmic	.066	254.192	
Inverse	.071	274.904	
Quadratic	.101	200.730	
Cubic	.113	151.853	
Compound	.060	227.857	
Power	.072	276.589	
S	.073	284.137	
Growth	.060	227.857	
Exponential	.060	227.857	
Logistic	.060	227.857	

Dependent Variable: Heating Energy
The independent variable is WWR of North Facade.

In this section, the relationship between lighting demand and the window-to-wall ratio is examined. According to the findings of the curvilinear regression test, the highest F-statistic value and the highest R-squared value are associated with the power relationship. Therefore, the relationship between lighting demand and the window-to-wall ratio is identified as a **power equation** (Table 4-69).

Table 4-69. Results of Curve Regression Between Lighting Demand and the WWR

Model formula	Model Results		Model Diagram
	R Square	F	
Linear	.386	2255.584	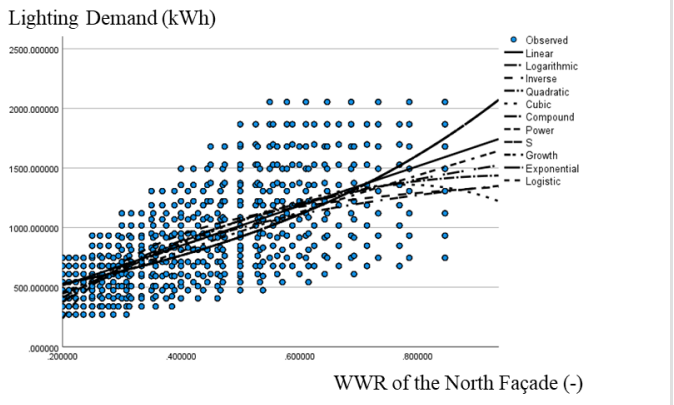
Logarithmic	.395	2339.908	
Inverse	.372	2119.458	
Quadratic	.399	1189.241	
Cubic	.401	799.153	
Compound	.396	2349.876	
Power	.422	2617.467	
S	.414	2534.034	
Growth	.396	2349.876	
Exponential	.396	2349.876	
Logistic	.396	2349.876	

Dependent Variable: Lighting Energy
The independent variable is WWR of North Facade.

In this section, the relationship between energy consumption and the window-to-wall ratio is examined. According to the findings, the highest F-statistic value is associated with the linear equation, while the highest R-squared value corresponds to the cubic curve. Based on the obtained statistics, the relationship between energy consumption and the window-to-wall ratio is identified as a **linear equation** (Table 4-70).

Table 4-70. Results of Curve Regression Between Average UDI and the WWR

Model formula	Model Results		Model Diagram
	R Square	F	
Linear	.727	9553.297	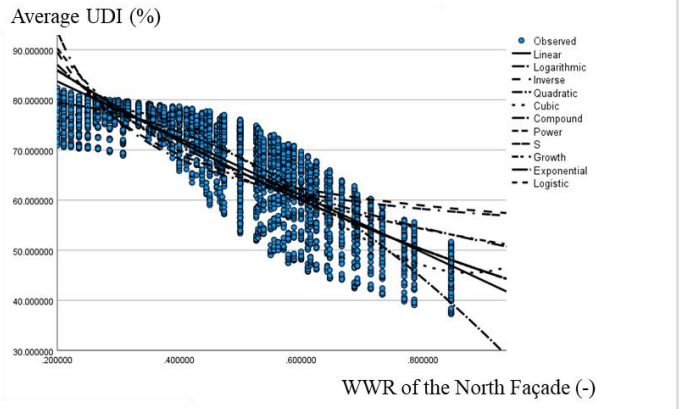
Logarithmic	.636	6261.378	
Inverse	.509	3706.833	
Quadratic	.763	5767.328	
Cubic	.784	4340.711	
Compound	.703	8485.312	
Power	.604	5468.517	
S	.475	3246.391	
Growth	.703	8485.312	
Exponential	.703	8485.312	
Logistic	.703	8485.312	

Dependent Variable: UDI Average

The independent variable is WWR of North Facade

In this section, the relationship between the average daylight autonomy and the window-to-wall ratio is examined. According to the findings, the highest F-statistic value and the highest R-squared value are associated with the power relationship. Therefore, the relationship between the average daylight autonomy and the window-to-wall ratio is identified as a **power equation**. In addition, based on the results of the regression test, a strong and direct relationship is detected between the two variables (Table 4-71).

Table 4-71. Results of Curve Regression Between Average DA and the WWR

Model formula	Model Results		Model Diagram
	R Square	F	
Linear	.838	18483.958	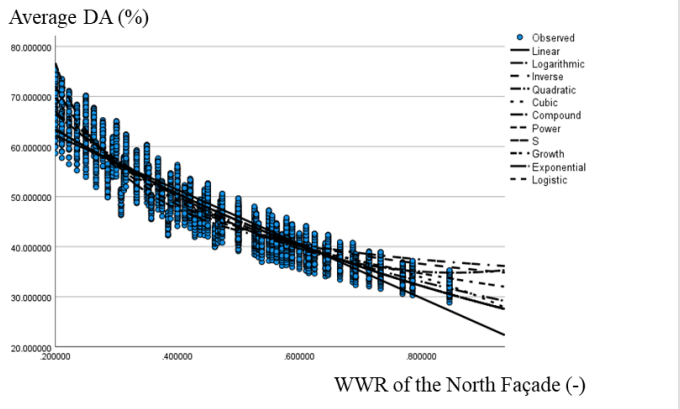
Logarithmic	.887	28028.032	
Inverse	.875	24980.676	
Quadratic	.885	13749.066	
Cubic	.890	9620.678	
Compound	.875	25137.646	
Power	.893	29991.614	
S	.850	20284.835	
Growth	.875	25137.646	
Exponential	.875	25137.646	
Logistic	.875	25137.646	

Dependent Variable: DA Average

The independent variable is WWR of North Facade.

In this section, the relationship between energy consumption per square meter and the width of the northern window is examined. According to the findings of the curvilinear regression test, the highest F-statistic value is associated with the inverse equation, and the highest R-squared value is associated with both the inverse and cubic curve relationships. Therefore, the relationship between the two variables is identified as an **inverse equation** (Table 4-72).

Table 4-72. Results of Curve Regression Between Energy Consumption per Square Meter and the Width of the Window

Model formula	Model Results		Model Diagram
	R Square	F	
Linear	.596	5276.189	
Logarithmic	.644	6492.486	
Inverse	.652	6696.578	
Quadratic	.634	3095.178	
Cubic	.652	2239.001	
Compound	.610	5607.835	
Power	.649	6637.132	
S	.645	6510.034	
Growth	.610	5607.835	
Exponential	.610	5607.835	
Logistic	.610	5607.835	

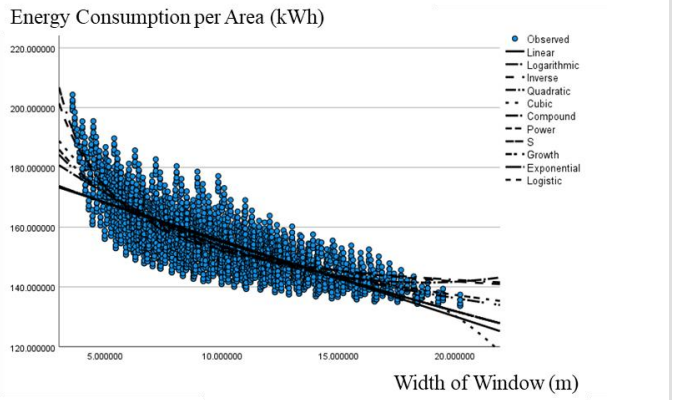

Dependent Variable: Global Energy Per Area
The independent variable is Width of Window.

In this section, the relationship between cooling demand per square meter and the width of the northern window has been examined. According to the findings from the curvilinear regression test, the highest F-statistic corresponds to the compound, growth, and logistic relationships, while the R-squared value remains constant. Based on these findings, the relationship between the two variables is identified as a **compound equation** (Table 4-73).

Table 4-73. Results of Curve Regression Between Cooling Demand per Square Meter and the Width of the Window

Model formula	Model Results		Model Diagram
	R Square	F	
Linear	.005	17.191	
Logarithmic	.005	16.951	
Inverse	.005	16.262	
Quadratic	.005	8.612	
Cubic	.005	6.175	
Compound	.005	17.663	
Power	.005	17.440	
S	.005	16.749	
Growth	.005	17.663	
Exponential	.005	17.663	
Logistic	.005	17.663	

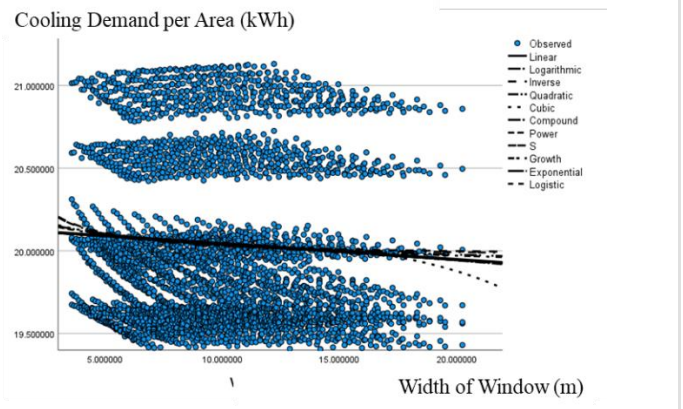

Dependent Variable: Cooling Energy Per Area
The independent variable is Width of Window.

In this section, the relationship between heating demand per square meter and the width of the north-facing window is examined. Based on the findings from the curvilinear regression test, the highest F-statistic is associated with the power function, and the highest R-squared value corresponds to the cubic curve function. Based on the Results, the relationship between the two variables is identified as a **power function** (Table 4-74).

Table 4-74. Results of Curve Regression Between Heating Demand per Square Meter and the Width of the Window

Model formula	Model Results		Model Diagram
	R Square	F	
Linear	.601	5387.897	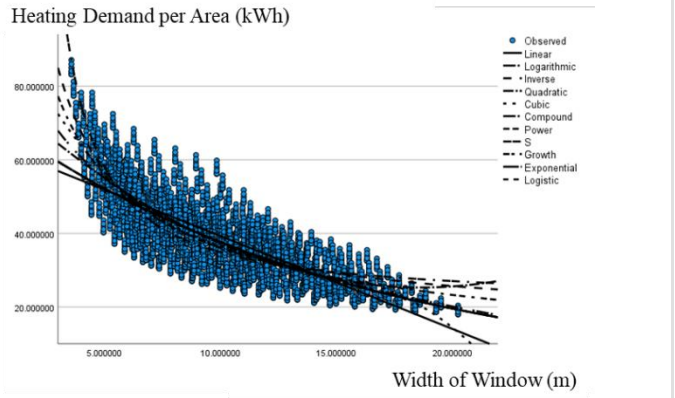
Logarithmic	.650	6655.784	
Inverse	.657	6872.229	
Quadratic	.639	3172.359	
Cubic	.658	2297.029	
Compound	.644	6493.516	
Power	.655	6804.488	
S	.620	5846.724	
Growth	.644	6493.516	
Exponential	.644	6493.516	
Logistic	.644	6493.516	

Dependent Variable: Heating Energy Per Area
The independent variable is Width of Window.

In this section, the relationship between energy consumption and the width of the north-facing window has been examined. Based on the findings of the curvilinear regression analysis, the highest F-statistic and the highest R-squared value were associated with the power-law relationship. The relationship between the two variables, energy consumption and the width of the north-facing window, is identified as a **power equation** (Table 4-75).

Table 4-75. Results of Curve Regression Between Energy Consumption and the Width of the Window

Model formula	Model Results		Model Diagram
	R Square	F	
Linear	.812	15436.922	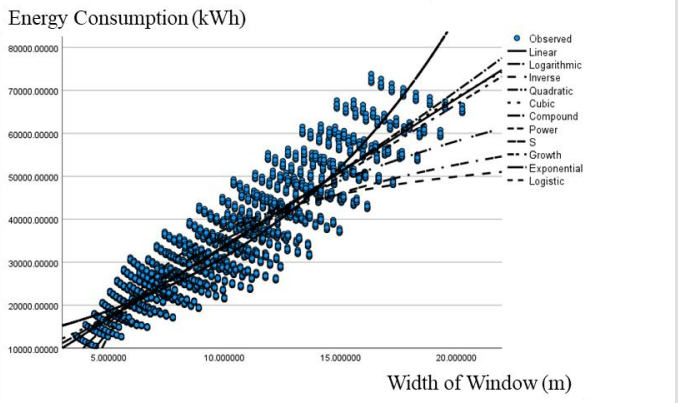
Logarithmic	.770	12019.150	
Inverse	.671	7289.413	
Quadratic	.812	7750.786	
Cubic	.813	5173.976	
Compound	.792	13636.410	
Power	.816	15893.445	
S	.775	12353.893	
Growth	.792	13636.410	
Exponential	.792	13636.410	
Logistic	.792	13636.410	

Dependent Variable: Global Energy
The independent variable is Width of Window.

In this section, the relationship between cooling demand and the width of the northern window is examined. Based on the findings, the highest F-statistic and the highest R-squared value were associated with the power-law relationship. Accordingly, the relationship between the two variables, cooling demand and the width of the northern window, is identified as a **power equation**. In addition, based on the results of the regression test, a strong and direct relationship is detected between the two variables (Table 4-76).

Table 4-76. Results of Curve Regression Between Cooling Demand and the Width of the Window

Model formula	Model Results		Model Diagram
	R Square	F	
Linear	.864	22831.660	
Logarithmic	.812	15521.023	
Inverse	.701	8383.151	
Quadratic	.867	11678.356	
Cubic	.867	7787.057	
Compound	.839	18683.508	
Power	.869	23693.986	
S	.830	17527.301	
Growth	.839	18683.508	
Exponential	.839	18683.508	
Logistic	.839	18683.508	

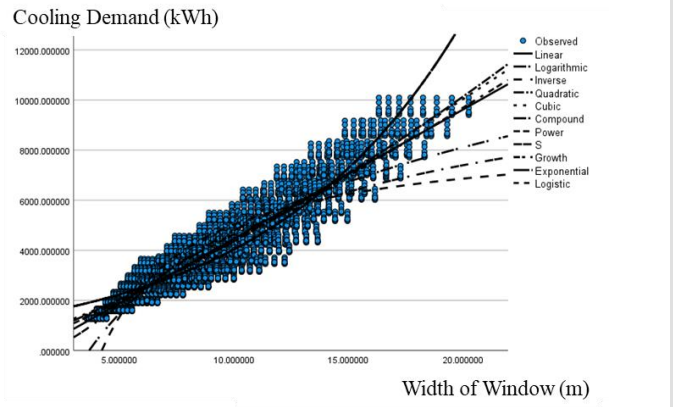

Dependent Variable: Cooling Energy
The independent variable is Width of Window

In this section, the relationship between heating demand and the width of the northern window is examined. Based on the findings from the curvilinear regression test, the highest F-statistic and the highest R-squared value were associated with the power-law relationship. Accordingly, the relationship between the two variables, heating demand and the width of the northern window, is identified as a **power equation** (Table 4-77).

Table 4-77. Results of Curve Regression Between Heating Demand and the Width of the Window

Model formula	Model Results		Model Diagram
	R Square	F	
Linear	.350	1929.894	
Logarithmic	.358	1994.110	
Inverse	.333	1785.017	
Quadratic	.361	1011.887	
Cubic	.364	682.748	
Compound	.357	1991.586	
Power	.378	2177.444	
S	.366	2064.766	
Growth	.357	1991.586	
Exponential	.357	1991.586	
Logistic	.357	1991.586	

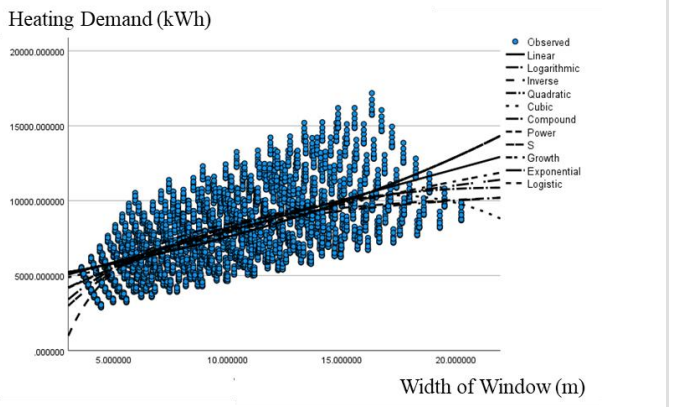

Dependent Variable: Heating Energy
The independent variable is Width of Window.

In this section, the relationship between lighting demand and the width of the northern window is examined. Based on the findings, the highest F-statistic and the highest R-squared value were associated with the power-law relationship. Accordingly, the relationship between the two variables, lighting demand and the width of the northern window, is identified as a **power equation**. In addition, based on the results of the regression test, a strong and direct relationship is detected between the two variables (Table 4-78).

Table 4-78. Results of Curve Regression Between Lighting Demand and the Width of the Window

Model formula	Model Results		Model Diagram
	R Square	F	
Linear	.865	22919.384	
Logarithmic	.812	15505.523	
Inverse	.700	8361.957	
Quadratic	.868	11744.939	
Cubic	.868	7830.743	
Compound	.839	18617.070	
Power	.868	23557.204	
S	.830	17450.900	
Growth	.839	18617.070	
Exponential	.839	18617.070	
Logistic	.839	18617.070	

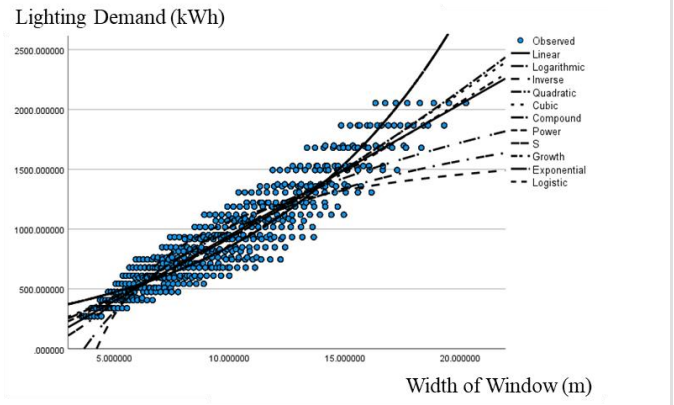

Dependent Variable: Lighting Energy
The independent variable is Width of Window.

In this section, the relationship between the average useful daylight and the width of the northern window is examined. Based on the findings from the curvilinear regression test, the highest F-statistic and the highest R-squared value were associated with the cubic curve relationship. Accordingly, the relationship between the two variables, average useful daylight and the width of the northern window, is identified as a **cubic curve** (Table 4-79).

Table 4-79. Results of Curve Regression Between Average UDI and the Width of the Window

Model formula	Model Results		Model Diagram
	R Square	F	
Linear	.015	52.997	
Logarithmic	.015	54.314	
Inverse	.018	66.029	
Quadratic	.018	32.041	
Cubic	.070	89.610	
Compound	.009	31.060	
Power	.009	32.549	
S	.012	42.901	
Growth	.009	31.060	
Exponential	.009	31.060	
Logistic	.009	31.060	

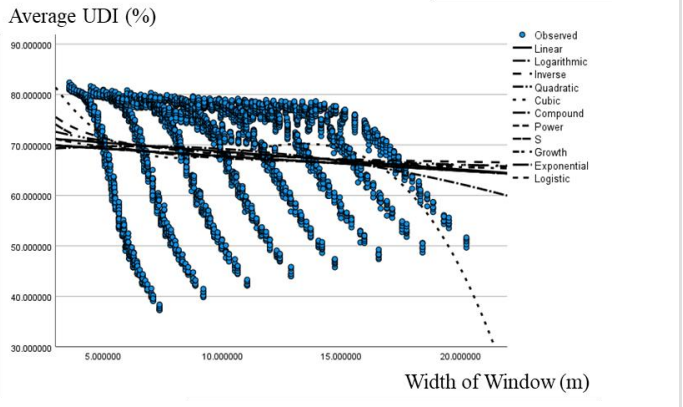

Dependent Variable: UDI Average
The independent variable is Width of Window.

In this section, the relationship between the average daylight autonomy and the width of the northern window is examined. Based on the findings, the highest F-statistic corresponds to the linear equation, while the highest R-squared value is associated with the cubic curve. However, considering the F-statistic and R-squared values for both equations, the relationship between the two variables is identified as a **linear model** (Table 4-80).

Table 4-80. Results of Curve Regression Between Average DA and the Width of the Window

Model formula	Model Results		Model Diagram
	R Square	F	
Linear	.124	504.733	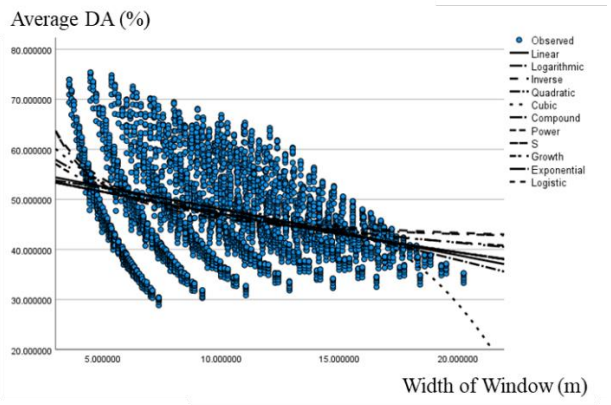
Logarithmic	.123	502.801	
Inverse	.122	495.903	
Quadratic	.124	253.258	
Cubic	.142	197.878	
Compound	.112	452.916	
Power	.110	441.529	
S	.107	429.550	
Growth	.112	452.916	
Exponential	.112	452.916	
Logistic	.112	452.916	

Dependent Variable: DA Average
The independent variable is Width of Window.

In this section, the relationship between energy consumption per square meter and the height of the northern window is examined. Based on the findings from the curvilinear regression test, the highest F-statistic corresponds to the inverse equation, while the highest R-squared value is associated with the cubic curve. However, considering the F-statistic and R-squared values for both equations, the relationship between the two variables is identified as an **inverse equation** (Table 4-81).

Table 4-81. Results of Curve Regression Between Energy Consumption per Square Meter and the Height of the Window

Model formula	Model Results		Model Diagram
	R Square	F	
Linear	.049	186.049	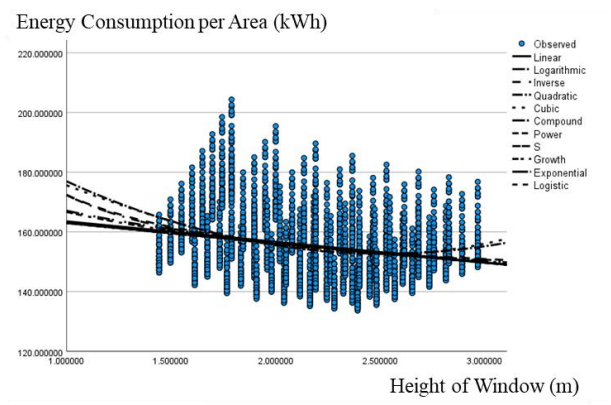
Logarithmic	.054	203.051	
Inverse	.056	211.865	
Quadratic	.068	130.689	
Cubic	.071	136.862	
Compound	.048	180.180	
Power	.052	198.472	
S	.055	208.909	
Growth	.048	180.180	
Exponential	.048	180.180	
Logistic	.048	180.180	

Dependent Variable: Global Energy Per Area
The independent variable is Height of Window.

In this section, the relationship between cooling demand per square meter and the height of the northern window is examined. Based on the findings from the curvilinear regression test, the highest F-statistic corresponds to the power-law equation, while the R-squared value was identical across all equations. Accordingly, the relationship between the two variables is identified as a **power equation** (Table 4-82).

Table 4-82. Results of Curve Regression Between Cooling Demand per Square Meter and the Height of the Window

Model formula	Model Results		Model Diagram
	R Square	F	
Linear	.018	64.453	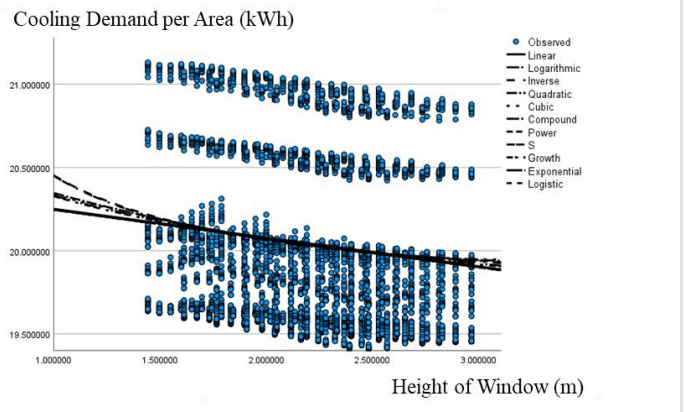
Logarithmic	.018	65.760	
Inverse	.018	65.609	
Quadratic	.018	33.197	
Cubic	.018	33.289	
Compound	.018	65.440	
Power	.018	66.759	
S	.018	66.595	
Growth	.018	65.440	
Exponential	.018	65.440	
Logistic	.018	65.440	

Dependent Variable: Cooling Energy Per Area
The independent variable is Height of Window.

In this section, the relationship between heating demand per square meter and the height of the northern window is examined. Based on the findings, the highest F-statistic corresponds to the inverse equation, while the highest R-squared value is associated with the cubic curve. However, considering the F-statistic and R-squared values, the relationship between the two variables is identified as an **inverse equation** (Table 4-83).

Table 4-83. Results of Curve Regression Between Heating Demand per Square Meter and the Height of the Window

Model formula	Model Results		Model Diagram
	R Square	F	
Linear	.048	179.337	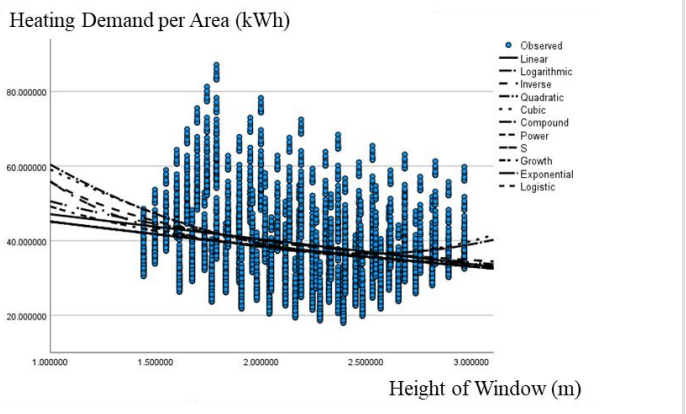
Logarithmic	.052	196.024	
Inverse	.054	204.744	
Quadratic	.066	127.267	
Cubic	.069	133.447	
Compound	.041	153.888	
Power	.047	174.932	
S	.050	189.481	
Growth	.041	153.888	
Exponential	.041	153.888	
Logistic	.041	153.888	

Dependent Variable: Heating Energy Per Area
The independent variable is Height of Window.

In this section, the relationship between energy consumption and the height of the northern window is examined. Based on the findings, the highest F-statistic and the highest R-squared value were associated with the power-law relationship. Accordingly, the relationship of the two variables, energy consumption and the height of the northern window, is identified as a **power equation**. In addition, based on the results of the regression test, a moderate and direct relationship is detected between the two variables (Table 4-84).

Table 4-84. Results of Curve Regression Between Energy Consumption and the Height of the Window

Model formula	Model Results		Model Diagram
	R Square	F	
Linear	.453	2970.320	
Logarithmic	.449	2919.045	
Inverse	.436	2769.928	
Quadratic	.453	1484.794	
Cubic	.453	1484.925	
Compound	.469	3167.717	
Power	.476	3251.453	
S	.473	3217.039	
Growth	.469	3167.717	
Exponential	.469	3167.717	
Logistic	.469	3167.717	

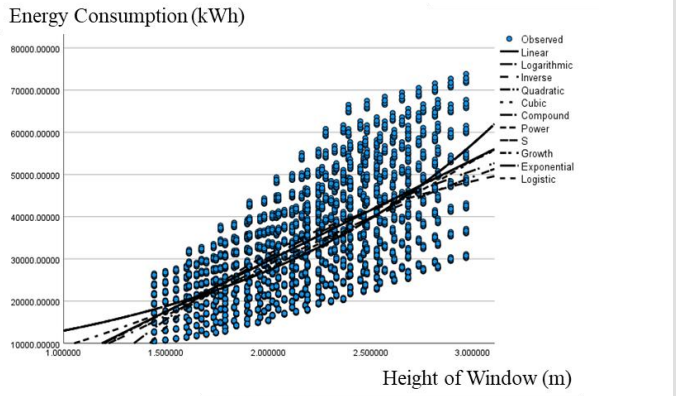

Dependent Variable: Global Energy
The independent variable is Height of Window.

In this section, the relationship between cooling demand and the height of the northern window is examined. Based on the findings from the curvilinear regression test, the highest F-statistic and the highest R-squared value were associated with the power-law relationship. Accordingly, the relationship between the two variables, cooling demand and the height of the northern window, is identified as a **power equation** (Table 4-85).

Table 4-85. Results of Curve Regression Between Cooling Demand and the Height of the Window

Model formula	Model Results		Model Diagram
	R Square	F	
Linear	.391	2301.831	
Logarithmic	.390	2291.636	
Inverse	.381	2205.710	
Quadratic	.392	1154.734	
Cubic	.392	1155.950	
Compound	.409	2480.273	
Power	.417	2557.739	
S	.416	2546.766	
Growth	.409	2480.273	
Exponential	.409	2480.273	
Logistic	.409	2480.273	

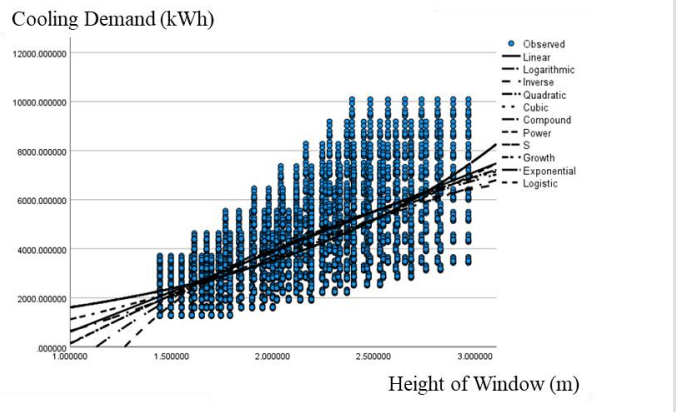

Dependent Variable: Cooling Energy
The independent variable is Height of Window.

In this section, the relationship between heating demand and the height of the northern window is examined. Based on the findings from the curvilinear regression test, the highest F-statistic corresponds to the compound equation, while the highest R-squared value is associated with the cubic curve. Accordingly, the relationship between the two variables is identified as a **compound equation** (Table 4-86).

Table 4-86. Results of Curve Regression Between Heating Demand and the Height of the Window

Model formula	Model Results		Model Diagram
	R Square	F	
Linear	.558	4530.988	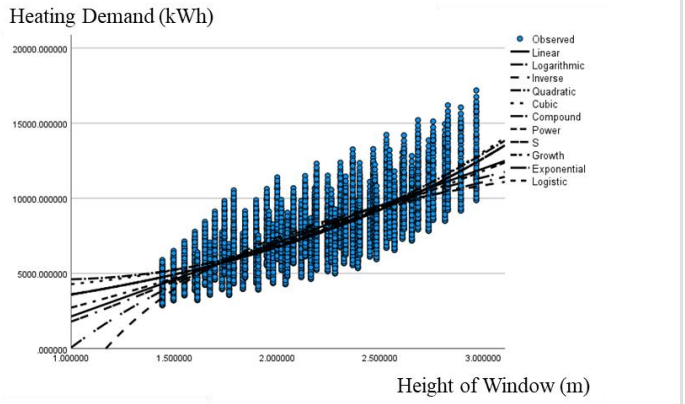
Logarithmic	.539	4185.042	
Inverse	.512	3754.833	
Quadratic	.572	2397.622	
Cubic	.574	2408.439	
Compound	.565	4655.698	
Power	.560	4564.494	
S	.547	4327.532	
Growth	.565	4655.698	
Exponential	.565	4655.698	
Logistic	.565	4655.698	

Dependent Variable: Heating Energy
The independent variable is Height of Window.

In this section, the relationship between lighting demand and the height of the northern window is examined. Based on the findings, the highest F-statistic and the highest R-squared value were associated with the power-law relationship. Accordingly, the relationship of the two variables, lighting demand and the height of the northern window, is identified as a **power equation**. In addition, based on the results of the regression test, a moderate and direct relationship is detected between the two variables (Table 4-87).

Table 4-87. Results of Curve Regression Between Lighting Demand and the Height of the Window

Model formula	Model Results		Model Diagram
	R Square	F	
Linear	.396	2351.024	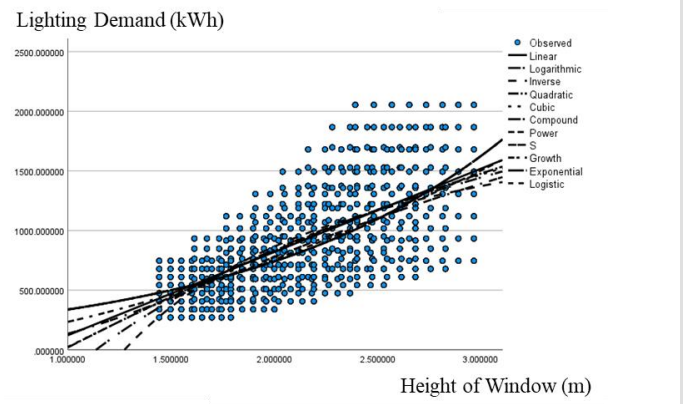
Logarithmic	.395	2339.908	
Inverse	.386	2250.828	
Quadratic	.397	1179.309	
Cubic	.397	1180.552	
Compound	.415	2537.371	
Power	.422	2617.467	
S	.421	2606.133	
Growth	.415	2537.371	
Exponential	.415	2537.371	
Logistic	.415	2537.371	

Dependent Variable: Lighting Energy
The independent variable is Height of Window.

In this section, the relationship between energy consumption and the height of the northern window is examined. Based on the findings from the curvilinear regression test, the highest F-statistic corresponds to the logarithmic equation, while the highest R-squared value is associated with the cubic curve. Considering the F-statistic and R-squared values, the relationship between the two variables is identified as a **logarithmic equation** (Table 4-88).

Table 4-88. Results of Curve Regression Between Average UDI and the Height of the Window

Model formula	Model Results		Model Diagram
	R Square	F	
Linear	.248	1182.019	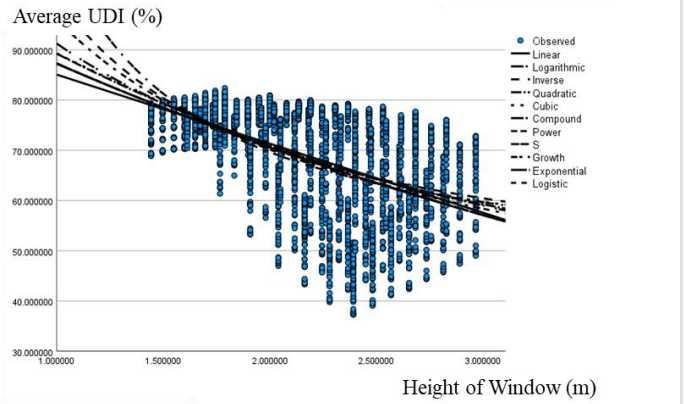
Logarithmic	.248	1183.701	
Inverse	.242	1145.019	
Quadratic	.250	598.047	
Cubic	.251	601.378	
Compound	.229	1063.139	
Power	.230	1069.510	
S	.225	1039.483	
Growth	.229	1063.139	
Exponential	.229	1063.139	
Logistic	.229	1063.139	

Dependent Variable: UDI Average

The independent variable is Height of Window.

In this section, the relationship between the average daylight autonomy and the height of the northern window is examined. Based on the findings, the highest F-statistic corresponds to the logarithmic equation, while the highest R-squared value is associated with the cubic curve. Considering the F-statistic and R-squared values for both equations, the relationship between the two variables is identified as a **logarithmic equation** (Table 4-89).

Table 4-89. Results of Curve Regression Between Average DA and the Height of the Window

Model formula	Model Results		Model Diagram
	R Square	F	
Linear	.266	1296.350	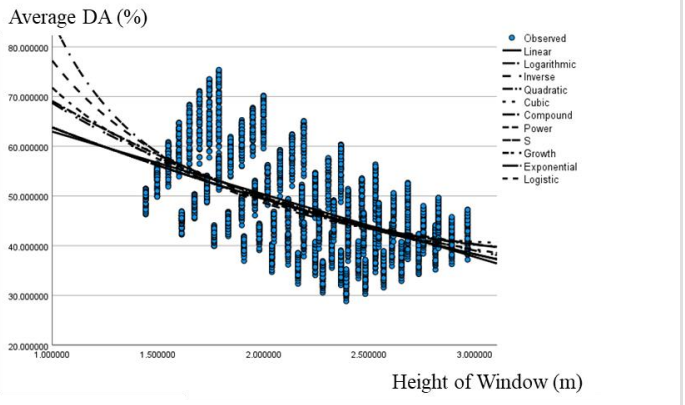
Logarithmic	.269	1315.130	
Inverse	.264	1284.105	
Quadratic	.272	669.014	
Cubic	.274	675.447	
Compound	.260	1259.774	
Power	.264	1287.599	
S	.261	1267.276	
Growth	.260	1259.774	
Exponential	.260	1259.774	
Logistic	.260	1259.774	

Dependent Variable: DA Average

The independent variable is Height of Window.

In this section, the relationship between energy consumption per square meter and the area of the northern window is examined. Based on the findings, the highest F-statistic and the highest R-squared value were associated with the power-law relationship. Accordingly, the relationship between the two variables, energy consumption and the area of the northern window, is identified as a **power equation** (Table 4-90).

Table 4-90. Results of Curve Regression Between Energy Consumption per Square Meter and the Area of the Window

Model formula	Model Results		Model Diagram
	R Square	F	
Linear	.476	3249.413	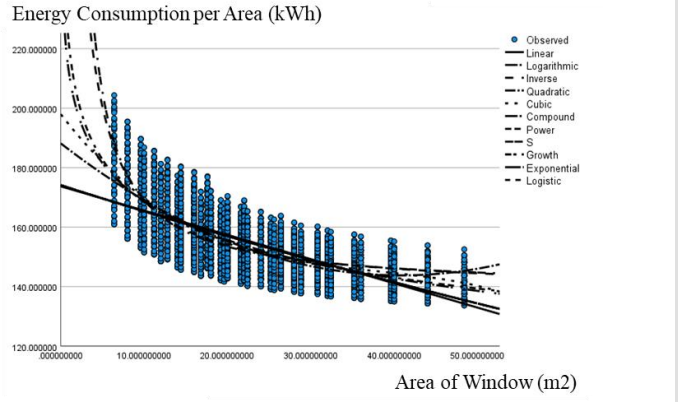
Logarithmic	.541	4217.513	
Inverse	.533	4085.119	
Quadratic	.539	2093.510	
Cubic	.546	1436.752	
Compound	.486	3384.299	
Power	.543	4256.749	
S	.525	3958.873	
Growth	.486	3384.299	
Exponential	.486	3384.299	
Logistic	.486	3384.299	

Dependent Variable: Global Energy Per Area
The independent variable is Area of Window

In this section, the relationship between cooling demand per square meter and the area of the northern window is examined. Based on the findings from the curvilinear regression test, the highest F-statistic and the highest R-squared value were associated with the compound equation, growth, and logistics. Accordingly, the relationship between the two variables is identified as a **compound equation** (Table 4-91).

Table 4-91. Results of Curve Regression Between Cooling Demand per Square Meter and the Area of the Window

Model formula	Model Results		Model Diagram
	R Square	F	
Linear	.011	38.707	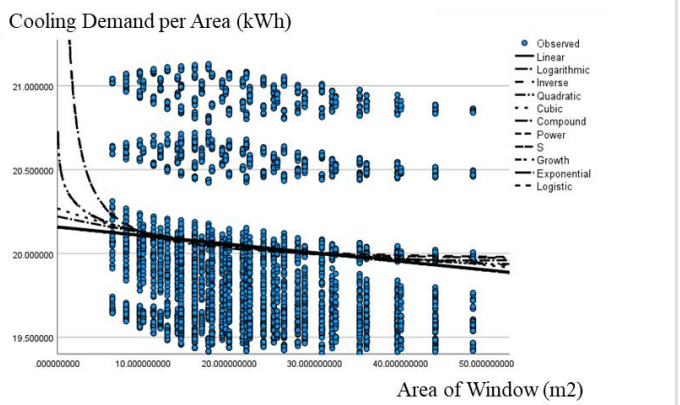
Logarithmic	.011	41.411	
Inverse	.011	38.412	
Quadratic	.011	20.481	
Cubic	.011	13.769	
Compound	.011	39.555	
Power	.012	42.334	
S	.011	39.284	
Growth	.011	39.555	
Exponential	.011	39.555	
Logistic	.011	39.555	

Dependent Variable: Cooling Energy Per Area
The independent variable is Area of Window.

In this section, the relationship between heating demand per square meter and the area of the northern window is examined. Based on the findings from the curvilinear regression test, the highest F-statistic and the highest R-squared value were associated with the logarithmic relationship. Accordingly, the relationship between the two variables is identified as a **logarithmic equation**. In addition, based on the results of the regression test, a moderate and direct relationship is detected between the two variables (Table 4-92).

Table 4-92. Results of Curve Regression Between Heating Demand per Square Meter and the Area of the Window

Model formula	Model Results		Model Diagram
	R Square	F	
Linear	.477	3270.088	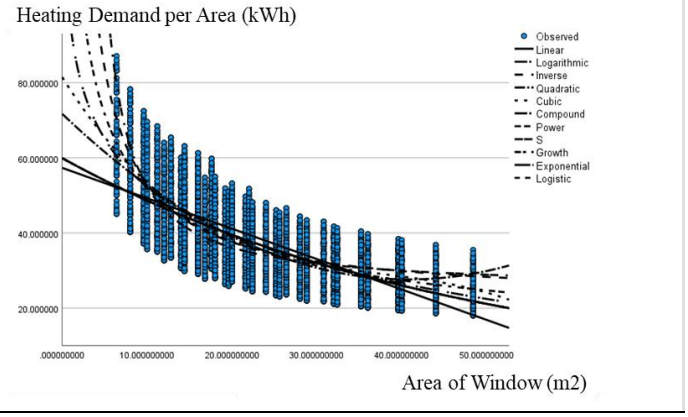
Logarithmic	.543	4251.744	
Inverse	.535	4120.903	
Quadratic	.541	2111.010	
Cubic	.548	1449.057	
Compound	.505	3657.595	
Power	.540	4198.636	
S	.496	3528.546	
Growth	.505	3657.595	
Exponential	.505	3657.595	
Logistic	.505	3657.595	

Dependent Variable: Heating Energy Per Area
The independent variable is Area of Window.

In this section, the relationship between energy consumption and the area of the northern window is examined. Based on the findings from the curvilinear regression test, the highest F-statistic corresponds to the linear equation, while the highest R-squared values were associated with the linear, quadratic, and cubic relationships. Accordingly, the relationship between the two variables is identified as a **linear equation** (Table 4-93).

Table 4-93. Results of Curve Regression Between Energy Consumption and the Area of the Window

Model formula	Model Results		Model Diagram
	R Square	F	
Linear	.986	245360.411	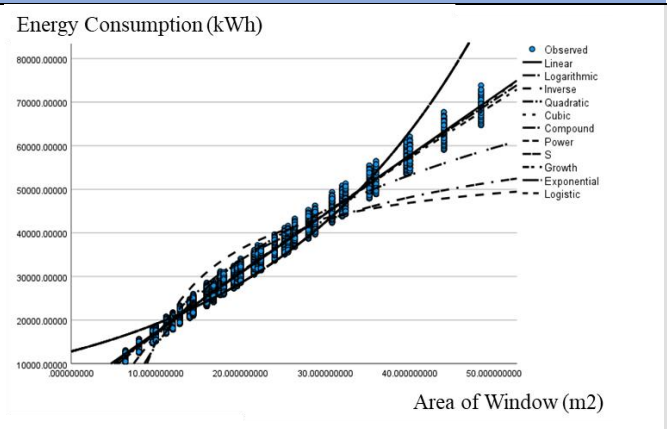
Logarithmic	.930	47618.198	
Inverse	.750	10758.711	
Quadratic	.986	124346.244	
Cubic	.986	83204.276	
Compound	.928	45869.874	
Power	.985	239744.598	
S	.905	34066.045	
Growth	.928	45869.874	
Exponential	.928	45869.874	
Logistic	.928	45869.874	

Dependent Variable: Global Energy
The independent variable is Area of Window.

In this section, the relationship between cooling demand and the area of the northern window is examined. Based on the findings from the curvilinear regression test, the highest F-statistic and R-squared value were associated with the power-law relationship. Accordingly, the relationship between the two variables, cooling demand and the area of the northern window, is identified as a **power equation** (Table 4-94).

Table 4-94. Results of Curve Regression Between Cooling Demand and the Area of the Window

Model formula	Model Results		Model Diagram
	R Square	F	
Linear	.996	955625.134	
Logarithmic	.933	49912.159	
Inverse	.746	10504.488	
Quadratic	.996	477937.126	
Cubic	.996	318537.805	
Compound	.933	50100.782	
Power	.997	1291578.100	
S	.921	42000.537	
Growth	.933	50100.782	
Exponential	.933	50100.782	
Logistic	.933	50100.782	

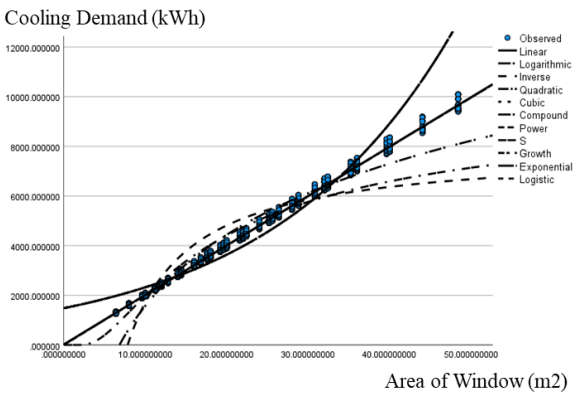

Dependent Variable: Cooling Energy
The independent variable is Area of Window.

In this section, the relationship between heating demand and the area of the northern window is examined. Based on the findings, the highest F-statistic and the highest R-squared value were both associated with the power-law relationship. Accordingly, the relationship between the two variables, heating demand and the area of the northern window, is identified as a **power equation**. In addition, based on the results of the regression test, a moderate and direct relationship is detected between the two variables (Table 4-95).

Table 4-95. Results of Curve Regression Between Heating Demand and the Area of the Window

Model formula	Model Results		Model Diagram
	R Square	F	
Linear	.589	5138.022	
Logarithmic	.583	5016.700	
Inverse	.498	3555.301	
Quadratic	.595	2627.689	
Cubic	.596	1763.109	
Compound	.574	4816.935	
Power	.613	5674.794	
S	.569	4724.550	
Growth	.574	4816.935	
Exponential	.574	4816.935	
Logistic	.574	4816.935	

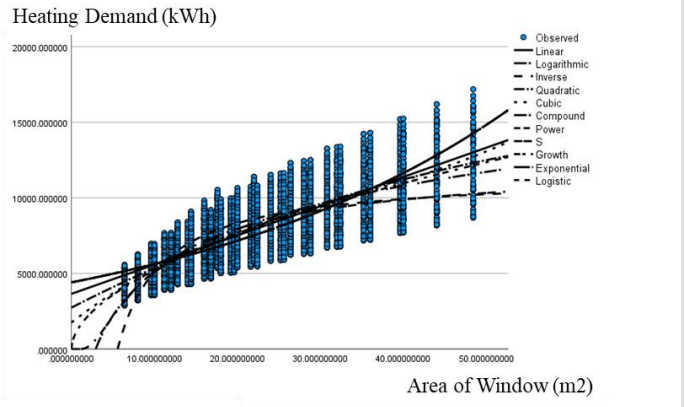

Dependent Variable: Heating Energy
The independent variable is Area of Window.

In this section, the relationship between lighting demand and the area of the northern window is analysed. Based on the results, the highest F-statistic corresponds to the linear equation, while the highest R-squared values are observed for linear, quadratic, cubic, and power-law relationships. Considering the F-statistic and R-squared values, the relationship between the two variables is identified as **linear model** (Table 4-96).

Table 4-96. Results of Curve Regression Between Lighting Demand and the Area of the Window

Model formula	Model Results		Model Diagram
	R Square	F	
Linear	1.000	33399366180619848	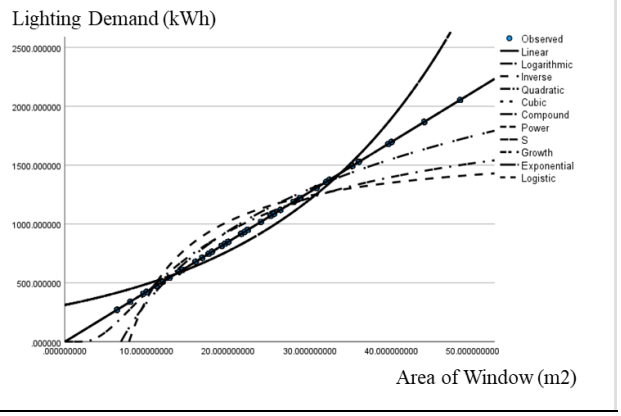
Logarithmic	.936	52263.310	
Inverse	.747	10597.661	
Quadratic	1.000	16695465794018060	
Cubic	1.000	11127364128593224	
Compound	.936	52263.312	
Power	1.000	35299548939254880	
S	.924	43549.410	
Growth	.936	52263.312	
Exponential	.936	52263.312	
Logistic	.936	52263.312	

Dependent Variable: Lighting Energy
The independent variable is Area of Window.

In this section, the relationship between the average useful daylight and the area of the northern window is examined. Based on the findings from the curvilinear regression test, the highest F-statistic corresponds to the inverse equation, while the highest R-squared value is associated with the cubic curve. Considering the F-statistic and R-squared values, the relationship between the two variables is identified as an **inverse equation** (Table 4-97).

Table 4-97. Results of Curve Regression Between Average UDI and the Area of the Window

Model formula	Model Results		Model Diagram
	R Square	F	
Linear	.065	248.758	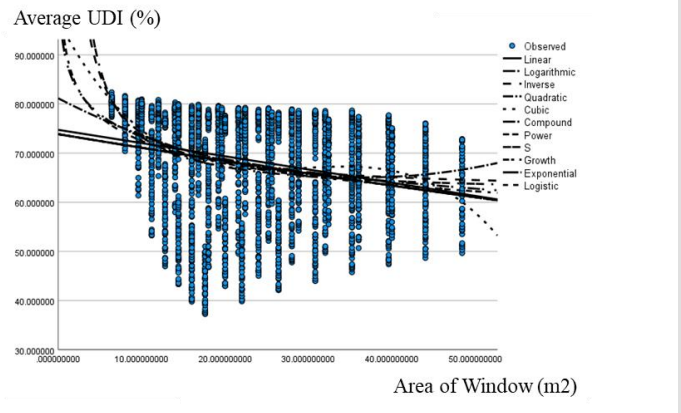
Logarithmic	.084	329.238	
Inverse	.098	389.941	
Quadratic	.081	157.002	
Cubic	.104	138.800	
Compound	.051	191.318	
Power	.068	261.588	
S	.082	318.723	
Growth	.051	191.318	
Exponential	.051	191.318	
Logistic	.051	191.318	

Dependent Variable: UDI Average
The independent variable is Area of Window.

In this section, the relationship between the average daylight autonomy and the area of the northern window is examined. Based on the findings from the curvilinear regression test, the highest F-statistic corresponds to the inverse equation, while the highest R-squared values are associated with both the inverse relationship and the cubic curve. Accordingly, the relationship between the two variables is identified as an **inverse equation**. In addition, based on the results of the regression test, a moderate and direct relationship is detected between the two variables. The R-squared values in this test were less than 0.25 in all equations (Table 4-98).

Table 4-98. Results of Curve Regression Between Average DA and the Area of the Window

Model formula	Model Results		Model Diagram
	R Square	F	
Linear	.199	890.749	
Logarithmic	.232	1082.941	
Inverse	.238	1116.587	
Quadratic	.228	529.441	
Cubic	.238	372.720	
Compound	.187	822.402	
Power	.216	985.550	
S	.219	1004.211	
Growth	.187	822.402	
Exponential	.187	822.402	
Logistic	.187	822.402	

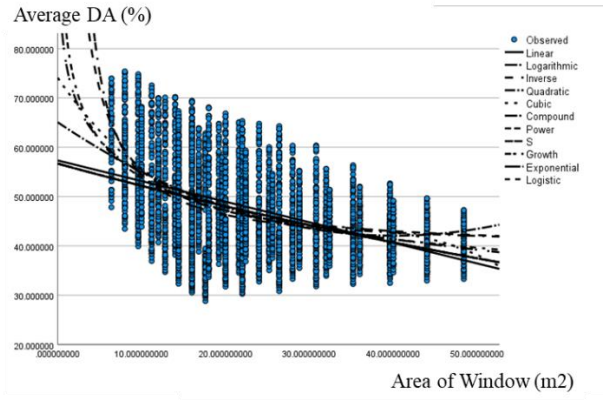

Dependent Variable: DA Average
The independent variable is Area of Window.

Based on the results of the curvilinear regression test, analyses of the relationships can be conducted; however, due to the extensive number of tests performed, this will not be addressed here. Instead, the subsequent section will focus on modelling the relationships based on the findings from the curvilinear regression.

4-2-3 Linear Modeling of Building Energy Performance Relationships

Linear regression is one of the methods of regression analysis. In general, regression is a type of statistical model used to predict a variable based on one or more other variables. Linear regression is a type of linear predictive function where the dependent variable is predicted as a linear combination of independent variables; each of the independent variables is multiplied by a coefficient obtained during the estimation process for that variable. The final result is the sum of these products plus a constant value, which is also derived in the estimation process. The simplest form of linear regression analysis is simple linear regression, which, unlike multiple linear regression, has only one independent variable.

Another type of linear regression is multivariate linear regression, where multiple dependent variables are predicted instead of just one. The estimation process aims to select the coefficients of the linear regression model in such a way that they align closely with the available data, meaning that the predictions are near the observed values in the data. One of the most critical issues in linear regression is minimizing the difference between these two. Various methods exist to address this issue. In probabilistic methods, linear regression models attempt to estimate the conditional probability distribution of the dependent variable (rather than the joint probability distribution), using this to derive a statistic of the dependent variable as the final prediction. The mean is one of the most used statistics, although other statistics such as the median or quantiles are also utilized. In this research, linear regression analysis is defined between performance objectives as the dependent variable and spatial factors as the predictor or independent variable. The findings from the nonlinear regression section indicate that, in most relationships, the linear model is appropriate. Therefore, in this section, assuming the linearity of the relationships, a linear regression test will be conducted on four potential relationships between the area of interior spaces and the length and width of these spaces as independent variables, and the environment of the final plan and the area of the environmental rectangle as dependent variables. The assumption of linearity implies that the dependent variable comprises the sum of a constant value with the effect of all influencing independent variables, each multiplied by its specific coefficient, as described in the following equation.

$$A = a + (b_1 B_1) + (b_2 B_2) + (b_3 B_3) + (b_4 B_4) + (b_5 B_5)$$

In the above equation, A is the dependent variable influenced by five independent variables, Bi. Initially, a linear regression analysis was conducted with energy consumption per square meter as the dependent variable and the spatial factors as the predictor variables, as detailed in the variable description table 4-99.

Table 4-99. Results of Linear Regression between Spatial Factors and Global Energy Per Area

Model	R	R Square	Adjusted R Square	Std. Error of the Estimate
1	.979[a]	.959	.959	2.386246721

a. Predictors: (Constant), Area of Window, NS Direction towards the North, Height of Building, NS Side Dimention, EW Side Dimention, WWR of North Facade, Volume of Building, Height of Window, Width of Window

According to the results of the linear regression analysis, an R Square value of 0.959 was obtained, indicating that the resulting equation predicts approximately 95.9% of the variations in energy consumption per square meter.

Additionally, based on the ANOVA test regarding energy consumption per square meter as the dependent variable and spatial factors, a significance level of less than 0.05 was obtained, confirming the significance of the regression test.

The significance of all spatial factors in the equation has also been found to be less than 0.05, confirming their relevance. In the conducted regression test, based on standardized coefficients, the largest contribution to the equation is associated with the dimensions of the north-south side, with a standardized beta coefficient of 3.637. Following that, the window height is the most influential variable in the equation (Table 4-100).

Table 4-100. Results of Linear Regression Between Spatial Factors and Global Energy Per Area

Model		Unstandardized Coefficients B	Unstandardized Coefficients Std. Error	Standardized Coefficients Beta	t	Sig.
1	(Constant)	154.609	1.333		115.977	.000
	EW Side Dimention	-3.615	.150	-1.409	-24.046	.000
	NS Side Dimention	9.329	.295	3.637	31.645	.000
	Height of Building	46.781	.743	1.824	62.963	.000
	NS Direction towards the North	-.023	.001	-.060	-17.560	.000
	Volume of Building	.010	.003	.300	3.500	.000
	WWR of North Facade	-90.658	3.360	-1.215	-26.981	.000
	Width of Window	6.626	.455	2.017	14.551	.000
	Height of Window	-105.993	2.796	-3.432	-37.912	.000
	Area of Window	-1.741	.198	-1.474	-8.786	.000

a. Dependent Variable: Global Energy Per Area

Additionally, the least contribution to the equation is for the orientation of the building relative to the north axis. Furthermore, the variable representing the area of the building has been excluded from the equation based on the test. This is due to its high correlation with the building volume and the dimensions of the building's sides included in the equation. Based on the results of the test, the equation for global energy consumption per square meter is obtained as follows:

$$GEPA = 154.609 - (3.615 \times EW) + (9.329 \times NS) + (46.781 \times H) - (0.023 \times D) + (0.010 \times V) - (90.658 \times WWR) + (6.626 \times WW) - (105.993 \times WH) - (1.741 \times WA)$$

Additionally, a linear regression test was conducted with cooling demand per square meter as the dependent variable and spatial factors as the independent predictive variables, which can be seen in the variable description table 4-101. According to the results of the linear regression test, an R-squared value of 0.593 was obtained, indicating that the resulting equation predicts approximately 59.3% of the changes in cooling demand per square meter. Furthermore, based on the ANOVA test regarding the cooling load per square meter as the

dependent variable and spatial factors, a significance level of less than 0.05 was obtained, confirming the significance of the regression test.

Table 4-101. Results of Linear Regression Between Spatial Factors and Cooling Energy Per Area

Model	R	R Square	Adjusted R Square	Std. Error of the Estimate
1	.770[a]	.593	.592	.315350619

a. Predictors: (Constant), Area of Window, NS Direction towards the North, Height of Building, NS Side Dimention, EW Side Dimention, WWR of North Facade, Volume of Building, Height of Window, Width of Window

The significance of the orientation in the equation has also been found to be less than 0.05, confirming its relevance. However, other factors have significance levels greater than 0.05, and their significance is not confirmed. Although according to modern statistical science, a significance level greater than 0.05 does not necessarily reject the significance of the test. In the conducted regression analysis, based on standardized coefficients, the largest contribution to the equation is attributed to the building orientation, with a standardized beta coefficient of -0.754. Following that, the window height is identified as the most influential variable in the equation (Table 4-102).

Table 4-102. Results of Linear Regression Between Spatial Factors and Cooling Energy Per Area

Model		Unstandardized Coefficients		Standardized Coefficients	t	Sig.
		B	Std. Error	Beta		
1	(Constant)	20.418	.176		115.898	.000
	EW Side Dimention	-.016	.020	-.147	-.798	.425
	NS Side Dimention	.043	.039	.399	1.103	.270
	Height of Building	.136	.098	.126	1.388	.165
	NS Direction towards the North	-.012	.000	-.754	-70.706	.000
	Volume of Building	.000	.000	.161	.596	.551
	WWR of North Facade	-.630	.444	-.201	-1.419	.156
	Width of Window	.048	.060	.350	.803	.422
	Height of Window	-.539	.369	-.416	-1.459	.145
	Area of Window	-.018	.026	-.369	-.699	.485

a. Dependent Variable: Cooling Energy Per Area

In the regression analysis, based on standardized coefficients, the smallest contribution to the equation is related to the building height, with a standardized beta coefficient of 0.126. Subsequently, the dimensions of the east-west side have the least influence in the equation. Additionally, the variable representing the area of the building has also been excluded from this equation. This is due to its high correlation with the building volume and the dimensions of the building sides included in the equation. Based on the results of the analysis, the equation for cooling demand per square meter is derived as follows:

$$CEPA = 20.418 - (0.016 \times EW) + (0.043 \times NS) + (0.136 \times H) - (0.012 \times D) - (0.630 \times WWR) + (0.048 \times WW) - (0.539 \times WH) - (0.018 \times WA)$$

Also, a linear regression test was conducted with heating demand per square meter as the dependent variable and spatial factors as the predictor variables, as detailed in the variable description table. According to the results of the linear regression test, an R-squared value of 0.964 was obtained, indicating that the resulting equation predicts approximately 96.4% of the variations in heating demand per square meter (Table 4-103).

Additionally, based on the ANOVA test regarding heating demand per square meter as the dependent variable and spatial factors, a significance level of less than 0.05 was obtained, confirming the significance of the regression test.

Table 4-103. Results of Linear Regression Between Spatial Factors and Heating Energy Per Area

Model	R	R Square	Adjusted R Square	Std. Error of the Estimate
1	.982[a]	.964	.964	2.226089680

a. Predictors: (Constant), Area of Window, NS Direction towards the North, Height of Building, NS Side Dimention, EW Side Dimention, WWR of North Facade, Volume of Building, Height of Window, Width of Window

Furthermore, the significance of all spatial factors in the equation was also found to be less than 0.05, confirming their relevance. In the conducted regression test, based on standardized coefficients, the largest contribution to the equation is associated with the north-south dimensions, with a standardized beta coefficient of 3.649 (Table 4-104).

Table 4-104. Results of the Linear Regression between Spatial Factors and Heating Energy Per Area

Model		Unstandardized Coefficients		Standardized Coefficients	t	Sig.
		B	Std. Error	Beta		
1	(Constant)	37.988	1.244		30.546	.000
	EW Side Dimention	-3.599	.140	-1.414	-25.663	.000
	NS Side Dimention	9.286	.275	3.649	33.766	.000
	Height of Building	46.645	.693	1.833	67.296	.000
	NS Direction towards the North	-.011	.001	-.028	-8.807	.000
	Volume of Building	.010	.003	.296	3.668	.000
	WWR of North Facade	-90.028	3.135	-1.216	-28.721	.000
	Width of Window	6.578	.425	2.018	15.484	.000
	Height of Window	-105.454	2.608	-3.442	-40.433	.000
	Area of Window	-1.723	.185	-1.470	-9.319	.000

a. Dependent Variable: Heating Energy Per Area

Following that, the window height is the most influential variable in the equation, which has a negative effect. In the conducted regression test, based on standardized coefficients, the least contribution to the equation is associated with the building orientation, with a standardized beta coefficient of -0.028. Following that, the building volume has the least influence in the equation. Additionally, in this case as well, the variable of building area has

been excluded from the equation. Based on the results of the test, the heating demand equation per square meter is obtained as follows:

$$HEPA = 37.988 - (3.599 \times EW) + (9.286 \times NS) + (46.645 \times H) - (0.011 \times D) + (0.010 \times V) - (90.028 \times WWR) + (6.578 \times WW) - (105.454 \times WH) - (1.723 \times WA)$$

Subsequently, a linear regression test was conducted with energy consumption as the dependent variable and spatial factors as the predictor variables, which can be seen in the variable description table. According to the results of the linear regression test, the R-squared value obtained is 0.999, indicating that the resulting equation predicts approximately 99.9% of the variations in energy consumption (Table 4-105).

Additionally, based on the ANOVA test regarding energy consumption as the dependent variable and spatial factors, a significance level of less than 0.05 has been obtained, confirming the significance of the regression test. The significance of all spatial factors, except for the window-to-wall ratio, in the equation has also been found to be less than 0.05, confirming their relevance.

Table 4-105. Results of the Linear Regression Between Spatial Factors and Global Energy

Model	R	R Square	Adjusted R Square	Std. Error of the Estimate
1	1.000[a]	.999	.999	331.34724812

a. Predictors: (Constant), Area of Window, NS Direction towards the North, Height of Building, NS Side Dimention, EW Side Dimention, WWR of North Facade, Volume of Building, Height of Window, Width of Window

In the conducted regression test, based on standardized coefficients, the largest contribution to the equation is associated with the window area, with a standardized beta coefficient of 0.643. Following that, the building volume is the most influential variable in the equation, with a standardized beta coefficient of 0.232 (Table 4-106).

Other standardized coefficients of the variables have been found to be less than 0.12. Therefore, the impact of the building area on predicting energy consumption is significantly greater than that of other factors. Furthermore, the least contribution to the equation is from the window-to-wall ratio. Additionally, similar to previous tests, the variable representing the building area has been excluded from the equation based on the test results. Subsequently, a linear regression test was conducted with cooling load as the dependent variable and spatial factors as the predictor variables, as outlined in the variable description table. According to the results of the linear regression test, the R-squared value obtained is

0.998, indicating that the resulting equation predicts approximately 99.8% of the variations in the cooling load (Table 4-106).

Table 4-106. Results of Linear Regression Test Between Spatial Factors and Global Energy

Model		Unstandardized Coefficients		Standardized Coefficients	t	Sig.
		B	Std. Error	Beta		
1	(Constant)	-4580.788	185.112		-24.746	.000
	EW Side Dimention	141.485	20.873	.048	6.778	.000
	NS Side Dimention	340.867	40.934	.115	8.327	.000
	Height of Building	2027.022	103.171	.068	19.647	.000
	NS Direction towards the North	-5.221	.184	-.012	-28.298	.000
	Volume of Building	9.063	.404	.232	22.452	.000
	WWR of North Facade	-632.830	466.573	-.007	-1.356	.175
	Width of Window	203.657	63.230	.054	3.221	.001
	Height of Window	-1560.292	388.214	-.044	-4.019	.000
	Area of Window	877.495	27.525	.643	31.880	.000

a. Dependent Variable: Global Energy

The R-squared value obtained allows the use of this model in forecasting tools. Based on the results of the test, the global energy consumption equation is obtained as follows:

$$GE = -4580.788 + (141.485 \times EW) + (340.867 \times NS) + (2027.022 \times H) - (5.221 \times D) + (9.063 \times V) - (632.830 \times WWR) + (203.657 \times WW) - (1560.292 \times WH) + (877.495 \times WA)$$

Additionally, based on the ANOVA test concerning cooling load as the dependent variable and spatial factors, the significance coefficient was found to be less than 0.05, confirming the significance of the regression test. The significance of all spatial factors, except for the window area, was found to be greater than 0.05, which does not confirm their relevance. Only the area showed a significance level of less than 0.05. In the conducted regression test, based on standardized coefficients, the largest contribution to the equation is associated with the window area, with a coefficient of 0.980 (Table 4-107).

Table 4-107. Results of Linear Regression Between Spatial Factors and Cooling Energy

Model	R	R Square	Adjusted R Square	Std. Error of the Estimate
1	.999[a]	.998	.998	84.560981754

a. Predictors: (Constant), Area of Window, NS Direction towards the North, Height of Building, NS Side Dimention, EW Side Dimention, WWR of North Facade, Volume of Building, Height of Window, Width of Window

The R-squared value obtained allows the use of this model in forecasting tools. Following that, the building orientation is the next most influential variable in the equation. However, there is a significant and substantial difference between the impact of the window area and that of other spatial factors on the cooling demand. Additionally, the least contribution in

the equation is attributed to the WWR. Furthermore, similar to previous tests, the variable for building area has been excluded from the equation based on the analysis (Table 4-106).

Table 4-108. Results of Linear Regression between Spatial Factors and Cooling Energy

Model		Unstandardized Coefficients		Standardized Coefficients	t	Sig.
		B	Std. Error	Beta		
1	(Constant)	-44.671	47.241		-.946	.344
	EW Side Dimention	1.302	5.327	.003	.244	.807
	NS Side Dimention	-8.762	10.446	-.020	-.839	.402
	Height of Building	-13.429	26.330	-.003	-.510	.610
	NS Direction towards the North	-2.873	.047	-.043	-61.030	.000
	Volume of Building	.038	.103	.007	.373	.709
	WWR of North Facade	68.857	119.071	.005	.578	.563
	Width of Window	5.869	16.137	.011	.364	.716
	Height of Window	85.233	99.074	.016	.860	.390
	Area of Window	195.542	7.024	.980	27.837	.000

a. Dependent Variable: Cooling Energy

Additionally, the least contribution in the equation is attributed to the window-to-wall ratio. Furthermore, similar to previous tests, the variable for building area has been excluded from the equation based on the analysis. Based on the results of the test, the equation for cooling demand is derived as follows:

$$CE = -44.671 + (1.302 \times EW) - (8.762 \times NS) - (13.429 \times H) - (2.873 \times D) + (0.038 \times V) + (68.857 \times WWR) + (5.869 \times WW) + (85.233 \times WH) + (195.542 \times WA)$$

In the continuation, a linear regression test was conducted with heating demand as the dependent variable and spatial factors as the predictor variables, which can be seen in the table of variable descriptions. According to the results of the linear regression test, the R-squared value obtained was 0.989, indicating that the resulting equation predicts approximately 98.9% of the variations in heating demand (Table 4-109).

Table 4-109. Results of the Linear Regression Test Between Spatial Factors and Heating Energy

Model	R	R Square	Adjusted R Square	Std. Error of the Estimate
1	.995[a]	.989	.989	257.910427810

a. Predictors: (Constant), Area of Window, NS Direction towards the North, Height of Building, NS Side Dimention, EW Side Dimention, WWR of North Facade, Volume of Building, Height of Window, Width of Window

Additionally, based on the ANOVA test regarding heating demand as the dependent variable and spatial factors, a significance level of less than 0.05 was obtained, confirming the significance of the regression test. Additionally, the significance of all spatial factors in the equation, except for the window-to-wall ratio, is found to be less than 0.05, confirming their

relevance, while the coefficient of the window-to-wall ratio has a somewhat minor error (Table 4-110).

Table 4-110. Results of the Linear Regression Test Between Spatial Factors and Heating Energy

Model		Unstandardized Coefficients B	Unstandardized Coefficients Std. Error	Standardized Coefficients Beta	t	Sig.
1	(Constant)	-4536.123	144.085		-31.482	.000
	EW Side Dimention	140.183	16.247	.256	8.628	.000
	NS Side Dimention	349.627	31.862	.640	10.973	.000
	Height of Building	2040.449	80.305	.373	25.409	.000
	NS Direction towards the North	-2.347	.144	-.028	-16.345	.000
	Volume of Building	9.025	.314	1.250	28.722	.000
	WWR of North Facade	-701.670	363.166	-.044	-1.932	.053
	Width of Window	197.785	49.217	.282	4.019	.000
	Height of Window	-1645.514	302.174	-.250	-5.446	.000
	Area of Window	-280.074	21.424	-1.112	-13.073	.000

a. Dependent Variable: Heating Energy

In the conducted regression test, based on standardized coefficients, the largest contribution to the equation is associated with the building volume, with a coefficient of 1.250. Following that, the window area is the most influential variable in the equation. There is a significant and substantial difference between the impact of these two factors and other spatial factors concerning the cooling demand. Additionally, the least contribution in the equation is for the building orientation. Also, similar to previous tests, the variable of building area has been excluded from the equation based on the test. Based on the results of the test, the equation for heating demand is as follows:

$$HE = -4536.123 + (140.183 \times EW) + (349.627 \times NS) + (2040.449 \times H) - (2.347 \times D) + (9.025 \times V) - (701.670 \times WWR) + (197.785 \times WW) - (1645.514 \times WH) - (280.074 \times WA)$$

Furthermore, a linear regression test was conducted with lighting demand as the dependent variable and spatial factors as predictor variables, as detailed in the table of variable descriptions. According to the results of the linear regression test, an R-squared value of 1.000 was obtained, indicating that the resulting equation predicts approximately 100% of the variations in lighting demand. This is due to the specific formula for lighting demand based on each square meter of space (Table 4-111).

Additionally, based on the ANOVA test regarding lighting demands as the dependent variable and spatial factors, a significance level of less than 0.05 has been obtained, confirming the significance of the regression test. Furthermore, the significance of all spatial

factors, except for the height and orientation of the building, is found to be less than 0.05 in the equation, confirming their relevance (Table 4-111).

Table 4-111. Results of the Linear Regression Test Between Spatial Factors and Lighting Energy

Model	R	R Square	Adjusted R Square	Std. Error of the Estimate
1	1.000[a]	1.000	1.000	.000130653

a. Predictors: (Constant), Area of Window, NS Direction towards the North, Height of Building, NS Side Dimention, EW Side Dimention, WWR of North Facade, Volume of Building, Height of Window, Width of Window

The data regarding orientation indicates that there is no definitive relationship between this variable and the lighting requirement. In the conducted regression test, based on standardized coefficients, the largest contribution in the equation is attributed to the window area, with a coefficient of 1.000. Other variables yielded values close to zero. There is a significant and substantial difference between the impact of window area and other spatial factors on the lighting requirement (Table 4-112).

Table 4-112. Results of the Linear Regression Test Between Spatial Factors and Lighting Energy

Model		Unstandardized Coefficients		Standardized Coefficients	t	Sig.
		B	Std. Error	Beta		
1	(Constant)	.000	.000		4.357	.000
	EW Side Dimention	-3.459E-5	.000	.000	-4.201	.000
	NS Side Dimention	5.873E-5	.000	.000	3.638	.000
	Height of Building	6.551E-5	.000	.000	1.610	.107
	NS Direction towards the North	.000	.000	.000	.000	1.000
	Volume of Building	7.767E-7	.000	.000	4.878	.000
	WWR of North Facade	-.001	.000	.000	-3.932	.000
	Width of Window	.000	.000	.000	4.081	.000
	Height of Window	.000	.000	.000	-3.206	.001
	Area of Window	42.431	.000	1.000	3908624.426	.000

a. Dependent Variable: Lighting Energy

The variable of building area has been excluded from the equation based on the test, similar to previous tests. According to the results of the test, the equation for lighting requirements is derived as follows:

$$LE = -(3.459\text{E} - 5 \times EW) + (5.873\text{E} - 5 \times NS) + (6.551E - 5 \times H) + (7.767E - 7 \times V) - (0.001 \times WWR) + (42.431 \times WA)$$

Subsequently, a linear regression test was conducted with the average useful daylight as the dependent variable and spatial factors as the predictor variables, which can be seen in the table describing the variables. This test can define the performance of daylight based on the useful daylight illuminance. According to the results of the linear regression test, the R-

squared value obtained is 0.957, indicating that the resulting equation predicts approximately 95.7% of the changes in the average useful daylight (Table 4-113).

Table 4-113. Results of the linear regression test between spatial factors and UDI Average

Model	R	R Square	Adjusted R Square	Std. Error of the Estimate
1	.978[a]	.957	.957	2.174983178

a. Predictors: (Constant), Area of Window, NS Direction towards the North, Height of Building, NS Side Dimention, EW Side Dimention, WWR of North Facade, Volume of Building, Height of Window, Width of Window

Furthermore, based on the ANOVA test regarding the mean useful daylight as the dependent variable and spatial factors, a significance level of less than 0.05 has been obtained, confirming the significance of the regression test.

The significance of all spatial factors, except for the window area, has also been found to be less than 0.05, which is confirmed. Regarding the window area, the test indicates that the relationship has considerable error. In the linear regression test conducted, based on the standardized coefficients, the greatest contribution to the equation is related to the dimensions of the north-south facade, with a standardized regression coefficient of -3.676 (Table 4-114).

Table 4-114. Results of Linear Regression Test Between Physical Factors and UDI Average

Model		Unstandardized Coefficients B	Unstandardized Coefficients Std. Error	Standardized Coefficients Beta	t	Sig.
1	(Constant)	97.605	1.215		80.327	.000
	EW Side Dimention	-2.935	.137	-1.281	-21.418	.000
	NS Side Dimention	-8.425	.269	-3.676	-31.354	.000
	Height of Building	-15.559	.677	-.679	-22.975	.000
	NS Direction towards the North	.015	.001	.042	12.246	.000
	Volume of Building	.017	.003	.546	6.241	.000
	WWR of North Facade	-25.144	3.063	-.377	-8.210	.000
	Width of Window	3.965	.415	1.351	9.554	.000
	Height of Window	68.794	2.548	2.494	26.997	.000
	Area of Window	.066	.181	.063	.367	.714

a. Dependent Variable: UDI Average

Additionally, the window height follows the dimensions of the north-south facade with a standardized regression coefficient of 2.494, having the most significant impact. Additionally, in this test, the width of the north-facing window and the dimensions of the east-west side, with coefficients of 1.351 and -1.281, respectively, hold the greatest significance in predicting the daylighting index. The least importance in this test is attributed to the orientation of the building.

Additionally, the variable of the building's floor area has been excluded from the equation, similar to previous tests. This is due to the high correlation of this variable with the variables present in the linear equation, as previously mentioned. Based on the results of the test, the equation for the average useful daylight is obtained as follows:

$$UDIA = 97.605 - (2.935 \times EW) - (8.425 \times NS) - (15.559 \times H) + (0.015 \times D) + (0.017 \times V) - (25.144 \times WWR) + (3.965 \times WW) + (68.794 \times WH) + (0.066 \times WA)$$

Next, a linear regression test was conducted with the average daylight autonomy as the dependent variable and spatial factors as the predictor variables, which can be seen in the table describing the variables. According to the results of the linear regression test, the R-squared value obtained is 0.969, indicating that the resulting equation predicts approximately 96.9% of the changes in average daylight autonomy (Table 4-115).

Table 4-115. Results of Linear Regression Between Spatial Factors and DA Average

Model	R	R Square	Adjusted R Square	Std. Error of the Estimate
1	.985[a]	.969	.969	1.631313322

a. Predictors: (Constant), Area of Window, NS Direction towards the North, Height of Building, NS Side Dimention, EW Side Dimention, WWR of North Facade, Volume of Building, Height of Window, Width of Window

Additionally, based on the ANOVA test regarding the average daylight autonomy as the dependent variable and the spatial factors, a significance level of less than 0.05 was obtained, confirming the significance of the regression test (Table 4-116).

Table 4-116. Results of Linear Regression between Spatial Factors and DA Average

Model		Unstandardized Coefficients B	Unstandardized Coefficients Std. Error	Standardized Coefficients Beta	t	Sig.
1	(Constant)	44.677	.911		49.023	.000
	EW Side Dimention	-.320	.103	-.158	-3.114	.002
	NS Side Dimention	.509	.202	.250	2.524	.012
	Height of Building	23.915	.508	1.178	47.082	.000
	NS Direction towards the North	.033	.001	.105	36.030	.000
	Volume of Building	-.002	.002	-.074	-1.005	.315
	WWR of North Facade	3.701	2.297	.063	1.611	.107
	Width of Window	-.902	.311	-.347	-2.898	.004
	Height of Window	-40.217	1.911	-1.645	-21.042	.000
	Area of Window	.822	.136	.879	6.069	.000

a. Dependent Variable: DA Average

Furthermore, the significance of all spatial factors, except for building volume and the window-to-wall ratio, has been found to be less than 0.05, confirming their relevance in the equation. In the case of building volume and the window-to-wall ratio, the tests indicate that there is a considerable error in the relationship. In the conducted regression analysis, based

on the standardized coefficients, the highest contribution in the equation is attributed to the height of the window, with a standardized coefficient of -1.645.

Following this, the height of the building has the next highest impact, with a standardized regression coefficient of 1.178. There is a substantial difference between the effects of these two variables and other variables on the mean daylight autonomy. Therefore, these two variables can be regarded as having a significantly higher importance compared to the others. Additionally, the least importance in this analysis pertains to three variables: the aspect ratio, building volume, and building orientation, with coefficients of 0.063, -0.074, and 0.105, respectively (Table 4-116).

The variable of the building's floor area has been automatically excluded from the equation based on the test results, similar to all previous tests. The R-squared value obtained allows the use of this model in forecasting tools. Based on the results of the test, the equation for the mean daylight autonomy is obtained as follows:

$$DAA = 44.677 - (0.320 \times EW) + (0.509 \times NS) + (23.915 \times H) + (0.033 \times D) - (0.002 \times V) + (3.701 \times WWR) - (0.902 \times WW) - (40.217 \times WH) + (0.822 \times WA)$$

The results of the linear modeling indicate that in most cases, the linear equation can provide satisfactory predictions. However, to enhance the accuracy of predictions, it is necessary to conduct a nonlinear analysis.

4-2-4- Nonlinear Modeling of Building Energy Performance Relationships

In this section, based on the findings of the nonlinear regression analysis, nonlinear models are defined to achieve higher accuracy coefficients for the relationships between each energy performance objective of the residential building, considered as the dependent variable, and the physical factors of the residential building, considered as independent and predictive variables.

To this end, the results of the curve regression tests are first presented in the table 4-117, and based on those results, a nonlinear equation is formulated and tested for each performance objective. Based on the results of the curvilinear regression tests, nonlinear equations have been defined for total energy consumption, energy consumption per square meter, cooling demand, cooling demand per square meter, heating demand, heating demand per square meter, average daylight factor, and average daylight autonomy index. Following

the explanation of each equation, nonlinear regression testing based on the coding of the relevant equation in SPSS software has been conducted, and the results are presented.

Table 4-117. Results of Curvilinear Regression Tests

	Global Energy Per Area	Cooling Energy Per Area	Heating Energy Per Area	Global Energy	Cooling Energy	Heating Energy	Lighting Energy	UDI Average	DA Average
EW Side Dimention	Inverse	Linear	Inverse	Power	Power	Compound	Power	S	S
NS Side Dimention	Inverse	Power	Inverse	Power	Power	Compound	Power	Linear	Logarithmic
Area of Building	Power	Power	Logarithmic	Linear	Power	Power	Linear	Inverse	Inverse
Height of Building	Compound	Compound	Power	Compound	Compound	Power	-	Inverse	S
NS Direction	Quadratic	Quadratic	Quadratic	Quadratic	Linear	Quadratic	-	Linear	Compound
Volume of Building	Logarithmic	Power	Logarithmic	Power	Power	Power	Power	Inverse	Inverse
WWR of N Facade	Inverse	Power	Power	Power	Power	Power	Power	Linear	Power
Width of Window	Inverse	Compound	Inverse	Power	Power	Power	Power	Cubic	Linear
Height of Window	Inverse	Power	Inverse	Power	Power	Compound	Linear	Logarithmic	Logarithmic
Area of Window	Power	Power	Logarithmic	Linear	Power	Power	Power	Inverse	Inverse

According to the findings from the curvilinear regression tests, the nonlinear equation for energy consumption per square meter has been derived and is presented as follows:

$$GEPA = a + (b / EW) + (c / NS) + (d \times A^{e}) + (f \times g^{H}) + (h \times D) + (i \times D^{2}) + (j \times \log V) + (k / WWR) + (l / WW) + (m / WH) + (n \times WA^{o})$$

In this equation, energy consumption per square meter (GEPA) is defined based on the dimensions of the east-west side (EW), dimensions of the north-south side (NS), building orientation (D), building floor area (A), building volume (V), window-to-wall ratio of the north façade (WWR), width of the north window (WW), height of the north window (WH), and area of the north window (WA). Based on the established equation, the coded nonlinear regression test is conducted and executed. According to the results of the linear regression test, the coefficients of the equation are presented in the table 4-118.

Table 4-118. Results of Nonlinear Regression Between Spatial Factors and Global Energy Per Area

Parameter	Estimate	Std. Error	95% Confidence Interval	
			Lower Bound	Upper Bound
a	.802	3151.409	-6177.941	6179.545
b	-30.154	3.914	-37.827	-22.481
c	468.803	11.479	446.297	491.308
d	-288.025	226981.565	-445314.641	444738.590
e	.151	12.676	-24.703	25.004
f	-.029	194.418	-381.209	381.152
g	-6.066	10746.537	-21076.037	21063.905
h	-.023	.000	-.024	-.023
i	.002	.000	.002	.002
j	380.597	1579.122	-2715.477	3476.670
k	2.514	.152	2.216	2.811
l	381.321	3.326	374.799	387.842
m	-91.027	2.647	-96.217	-85.838
n	-199.147	319737.428	-627085.586	626687.292
o	.147	31.405	-61.427	61.721

Based on the results of the test, a significance level close to zero and less than 0.05 has been obtained, thus confirming the significance. Additionally, the adjusted R-squared value is 0.998 (Table 4-119).

Table 4-119. Results of Non-Linear Regression between Spacial Factors and Global Energy Per Area

Source	Sum of Squares	df	Mean Squares
Regression	22718467.368	15	1514564.491
Residual	304.945	3569	.085
Uncorrected Total	22718772.313	3584	
Corrected Total	150110.291	3583	

Dependent variable: Global Energy Per Area
a. R squared = 1 - (Residual Sum of Squares) / (Corrected Sum of Squares) = .998.

Therefore, with 95% confidence, the equation obtained from the non-linear regression test can predict 99.8% of the changes in energy consumption per square meter. The equation based on the results is presented as follows:

$$GEPA = 0.802 + (-30.154 / EW) + (468.803 / NS) + (-288.025 \times A^{0.151}) + (-0.029 \times -6.066^{H}) + (-0.023 \times D) + (0.002 \times D^{2}) + (380.597 \times \log V) + (2.514 / WWR) + (381.321 / WW) + (-91.027 / WH) + (-199.147 \times WA^{0.147})$$

Also, based on the findings from the set of curvature regression tests conducted in the previous section, the nonlinear equation for the cooling requirement per square meter was obtained and presented as follows:

$$CEPA = a + (b \times EW) + (c \times NS^{d}) + (e \times A^{f}) + (g \times h^{H}) + (i \times D) + (j \times D^{2}) + (k \times V^{l}) + (m \times WWR^{n}) + (o \times p^{WW}) + (q \times WH^{r}) + (s \times WA^{t})$$

In this equation, the cooling demand per square meter (CEPA) is defined based on the dimensions of the east-west side (EW), the dimensions of the north-south side (NS), the orientation of the building (D), the floor area of the building (A), the volume of the building (V), the window-to-north wall ratio (WWR), the width of the north window (WW), the height of the north window (WH), and the area of the north window (WA).

Table 4-120. Results of Non-Linear Regression Between Factors and Cooling Energy Per Area

Parameter	Estimate	Std. Error	95% Confidence Interval	
			Lower Bound	Upper Bound
a	14284.310	.000	14284.310	14284.310
b	-.274	28.286	-55.732	55.184
c	-3452.202	.000	-3452.202	-3452.202
d	-.002	.961	-1.886	1.883
e	.021	268563.289	-526553.175	526553.216
f	-2.548	.422	-3.376	-1.720
g	46.325	.131	46.068	46.582
h	1.002	119374.483	-234048.169	234050.173
i	-.012	1341.526	-2630.248	2630.224
j	.000	.035	-.068	.069
k	-1924.031	43815.731	-87830.460	83982.398
l	-.003	123333.957	-241812.237	241812.231
m	-.098	.053	-.203	.007
n	1.347	4.123	-6.737	9.431
o	1.085	91612.392	-179616.902	179619.073
p	1.006	.000	1.006	1.006
q	-4126.519	.037	-4126.593	-4126.446
r	.003	.023	-.042	.047
s	-4833.290	.000	-4833.290	-4833.290
t	.001	.056	-.109	.111

Based on the defined equation, a coded non-linear regression test has been executed (Table 4-120). The coefficients of the equation, according to the results of the non-linear regression test, are presented in the following table. Based on the results of the nonlinear regression test presented in the form of a table, the coefficients of the coded equation can be defined.

Table 4-121. Results of Non-linear Regression Between Spatial Factors and Cooling Energy Per Area

Source	Sum of Squares	df	Mean Squares
Regression	1440979.338	20	72048.967
Residual	32.812	3564	.009
Uncorrected Total	1441012.149	3584	
Corrected Total	874.080	3583	

Dependent variable: Cooling Energy Per Area
a. R squared = 1 - (Residual Sum of Squares) / (Corrected Sum of Squares) = .962.

Based on the test results, a significance level close to zero, less than 0.05, has been obtained. Therefore, the significance is confirmed. Additionally, the R-squared value is 0.962 (Table 4-121). Therefore, with 95% confidence, the equation obtained from the non-linear

regression test can predict 96.2% of the variations in cooling energy consumption per square meter (Table 4-121).

The R-squared value obtained indicates that the formula obtained from the nonlinear regression test can be used as an efficient tool for prediction. The equation resulting from the nonlinear regression test is presented as follows:

$$CEPA = 14284.310 + (-0.274 \times EW) + (-3452.202 \times NS^{-0.002}) + (0.021 \times A^{-2.548}) + (46.325 \times 1.002^{H}) + (-0.012 \times D) + (-1924.031 \times V^{-0.003}) + (-0.098 \times WWR^{1.347}) + (1.085 \times 1.006^{WW}) + (-4126.519 \times WH^{0.003}) + (-4833.290 \times WA^{0.001})$$

Based on the findings from the curvature regression tests, the non-linear equation for heating demand per square meter has been derived, as presented below:

$$HEPA = a + (b / EW) + (c / NS) + (d \times \log A) + (e \times H^{f}) + (g \times D) + (h \times D^{2}) + (i \times \log V) + (j \times WWR^{k}) + (l / WW) + (m / WH) + (n \times \log WA)$$

In this equation, the heating demand per square meter (HEPA) is defined based on the east-west dimensions (EW), the north-south dimensions (NS), the building orientation (D), the building's area (A), the building volume (V), the WWR of the north facade (WWR), the width of the window (WW), the height of the window (WH), and the window's area (WA).

Table 4-122. Results of Non-Linear Regression Between Spatial Factors and Heating Energy Per Area

Parameter	Estimate	Std. Error	95% Confidence Interval	
			Lower Bound	Upper Bound
a	-17.081	80013.874	-156894.580	156860.418
b	118.624	5.938	106.982	130.265
c	-103.736	31.882	-166.245	-41.227
d	1.322	80016.273	-156880.881	156883.525
e	4.178	11.385	-18.143	26.498
f	1.454	1.064	-.631	3.539
g	-.011	.001	-.012	-.010
h	.001	.000	.001	.001
i	-8.483	57.567	-121.350	104.385
j	5.494	.624	4.271	6.718
k	-1.207	.056	-1.317	-1.098
l	101.972	2.402	97.262	106.682
m	10.892	9.678	-8.082	29.867
n	13.532	80013.714	-156863.652	156890.716

Based on the established equation, the non-linear regression test is coded and executed (Table 4-122). The coefficients of the equation are presented based on the results of the test.

Based on the results of the test, the significance level is found to be close to zero and less than 0.05. Therefore, the significance is confirmed. Additionally, the R-squared value obtained is 0.992 (Table 4-123).

Table 4-123. Results of Non-linear Regression Between Spatial Factors and Heating Energy Per Area

Source	Sum of Squares	df	Mean Squares
Regression	5969255.224	14	426375.373
Residual	3829.197	3570	1.073
Uncorrected Total	5973084.421	3584	
Corrected Total	487306.561	3583	

Dependent variable: Heating Energy Per Area
a. R squared = 1 - (Residual Sum of Squares) / (Corrected Sum of Squares) = .992.

Therefore, with 95% confidence, the equation resulting from the linear regression test can predict 99.2% of the changes in heating demand per square meter. This rate provides a very good prediction of the building's energy performance. The prediction error of this equation is less than one percent. The equation based on the results is presented as follows:

$$HEPA = -17.081 + (118.624 / EW) + (-103.736 / NS) + (1.322 \times \log A) + (4.178 \times H^{1.454}) + (-0.011 \times D) + (0.001 \times D^2) + (-8.483 \times \log V) + (5.494 \times WWR^{-1.207}) + (101.972 / WW) + (10.892 / WH) + (13.532 \times \log WA)$$

Based on the findings of the curvature regression tests, the nonlinear equation for total energy consumption has been obtained, which is presented as follows:

$$GE = a + (b \times EW^c) + (d \times NS^e) + (f \times A) + (g \times h^H) + (i \times D) + (j \times D^2) + (k \times V^l) + (m \times WWR^n) + (o \times WW^p) + (q \times WH^r) + (s \times WA)$$

In this equation, total energy consumption (GE) is defined based on the dimensions of the east-west side (EW), dimensions of the north-south side (NS), building orientation (D), building floor area (A), building volume (V), window-to-wall ratio of the north wall (WWR), width of the north window (WW), height of the north window (WH), and area of the north window (WA).

Based on the established equation, the nonlinear regression test has been coded and executed. The test was performed several times to achieve high accuracy. The regression test results confirm the high convergence of the output equation based on the input data. According to the results of the nonlinear regression test, the coefficients of the equation are presented in the table below. The standard error of the obtained coefficients is very low and accurate estimated coefficients have been obtained (Table 4-124).

Table 4-124. Results of the Nonlinear Regression Test Between Physical Factors and Global Energy

Parameter	Estimate	Std. Error	95% Confidence Interval	
			Lower Bound	Upper Bound
a	-3022.149	1921.210	-6788.931	744.634
b	43.835	15.843	12.772	74.898
c	1.364	.093	1.181	1.547
d	252.913	308.256	-351.464	857.290
e	.926	.271	.396	1.457
f	45.943	79518.637	-155860.653	155952.540
g	359.905	355.509	-337.116	1056.927
h	1.647	.243	1.171	2.122
i	-5.221	.078	-5.374	-5.067
j	.377	.003	.371	.383
k	30.581	4.639	21.486	39.677
l	.853	.016	.821	.884
m	350.145	875.912	-1367.194	2067.483
n	-.819	.707	-2.205	.567
o	.002	.004	-.006	.010
p	4.400	.757	2.915	5.884
q	.216	.498	-.761	1.192
r	6.729	1.845	3.112	10.345
s	459.515	795186.422	-1558606.554	1559525.584

Based on the results of the test, a significance level close to zero and less than 0.05 has been obtained. Therefore, the significance is confirmed. Additionally, the R-squared value is found to be 1.000 (Table 4-125).

Table 4-125. Results of Non-Linear Regression Tests Between Physical Factors and Global Energy

Source	Sum of Squares	df	Mean Squares
Regression	4840147307213.824	19	254744595116.517
Residual	70397105.113	3565	19746.734
Uncorrected Total	4840217704318.937	3584	
Corrected Total	659886080983.070	3583	

Dependent variable: Global Energy
a. R squared = 1 - (Residual Sum of Squares) / (Corrected Sum of Squares) = 1.000.

Therefore, with 95% confidence, the equation derived from the non-linear regression test can predict 100% of the changes in total energy consumption. The equation based on the results is presented as follows:

$$GE = -3022.149 + (43.835 \times EW^{1.364}) + (252.913 \times NS^{0.926}) + (45.943 \times A) + (359.905 \times 1.647^{H}) + (-5.221 \times D) + (0.377 \times D^{2}) + (30.581 \times V^{0.853}) + (350.145 \times WWR^{-0.819}) + (0.002 \times WW^{4.400}) + (0.216 \times WH^{6.729}) + (459.515 \times WA)$$

Based on the findings of the curvature regression tests, the non-linear equation for total cooling demand has been derived, which is presented as follows:

$$CE = a + (b \times EW^{c}) + (d \times NS^{e}) + (f \times A^{g}) + (h \times i^{H}) + (j \times D) + (k \times V^{l}) + (m \times WWR^{n}) + (o \times WW^{p}) + (q \times WH^{r}) + (s \times WA^{t})$$

In this equation, total cooling demand (CE) is defined based on the dimensions of the east-west side (EW), dimensions of the north-south side (NS), building orientation (D), building floor area (A), building volume (V), window-to-north wall ratio (WWR), width of the north window (WW), height of the north window (WH), and area of the north window (WA).

Table 4-126. Results of Nonlinear Regression Tests Between Physical Factors and Cooling Energy

Parameter	Estimate	Std. Error	95% Confidence Interval	
			Lower Bound	Upper Bound
a	2348.056	1053704.790	-2063576.985	2068273.097
b	-106.063	2083.784	-4191.593	3979.466
c	.438	2.182	-3.840	4.715
d	74.660	11212.342	-21908.592	22057.911
e	.401	14.813	-28.642	29.443
f	4.304	203662.761	-399302.980	399311.588
g	1.017	7239.547	-14193.054	14195.088
h	-.001	.117	-.230	.229
i	10.541	448.068	-867.954	889.036
j	-2.873	.047	-2.966	-2.781
k	7.091	146.422	-279.988	294.169
l	.594	1.820	-2.974	4.162
m	-2404.608	1039918.400	-2041299.642	2036490.426
n	.025	12.209	-23.913	23.962
o	63.288	892.938	-1687.434	1814.009
p	.794	2.393	-3.897	5.485
q	-83.279	7417.757	-14626.754	14460.196
r	.922	23.787	-45.716	47.560
s	126.456	1396603.878	-2738096.764	2738349.676
t	1.017	2563.127	-5024.326	5026.360

Based on the established equation, the coded nonlinear regression test is executed and the R-squared value obtained is 0.998 (Table 4-127).

Table 4-127. Results of Nonlinear Regression Between Physical Factors and Cooling Energy

Source	Sum of Squares	df	Mean Squares
Regression	86826602028.383	20	4341330101.419
Residual	25552930.118	3564	7169.733
Uncorrected Total	86852154958.501	3584	
Corrected Total	14109248383.495	3583	

Dependent variable: Cooling Energy
a. R squared = 1 - (Residual Sum of Squares) / (Corrected Sum of Squares) = .998.

The R-squared value obtained allows the use of this model in forecasting tools. Therefore, , the equation obtained from the nonlinear regression test can predict 99.8% of the changes in total cooling demand. The equation based on the results is presented as follows:

$$CE = 2348.056 + (-106.063 \times EW^{0.438}) + (74.660 \times NS^{.0401}) + (4.304 \times A^{1.017}) + (-0.001 \times 10.541^{H}) + (-2.873 \times D) + (7.091 \times V^{0.594}) + (-2404.608 \times WWR^{0.025}) + (63.288 \times WW^{0.794}) + (-83.279 \times WH^{0.922}) + (126.456 \times WA^{1.017})$$

Based on the findings of the curvilinear regression tests, the nonlinear equation for total heating demand has been obtained, which is presented as follows:

$$HE = a + (b \times c^{EW}) + (d \times e^{NS}) + (f \times A^{g}) + (h \times H^{i}) + (j \times D) + (k \times D^{2}) + (l \times V^{m}) + (n \times WWR^{o}) + (p \times WW^{q}) + (r \times s^{WH}) + (t \times WA^{u})$$

In this equation, the total heating demand (HE) is defined based on the dimensions of the east-west side (EW), the dimensions of the north-south side (NS), the orientation of the building (D), the building's floor area (A), the building volume (V), the window-to-north wall ratio (WWR), the width of the north window (WW), the height of the north window (WH), and the area of the north window (WA).

Table 4-128. Results of the Nonlinear Regression Between Physical Factors and Heating Energy

Parameter	Estimate	Std. Error	95% Confidence Interval	
			Lower Bound	Upper Bound
a	-13098.801	129994.477	-267969.875	241772.273
b	604.096	578.568	-530.261	1738.454
c	1.071	.023	1.026	1.117
d	553.985	1037.462	-1480.094	2588.064
e	1.063	.043	.979	1.146
f	-227.868	781624.349	-1532704.027	1532248.291
g	.621	17.639	-33.963	35.206
h	.797	1.023	-1.208	2.803
i	5.070	.775	3.552	6.589
j	-2.347	.059	-2.462	-2.232
k	.293	.002	.288	.297
l	167.483	109.503	-47.211	382.178
m	.657	.058	.542	.771
n	1.643	3.486	-5.191	8.477
o	-3.254	1.091	-5.393	-1.115
p	8936.631	125615.715	-237349.311	255222.573
q	.083	1.065	-2.005	2.170
r	2641.833	7365.165	-11798.530	17082.197
s	1.258	.396	.482	2.034
t	-611.251	3253430.920	-6379385.562	6378163.060
u	.617	27.971	-54.224	55.459

Based on the established equation, the nonlinear regression test is coded and executed (Table 4-128). According to the results of the nonlinear regression test, the coefficients of the equation are presented in the following table. The results indicate a high convergence of the thermal energy performance modeling process. The results show that the prediction can be made to a satisfactory extent based on the equation.

Based on the results of the test, a significance level close to zero and less than 0.05 has been obtained. Therefore, the significance is confirmed. Additionally, the R-squared value of 0.998 has been achieved .Therefore, with 95% confidence, the equation derived from the

nonlinear regression test can predict 99.8% of the changes in total heating demandof the residential building (Table 4-129).

Table 4-129. Results of the Nonlinear Regression Between Physical Factors and Heating Energy

Source	Sum of Squares	df	Mean Squares
Regression	251920978382.247	21	11996237065.821
Residual	39496734.744	3563	11085.247
Uncorrected Total	251960475116.991	3584	
Corrected Total	22492694886.524	3583	

Dependent variable: Heating Energy
a. R squared = 1 - (Residual Sum of Squares) / (Corrected Sum of Squares) = .998.

The equation based on the results is presented as follows:

$$HE = -13098.801 + (604.096 \times 1.071^{EW}) + (553.985 \times 1.063^{NS}) + (-227.868 \times A^{0.621}) + (0.797 \times H^{5.070}) + (-2.347 \times D) + (0.293 \times D^2) + (167.483 \times V^{0.657}) + (1.643 \times WWR^{-3.254}) + (8936.631 \times WW^{0.083}) + (2641.833 \times 1.258^{WH}) + (-611.251 \times WA^{0.617})$$

Based on the findings of the curvature regression tests, the nonlinear equation for lighting demand has been derived, which is presented as follows:

$$LE = a + (b \times EW^c) + (d \times NS^e) + (f \times A) + (g \times V^h) + (i \times WWR^j) + (k \times WW^l) + (m \times WH) + (n \times WA^o)$$

In this equation, the total lighting demand (LE) is defined based on the east-west dimensions (EW), the north-south dimensions (NS), the orientation of the building (D), the area of the building (A), the volume of the building (V), the window-to-north wall ratio (WWR), the width of the north window (WW), the window height (WH), and the window area (WA).

Table 4-130. Results of the Nonlinear Regression Test Between Spatial Factors and Lighting Energy

Parameter	Estimate	Std. Error	95% Confidence Interval	
			Lower Bound	Upper Bound
a	-2.621E-5	.000	-2.621E-5	-2.621E-5
b	-1.530E-13	.000	-1.530E-13	-1.530E-13
c	1.000	.000	1.000	1.000
d	-5.783E-1217	.000	-5.788E-12	-5.778E-12
e	1.000	.000	1.000	1.000
f	4.243	.000	4.243	4.243
g	9.827E-6	.000	9.827E-6	9.827E-6
h	-3.550E-7	.000	-3.550E-7	-3.550E-7
i	3.828E-5	.000	3.828E-5	3.828E-5
j	2.363E-6	.000	2.363E-6	2.363E-6
k	-2.517E-5	.000	-2.517E-5	-2.517E-5
l	-1.365E-6	.000	-1.365E-6	-1.365E-6
m	2.476E-11	.000	2.476E-11	2.476E-11
n	3.276E-6	.000	3.276E-6	3.276E-6
o	2.855E-6	.000	2.855E-6	2.855E-6

Based on the established equation, the nonlinear regression test has been coded and executed (Table 4-130). The test was performed several times to achieve high accuracy. The regression test results confirm the high convergence of the output equation based on the input data. According to the results of the nonlinear regression test, the coefficients of the equation are presented in the table below. The standard error of the obtained coefficients is very low and accurate estimated coefficients have been obtained.

Based on the test results, a significance level close to zero, less than 0.05, has been obtained. Therefore, the significance is confirmed. Additionally, the R-squared value obtained is 1.000. The R-squared value obtained allows the use of this model in forecasting tool (Table 4-131). The results indicate a high convergence of the thermal energy performance modeling process. Also, the results show that the prediction can be made to a satisfactory extent based on the equation.

Table 4-131. Results of the Nonlinear Regression Between Physical Factors and Lighting Energy

Source	Sum of Squares	df	Mean Squares
Regression	3904906918.683	15	260327127.912
Residual	.000	3569	.000
Uncorrected Total	3904906918.683	3584	
Corrected Total	638235083.824	3583	

Dependent variable: Lighting Energy
a. R squared = 1 - (Residual Sum of Squares) / (Corrected Sum of Squares) = 1.000.

Therefore, with 95% confidence, the equation resulting from the nonlinear regression test can predict 100% of the changes in lighting demand. The equation based on the results is presented as follows:

$$LE = -2.621\text{E}-5 + \left((-1.530\text{E}-13) \times EW\right) + \left((-5.783\text{E}-12) \times NS\right) + (4.243 \times A) + \left((9.827\text{E}-6) \times V^{-3.550\text{E}-7}\right) + \left((3.828\text{E}-5) \times WWR^{2.363\text{E}-6}\right) + (-2.517\text{E}-5 \times WW^{-1.365\text{E}-6}) + \left((2.476\text{E}-11) \times WH\right) + \left((3.276\text{E}-6) \times WA^{2.855\text{E}-6}\right)$$

Based on the findings of the curvature regression tests and based on the obtained coefficients, the nonlinear equation for the average useful daylight illuminance has been derived, which is presented as follows:

$$UDIA = a + (b \times EW^{c}) + (d \times NS) + (e \,/\, A) + (f \,/\, H) + (g \times D) + (h \,/\, V) + (i \times WWR) + (j \times WW) + (k \times WW^{2}) + (l \times WW^{3}) + (m \times \log WH) + (n \,/\, WA)$$

The average Useful Daylight Illuminance (UDIA) is defined based on east-west dimension (EW), north-south dimension (NS), building orientation (D), floor area (A), building volume

(V), window-to-wall ratio on the northern facade (WWR), width of northern window (WW), height of the northern window (WH), and area of the northern window (WA).

Table 4-132. Results of the Nonlinear Regression Test Between Physical Factors and UDI Average

Parameter	Estimate	Std. Error	95% Confidence Interval	
			Lower Bound	Upper Bound
a	139.180	11.336	116.955	161.405
b	-16.632	2.473	-21.480	-11.785
c	.738	.029	.682	.795
d	-3.616	.078	-3.768	-3.464
e	-1065.194	241.191	-1538.079	-592.309
f	-42.501	13.759	-69.478	-15.524
g	.015	.001	.013	.017
h	4453.090	563.873	3347.543	5558.636
i	-101.211	2.040	-105.210	-97.212
j	17.195	.904	15.423	18.966
k	-.551	.051	-.651	-.452
l	.008	.001	.006	.011
m	77.554	9.515	58.899	96.208
n	.708	.057	.596	.820

Based on the specified equation, the nonlinear regression test is coded and executed (Table 4-133). The test was performed several times to achieve high accuracy. The regression test results confirm the high convergence of the output equation based on the input data.

Table 4-133. Results of the Nonlinear Regression Test Between Physical Factors and UDI Average

Source	Sum of Squares	df	Mean Squares
Regression	17294170.728	14	1235297.909
Residual	10208.130	3570	2.859
Uncorrected Total	17304378.859	3584	
Corrected Total	395196.902	3583	

Dependent variable: UDI Average
a. R squared = 1 - (Residual Sum of Squares) / (Corrected Sum of Squares) = .974.

According to the results of the nonlinear regression test, the coefficients of the equation are presented in the table below. The standard error of the obtained coefficients is very low and accurate estimated coefficients have been obtained. Based on the results of the test, a significance level close to zero and less than 0.05 has been obtained. Therefore, the significance is confirmed. Additionally, the R-squared value obtained is 0.974. Therefore, with 95% confidence, the equation resulting from the nonlinear regression test can predict 97.4% of the variations in the average Useful Daylight Illuminance (UDIA). The equation based on the results is presented as follows:

$$UDIA = 139.180 + (-16.632 \times EW^{0.738}) + (-3.616 \times NS) + (-1065.194 / A) + (-42.501 / H) + (0.015 \times D) + (4453.090 / V) + (-101.211 \times WWR) + (17.195 \times WW) + (-0.551 \times WW^2) + (0.008 \times WW^3) + (77.554 \times \log WH) + (0.708 / WA)$$

Based on the findings of the curvature regression tests, the nonlinear equation for the average Daylight autonomy has been obtained, which is presented as follows:

$$DAA = a + (b \times EW^{c}) + (d \times \log NS) + (e \,/\, A) + (f \times H^{g}) + (h \times i^{D}) + (j \,/\, V) + (k \times WWR^{l}) + (m \times WW) + (n \times \log WH) + (o \,/\, WA)$$

In this equation, the average Daylight autonomy Index (DAA) is defined based on the east-west dimension (EW), north-south dimension (NS), building orientation (D), building floor area (A), building volume (V), window-to-wall ratio on the northern facade (WWR), width of the northern window (WW), height of the northern window (WH), and the area of the northern window (WA).

Table 4-134. Results of the Linear Regression Test Between Physical Factors and DA Average

Parameter	Estimate	Std. Error	95% Confidence Interval	
			Lower Bound	Upper Bound
a	-15592.661	2224115.316	-4376257.413	4345072.090
b	6778.397	39266.741	-70209.110	83765.903
c	.005	.029	-.052	.062
d	524.188	38915.006	-75773.698	76822.074
e	685059.409	31587602.433	-61246506.618	62616625.436
f	718.180	39942.819	-77594.865	79031.224
g	.161	4.127	-7.929	8.252
h	5216.455	2117170.997	-4145770.176	4156203.086
i	1.000	.003	.995	1.005
j	-8598.934	423.413	-9429.089	-7768.778
k	2318.205	784826.825	-1536435.945	1541072.354
l	-.021	3.522	-6.925	6.884
m	-1.839	.142	-2.118	-1.560
n	-819.127	41364.462	-81919.486	80281.232
o	-67992.515	3158758.225	-6261145.162	6125160.131

Based on the specified equation, the linear regression test is coded and executed (Table 4-134). According to the results of the linear regression test, the coefficients of the equation are presented in the table below. Based on the results of the test, a significance level close to zero and less than 0.05 has been obtained. Therefore, the significance is confirmed. Additionally, the R-squared value obtained is 0.961. The R-squared value obtained allows the use of this model in forecasting tools (Table 4-135).

Table 4-135. Results of the Nonlinear Regression Test Between Physical Factors and DA Average

Source	Sum of Squares	df	Mean Squares
Regression	8531541.833	15	568769.456
Residual	12155.810	3569	3.406
Uncorrected Total	8543697.643	3584	
Corrected Total	310423.064	3583	

Dependent variable: DA Average

a. R squared = 1 - (Residual Sum of Squares) / (Corrected Sum of Squares) = .961.

Therefore, with 95% confidence, the equation resulting from the linear regression test can predict 96.1% of the variations in the average Useful Daylight Illuminance (UDIA).

$$DAA = -15592.661 + (6778.397 \times EW^{0.005}) + (524.188 \times \log NS) + (685059.409 \,/\, A) + (718.180 \times H^{0.161}) + (5216.455 \times 1^{D}) + (-8598.934 \,/\, V) + (2318.205 \times WWR^{-0.021}) + (-1.839 \times WW) + (-819.127 \times \log WH) + (-67992.515 \,/\, WA)$$

The results obtained from the nonlinear regression tests achieved higher R-squared values in all cases. Based on the results of the tests, overall, the equations derived from them can predict more than 95% of energy performance with over 95% confidence, which is a very high level. In general, equations resulting from nonlinear regression testing provide better results than equations resulting from linear regression testing. In the next chapter, a comparative study of the results of the equations obtained from the nonlinear regression test and the equations obtained from the linear regression test is presented.

Providing energy performance prediction models using nonlinear regression method is one of the research innovations; it has been able to predict energy performance with an accuracy of over 95% compared to simulated models and with high accuracy compared to actual energy consumption. In the studies conducted in various researches, a model that is accurately presented by defining a mathematical equation and has high accuracy has not been seen. The models obtained in this section can be used in various sectors and can be utilized in future research.

4-3- Optimization of Energy Performance in Residential buildings

Following the energy performance modeling of the residential building, the energy performance optimization process was taken into consideration through the Non-Dominated Sorting Genetic Algorithm II (NSGA-II). The performance objectives for the optimization process include cooling demand per square meter, heating demand per square meter, and useful daylight illuminace index. The modeling results of the residential building indicated that various spatial and physical factors influence energy performance goals. The diversity of the impacts of these spatial layout factors, combined with the inability to quantitatively define many of them, has added significant complexity to the energy performance assessment process.

Accordingly, this research aims to optimize the building envelope to achieve the best geometric specifications for residential buildings based on energy performance. To this end,

a larger and more precise stepwise approach was employed for the modeling process, considering all possible scenarios. An optimization process was carried out using the Non-dominated Sorting Genetic Algorithm II (NSGA-II) within the Wallacei plugin in Grasshopper coding environment.

Table 4-136. Stepwise Breakdown of Genes in Spatial layout Models for Optimization Process

	North-South Dimension	East-West Dimension	Building Height	Building Orientation
Minimum Step	**8**	**8**	**2.6**	**-45**
Maximum Step	**22**	**22**	**4**	**45**
Step Value	**1**	**1**	**0.1**	**5**
Number of Step Scenarios	**800**	**800**	**140**	**17**

In this process, four input genes, including the north-south dimension, the east-west dimension, the internal height of the units, and the building orientation, were defined and stepwise configured according to the table for initiating the optimization process (Table 4-136; Figure 4-1).

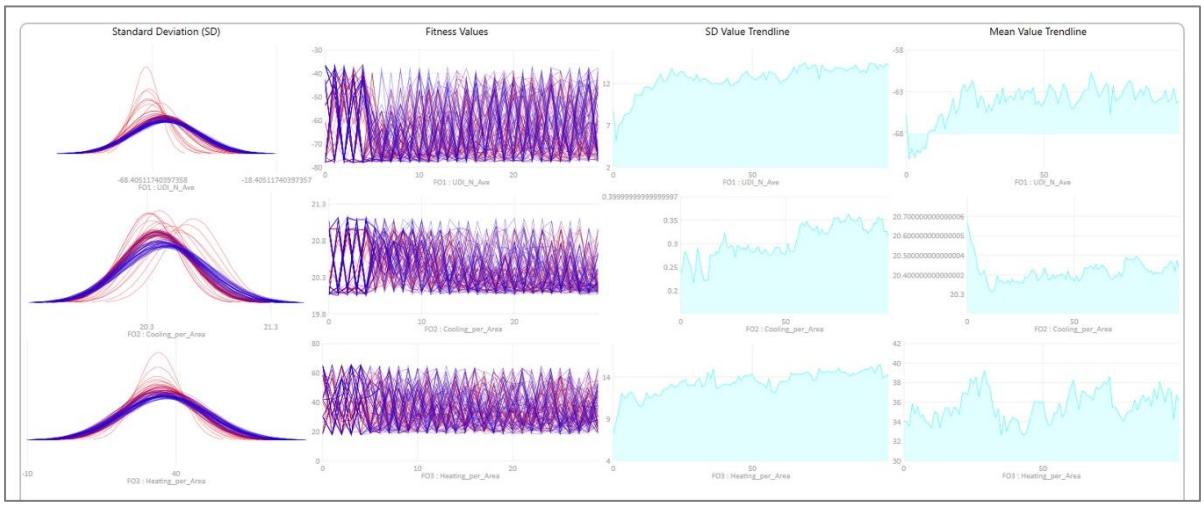

Figure 4-1. Results of Performance Objective Values and Standard Deviation of Responses in the Optimization Process

Additionally, three energy performance objectives, including cooling demand per square meter, heating demand per square meter, and the average Useful daylight illuminance (UDI), were defined as optimization targets. The optimization process was conducted over 100 generations with a population of 30 samples per generation, based on building energy performance simulations with the settings specified in the methodology chapter and according to the climatic characteristics of Melbourne (Figure 4-1).

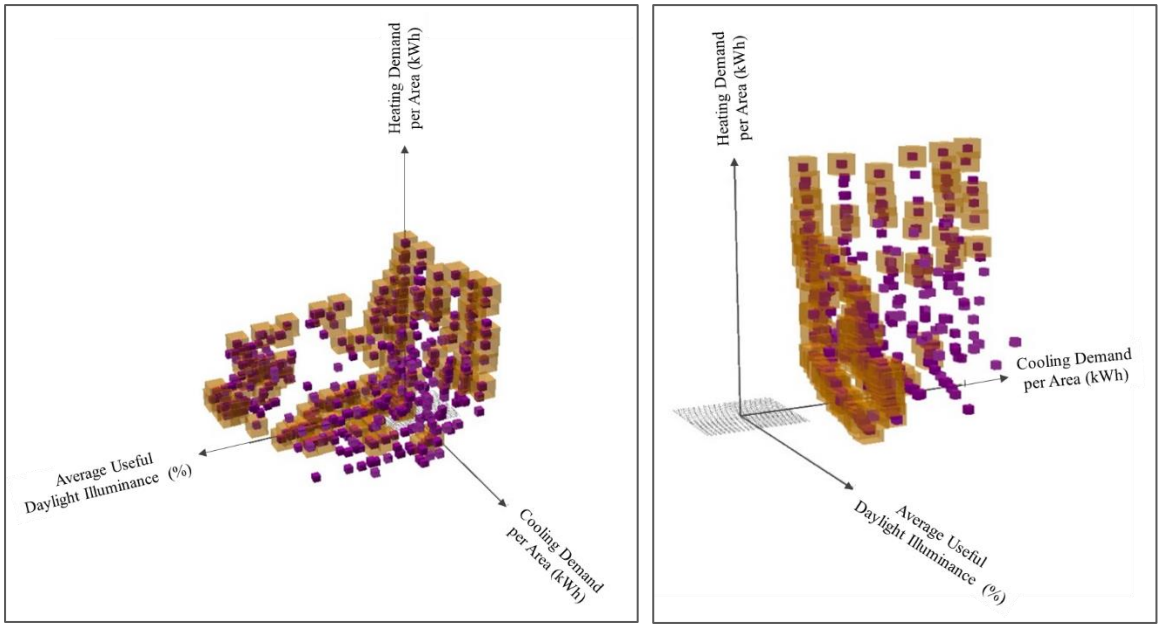

Figure 4-2. Performance Objective Chart of All Responses

The reproduction probability coefficient was set at 0.9, and the mutation probability coefficient was determined as one divided by the number of genes. Based on the results, 30 responses from generation 99 were obtained as the Pareto frontier optimal solutions.

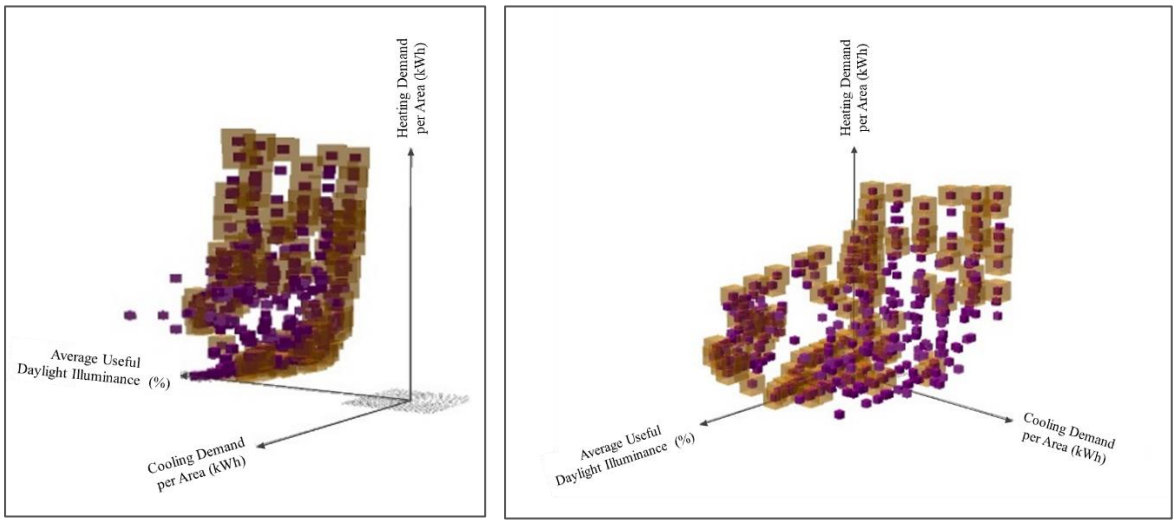

Figure 4-3. Performance Objective Chart of All Responses

In the image, the 3D chart of the Pareto frontier performance objective responses and all responses can be observed together. The responses enclosed by a brown cube represent the Pareto frontier solutions. Based on the Pareto frontier responses, it can be understood that the optimization was conducted with high convergence across the entire set of responses (Figure 4-2; Figure 4-3).

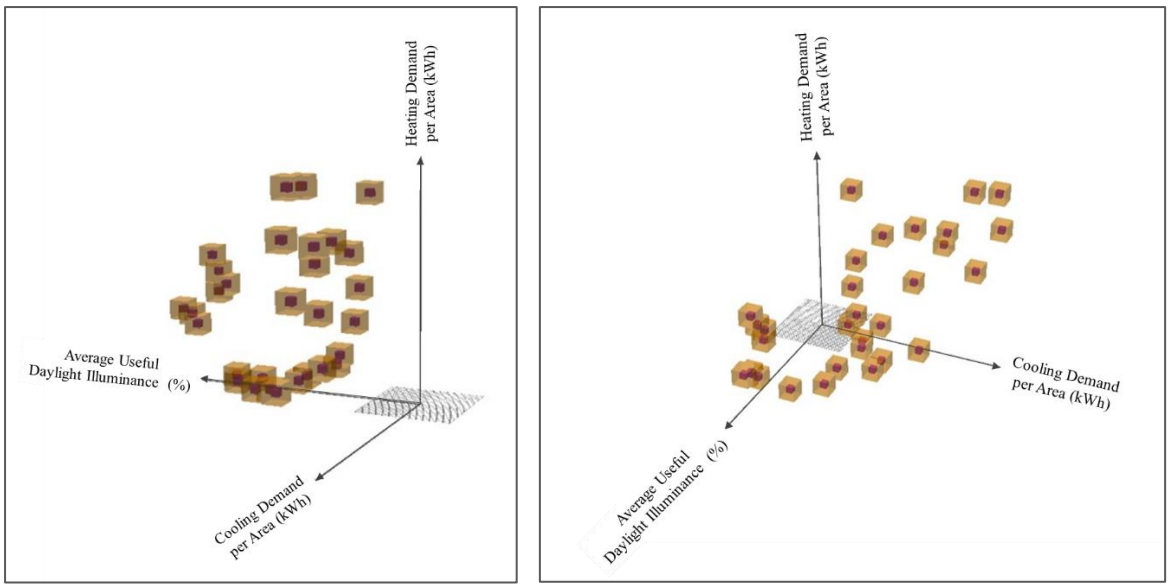

Figure 4-4. Performance Objective Chart of Pareto Frontier Responses

In general, the responses do not show a specific correlation between performance objectives. Instead, some contradiction between the Useful daylight illuminance and the cooling demand per square meter and heating demand per square meter can be observed in the chart. Additionally, there is no visible unit convergence in the scale of the Pareto frontier responses (Figure 4-4; Figure 4-5).

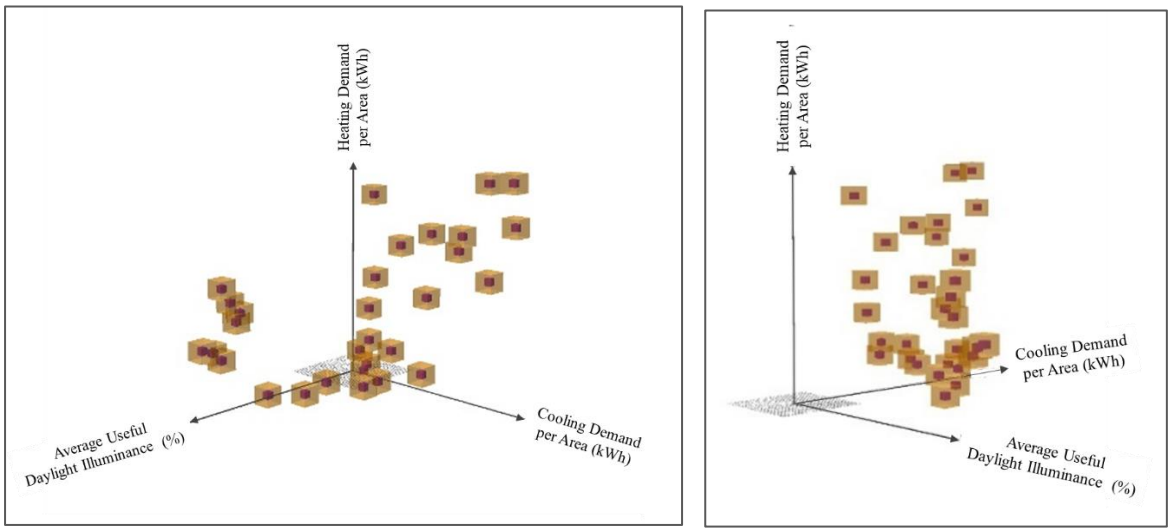

Figure 4-5. Performance Objective Chart of Pareto Frontier Responses

The Pareto frontier responses generally exhibit an irregular spread and distinct categorizations, which need to be addressed further. Additionally, an analysis of the standard deviation chart and the median values of the performance objectives shows that the

responses have high variance. However, overall, after three-quarters of the optimization process, they have reached a specific convergence (Table 4-137).

Table 4-137. Specifications of Pareto Frontier Responses

Gene Number	East-West Dimension	North-South Dimension	Aspect Ratio	Area	Unit Height	Orientation	Cooling Demand Per Square Meter	Heating Demand Per Square Meter	Average Index Useful daylight illuminance
0	8	8	1	64	3.3	-40	21.076363	65.53545	77.826042
1	8	22	2.75	176	2.6	-15	20.082405	30.252622	36.178529
2	10	8	0.8	80	3.2	-40	21.102558	56.294063	77.476222
3	8	22	2.75	176	3.3	-15	20.053713	42.422477	42.157843
4	22	22	1	484	2.6	-15	20.166913	17.795507	49.238417
5	22	20	0.909091	440	2.6	-20	20.328846	18.665567	53.316917
6	8	8	1	64	3.3	-35	20.93853	64.882879	77.832083
7	22	19	0.863636	418	2.7	-20	20.34265	20.040111	57.461024
8	10	8	0.8	80	2.7	-35	20.974196	43.928747	76.253556
9	22	15	0.681818	330	2.7	-30	20.726819	22.90011	68.383517
10	10	8	0.8	80	3.1	-30	20.795727	52.684989	77.271056
11	22	17	0.772727	374	2.6	-25	20.533158	20.243198	61.139672
12	10	22	2.2	220	3.3	-15	20.079333	36.524307	45.609824
13	9	8	0.888889	72	3.3	-15	20.215894	59.247004	77.23881
14	22	12	0.545455	264	3.3	-15	20.242718	32.752513	74.802418
15	10	9	0.9	90	3.1	-20	20.413477	48.459458	76.665571
16	22	16	0.727273	352	2.6	-25	20.547681	20.791705	63.867318
17	10	9	0.9	90	2.6	-25	20.626086	38.13514	74.443333
18	10	22	2.2	220	2.7	-15	20.108298	27.497972	39.556667
19	22	11	0.5	242	2.7	-15	20.292561	25.975291	72.759118
20	10	9	0.9	90	3.1	-30	20.779745	49.330405	76.797952
21	10	8	0.8	80	3.1	-25	20.608045	52.195132	76.959444
22	22	15	0.681818	330	2.6	-20	20.396524	21.132887	66.743031
23	9	22	2.444444	198	2.7	-15	20.09364	29.428601	38.232773
24	22	12	0.545455	264	2.6	-15	20.254963	23.457859	71.73781
25	22	11	0.5	242	2.6	-20	20.451246	24.89474	72.02436
26	10	22	2.2	220	3.2	-15	20.092185	34.95718	44.765196
27	22	15	0.681818	330	2.7	-20	20.384967	22.244464	68.032788
28	10	8	0.8	80	2.6	-15	20.25687	40.051826	75.774
29	9	22	2.444444	198	3.3	-15	20.066371	39.113304	44.403193

In the tables, the specifications of the Pareto frontier responses include geometric specifications and three energy performance objectives: the Useful daylight illuminance, heating demand per square meter, and cooling demand per square meter. Additionally, the energy performance specifications of the Pareto frontier responses are presented in the tables. Descriptive statistics for these responses are also provided in another table, which can indicate the orientation of the Pareto frontier responses. Based on this, all 30 responses have a negative orientation ranging from -40 to -15 degrees. The building height varies from 2.6 to 3.3 meters (Table 4-138).

Table 4-138. Descriptive Statistics of Pareto Frontier Response Specifications

	Number	Minimum	Maximum	Median	Standard Deviation
East-West Dimensions of the Building	30	8	22	14.43	6.317
North-South Dimensions of the Building	30	8	22	14.33	5.797
Building Height	30	2.6	3.3	2.893	.3016
Building Area	30	64	484	211.60	126.161
Building Volume	30	208.0	1258.4	592.573	324.9051
Length to Width Ratio of the Building	30	.500000	2.750000	1.166	.728746092
Building Orientation	30	-40	-15	-21.83	8.039
Cooling Demand per Square Meter	30	1340.065	9760.785	4308.481	2560.330
Heating Demand per Square Meter	30	3204.146	8646.663	6056.990	1767.575
Average Useful Daylight	30	36.178	77.832	63.831	14.566

Additionally, other geometric specifications of the Pareto frontier responses were obtained with variability (Table 4-139).

Table 4-139. Specifications of Pareto Frontier Response

Gene Number	Energy Consumption per Square	Total Energy Consumption	Cooling Demand per Square Meter	Cooling Demand	Heating Demand per Square Meter	Heating Demand	Average Index Useful daylight illuminance	Average Daylight Availability Index
0	184.7241	11822.34	21.07636	1348.887	65.53545	4194.269	77.82604	61.59215
1	148.4473	26126.72	20.08241	3534.503	30.25262	5324.461	36.17853	29.10216
2	175.5089	14040.71	21.10256	1688.205	56.29406	4503.525	77.47622	61.51067
3	160.5884	28263.57	20.05371	3529.453	42.42248	7466.356	42.15784	33.85444
4	136.0747	65860.14	20.16691	9760.786	17.79551	8613.025	49.23842	33.90837
5	137.1067	60326.93	20.32885	8944.692	18.66557	8212.849	53.31692	35.53514
6	183.9337	11771.75	20.93853	1340.066	64.88288	4152.504	77.83208	61.82194
7	138.495	57890.91	20.34265	8503.228	20.04011	8376.766	57.46102	37.49829
8	163.0152	13041.22	20.9742	1677.936	43.92875	3514.3	76.25356	51.55
9	141.7392	46773.93	20.72682	6839.85	22.90011	7557.036	68.38352	40.76091
10	171.593	13727.44	20.79573	1663.658	52.68499	4214.799	77.27106	59.70661
11	138.8886	51944.34	20.53316	7679.401	20.2432	7570.956	61.13967	38.11576
12	154.7159	34037.5	20.07933	4417.453	36.52431	8035.348	45.60982	35.50578
13	177.5751	12785.41	20.21589	1455.544	59.247	4265.784	77.23881	62.20649
14	151.1075	39892.37	20.24272	5344.078	32.75251	8646.663	74.80242	52.23582
15	166.9852	15028.67	20.41348	1837.213	48.45946	4361.351	76.66557	55.96176
16	139.4516	49086.98	20.54768	7232.784	20.79171	7318.68	63.86732	38.64042
17	156.8735	14118.61	20.62609	1856.348	38.13514	3432.163	74.44333	47.15962
18	145.7185	32058.07	20.1083	4423.826	27.49797	6049.554	39.55667	31.33973
19	144.3801	34939.98	20.29256	4910.8	25.97529	6286.02	72.75912	44.15213
20	168.2224	15140.02	20.77975	1870.177	49.33041	4439.736	76.79795	56.00448
21	170.9154	13673.23	20.60805	1648.644	52.19513	4175.611	76.95944	59.40394
22	139.6417	46081.75	20.39652	6730.853	21.13289	6973.853	66.74303	39.49333
23	147.6345	29231.63	20.09364	3978.541	29.4286	5826.863	38.23277	30.54767
24	141.8251	37441.82	20.25496	5347.31	23.45786	6192.875	71.73781	41.44624
25	143.4582	34716.89	20.45125	4949.202	24.89474	6024.527	72.02436	42.59183
26	153.1616	33695.56	20.09219	4420.281	34.95718	7690.58	44.7652	34.757
27	140.7417	46444.75	20.38497	6727.039	22.24446	7340.673	68.03279	40.45679
28	158.4209	12673.68	20.25687	1620.55	40.05183	3204.146	75.774	49.22028
29	157.2919	31143.8	20.06637	3973.141	39.1133	7744.434	44.40319	34.70071

Based on this, all 30 responses have a negative orientation ranging from -40 to -15 degrees. The building height varies from 2.6 to 3.3 meters (Table 4-140).

Table 4-140. Specifications of Pareto Frontier Responses

Gene Number	Energy Consumption per Square	Total Energy Consumption	Cooling Demand per Square Meter	Cooling Demand	Heating Demand per Square Meter	Heating Demand	Average Index Useful daylight	Average Daylight Availability Index
0	184.7241	11822.34	21.07636	1348.887	65.53545	4194.269	77.82604	61.59215
1	148.4473	26126.72	20.08241	3534.503	30.25262	5324.461	36.17853	29.10216
2	175.5089	14040.71	21.10256	1688.205	56.29406	4503.525	77.47622	61.51067
3	160.5884	28263.57	20.05371	3529.453	42.42248	7466.356	42.15784	33.85444
4	136.0747	65860.14	20.16691	9760.786	17.79551	8613.025	49.23842	33.90837
5	137.1067	60326.93	20.32885	8944.692	18.66557	8212.849	53.31692	35.53514
6	183.9337	11771.75	20.93853	1340.066	64.88288	4152.504	77.83208	61.82194
7	138.495	57890.91	20.34265	8503.228	20.04011	8376.766	57.46102	37.49829
8	163.0152	13041.22	20.9742	1677.936	43.92875	3514.3	76.25356	51.55
9	141.7392	46773.93	20.72682	6839.85	22.90011	7557.036	68.38352	40.76091
10	171.593	13727.44	20.79573	1663.658	52.68499	4214.799	77.27106	59.70661
11	138.8886	51944.34	20.53316	7679.401	20.2432	7570.956	61.13967	38.11576
12	154.7159	34037.5	20.07933	4417.453	36.52431	8035.348	45.60982	35.50578
13	177.5751	12785.41	20.21589	1455.544	59.247	4265.784	77.23881	62.20649
14	151.1075	39892.37	20.24272	5344.078	32.75251	8646.663	74.80242	52.23582
15	166.9852	15028.67	20.41348	1837.213	48.45946	4361.351	76.66557	55.96176
16	139.4516	49086.98	20.54768	7232.784	20.79171	7318.68	63.86732	38.64042
17	156.8735	14118.61	20.62609	1856.348	38.13514	3432.163	74.44333	47.15962
18	145.7185	32058.07	20.1083	4423.826	27.49797	6049.554	39.55667	31.33973
19	144.3801	34939.98	20.29256	4910.8	25.97529	6286.02	72.75912	44.15213
20	168.2224	15140.02	20.77975	1870.177	49.33041	4439.736	76.79795	56.00448
21	170.9154	13673.23	20.60805	1648.644	52.19513	4175.611	76.95944	59.40394
22	139.6417	46081.75	20.39652	6730.853	21.13289	6973.853	66.74303	39.49333
23	147.6345	29231.63	20.09364	3978.541	29.4286	5826.863	38.23277	30.54767
24	141.8251	37441.82	20.25496	5347.31	23.45786	6192.875	71.73781	41.44624
25	143.4582	34716.89	20.45125	4949.202	24.89474	6024.527	72.02436	42.59183
26	153.1616	33695.56	20.09219	4420.281	34.95718	7690.58	44.7652	34.757
27	140.7417	46444.75	20.38497	6727.039	22.24446	7340.673	68.03279	40.45679
28	158.4209	12673.68	20.25687	1620.55	40.05183	3204.146	75.774	49.22028
29	157.2919	31143.8	20.06637	3973.141	39.1133	7744.434	44.40319	34.70071

Additionally, other geometric specifications of the Pareto frontier responses have been obtained with variability (Table 4-141).

Table 4-141. Descriptive Statistics of Pareto Frontier Response Specifications

	Number	Minimum	Maximum	Median	Standard Deviation
Energy Consumption per Square Meter	30	136.074669	184.724061	154.60784837	14.736757153
Total Energy Consumption	30	11771.75411	65860.13980	31126.0237220	16490.22831900
Cooling Demand per Square Meter	30	20.053713	21.102558	20.43441607	.319635025
Total Cooling Demand	30	1340.065920	9760.785892	4308.48158000	2560.330128586
Heating Demand per Square Meter	30	17.795507	65.535450	36.06118360	14.570489881
Total Heating Demand	30	3204.146080	8646.663432	6056.99030287	1767.575829207
Total Lighting Demand	30	393.762432	2977.828392	1301.87704080	776.208547513
Average Useful Daylight	30	36.178529	77.832083	63.83161613	14.566192719
Average Daylight Availability	30	29.102157	62.206488	44.69268180	10.867913425

the floor area, a negative orientation of the building and a reduction in building height lead to optimal energy performance in terms of cooling and heating demands, as well as daylight performance. Additionally, the variables of area and length-to-width ratio alone do not have a significant impact on optimal energy performance. The findings indicate that for buildings with north-facing windows covering 10 percent of Based on these results, further investigations are necessary to elucidate the role of geometric specifications of buildings on energy performance.

4-3-1: Best Solutions for Optimizing Energy Performance

To conduct a more detailed analysis, the best responses for each performance objective among all optimization responses will be examined, as shown in the image below. Accordingly, the best average Useful daylight illuminance, cooling demand per square meter, and heating demand per square meter are presented below (Figure 4-6).

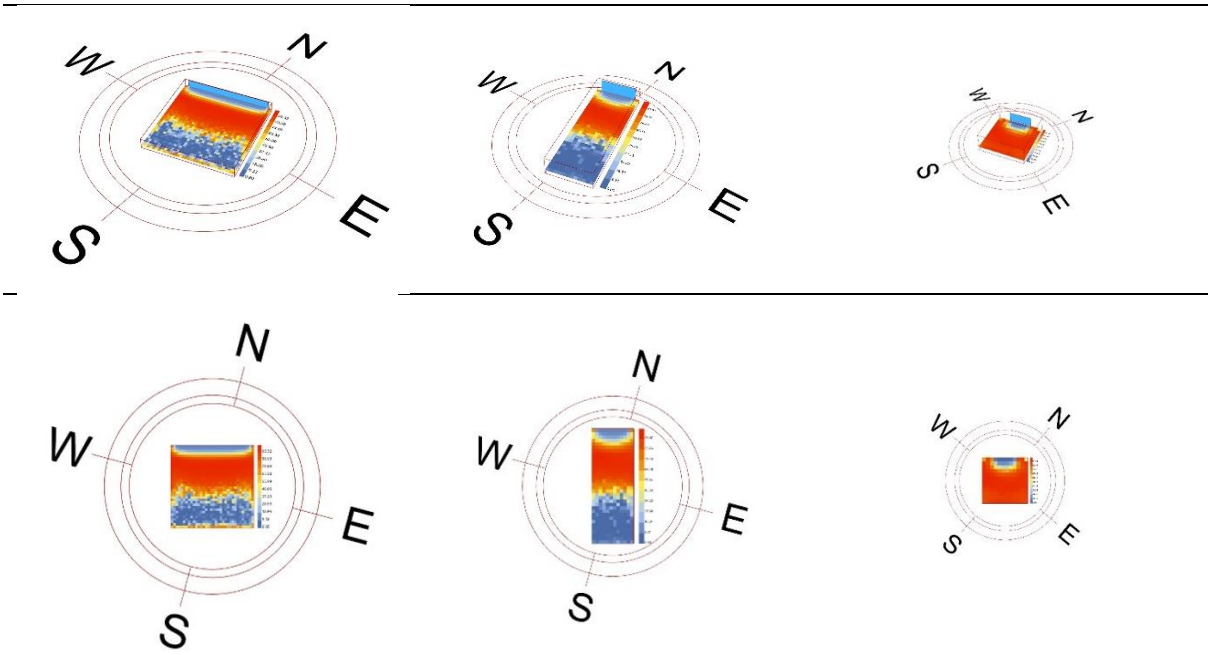

Best heating demand per square meter	Best cooling demand per square meter	Best average useful daylight illuminance
Dimension: 8*8	Dimension: 8*22	Dimension: 8*8
Length to Width Ratio: 1	Length to Width Ratio: 2.75	Length to Width Ratio: 1
Orientation Angle: -15 degrees	Orientation Angle: -15 degrees	Orientation Angle: -40 degrees
Internal Height of Units: 2.6 meters	Internal Height of Units: 3.3 meters	Internal Height of Units: 3.3 meters
Total Energy Consumption: 65860.13 kWh	Total Energy Consumption: 28263.56 kWh	Total Energy Consumption: 11,822.33 kWh
Total Cooling Demand: 9760.78 kWh	Total Cooling Demand: 3529.45 kWh	Total Cooling Demand: 1,348.88 kWh
Total Heating Demand: 8613.02 kWh	Total Heating Demand: 7466.35 kWh	Total Heating Demand: 4,194.26 kWh
Energy Consumption per m2: 136.07 kWh	Energy Consumption per m2: 160.58 kWh	Energy Consumption per m2: 184.72 kWh
Cooling Demand per m2: 20.16 kWh	Cooling Demand per m2: 20.05 kWh	Cooling Demand per m2: 21.07 kWh
Heating Demand per m2: 17.79 kWh	Heating Demand per m2: 42.42 kWh	Heating Demand per m2: 65.53 kWh
Average UDI: 48.63%	Average UDI: 41.89%	Average UDI: 77.94%
Average DA: 33.95%	Average DA: 33.88%	Average DA: 61.93%

Figure 4-6. Best Responses for Each Performance Objective Among All Optimization Responses

Based on this, the best average Useful daylight illuminance corresponds to response 4 from generation 74, which features a residential building with a floor area of 8 by 8 meters, a length-to-width ratio of 1, an orientation angle of -40 degrees, and an i height of 3.3 meters.

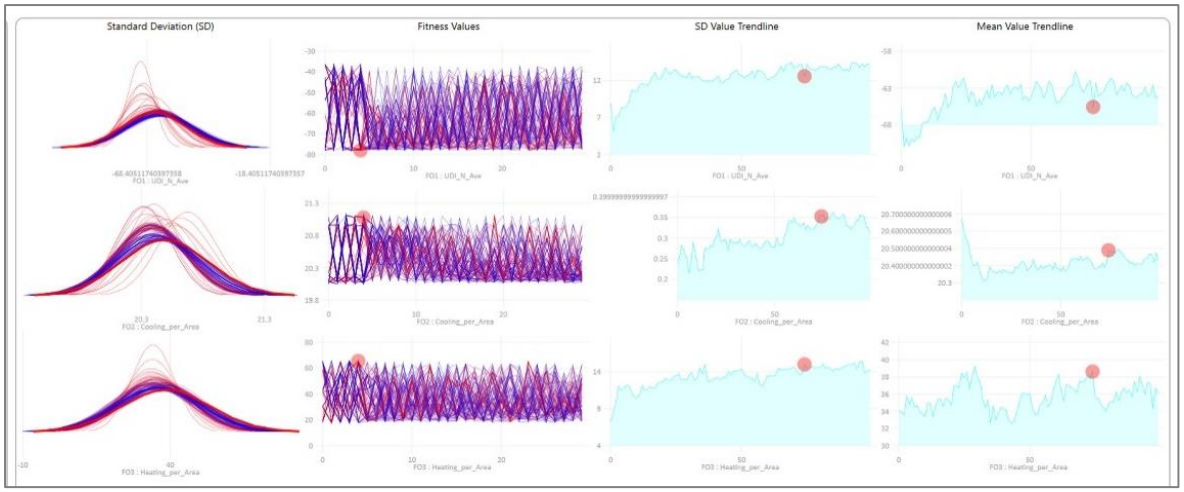

Figure 4-7. Specifications of the Best Response Based on Average Useful Daylight

In this model, the average Useful daylight illuminance is 77.94%, the Average Daylight Availability Index is 61.93%, the total energy consumption is 11822.33 kilowatt-hours, the energy consumption per square meter is 184.72 kilowatt-hours, the total cooling demand is 1348.88 kilowatt-hours, the cooling demand per square meter is 66.08 kilowatt-hours, the total heating demand is 4194.26 kilowatt-hours, and the heating demand per square meter is 50.64 kilowatt-hours (Figure 4-7).

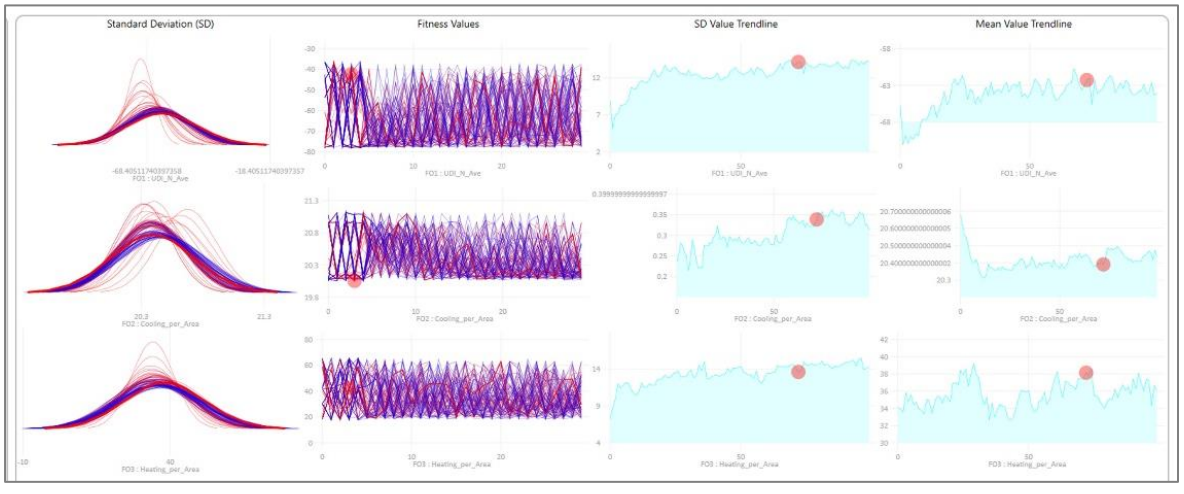

Figure 4-8. Specifications of the Best Response Based on Cooling Demand per Square Meter

Additionally, the best cooling demand per square meter corresponds to response 4 from generation 74, which features a residential building with a floor area of 8 by 22 meters, a

length-to-width ratio of 2.75, an orientation angle of -15 degrees, and an internal height of 2.6 meters. In this model, the average Useful daylight illuminance is 41.89%. In this model, the average Daylight Availability Index is 33.88%, the total energy consumption is 28,263.56 kilowatt-hours, the energy consumption per square meter is 160.58 kilowatt-hours, the total cooling demand is 3,529.45 kilowatt-hours, the cooling demand per square meter is 20.05 kilowatt-hours, the total heating demand is 4,194.26 kilowatt-hours, and the heating demand per square meter is 42.42 kilowatt-hours (Figure 4-8).

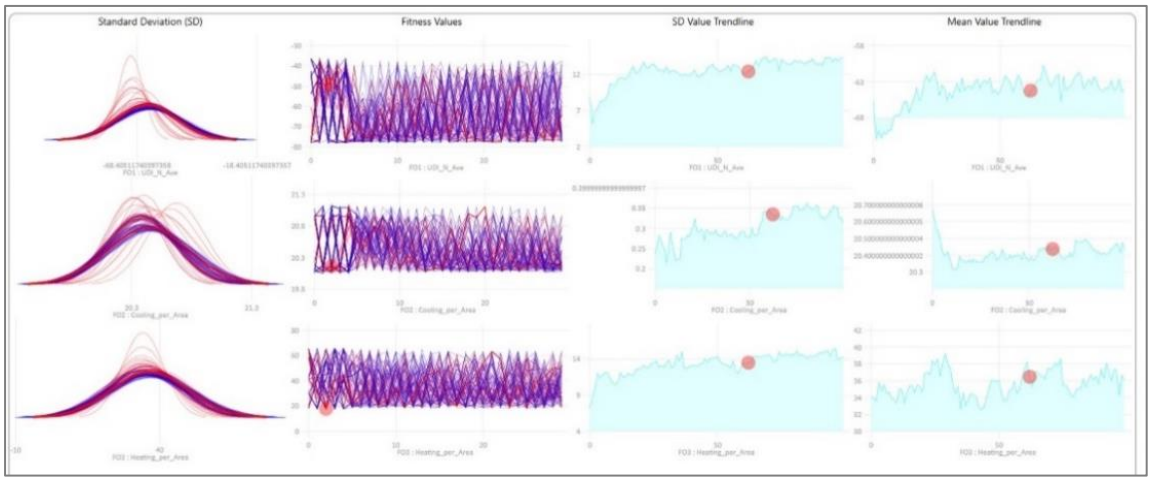

Figure 4-9. Specifications of the Best Response Based on Heating Demand per Square Meter

Additionally, the best heating demand per square meter corresponds to response 4 from generation 74, which features a residential building with a floor area of 22 by 22 meters, a length-to-width ratio of 1, an orientation angle of -15 degrees, and an internal height of 3.3 meters. In this model, the average Useful daylight illuminance is 48.63%, the average Daylight Availability Index is 33.95%, the total energy consumption is 65,860.13 kilowatt-hours, the energy consumption per square meter is 136.07 kilowatt-hours, the total cooling demand is 9,760.78 kilowatt-hours, the cooling demand per square meter is 20.16 kilowatt-hours, the total heating demand is 8,613.02 kilowatt-hours, and the heating demand per square meter is 17.79 kilowatt-hours (Figure 4-9).

4-3-1- Classification of Responses for Optimizing Energy Performance

Subsequently, through the K-means unsupervised machine learning process, the 30 Pareto frontier responses have been divided into three categories based on three optimization performance objectives, as shown in the image. Additionally, other specifications of the responses are provided for a better examination of the classification. Based on the

classification, it can be understood that the first group consists of east-west elongations and is positioned at an intermediate level in terms of energy performance (Figure 4-10).

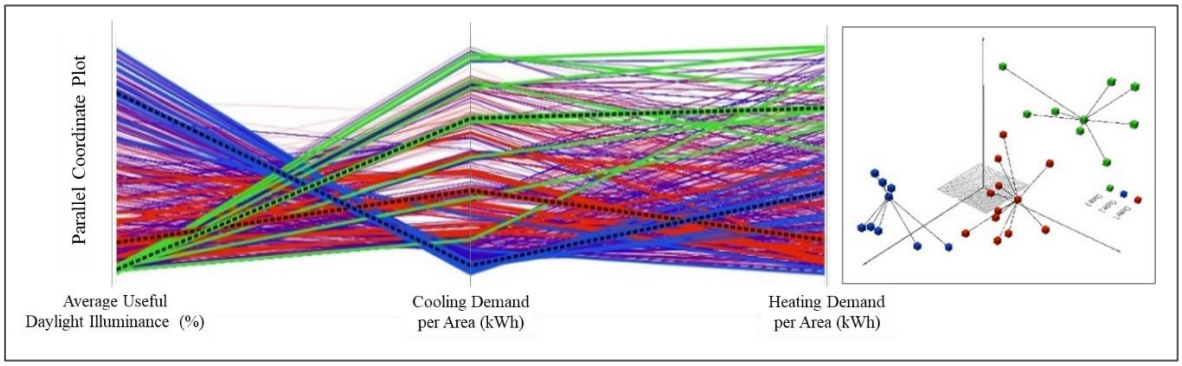

Figure 4-10. Diagram of Pareto Frontier Responses Classification via K-means Machine Learning

The responses in this class are very close to the optimal values for heating demand per square meter and the Useful daylight illuminance under optimal conditions (Table 4-142).

Table 4-142. Specifications of Classified Pareto Frontier Responses

Class	Gene Number	East-West Side Dimensions	North-South Side Dimensions	Aspect Ratio	Area	Unit Height	Orientation	Cooling Demand per Square Meter	Heating Demand per Square Meter	Average Useful daylight illuminance
Class 1	**25**	22	11	0.5	242	2.6	-20	20.451246	24.89474	72.02436
	27	22	15	0.681818	330	2.7	-20	20.384967	22.244464	68.032788
	22	22	15	0.681818	330	2.6	-20	20.396524	21.132887	66.743031
	19	22	11	0.5	242	2.7	-15	20.292561	25.975291	72.759118
	24	22	12	0.545455	264	2.6	-15	20.254963	23.457859	71.73781
	16	22	16	0.727273	352	2.6	-25	20.547681	20.791705	63.867318
	11	22	17	0.772727	374	2.6	-25	20.533158	20.243198	61.139672
	14	22	12	0.545455	264	3.3	-15	20.242718	32.752513	74.802418
	7	22	19	0.863636	418	2.7	-20	20.34265	20.040111	57.461024
	9	22	15	0.681818	330	2.7	-30	20.726819	22.90011	68.383517
	17	10	9	0.9	90	2.6	-25	20.626086	38.13514	74.443333
	28	10	8	0.8	80	2.6	-15	20.25687	40.051826	75.774
Class 2	**26**	10	22	2.2	220	3.2	-15	20.092185	34.95718	44.765196
	18	10	22	2.2	220	2.7	-15	20.108298	27.497972	39.556667
	23	9	22	2.444444	198	2.7	-15	20.09364	29.428601	38.232773
	12	10	22	2.2	220	3.3	-15	20.079333	36.524307	45.609824
	1	8	22	2.75	176	2.6	-15	20.082405	30.252622	36.178529
	29	9	22	2.444444	198	3.3	-15	20.066371	39.113304	44.403193
	3	8	22	2.75	176	3.3	-15	20.053713	42.422477	42.157843
	4	22	22	1	484	2.6	-15	20.166913	17.795507	49.238417
	5	22	20	0.909091	440	2.6	-20	20.328846	18.665567	53.316917
Class 3	**10**	10	8	0.8	80	3.1	-30	20.795727	52.684989	77.271056
	20	10	9	0.9	90	3.1	-30	20.779745	49.330405	76.797952
	21	10	8	0.8	80	3.1	-25	20.608045	52.195132	76.959444
	6	8	8	1	64	3.3	-35	20.93853	64.882879	77.832083
	8	10	8	0.8	80	2.7	-35	20.974196	43.928747	76.253556
	2	10	8	0.8	80	3.2	-40	21.102558	56.294063	77.476222
	15	10	9	0.9	90	3.1	-20	20.413477	48.459458	76.665571
	0	8	8	1	64	3.3	-40	21.076363	65.53545	77.826042
	13	9	8	0.888889	72	3.3	-15	20.215894	59.247004	77.23881

Additionally, regarding cooling demand per square meter, all responses are generally within a similar range; however, the responses in this class are positioned at an intermediate level among the responses. Two responses from this class have slight elongations and exhibit a form close to a square (Table 4-143).

Table 4-143. Specifications of Classified Pareto Frontier Responses

Gene Number	Energy Consumption per Square Meter	Total Energy Consumption	Cooling Demand per Square Meter	Cooling Demand	Heating Demand per Square Meter	Heating Demand	Average Index Useful daylight illuminance	Average Daylight Availability Index	Gene Number
Class 1	**25**	143.4582	34716.89	20.45125	4949.202	24.89474	6024.527	1488.914	72.02436
	27	140.7417	46444.75	20.38497	6727.039	22.24446	7340.673	2030.338	68.03279
	22	139.6417	46081.75	20.39652	6730.853	21.13289	6973.853	2030.338	66.74303
	19	144.3801	34939.98	20.29256	4910.8	25.97529	6286.02	1488.914	72.75912
	24	141.8251	37441.82	20.25496	5347.31	23.45786	6192.875	1624.27	71.73781
	16	139.4516	49086.98	20.54768	7232.784	20.79171	7318.68	2165.693	63.86732
	11	138.8886	51944.34	20.53316	7679.401	20.2432	7570.956	2301.049	61.13967
	14	151.1075	39892.37	20.24272	5344.078	32.75251	8646.663	1624.27	74.80242
	7	138.495	57890.91	20.34265	8503.228	20.04011	8376.766	2571.761	57.46102
	9	141.7392	46773.93	20.72682	6839.85	22.90011	7557.036	2030.338	68.38352
	17	156.8735	14118.61	20.62609	1856.348	38.13514	3432.163	553.7284	74.44333
	28	158.4209	12673.68	20.25687	1620.55	40.05183	3204.146	492.203	75.774
Class 2	**26**	153.1616	33695.56	20.09219	4420.281	34.95718	7690.58	1353.558	44.7652
	18	145.7185	32058.07	20.1083	4423.826	27.49797	6049.554	1353.558	39.55667
	23	147.6345	29231.63	20.09364	3978.541	29.4286	5826.863	1218.203	38.23277
	12	154.7159	34037.5	20.07933	4417.453	36.52431	8035.348	1353.558	45.60982
	1	148.4473	26126.72	20.08241	3534.503	30.25262	5324.461	1082.847	36.17853
	29	157.2919	31143.8	20.06637	3973.141	39.1133	7744.434	1218.203	44.40319
	3	160.5884	28263.57	20.05371	3529.453	42.42248	7466.356	1082.847	42.15784
	4	136.0747	65860.14	20.16691	9760.786	17.79551	8613.025	2977.828	49.23842
	5	137.1067	60326.93	20.32885	8944.692	18.66557	8212.849	2707.117	53.31692
Class 3	**10**	171.593	13727.44	20.79573	1663.658	52.68499	4214.799	492.203	77.27106
	20	168.2224	15140.02	20.77975	1870.177	49.33041	4439.736	553.7284	76.79795
	21	170.9154	13673.23	20.60805	1648.644	52.19513	4175.611	492.203	76.95944
	6	183.9337	11771.75	20.93853	1340.066	64.88288	4152.504	393.7624	77.83208
	8	163.0152	13041.22	20.9742	1677.936	43.92875	3514.3	492.203	76.25356
	2	175.5089	14040.71	21.10256	1688.205	56.29406	4503.525	492.203	77.47622
	15	166.9852	15028.67	20.41348	1837.213	48.45946	4361.351	553.7284	76.66557
	0	184.7241	11822.34	21.07636	1348.887	65.53545	4194.269	393.7624	77.82604
	13	177.5751	12785.41	20.21589	1455.544	59.247	4265.784	442.9827	77.23881

Additionally, the second group predominantly consists of rectangular-shaped responses with north-south elongations. These responses are positioned optimally in terms of cooling demand per square meter. However, the responses in this class are in unfavorable conditions regarding the Useful daylight illuminance among the Pareto frontier responses and are positioned at an intermediate level for heating demand per square meter (Table 4-143).

Furthermore, the third group generally includes responses with an aspect ratio close to one and limited east-west elongation. These responses are positioned optimally in terms of the Useful daylight illuminance. However, regarding cooling demand per square meter, they are in unfavourable conditions among the Pareto frontier responses. Moreover, the responses exhibit undesirable performance regarding heating demand per square meter among the Pareto frontier responses (Figure 4-11).

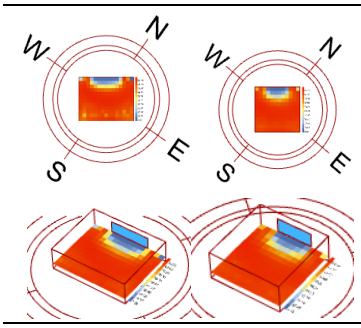	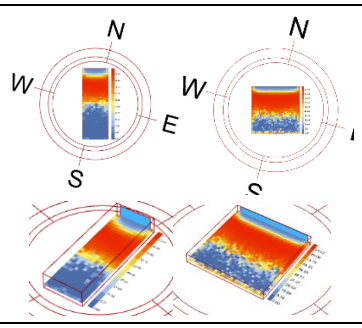	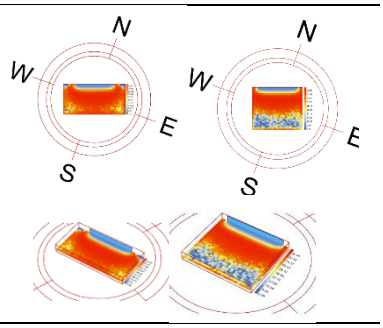
Dimension: 8*8 - 9*10	Dimension: 8*22 - 22*22	Dimension: 8*10 - 22*19
Length to Width Ratio: 0.8 to 1	Length to Width Ratio: 1 to 2.75	Length to Width Ratio: 0.5 to 0.9
Height: 2.7 - 3.3	Height: 2.6 - 3.3	Height: 2.6 - 3.3
Orientation: -15 to -40 degrees	Orientation: -15 to -20 degrees	Orientation: -30 to -15 degrees
Class 3 responses at the threshold of floor area proportions	Class 2 responses at the threshold of floor area proportions	Class 1 responses at the threshold of floor area proportions

Figure 4-11. Specifications of Classified Pareto Frontier Responses

Furthermore, in the table, a descriptive statistical analysis of the classified responses from the machine learning process has been conducted in two sections: geometric specifications and energy performance specifications of the building. Overall, the results of this optimization classification process indicate that east-west elongation leads to improvements in heating demand per square meter and the Useful daylight illuminance.

Additionally, north-south elongations lead to an improvement in cooling demands per square meter. Furthermore, a length-to-width ratio close to one can result in improved daylight performance and cooling demands per square meter. Overall, based on the results, limited east-west elongation indicates a better outcome for energy performance.

4-4- Comparative Analysis of the Impact of Orientation Angle and Height on the Energy Performance of Residential buildings

Based on the findings from the conducted optimization tests and the modelling process and considering the number of input genes in the optimization processes, it is evident that the angle of orientation and the height of the space have not reached definitive convergence.

Therefore, there is a need for a comparative analysis of the angle of orientation and the height of residential buildings (Table 4-144).

In this section, the energy performance is first examined by maintaining a height of 3 meters for the spaces while varying the angle of orientation across different areas. Based on the results of the variations in angle of orientation, it can be concluded that, in terms of energy consumption per square meter, the building performs optimally at angles of 0 degrees, 15 degrees, and -15 degrees, respectively (Table 4-144).

Furthermore, regarding the cooling requirements per square meter, the building's performance varies across different length-to-width ratios and areas; however, the best performance is observed at an angle of 15 degrees, followed by 0 degrees and -15 degrees, which also demonstrate acceptable performance.

Table 4-144 Energy Performance Based on Variations in Orientation Angle Across Different Areas with a Height of 3 Meters for Spaces

Average Daylight Availability Index	Average Useful daylight illuminance	Heating Demand per Square Meter	Cooling Demand per Square Meter	Energy Consumption per Square Meter	Orientation Angle	Building Dimensions
55.24021	79.69556	58.93351	21.02312	176.1595	-45	٦٤ m٢ 8*8 m H:3 m
56.91778	79.53028	57.03728	20.62313	173.8632	-30	
57.67611	79.62507	55.79645	20.06553	172.0648	-15	
58.48632	79.63715	55.268	19.64838	171.1192	0	
59.08111	79.86118	55.36405	19.66452	171.2314	15	
59.28313	80.20507	56.20937	19.96045	172.3727	30	
59.07889	80.3609	57.84443	20.16271	174.21	45	
31.58628	41.28838	40.46066	20.80008	157.4636	-45	١٧٦ m٢ 8*22 m H:3 m
32.14659	41.22547	38.80904	20.42186	155.4337	-30	
32.49186	41.59706	37.71581	19.90177	153.8204	-15	
32.8537	41.42336	37.23578	19.47125	152.9099	0	
33.10689	41.1524	37.31406	19.41701	152.9339	15	
33.12963	41.40105	38.05556	19.62339	153.8818	30	
33.49355	42.40578	39.4723	19.77658	155.4517	45	
51.88838	70.19003	40.49565	21.11436	157.8128	-45	١٧٦ m2 8*22 m H:3 m
53.31007	70.21172	38.83115	20.68917	155.7232	-30	
54.94387	70.39422	37.744	20.11379	154.0606	-15	
56.08282	70.51466	37.28456	19.66856	153.156	0	
56.52277	70.24613	37.37431	19.63108	153.2082	15	
56.51841	70.16253	38.12903	19.87707	154.2089	30	
55.37054	70.25429	39.56472	20.07413	155.8417	45	
36.88411	56.70587	24.37458	20.83913	141.4165	-45	٤٨٤ m2 22*22 m H:3 m
37.46752	57.33465	23.00772	20.46793	139.6785	-30	
38.14084	58.59439	22.12785	19.96874	138.2994	-15	
38.59989	57.65446	21.77434	19.57744	137.5546	0	
38.86683	58.52394	21.8924	19.4189	137.5141	15	
38.85016	58.50369	22.53725	19.57275	138.3128	30	
38.88907	58.70714	23.68162	19.68329	139.5677	45	

Subsequently, energy performance is examined by keeping the angle of orientation fixed at 0 degrees while varying the height of the space across different areas (Table 4-145).

Table 4-145. Energy Performance Based on Variations in Space Height Across Different Areas with an Orientation Angle of 0 Degrees

Average Daylight Availability Index	Average Useful daylight illuminance	Heating Demand per Square Meter	Cooling Demand per Square Meter	Energy Consumption per Square Meter	Height	Building Dimensions
50.51028	78.03882	45.05756	19.65558	160.916	2.6	٦٤ m² 8*8 m H:3 m
54.72569	79.21681	50.08108	19.64409	165.928	2.8	
58.48632	79.63715	55.268	19.64838	171.1192	3	
61.93299	79.79646	60.62449	19.65859	176.4859	3.2	
65.50639	80.14063	66.08023	19.65717	181.9402	3.4	
68.89236	80.46993	71.65113	19.66682	187.5208	3.6	
71.27389	80.58014	77.37068	19.66839	193.2419	3.8	
29.98177	37.3	30.41724	19.49387	146.114	2.6	١٧٦ m² 8*22 m H:3 m
31.51365	39.05838	33.77219	19.4805	149.4555	2.8	
32.8537	41.42336	37.23578	19.47125	152.9099	3	
34.16917	42.85338	40.81091	19.48838	156.5021	3.2	
35.40495	44.47159	44.49291	19.47799	160.1737	3.4	
36.52453	45.82025	48.26841	19.47871	163.95	3.6	
37.73927	48.11152	52.138	19.48844	167.8293	3.8	
50.55137	69.34824	30.46712	19.71161	146.3816	2.6	١٧٦ m² 8*22 m H:3 m
53.36525	69.68395	33.8278	19.68237	149.713	2.8	
56.08282	70.51466	37.28456	19.66856	153.156	3	
57.7838	70.5012	40.8662	19.67207	156.7411	3.2	
59.15279	70.56733	44.53514	19.66355	160.4015	3.4	
60.49887	70.8411	48.3192	19.65284	164.1749	3.6	
61.34284	70.8389	52.20157	19.64424	168.0486	3.8	
34.81005	51.22392	17.95056	19.56075	133.7142	2.6	٤٨٤ m² 22*22 m H:3 m
36.74242	54.45862	19.82271	19.54087	135.5664	2.8	
38.59989	57.65446	21.77434	19.57744	137.5546	3	
40.16574	61.76258	23.79078	19.59184	139.5855	3.2	
41.89912	64.58513	25.87398	19.56792	141.6447	3.4	
43.46481	68.44362	28.02018	19.55911	143.7821	3.6	
45.12689	70.72164	30.22704	19.55236	145.9822	3.8	

Based on the results of changes in space height, it can be concluded that a reduction in height leads to a decrease in energy consumption per square meter and a decrease in heating demand per square meter. Additionally, increasing the height of the space results in an increase in both the useful daylight illuminance and the daylight autonomy index. However, regarding cooling demand, variations in space height produce diverse effects.

4-5- Investigating the effect of the WWR on building energy performance

In this section, a comparative analysis of energy consumption is undertaken with respect to the window-to-wall ratio for a building with a floor area of 100 m², east–west dimensions of 7.07 m, north–south dimensions of 14.142 m, and an aspect ratio of 0.5. The results in -45-degree orientation indicate that the minimum energy consumption is achieved at a window-to-wall ratio of 0.5. Furthermore, the findings in -30-degree orientation indicate that the lowest energy consumption occurs at a WWR of 0.5 (Figure 4-12).

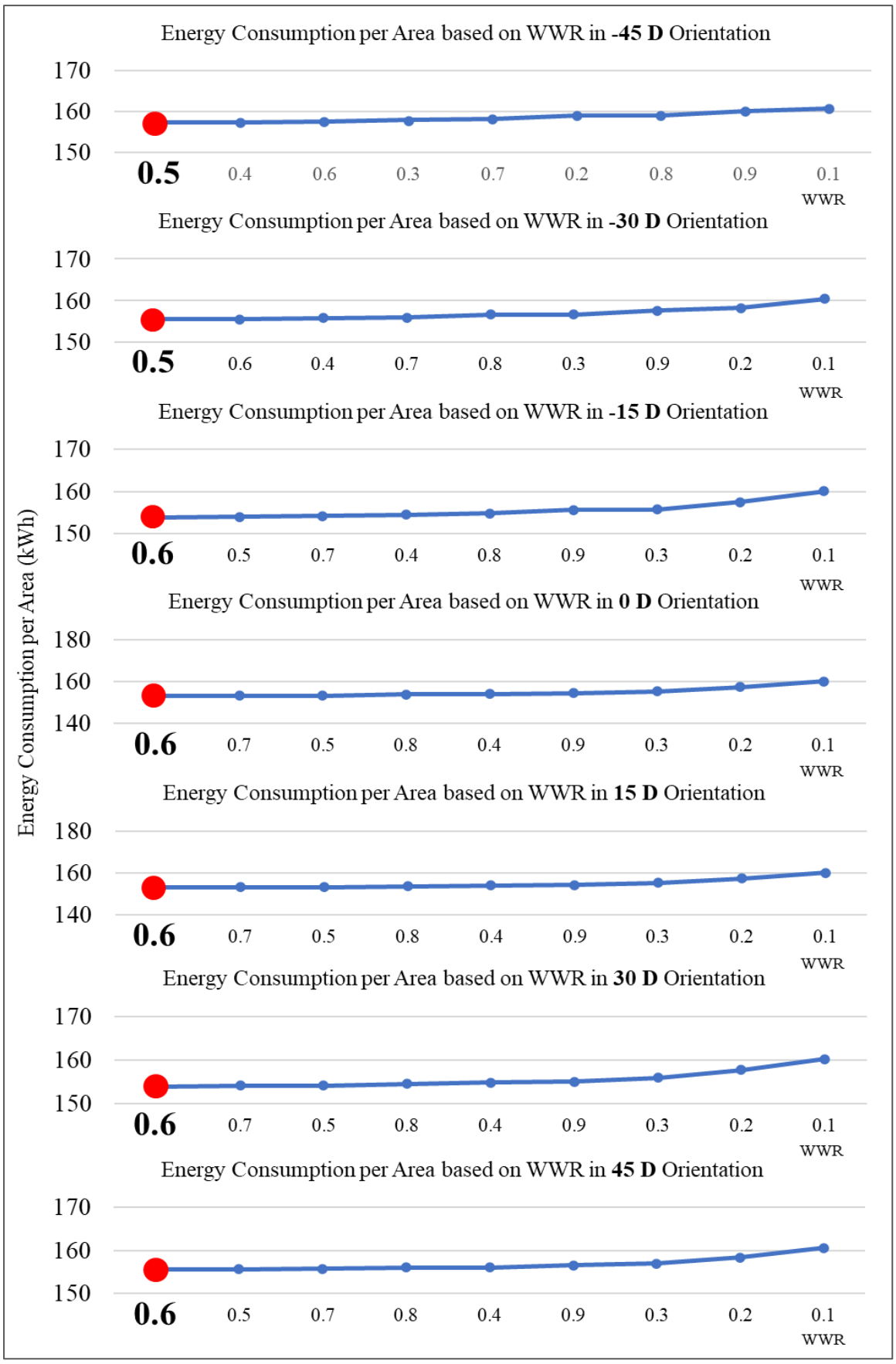

Figure 4-12. Comparative analysis of energy consumption based on the window-to-wall ratio for a 100 m² building with east–west dimensions of 7.07 m, north–south dimensions of 14.142 m.

Furthermore in -30 degrees orientation, findings indicate that the lowest energy consumption occurs at a WWR of 0.5. The results in -15-degree orientation, indicate that the minimum energy consumption is achieved at a WWR of 0.6. Based on a comparative analysis of building with 0-degree, the results show that the lowest energy consumption is achieved at a WWR of 0.6. Also, the results in 15-degree orientation indicate that the minimum energy consumption occurs at a WWR of 0.6 and the results in 30-degree orientation indicate that the minimum energy consumption occurs at a WWR of 0.6. Furthermore, based on a comparative analysis of a building with a floor area of 100 m², east–west dimensions of 7.07 m, north–south dimensions of 14.142 m, and an aspect ratio of 0.5, oriented at an azimuth of 45 degrees, the results indicate that the minimum energy consumption occurs at a window-to-wall ratio of 0.6 (Figure 4-12; Figure 4-13).

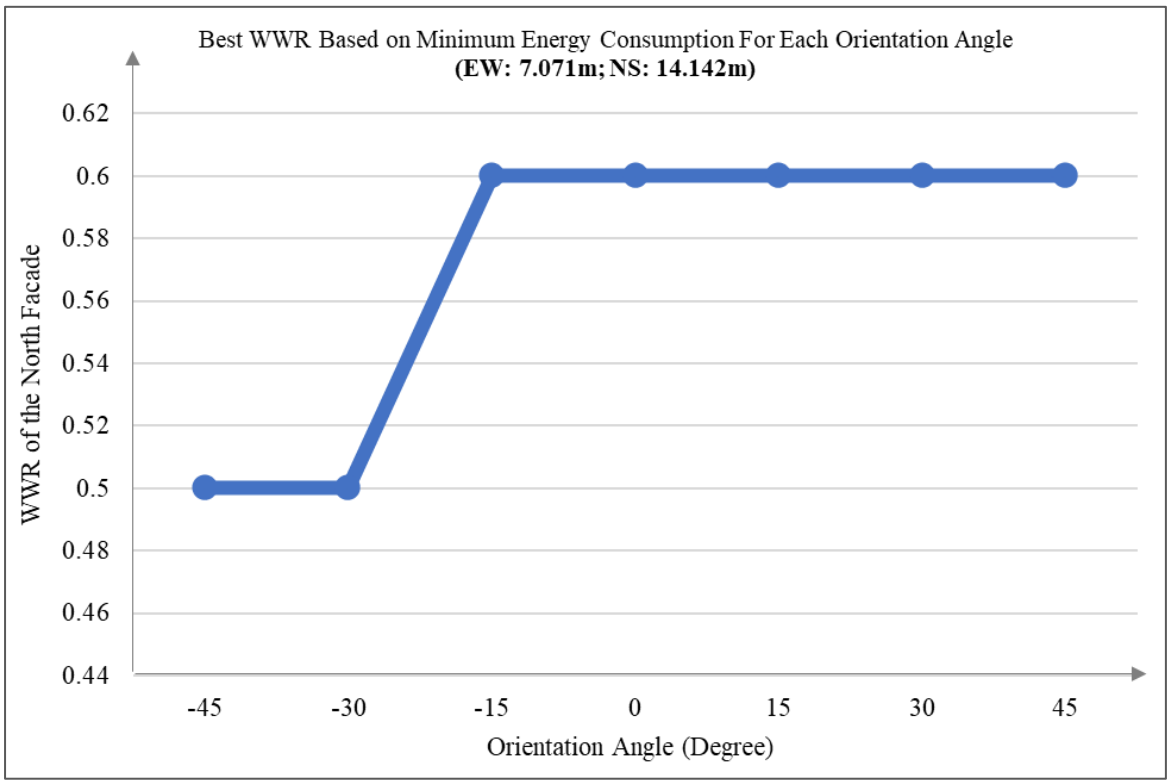

Figure 4-13. Analysis of the optimal window-to-wall ratio for a building with a floor area of 100 m², east–west dimensions of 7.07 m, north–south dimensions of 14.142 m, and an aspect ratio of 0.5 at various orientation angles.

Furthermore, a comparative analysis of energy consumption was conducted with respect to the window-to-wall ratio for a building with a floor area of 100 m², east–west and north–south dimensions of 10 m, and an aspect ratio of 1. The results in -45-degree orientation, indicate that the minimum energy consumption occurs at a WWR of 0.3 (Figure 4-14).

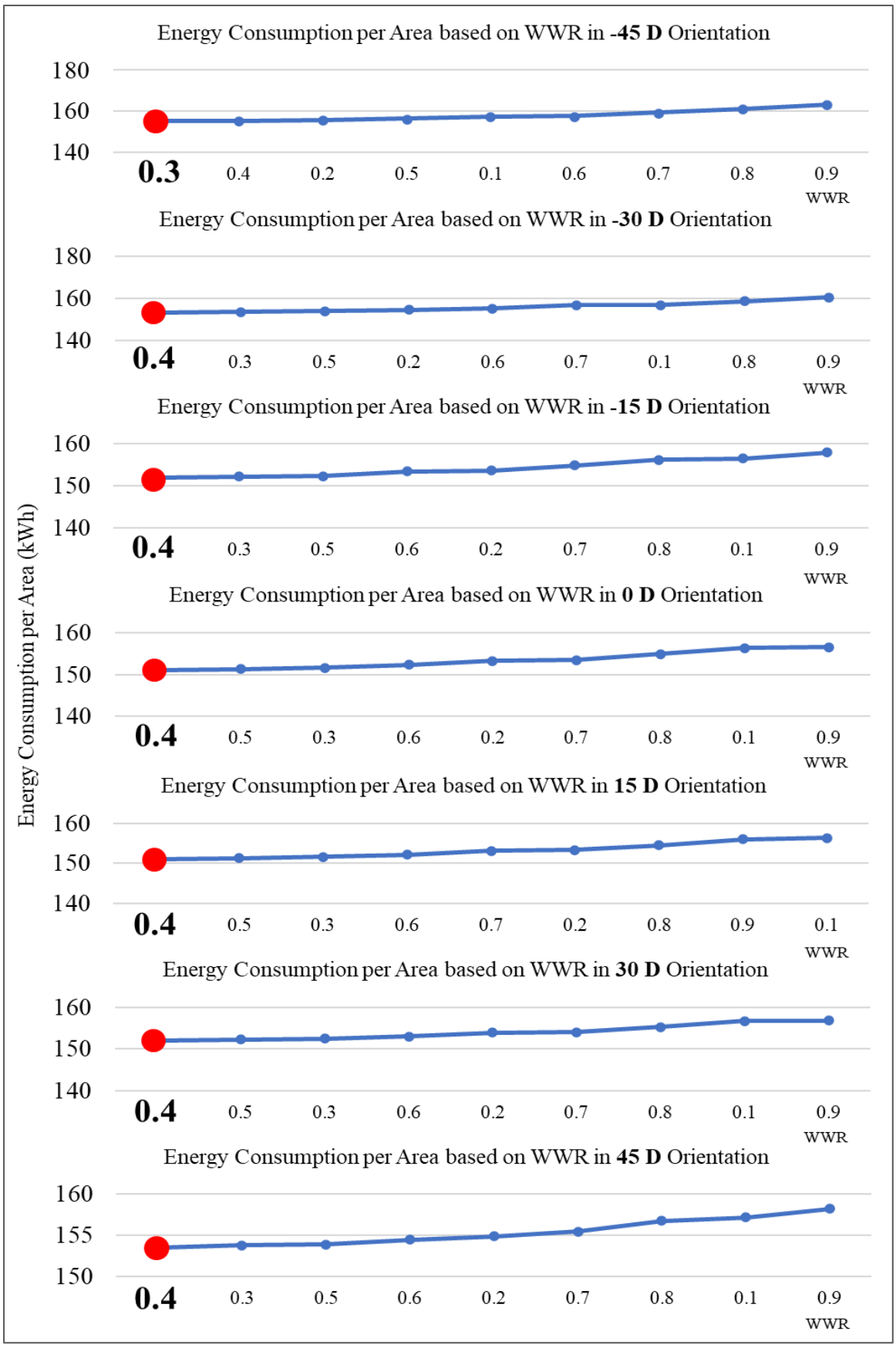

Figure 4-14. Comparative analysis of energy consumption based on the window-to-wall ratio for a 100 m² building with east–west and north–south dimensions of 10 m.

Also, in -30-degree and -15-degree orientation, findings indicate that the lowest energy consumption occurs at a WWR of 0.4 and 0.3 respectively. The results in 0-degree, 15-degree and 30-degree orientations, indicate that the minimum energy consumption is achieved at a WWR of 0.4 and 0.5. Based on a comparative analysis of building with 45-degree, the results show that the lowest energy consumption is achieved at a WWR of 0.4 (Figure 4-15).

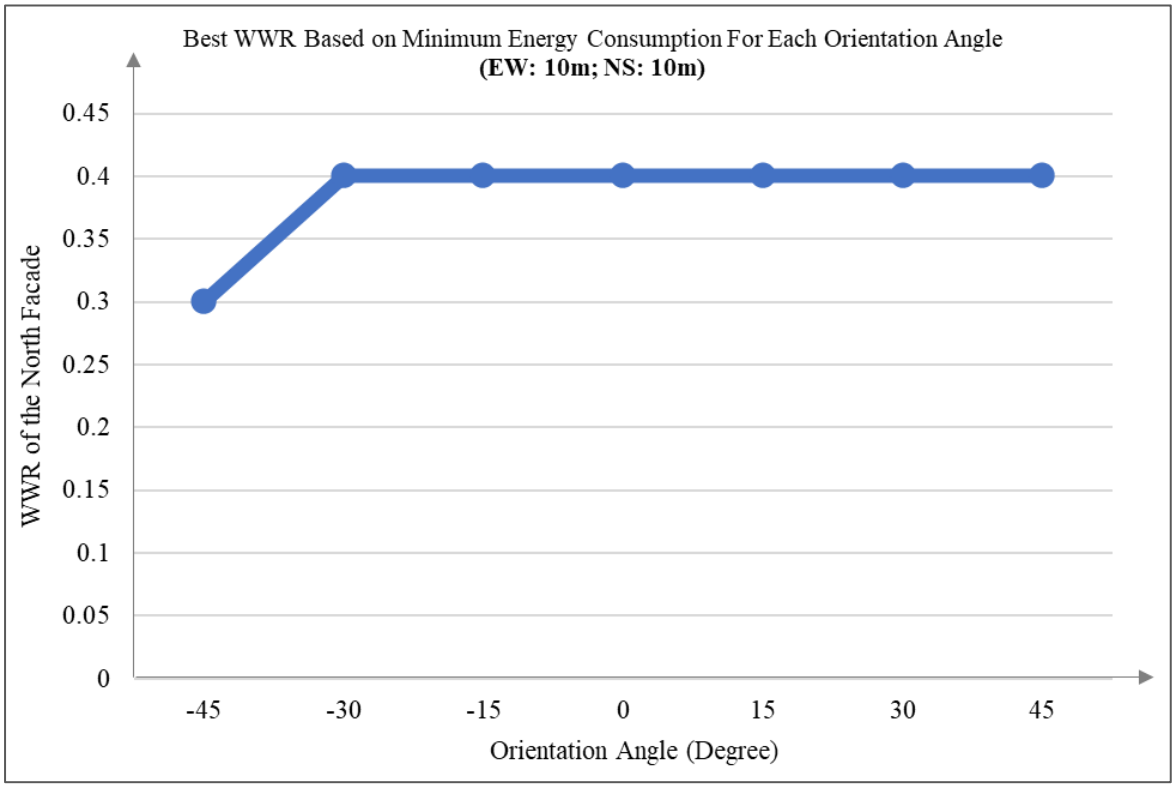

Figure 4-15. Comparative analysis of the optimal window-to-wall ratio for a building with a floor area of 100 m², east–west dimensions of 10 m, north–south dimensions of 10 m, and an aspect ratio of 1 at various orientation angles.

Furthermore, a comparative analysis of energy consumption was conducted with respect to the window-to-wall ratio for a building with a floor area of 100 m², east–west dimensions of 14.142 m, north–south dimensions of 7.07 m, and an aspect ratio of 2, oriented at an azimuth of -30 degrees. The results indicate that the minimum energy consumption occurs at a WWR of 0.3. Furthermore, a comparative analysis of energy consumption was conducted with respect to the window-to-wall ratio for a building with a floor area of 100 m², east–west dimensions of 14.142 m, north–south dimensions of 7.07 m, and an aspect ratio of 2, oriented at an azimuth of -30 degrees. The results indicate that the minimum energy consumption occurs at a WWR of 0.3. The results for the mentioned building, oriented at an azimuth of -15 degrees, indicate that the minimum energy consumption occurs at a WWR of 0.3

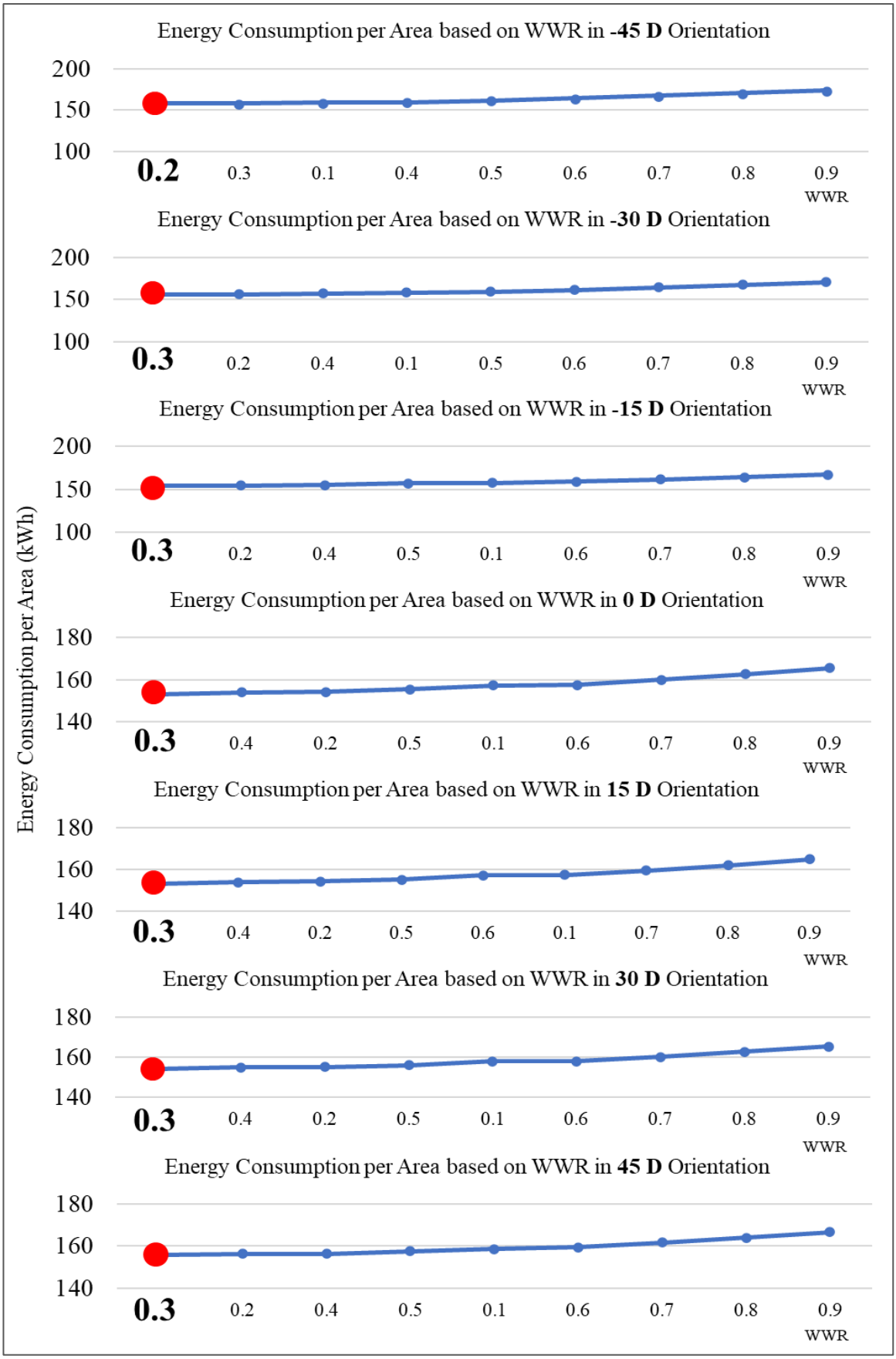

Figure 4-16. Comparative analysis of energy consumption based on the window-to-wall ratio for a 100 m² building with east–west dimensions of 14.142 m, north–south dimensions of 7.07 m

Furthermore. The results for a building with a floor area of 100 m², east–west dimensions of 14.142 m, north–south dimensions of 7.07 m, and an aspect ratio of 2, oriented at an azimuth of 0 degrees indicate that the minimum energy consumption occurs at a WWR of 0.3. Also, the best window-to-wall ratio for a building with a floor area of 100 m², east–west dimensions of 14.142 m, north–south dimensions of 7.07 m, and an aspect ratio of 2, oriented at an azimuth of 15 degree based on minimum energy consumption is at a WWR of 0.3. Furthermore, a comparative analysis of energy consumption was conducted with respect to the window-to-wall ratio for a building with a floor area of 100 m², east–west dimensions of 14.142 m, north–south dimensions of 7.07 m, and an aspect ratio of 2, oriented at an azimuth of 30 degrees. The results indicate that the minimum energy consumption occurs at a WWR of 0.3. The results for the mentioned building, oriented at an azimuth of 45 degrees indicate that the minimum energy consumption occurs at a WWR of 0.3 (Figure 4-16; Figure 4-17).

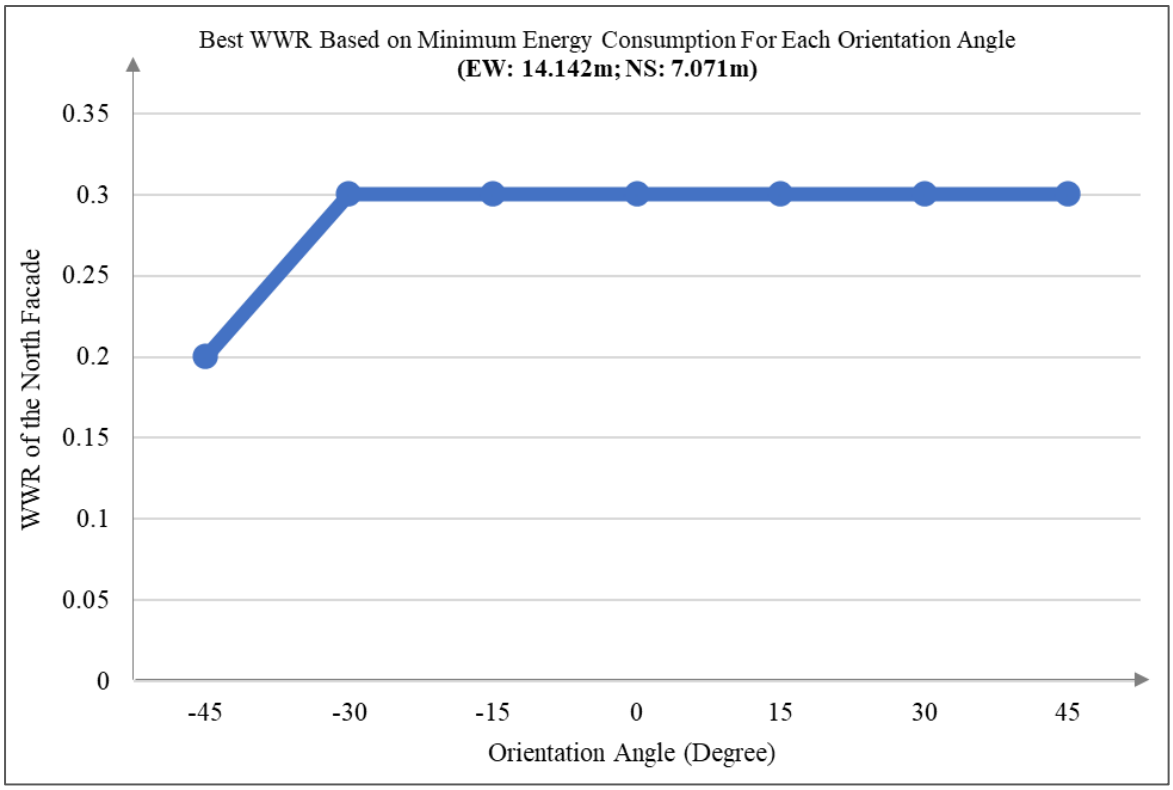

Figure 4-17. Comparative analysis of the optimal window-to-wall ratio for a building with a floor area of 100 m², east–west dimensions of 7.07 m, north–south dimensions of 14.142 m, and an aspect ratio of 0.5 at various orientation angles.

Furthermore, a comparative analysis of energy consumption was conducted with respect to the window-to-wall ratio for a building with a floor area of 150 m², east–west dimensions of 8.66 m, north–south dimensions of 17.32 m and the results are presented (Figure 4-18).

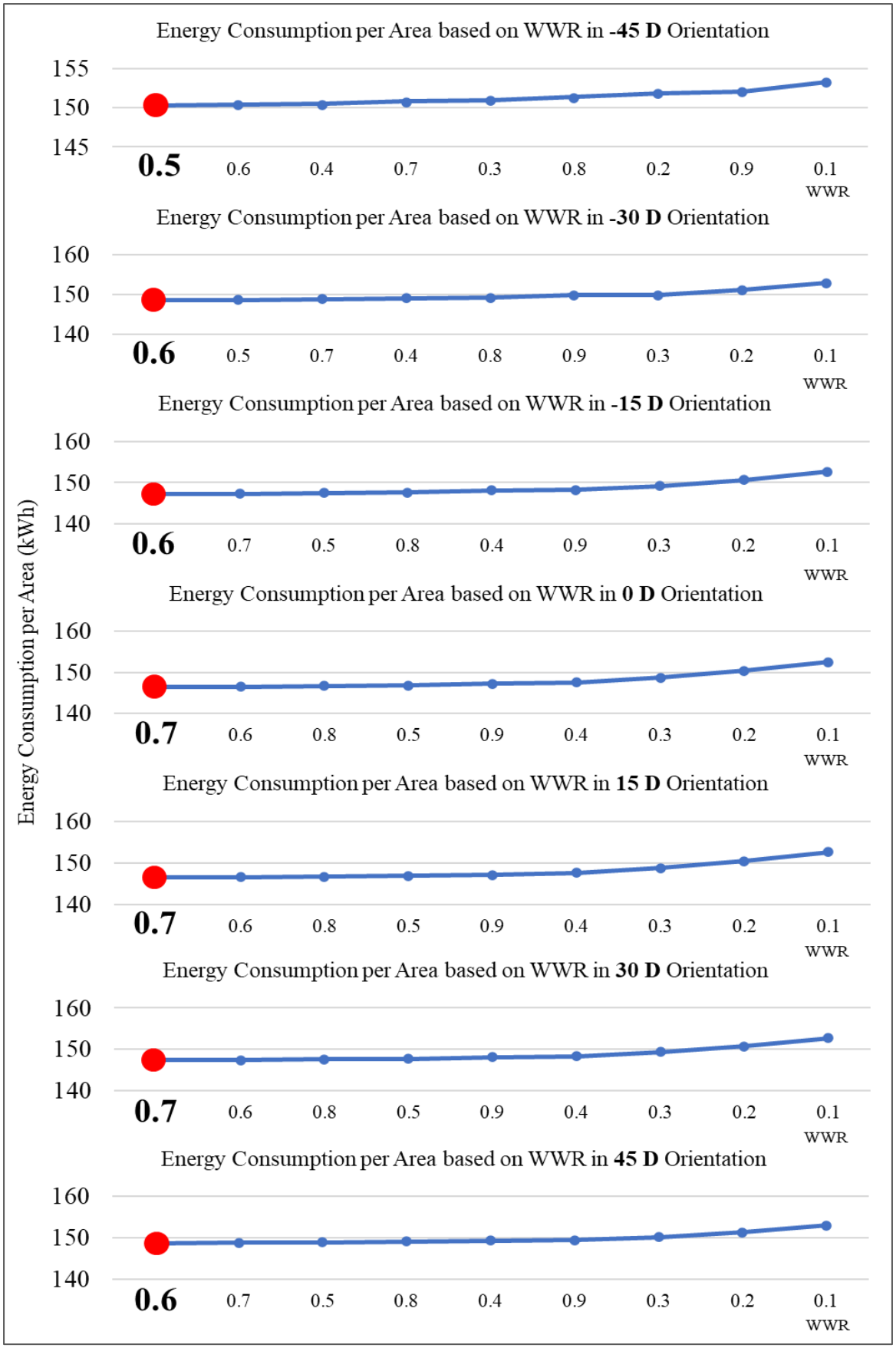

Figure 4-18. Comparative analysis of energy consumption based on the window-to-wall ratio for a 150 m² building with east–west dimensions of 8.66 m, north–south dimensions of 17.32 m

For a building with a floor area of 150 m², east–west dimensions of 8.66 m, north–south dimensions of 17.32 m, and an aspect ratio of 0.5, oriented at an azimuth of -45 degrees, the results indicate that the minimum energy consumption occurs at a window-to-wall ratio of 0.6. In addition, based on the reults, for a building with a floor area of 150 m², east–west dimensions of 8.66 m, north–south dimensions of 17.32 m, and an aspect ratio of 0.5, oriented at an azimuth of -30 and -15 degrees, the minimum energy consumption occurs at a WWR of 0.6. Also, for a building with a floor area of 150 m², east–west dimensions of 8.66 m, north–south dimensions of 17.32 m, and an aspect ratio of 0.5, oriented at an azimuth of 0, 15 and 30 degrees, the minimum energy consumption occurs at a WWR of 0.7. In addition, based on the results, for the building mentioned, oriented at an azimuth of 45 degrees, the minimum energy consumption occurs at a WWR of 0.6 (Figure 4-19).

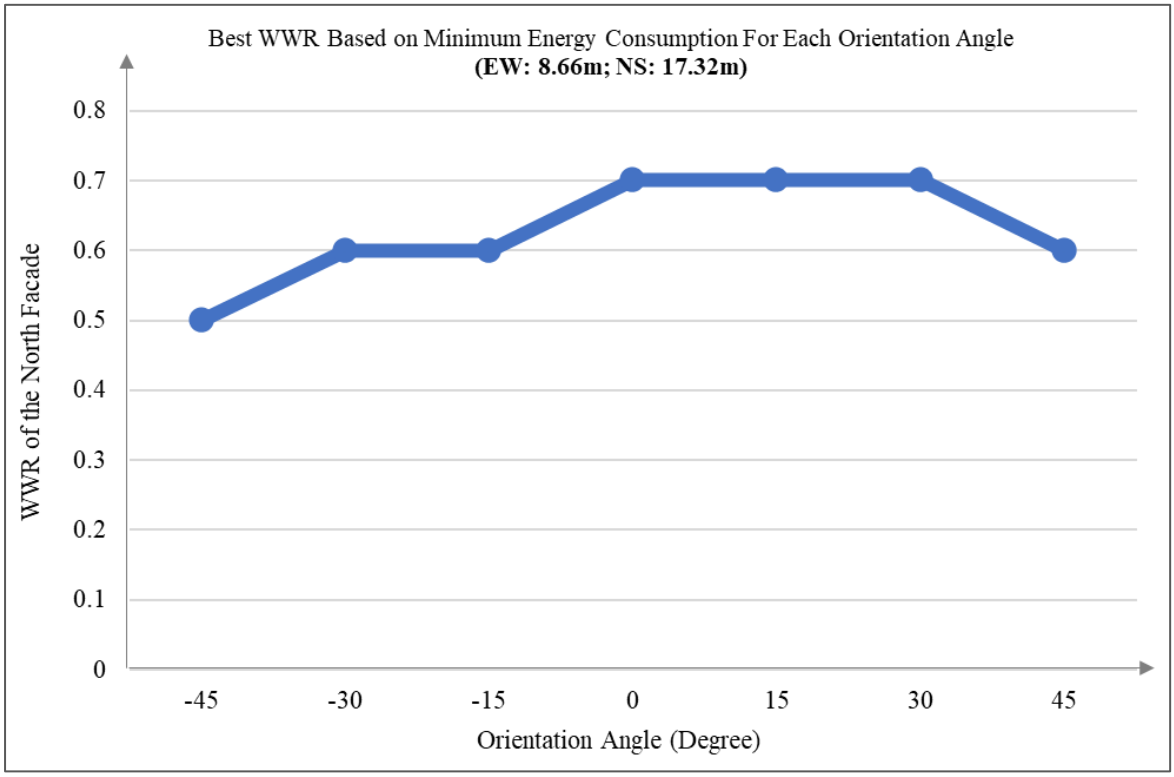

Figure 4-19. Comparative analysis of the optimal window-to-wall ratio for a building with a floor area of 150 m², east–west dimensions of 8.66 m, north–south dimensions of 17.32 m, and an aspect ratio of 0.5 at various orientation angles.

In this section, a comparative analysis of energy consumption was conducted with respect to the window-to-wall ratio for a building with a floor area of 150 m², east–west and north–south dimensions of 12.247 m, and an aspect ratio of 1. The results are presented below (Figure 4-20).

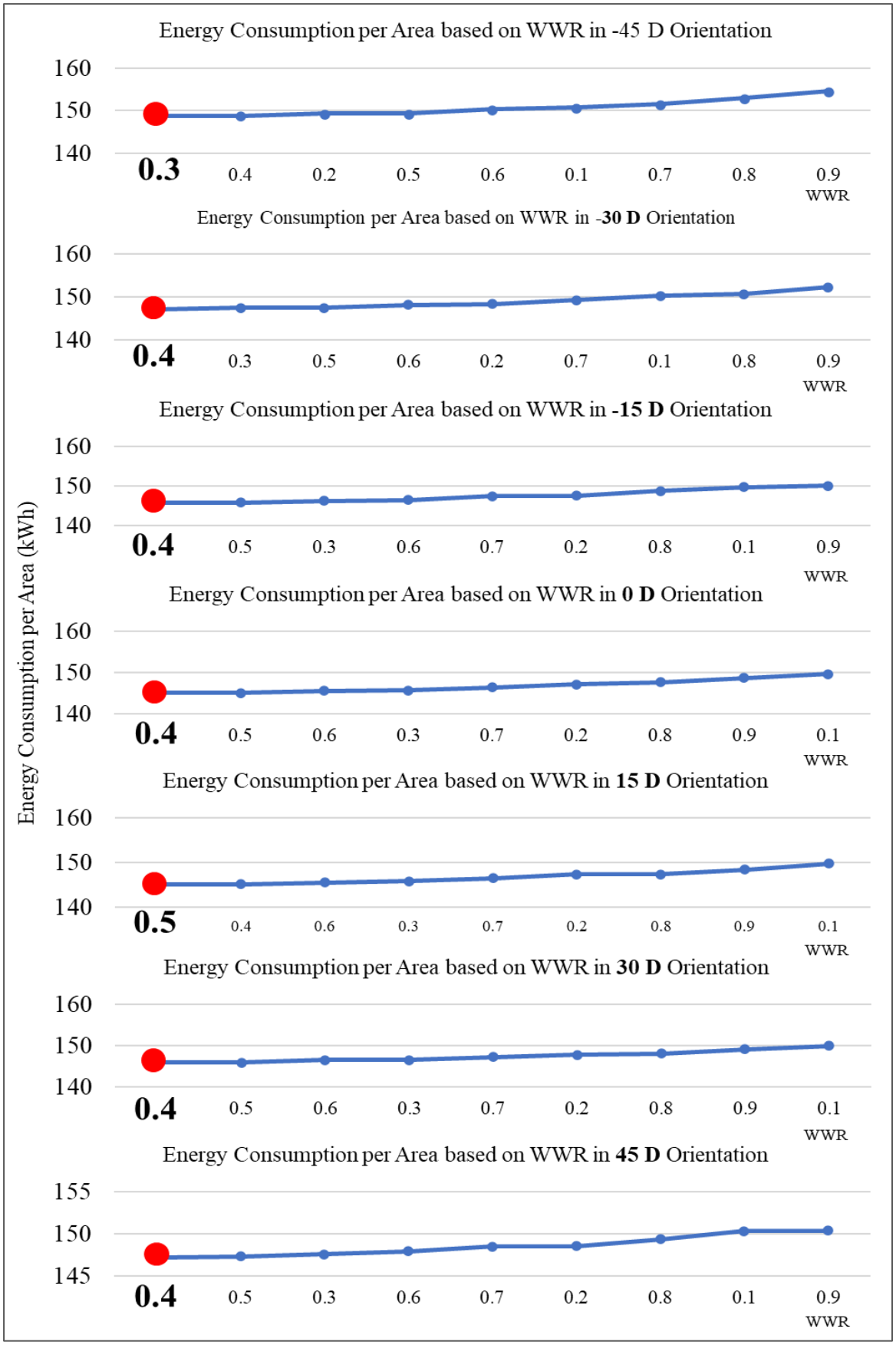

Figure 4-20. Comparative analysis of energy consumption based on the window-to-wall ratio for a 150 m² building with east–west and north–south dimensions of 12.247 m

Based on the results of the comparative analysis, the best WWR for a building with a floor area of 150 m², east–west and north–south dimensions of 12.247 m, and an aspect ratio of 1, oriented at an azimuth of -45 degrees is 0.4. In addition, for the mentioned building, oriented at an azimuth of -30, -15 and 45 degrees, the minimum energy consumption occurs at a WWR of 0.6. Furthermore, comparative analysis of energy consumption for a building with a floor area of 150 m², east–west and north–south dimensions of 12.247 m, and an aspect ratio of 1, oriented at an azimuth of 0, 15 and 30 degrees, indicate that the minimum energy consumption occurs at a WWR of 0.7. The weakest window-to-wall ratio for the building mentioned based on energy performance is 0.9 and 0.1. This indicates that too much reduction and too much increase in the window-to-wall ratio will increase energy consumption (Figure 4-21).

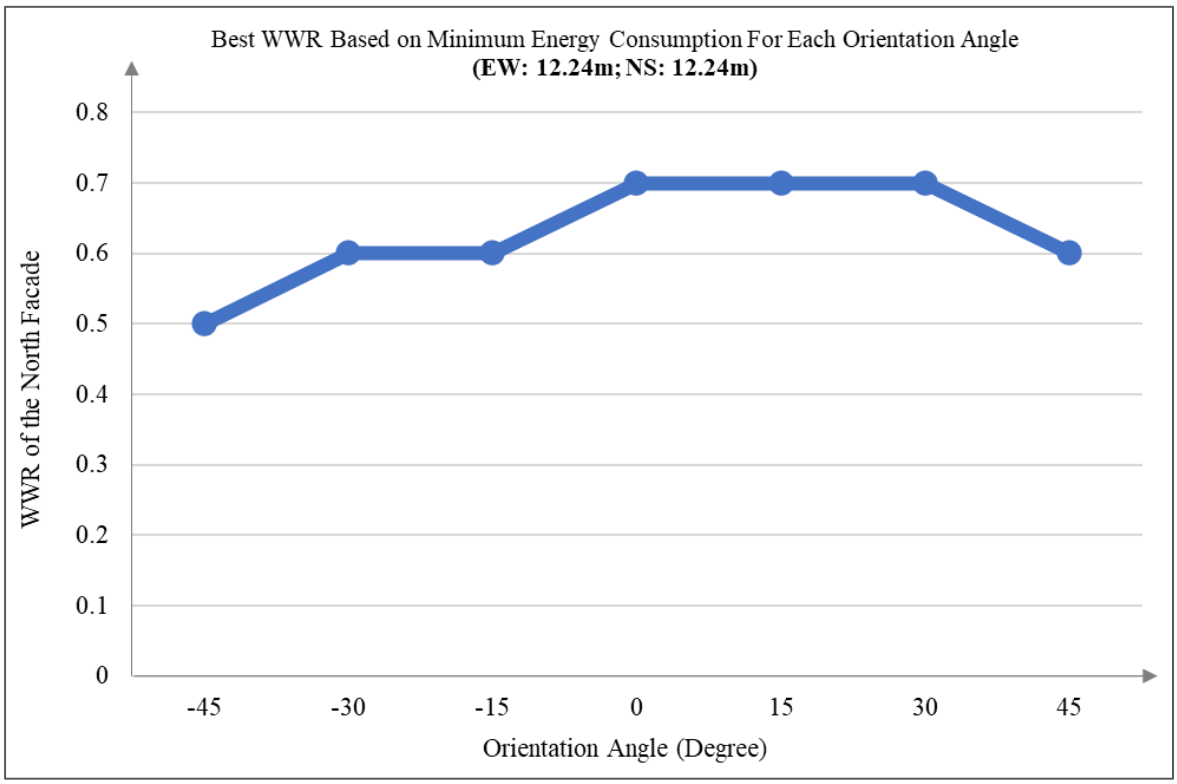

Figure 4-21. Comparative analysis of the optimal window-to-wall ratio for a building with a floor area of 150 m², east–west dimensions of 12.247 m, north–south dimensions of 12.247 m, and an aspect ratio of 1 at various orientation angles.

Furthermore, a comparative analysis of energy consumption was conducted with respect to the window-to-wall ratio for a building with a floor area of 150 m², east–west dimensions of 17.321 m, north–south dimensions of 8.66 m, and an aspect ratio of 2. The results of this comparative study are presented below (Figure 4-22).

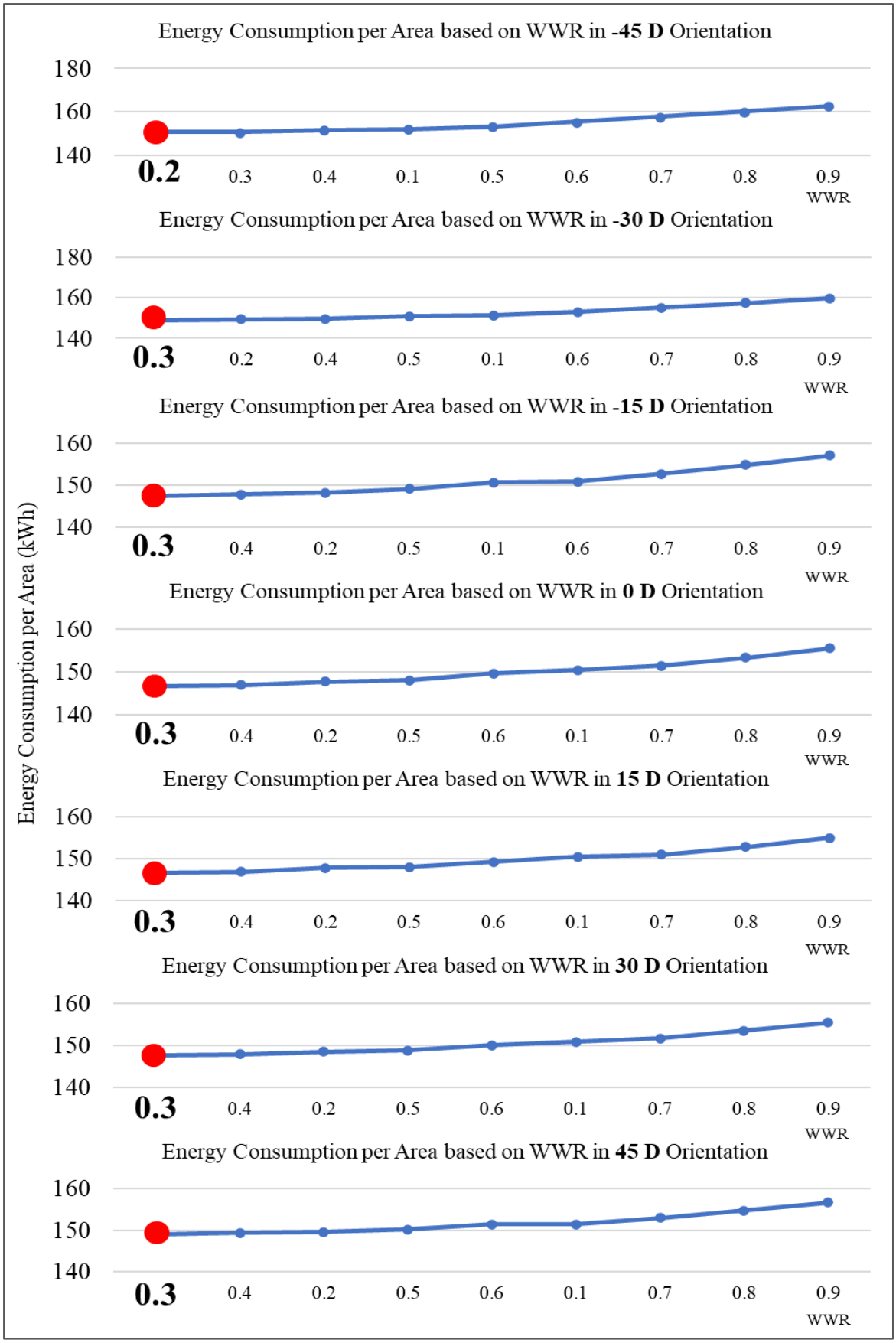

Figure 4-22. Comparative analysis of energy consumption based on the window-to-wall ratio for a 150 m² building with east–west dimensions of 17.321 m, north–south dimensions of 8.66 m

Based on the comparative analysis of energy consumption for a building with a floor area of 150 m², east–west dimensions of 17.321 m, north–south dimensions of 8.66 m, and an aspect ratio of 2, oriented at an azimuth of -45 degrees, the results indicate that the minimum energy consumption occurs at a WWR of 0.2 (Figure 4-23).

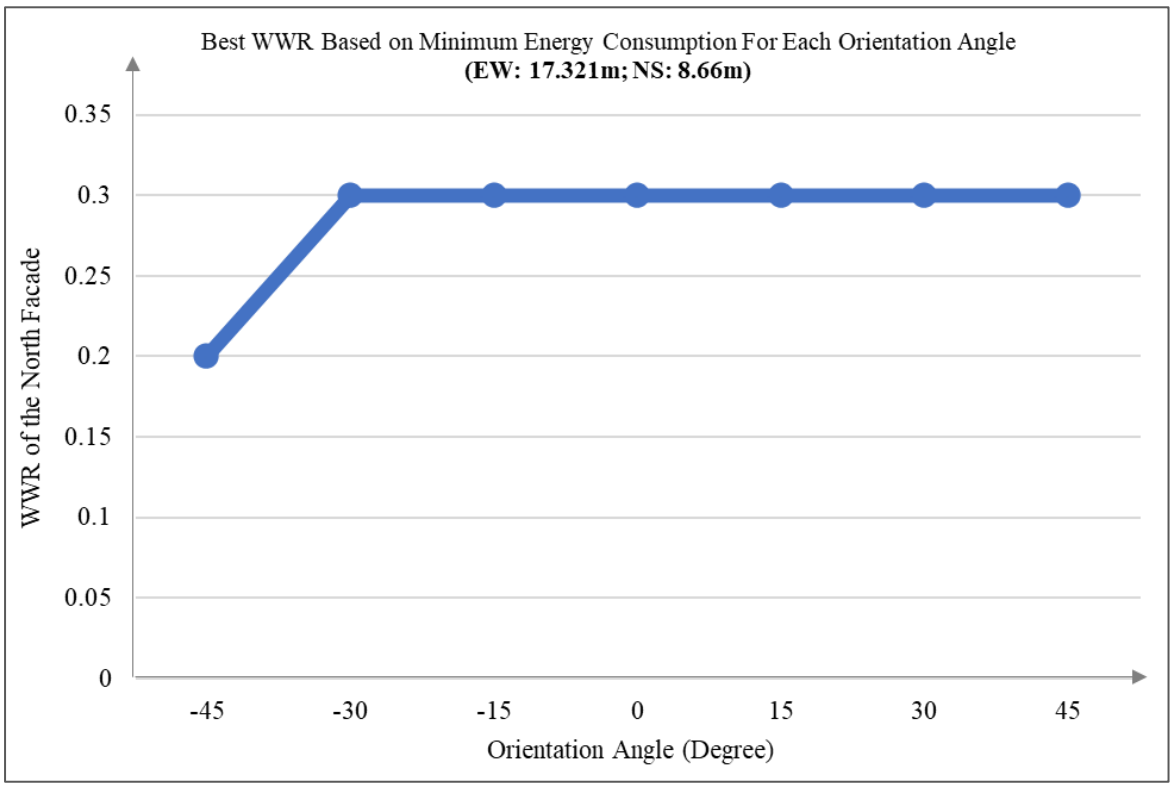

Figure 4-23. Comparative analysis of the optimal window-to-wall ratio for a building with a floor area of 150 m², east–west dimensions of 17.321 m, north–south dimensions of 8.66 m, and an aspect ratio of 2 at various orientation angles.

In addition, based on the reults of the comparative analysis of energy consumption was conducted with respect to the window-to-wall ratio for the mentioned building, oriented at an azimuth of -30, -15, 0, 15, 30 and 45 degrees, the results indicate that the minimum energy consumption occurs at a WWR of 0.3. Additionally, the weakest window-to-wall ratio for the building mentioned based on energy performance is 0.9. This indicates that too much increase in the window-to-wall ratio will increase energy consumption (Figure 4-24).

In this section, a comparative analysis of energy consumption based on the window-to-wall ratio was conducted for a building with a floor area of 200 m², east–west dimensions of 10 m, north–south dimensions of 20 m. The results of this comparative study are presented in the form of graphs below. The results of this section also confirm the previous results.

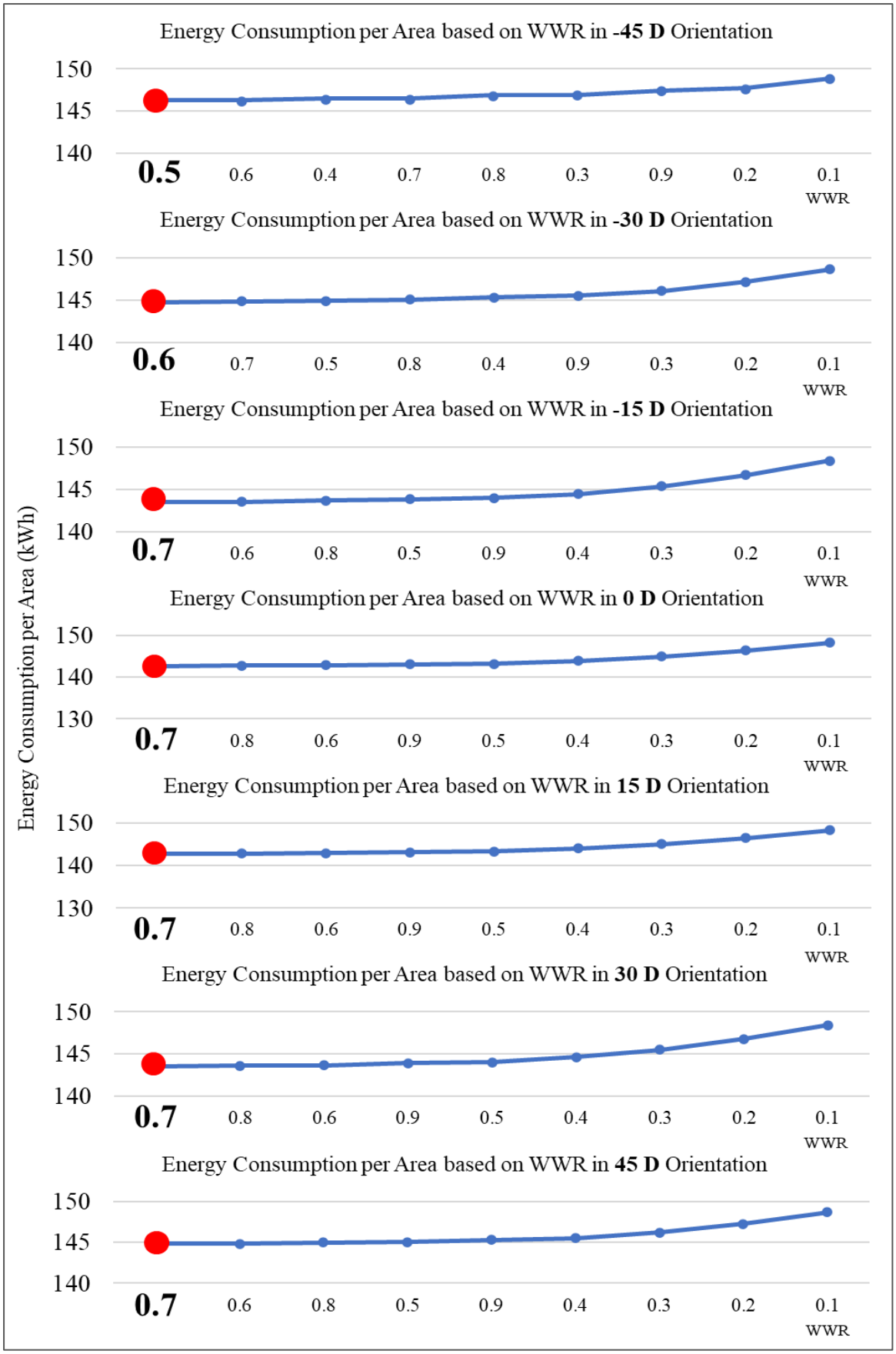

Figure 4-24. Comparative analysis of energy consumption based on the window-to-wall ratio for a building with a floor area of 200 m², east–west dimensions of 10m, north–south dimensions of 20 m

Based on the reults of the simulation for the building with a floor area of 200 m², east–west dimensions of 10 m, north–south dimensions of 20 m, and an aspect ratio of 0.5 at an orientation angle of -45°, the lowest energy consumption corresponds to a window-to-wall ratio of 0.5 and for the mentioned building at an orientation angle of -30°, the lowest energy consumption corresponds to a window-to-wall ratio of 0.6. Additionally, the lowest energy consumption for a building with a floor area of 200 m², east–west dimensions of 10 m, north–south dimensions of 20 m, and an aspect ratio of 0.5 at an orientation angle of -15°, 0°, 15°, 30° and 45°, corresponds to a window-to-wall ratio of 0.7. Furthermore, the weakest WWR for the building mentioned based on energy performance is 0.1. This indicates that too much reduction in the WWR will increase energy consumption (Figure 4-25).

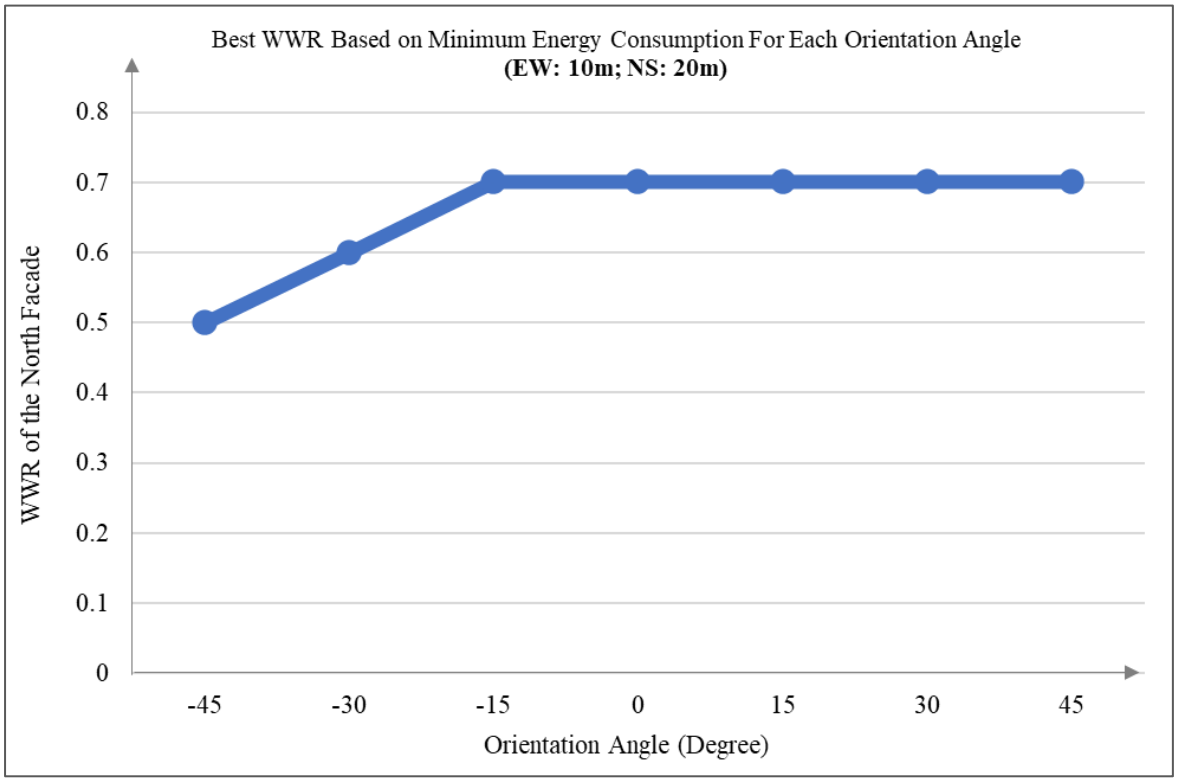

Figure 4-25. Comparative analysis of the optimal window-to-wall ratio for a building with a floor area of 200 m², east–west dimensions of 10 m, north–south dimensions of 20 m, and an aspect ratio of 0.5 at various orientation angles.

Additionally, a comparative analysis of energy consumption based on the window-to-wall ratio was conducted for a building with a floor area of 200 m², east–west dimensions of 14.142 m, north–south dimensions of 14.142 m, and an aspect ratio of 1 at various orientation angles. The results of this comparative study are presented in the form of graphs below. The results of this section also confirm the previous results (Figure 4-26).

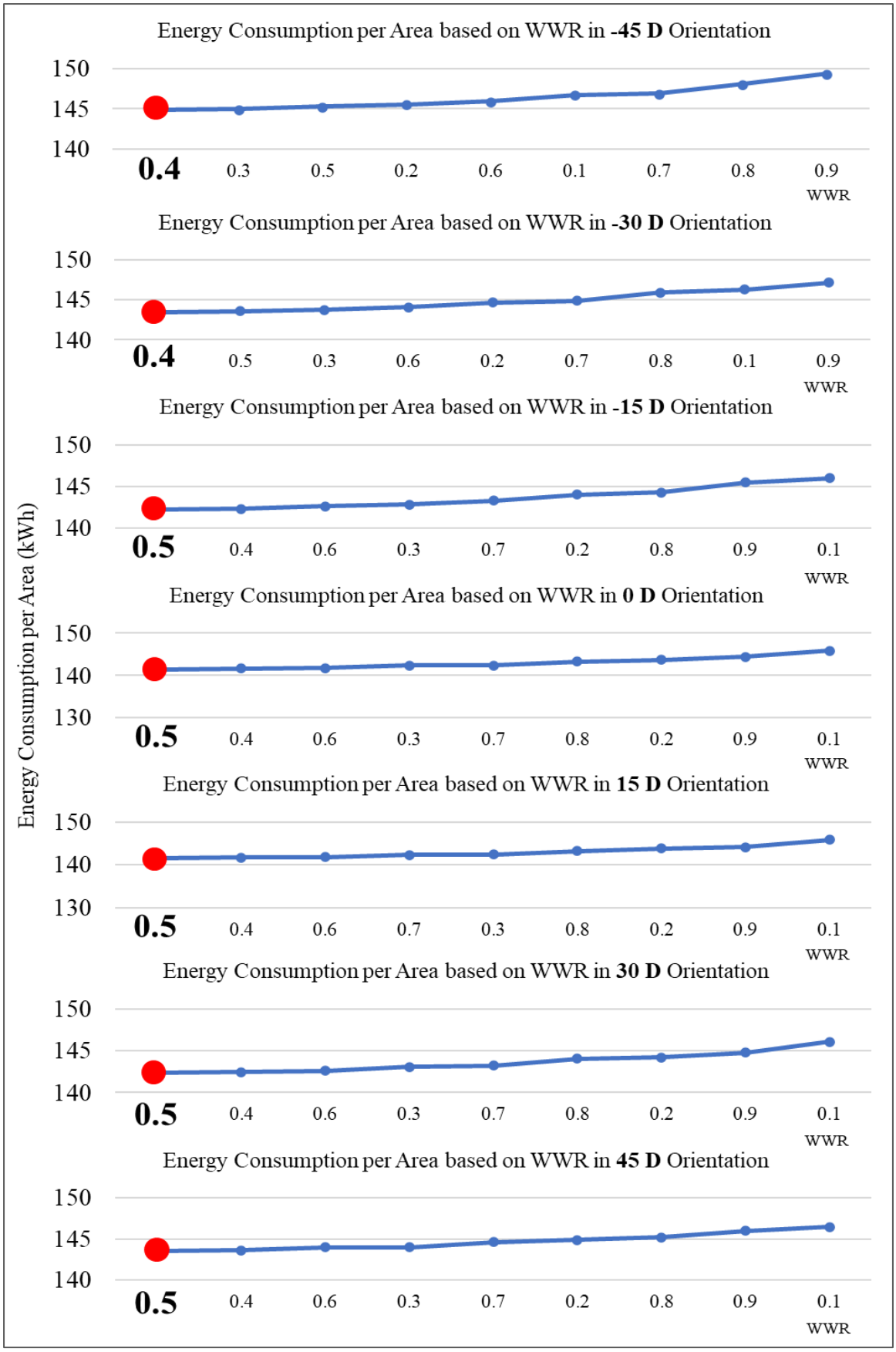

Figure 4-26. Comparative analysis of energy consumption based on the WWR for a building with a floor area of 200 m², east–west dimensions of 14.14 m, north–south dimensions of 14.14 m

Based on the reults of the Comparative analysis for the building with a floor area of 200 m², east–west dimensions of 14.14 m, north–south dimensions of 14.14 m, and an aspect ratio of 1 at an orientation angle of -45°, the lowest energy consumption corresponds to a window-to-wall ratio of 0.4 and 0.3. and for the mentioned building at an orientation angle of -30°, the lowest energy consumption corresponds to a window-to-wall ratio of 0.4 and 0.5 respectively. Additionally, the lowest energy consumption for a building with a floor area of 200 m², east–west dimensions of 14.142 m, north–south dimensions of 14.142 m, and an aspect ratio of 1 at an orientation angle of -15°, 0°, 15°, 30° and 45°, corresponds to a window-to-wall ratio of 0.5. Furthermore, the weakest window-to-wall ratio for the building mentioned based on energy performance is 0.1. This indicates that too much reduction in the window-to-wall ratio will increase energy consumption (Figure 4-27).

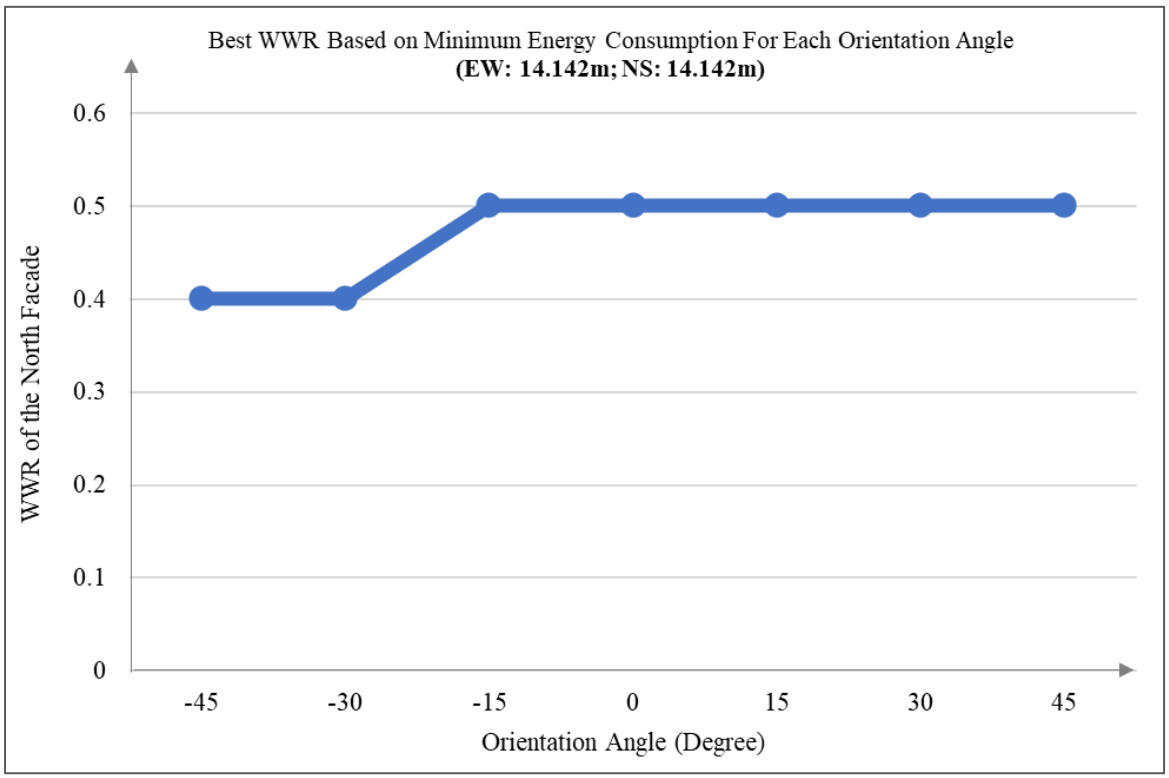

Figure 4-27. Comparative analysis of the optimal window-to-wall ratio for a building with a floor area of 200 m², east–west dimensions of 14.142 m, north–south dimensions of 14.142 m, and an aspect ratio of 1 at various orientation angles.

In this section, a comparative analysis of energy consumption based on the window-to-wall ratio was conducted for a building with a floor area of 200 m², east–west dimensions of 20 m, north–south dimensions of 10 m, and an aspect ratio of 2 at various orientation angles. The results are presented in the form of graphs below (Figure 4-28).

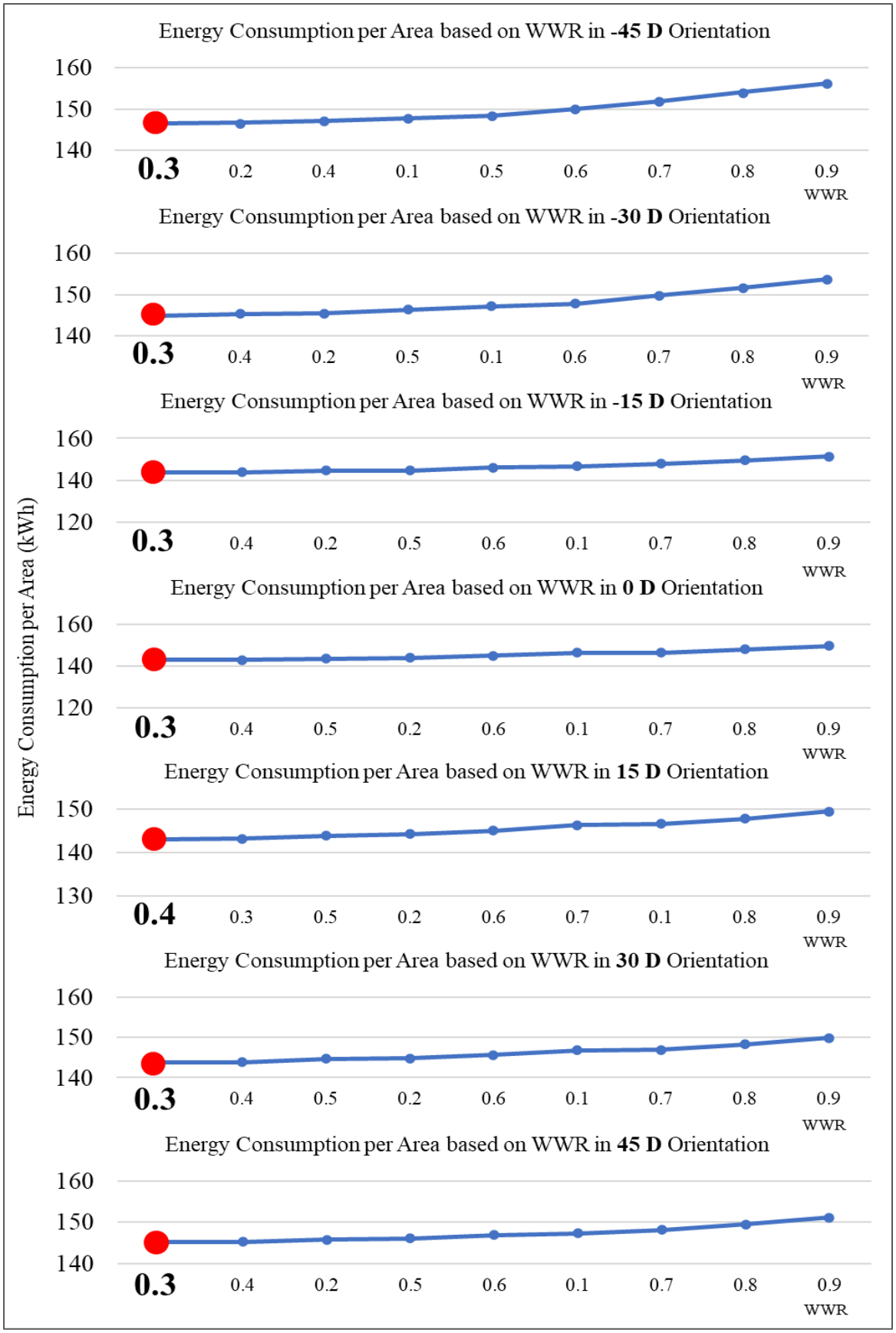

Figure 4-28. Comparative analysis of energy consumption based on the window-to-wall ratio for a building with a floor area of 200 m², east–west dimensions of 20m, north–south dimensions of 10 m

Based on the results, the lowest energy consumption for a building with a floor area of 200 m², east–west dimensions of 20 m, north–south dimensions of 10 m, and an aspect ratio of 2, at an orientation angle of -45°, -30°, -15°, 0°, 30° and 45°, corresponds to a window-to-wall ratio of 0.3 (Figure 4-29).

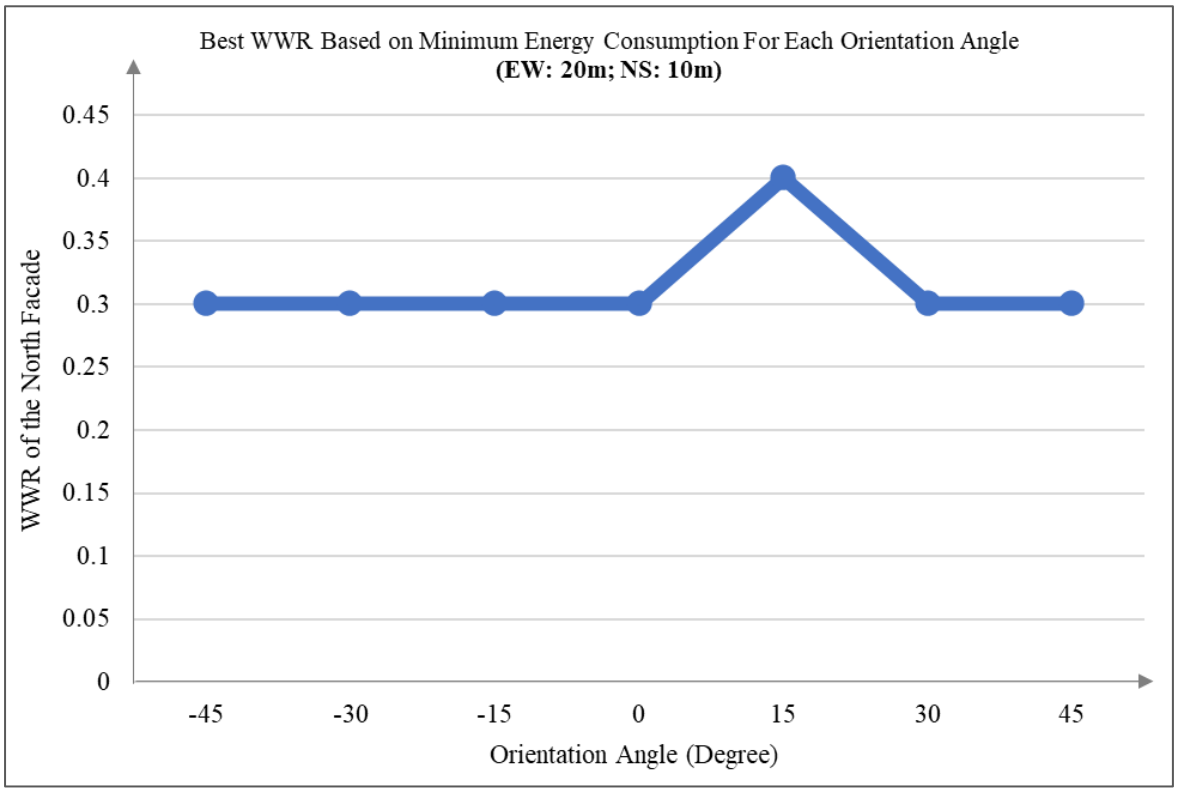

Figure 4-29. Comparative analysis of the optimal window-to-wall ratio for a building with a floor area of 200 m², east–west dimensions of 20 m, north–south dimensions of 10 m, and an aspect ratio of 2 at various orientation angles.

In this section, a comparative analysis of energy consumption based on the window-to-wall ratio was conducted for a building with a floor area of 200 m², east–west dimensions of 20 m, north–south dimensions of 10 m, and an aspect ratio of 2 at an orientation angle of 15°. The lowest energy consumption corresponds to a window-to-wall ratio of 0.4. Additionally, the weakest window-to-wall ratio for the building mentioned based on energy performance is 0.9. This indicates that too much increase in the window-to-wall ratio will increase energy consumption (Figure 4-30).

Based on the results, for a building with a floor area of 100 m², east–west dimensions of 7.07 m, north–south dimensions of 14.142 m, and an aspect ratio of 0.5, for orientation angles ranging from -15° to 15°, a window-to-wall ratio of 0.6 is recommended for the north-facing façade in Melbourne. Additionally, for a building with a floor area of 100 m², east–

west dimensions of 10 m, north–south dimensions of 10 m, and an aspect ratio of 1, for orientation angles ranging from -15° to 15°, a window-to-wall ratio of 0.4 is recommended for the north-facing façade in Melbourne. For a building with a floor area of 100 m², east–west dimensions of 14.142 m, north–south dimensions of 7.07 m, and orientation angles ranging from -15° to 15°, a window-to-wall ratio of 0.3 is recommended for the north-facing façade in Melbourne. The optimal window-to-wall ratio for the north-facing façade in Melbourne, for a building with a floor area of 150 m², east–west dimensions of 8.66 m, north–south dimensions of 17.32 m, and an aspect ratio of 0.5, for orientation angles ranging from -15° to 15°, is recommended to be between 0.6 and 0.7. A comparative analysis of the window-to-wall ratio for a building with a floor area of 150 m², east–west dimensions of 12.247 m, north–south dimensions of 12.247 m, and an aspect ratio of 1, showed that for orientation angles ranging from -15° to 15°, a window-to-wall ratio of 0.6 to 0.7 is recommended for the north-facing façade in Melbourne. For a building with a floor area of 150 m², east–west dimensions of 17.321 m, north–south dimensions of 8.66 m, and an aspect ratio of 2, for orientation angles ranging from -15° to 15°, a window-to-wall ratio of 0.3 is recommended for the north-facing façade in Melbourne. For a building with a floor area of 200 m², east–west dimensions of 10 m, north–south dimensions of 20 m, and orientation angles ranging from -15° to 15°, a window-to-wall ratio of 0.7 provides optimal energy performance for the north-facing façade in Melbourne. Additionally, the optimal window-to-wall ratio for the north-facing façade in Melbourne, for a building with a floor area of 200 m², east–west dimensions of 14.142 m, north–south dimensions of 14.142 m, and orientation angles ranging from -15° to 15°, is recommended to be 0.5. A comparative analysis of the window-to-wall ratio for a building with a floor area of 200 m², east–west dimensions of 20 m, north–south dimensions of 10 m, at various orientation angles, showed that, in general, for angles ranging from -15° to 15°, a window-to-wall ratio of 0.3 to 0.4 is recommended for the north-facing façade in Melbourne.

4-5 Summary

In this chapter, the findings of the research are elucidated and examined. The results of this study, adopting a quantitative approach, are based on coding, simulation, optimization, and modelling processes. Accordingly, the findings are presented in two main sections: the results of modelling the energy performance of the external shell of residential buildings and the optimization of the energy performance of the external shell of residential buildings.

Overall, this research involved an energy performance optimization process, 8 linear modelling processes, and 8 nonlinear modelling processes for various energy performance components, along with several analytical processes. In this context, over 6,000 simulations of the specifications and energy performance of residential buildings have been conducted. Additionally, a generative design algorithm for the external shell of residential buildings has been defined based on its spatial layout characteristics, which can effectively explore the solution space of a residential building.

Based on the results and analyses, the specifications of the residential building can be defined according to the optimization of three performance objectives: cooling demand per square meter, heating demand per square meter, and daylight factor. During the energy performance simulation of the residential building, the specifications of the materials used in common single-story residential buildings in Melbourne were extracted. Furthermore, a validation process of the energy simulation using Ladybug Tools was conducted by comparing the results with actual energy consumption.

Based on the findings, 8 predictive models for the energy performance of single-story residential buildingss with a high confidence level of over 95% have been developed. These models can be utilized in the urban planning of various areas in Melbourne. Additionally, they can serve as the basis for developing artificial intelligence tools aimed at predicting energy performance based on building specifications. In the following chapter, a discussion of the findings and conclusions of the research will be presented.

Chapter 5:

Summary, Conclusion, Recommendations

Chapter 5: Summary, Conclusion, Recommendations

5-1- Introduction

This research aims to optimize the spatial layout of a typical single-story house in Melbourne based on Building Energy Performance (BEP) through a Performative Computational Architecture (PCA) framework. The study adopts a quantitative approach grounded in coding, simulation, optimization, and modeling of the results. In the previous chapter, the findings were presented in two main sections. Based on those findings, this chapter summarizes the research results and then discusses and analyzes them. Subsequently, these results are compared with the findings of previous studies, and the potential factors influencing the achievement of such results are discussed. Finally, a general conclusion is drawn, and recommendations derived from the research are presented.

5-2- Analysis of the research results

In this section, a summary of the findings and results is initially presented, followed by an analysis of these results. Based on this, in the previous chapter, the findings were presented in two parts: modelling the energy performance of residential buildings and optimizing the energy performance of residential buildings. This ultimately led to the development of a set of predictive models for energy performance and building geometric specifications to improve energy performance. Accordingly, this section focuses on analysing these findings.

5-2-1- Analysis of the results of energy performance modeling for residential buildings

This section provides a summary and analysis of the results from the parametric simulation process of the building envelope for a residential building. After preparing the model, the initial step involved validating the generative design model of the building envelope by comparing simulation predictions with actual observations. The results of this validation revealed an average discrepancy of 1.3% between the algorithm's predictions and actual energy consumption. Based on this, the modelling results of the study, with an accuracy of 96.9%, can reflect the actual energy performance of residential buildings. Accordingly, a total of 3,584 single-story building morphologies were simulated for energy performance based on the climatic conditions of Melbourne.

According to the simulations, an increase in the building area leads to an increase in total energy consumption while reducing energy consumption per square meter. Additionally, in general, reducing the height of the building decreases energy consumption, while increasing the height improves daylight performance. Based on the findings, by altering the physical characteristics of the building as proposed in the study, it is possible to achieve changes in energy consumption of up to 71 kWh per square meter and approximately 34% in total annual energy consumption per square meter for the residential building. Furthermore, modifications in the building's physical characteristics as suggested in this study could result in changes of up to 2 kWh per square meter (around 9%) in cooling demand and up to 70 kWh per square meter (around 80%) in heating demand per square meter.

Subsequently, a correlation analysis conducted between the physical variables and performance objectives is briefly presented and analysed. Based on the correlation analysis findings, the highest correlations between performance objectives and physical factors are observed in the relationship between the floor area and energy consumption and cooling demand, with coefficients of 0.993 and 0.998, respectively. Similarly, the window area also correlates with energy consumption and cooling demand per square meter with coefficients of 0.993 and 0.998. Therefore, floor area and window area are identified as two critical factors that could be used for regulatory purposes.

Next, to model the energy performance objectives, a curvilinear regression analysis was performed between each energy performance objective of the residential building and its physical factors, and a model for each one-to-one relationship was developed. The findings from the curvilinear regression analysis indicate that in most relationships, the linear equation serves as a suitable model among the fitted models for the one-to-one relationships. Based on this, both linear and nonlinear models of the residential building's energy performance objectives, as dependent variables, and the physical factors of the residential building, as independent and predictive variables, have been evaluated.

Based on the conducted tests, the linear equation derived from the linear regression test, with a confidence level of over 99%, predicts approximately 99.9% of the energy consumption of the residential building per square meter. Additionally, the equation resulting from the nonlinear regression test, with a confidence level of over 95%, predicts 100% of the total energy consumption of the residential building. Accordingly, the nonlinear equation provides a slightly better prediction of total energy consumption by about 0.1%. Thus, the

nonlinear model is considered to better fit the total energy consumption of the residential building.

Based on the results for energy consumption per square meter, the equation from the linear regression test, with a confidence level of over 99%, predicts 95.9% of the energy consumption of the residential building per square meter. Meanwhile, the nonlinear equation derived from the physical factors of the single-story residential buildings, with a confidence level of over 95%, predicts 99.8% of the energy consumption of the residential building per square meter. Consequently, the nonlinear equation offers a better prediction by approximately 3.9%. Therefore, it can be concluded that the nonlinear model for energy consumption per square meter of the residential building is deemed more fitting.

Regarding the findings for total cooling demand, the linear equation based on the physical factors of the residential building, with a confidence level of over 99%, predicts approximately 99.8% of the total cooling demand of the residential building. Similarly, the nonlinear regression test equation, with a confidence level of over 95%, also predicts 99.8% of the cooling demand of the residential building. Hence, the nonlinear and linear equations provide identical predictions for the cooling demand of the residential building, suggesting that both the nonlinear and linear models are considered suitable for the total cooling demand of the residential building.

Further, based on the simulation results for the cooling demand per square meter of the residential building, derived from the physical factors of the residential building, the linear equation, with a confidence level of over 99%, predicts only 59.3% of the cooling demand per square meter. In contrast, based on the nonlinear regression results for cooling demand per square meter, the derived equation, with a confidence level of over 95%, predicts 96.2% of the cooling demand per square meter of the residential building. Accordingly, the resulting nonlinear equation offers a significantly better prediction of cooling demand per square meter, by about 36.9%. Thus, it can be concluded that the nonlinear model for cooling demand per square meter of the residential building is considered more fitting.

Regarding heating demand results, the equation derived from the linear regression test, with a confidence level of over 99%, predicts approximately 98.9% of the heating demand of the residential building. Furthermore, the equation derived from the nonlinear regression test, with a confidence level of over 95%, predicts 99.8% of the total heating demand of the

residential building. Accordingly, the resulting nonlinear equation provides a slightly better prediction of total heating demand by about 0.9%. Therefore, it can be concluded that the nonlinear model for the total heating demand of the residential building is considered more fitting.

In relation to heating demand per square meter, the equation derived from the linear regression test, with a confidence level of over 99%, predicts approximately 96.4% of the heating demand per square meter of the residential building. Meanwhile, the equation derived from the nonlinear regression test, with a confidence level of over 95%, predicts 99.2% of the heating demand per square meter of the residential building. Based on these findings, the resulting nonlinear equation offers a more precise prediction of heating demand per square meter, by about 2.8%. Hence, it can be concluded that the nonlinear model for heating demand per square meter of the residential building is considered more fitting.

Regarding lighting demand results, the equation derived from the linear regression test, with a confidence level of over 99%, predicts approximately 100% of the lighting demand of the residential building. Similarly, the equation derived from the nonlinear regression test, with a confidence level of over 95%, also predicts 100% of the total heating demand of the residential building. Therefore, both the nonlinear and linear equations provide identical predictions for the lighting demand of the residential building, suggesting that both the nonlinear and linear models are considered suitable for the total lighting demand of the residential building. The results of these two groups of energy performance objective models and their specific characteristics are presented in the table 5-1.

Regarding the useful daylight illuminance, the linear regression equation predicts approximately 95.7% of the changes in the average useful daylight illuminance, with a confidence level of over 99%. The nonlinear regression equation predicts 97.4% of the useful daylight illuminance of the residential building per square meter, with a confidence level of over 95%. Thus, the nonlinear equation provides approximately 1.7% more accurate prediction of the useful daylight illuminance per square meter of the residential building. Therefore, it can be concluded that the nonlinear model for the average useful daylight illuminance of the residential building is considered more accurate.

Regarding the average daylight factor, the linear regression equation predicts approximately 96.9% of the changes in the average daylight factor, with a confidence level of over 99%.

The nonlinear regression equation predicts 96.1% of the average daylight factor of the residential building, with a confidence level of over 95%. Thus, the linear equation provides approximately 0.8% more accurate prediction of the average daylight factor. Therefore, it can be concluded that the linear model for the average daylight factor of the residential building is considered more accurate.

Table 5-1: Linear and Nonlinear Equations for Energy Performance Objectives of the Study

Performance Objective	Type of Equation	Equation	Accuracy Percentage
Total energy consumption of the residential building	Linear	$GE = -4580.788 + (141.485 \times EW) + (340.867 \times NS) + (2027.022 \times H) - (5.221 \times D) + (9.063 \times V) - (632.830 \times WWR) + (203.657 \times WW) - (1560.292 \times WH) + (877.495 \times WA)$	**99.9 %**
	Nonlinear	$GE = -3022.149 + (43.835 \times EW^{1.364}) + (252.913 \times NS^{0.926}) + (45.943 \times A) + (359.905 \times 1.647^{H}) + (-5.221 \times D) + (0.377 \times D^{2}) + (30.581 \times V^{0.853}) + (350.145 \times WWR^{-0.819}) + (0.002 \times WW^{4.400}) + (0.216 \times WH^{6.729}) + (459.515 \times WA)$	**100 %**
Energy consumption of the residential building per square meter	Linear	$GEPA = 154.609 - (3.615 \times EW) + (9.329 \times NS) + (46.781 \times H) - (0.023 \times D) + (0.010 \times V) - (90.658 \times WWR) + (6.626 \times WW) - (105.993 \times WH) - (1.741 \times WA)$	**95.9 %**
	Nonlinear	$GEPA = 0.802 + (-30.154 / EW) + (468.803 / NS) + (-288.025 \times A^{0.151}) + (-0.029 \times -6.066^{H}) + (-0.023 \times D) + (0.002 \times D^{2}) + (380.597 \times \log V) + (2.514 / WWR) + (381.321 / WW) + (-91.027 / WH) + (-199.147 \times WA^{0.147})$	**99.8 %**
Total cooling demand of the residential building	Linear	$CE = -44.671 + (1.302 \times EW) - (8.762 \times NS) - (13.429 \times H) - (2.873 \times D) + (0.038 \times V) + (68.857 \times WWR) + (5.869 \times WW) + (85.233 \times WH) + (195.542 \times WA)$	**99.8 %**
	Nonlinear	$CE = 2348.056 + (-106.063 \times EW^{0.438}) + (74.660 \times NS^{.0401}) + (4.304 \times A^{1.017}) + (-0.001 \times 10.541^{H}) + (-2.873 \times D) + (7.091 \times V^{0.594}) + (-2404.608 \times WWR^{0.025}) + (63.288 \times WW^{0.794}) + (-83.279 \times WH^{0.922}) + (126.456 \times WA^{1.017})$	**99.8 %**
Cooling demand of the residential building per square meter	Linear	$CEPA = 20.418 - (0.016 \times EW) + (0.043 \times NS) + (0.136 \times H) - (0.012 \times D) - (0.630 \times WWR) + (0.048 \times WW) - (0.539 \times WH) - (0.018 \times WA)$	**59.3 %**
	Nonlinear	$CEPA = 14284.310 + (-0.274 \times EW) + (-3452.202 \times NS^{-0.002}) + (0.021 \times A^{-2.548}) + (46.325 \times 1.002^{H}) + (-0.012 \times D) + (-1924.031 \times V^{-0.003}) + (-0.098 \times WWR^{1.347}) + (1.085 \times 1.006^{WW}) + (-4126.519 \times WH^{0.003}) + (-4833.290 \times WA^{0.001})$	**96.2 %**
Total heating demand of the residential building	Linear	$HE = -4536.123 + (140.183 \times EW) + (349.627 \times NS) + (2040.449 \times H) - (2.347 \times D) + (9.025 \times V) - (701.670 \times WWR) + (197.785 \times WW) - (1645.514 \times WH) - (280.074 \times WA)$	**98.9 %**
	Nonlinear	$HE = -13098.801 + (604.096 \times 1.071^{EW}) + (553.985 \times 1.063^{NS}) + (-227.868 \times A^{0.621}) + (0.797 \times H^{5.070}) + (-2.347 \times D) + (0.293 \times D^{2}) + (167.483 \times V^{0.657}) + (1.643 \times WWR^{-3.254}) + (8936.631 \times WW^{0.083}) + (2641.833 \times 1.258^{WH}) + (-611.251 \times WA^{0.617})$	**99.8 %**
Heating demand of the residential building per square meter	Linear	$HEPA = 37.988 - (3.599 \times EW) + (9.286 \times NS) + (46.645 \times H) - (0.011 \times D) + (0.010 \times V) - (90.028 \times WWR) + (6.578 \times WW) - (105.454 \times WH) - (1.723 \times WA)$	**96.4 %**
	Nonlinear	$HDPA = -19.213 + (92.691 / FN) + (-39.599 \times EW^{0.098}) + (e\_n^{5.154 + (0.730 / NS)}) + (0.002 \times D) + (0.001 \times D^{2}) + (3.498 \times UH^{1.362}) + (-81.091 \times A^{0.078}) + (1.002 \times BV^{0.264}) + (e\_n^{5.193 + (0.044 / WLR)}) + (-71.646 \times SWW^{0.085}) + (3.288 \times SWH^{1.315}) + (-84.400 \times NWW^{0.069}) + (2.278 \times NWH^{1.386})$	**99.3 %**
Total lighting demand of the residential building	Linear	$LE = -(3.459\text{E}-5 \times EW) + (5.873\text{E}-5 \times NS) + (6.551E-5 \times H) + (7.767E-7 \times V) - (0.001 \times WWR) + (42.431 \times WA)$	**100 %**
	Nonlinear	$LE = -2.621\text{E}-5 + ((-1.530\text{E}-13) \times EW) + ((-5.783\text{E}-12) \times NS) + (4.243 \times A) + ((9.827\text{E}-6) \times V^{-3.550\text{E}-7}) + ((3.828\text{E}-5) \times WWR^{2.363\text{E}-6}) + (-2.517\text{E}-5 \times WW^{-1.365\text{E}-6}) + ((2.476\text{E}-11) \times WH) + ((3.276\text{E}-6) \times WA^{2.855\text{E}-6})$	**100 %**
Average useful daylight illuminance	Linear	$UDIA = 97.605 - (2.935 \times EW) - (8.425 \times NS) - (15.559 \times H) + (0.015 \times D) + (0.017 \times V) - (25.144 \times WWR) + (3.965 \times WW) + (68.794 \times WH) + (0.066 \times WA)$	**95.7 %**
	Nonlinear	$UDIA = 139.180 + (-16.632 \times EW^{0.738}) + (-3.616 \times NS) + (-1065.194 / A) + (-42.501 / H) + (0.015 \times D) + (4453.090 / V) + (-101.211 \times WWR) + (17.195 \times WW) + (-0.551 \times WW^{2}) + (0.008 \times WW^{3}) + (77.554 \times \log WH) + (0.708 / WA)$	**97.4 %**
Average daylight factor	Linear	$DAA = 44.677 - (0.320 \times EW) + (0.509 \times NS) + (23.915 \times H) + (0.033 \times D) - (0.002 \times V) + (3.701 \times WWR) - (0.902 \times WW) - (40.217 \times WH) + (0.822 \times WA)$	**96.9 %**
	Nonlinear	$DAA = -15592.661 + (6778.397 \times EW^{0.005}) + (524.188 \times \log NS) + (685059.409 / A) + (718.180 \times H^{0.161}) + (5216.455 \times 1^{D}) + (-8598.934 / V) + (2318.205 \times WWR^{-0.021}) + (-1.839 \times WW) + (-819.127 \times \log WH) + (-67992.515 / WA)$	**96.1 %**

As mentioned, all nonlinear equations provide more accurate predictions of the energy performance objectives and have been deemed more suitable. Accordingly, the final energy performance equations based on the nonlinear model are presented below. Therefore, the final equation for predicting the total energy consumption of the residential building (GE) is as follows:

$$\begin{aligned} GE = {} & -3022.149 + (43.835 \times EW^{1.364}) + (252.913 \times NS^{0.926}) + (45.943 \times A) \\ & + (359.905 \times 1.647^{H}) + (-5.221 \times D) + (0.377 \times D^{2}) + (30.581 \times V^{0.853}) \\ & + (350.145 \times WWR^{-0.819}) + (0.002 \times WW^{4.400}) + (0.216 \times WH^{6.729}) \\ & + (459.515 \times WA) \end{aligned}$$

Additionally, the final equation for predicting the energy consumption of the residential building per square meter (GEPA) is provided as follows:

$$\begin{aligned} GEPA = {} & 0.802 + (-30.154 \,/\, EW) + (468.803 \,/\, NS) + (-288.025 \times A^{0.151}) \\ & + (-0.029 \times -6.066^{H}) + (-0.023 \times D) + (0.002 \times D^{2}) + (380.597 \times \log V) \\ & + (2.514 \,/\, WWR) + (381.321 \,/\, WW) + (-91.027 \,/\, WH) \\ & + (-199.147 \times WA^{0.147}) \end{aligned}$$

The final equation for predicting the cooling demand of the residential building (CE) is provided as follows:

$$\begin{aligned} CE = {} & 2348.056 + (-106.063 \times EW^{0.438}) + (74.660 \times NS^{\cdot 0401}) + (4.304 \times A^{1.017}) \\ & + (-0.001 \times 10.541^{H}) + (-2.873 \times D) + (7.091 \times V^{0.594}) \\ & + (-2404.608 \times WWR^{0.025}) + (63.288 \times WW^{0.794}) \\ & + (-83.279 \times WH^{0.922}) + (126.456 \times WA^{1.017}) \end{aligned}$$

Additionally, the final equation for predicting the cooling demand of the residential building per square meter (CEPA) is provided as follows:

$$\begin{aligned} CEPA = {} & 14284.310 + (-0.274 \times EW) + (-3452.202 \times NS^{-0.002}) + (0.021 \times A^{-2.548}) \\ & + (46.325 \times 1.002^{H}) + (-0.012 \times D) + (-1924.031 \times V^{-0.003}) \\ & + (-0.098 \times WWR^{1.347}) + (1.085 \times 1.006^{WW}) \\ & + (-4126.519 \times WH^{0.003}) + (-4833.290 \times WA^{0.001}) \end{aligned}$$

The final equation for predicting the heating demand of the residential building (HE) is provided as follows:

$$\begin{aligned} HE = {} & -13098.801 + (604.096 \times 1.071^{EW}) + (553.985 \times 1.063^{NS}) \\ & + (-227.868 \times A^{0.621}) + (0.797 \times H^{5.070}) + (-2.347 \times D) \\ & + (0.293 \times D^{2}) + (167.483 \times V^{0.657}) + (1.643 \times WWR^{-3.254}) \\ & + (8936.631 \times WW^{0.083}) + (2641.833 \times 1.258^{WH}) \\ & + (-611.251 \times WA^{0.617}) \end{aligned}$$

Additionally, the final equation for predicting the heating demand of the residential building per square meter (HEPA) is provided as follows:

$$HDPA = -19.213 + (92.691 / FN) + (-39.599 \times EW^{0.098}) + \left(e\_n^{5.154 + (0.730 / NS)}\right) + (0.002 \times D) + (0.001 \times D^2) + (3.498 \times UH^{1.362}) + (-81.091 \times A^{0.078}) + (1.002 \times BV^{0.264}) + \left(e\_n^{5.193 + (0.044 / WLR)}\right) + (-71.646 \times SWW^{0.085}) + (3.288 \times SWH^{1.315}) + (-84.400 \times NWW^{0.069}) + (2.278 \times NWH^{1.386})$$

e_n = 2.7182818284590452353602874713 52

Additionally, the final equation for predicting the lighting demand of the residential building (LE) is provided as follows:

$$LE = -2.621\text{E}-5 + \left((-1.530\text{E}-13) \times EW\right) + \left((-5.783\text{E}-12) \times NS\right) + (4.243 \times A) + \left((9.827\text{E}-6) \times V^{-3.550\text{E}-7}\right) + \left((3.828\text{E}-5) \times WWR^{2.363\text{E}-6}\right) + \left(-2.517\text{E}-5 \times WW^{-1.365\text{E}-6}\right) + \left((2.476\text{E}-11) \times WH\right) + \left((3.276\text{E}-6) \times WA^{2.855\text{E}-6}\right)$$

Additionally, the final equation for predicting the average useful daylight illuminance of the residential building (UDIA) is provided as follows:

$$UDIA = 139.180 + (-16.632 \times EW^{0.738}) + (-3.616 \times NS) + (-1065.194 / A) + (-42.501 / H) + (0.015 \times D) + (4453.090 / V) + (-101.211 \times WWR) + (17.195 \times WW) + (-0.551 \times WW^2) + (0.008 \times WW^3) + (77.554 \times \log WH) + (0.708 / WA)$$

Additionally, the final equation for predicting the average daylight factor of the residential building (DAA) is provided as follows:

$$DAA = 44.677 - (0.320 \times EW) + (0.509 \times NS) + (23.915 \times H) + (0.033 \times D) - (0.002 \times V) + (3.701 \times WWR) - (0.902 \times WW) - (40.217 \times WH) + (0.822 \times WA)$$

In these equations, the physical factors include the dimensions of the east-west side (EW), the dimensions of the north-south side (NS), the height of the space (H), the orientation of the building (D), the floor area of the building (A), the volume of the building (V), the window-to-wall ratio of the building (WW), the width of the north-facing window of the building (WW), the height of the north-facing window of the building (WH), and the height of the north-facing window of the building (WA).

5-2-2- Analysis of the Results of Energy Performance Optimization for Residential building

The following section focuses on the analysis of the results from optimizing the energy performance of the building envelope for residential buildings. In this regard, an

optimization process was conducted on the energy performance of the building envelope of single-story residential buildingss. In the optimization process, the steps were defined with smaller intervals to achieve more precise outcomes. According to the findings, three performance objectives—cooling demand per square meter, heating demand per square meter, and Useful Daylight Illuminance (UDI)—exhibited conflicting behaviors with each other (Figure 5-1).

The results indicated that the building's floor area is the most critical factor influencing the building's energy performance. This factor significantly affects the impact of other factors in the optimization process. Moreover, the influence of this factor is largely predictable due to its high correlation with energy performance objectives. Generally, as the floor area increases, the total energy consumption also increases, while energy consumption per square meter decreases. The impact of this factor on energy consumption is illustrated in the chart.

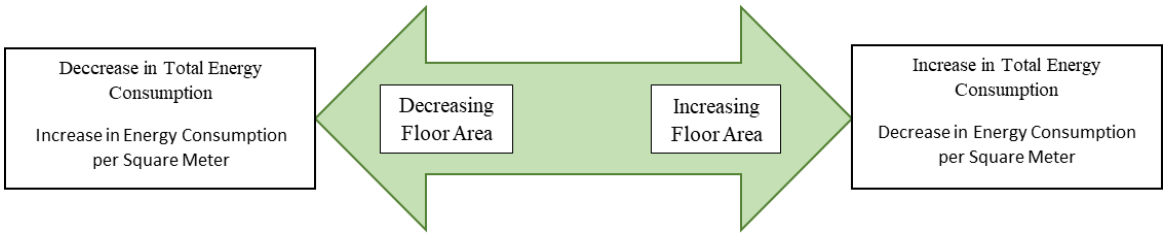

Figure 5-1. Analysis of the Impact of Floor Area on Energy Performance Based on Results

The results showed that the height of the building space also significantly impacts the building's energy performance. Generally, an increase in the floor area leads to higher total energy consumption as well as increased energy consumption per square meter. The effect of this factor on energy consumption is illustrated in the chart (Figure 5-2).

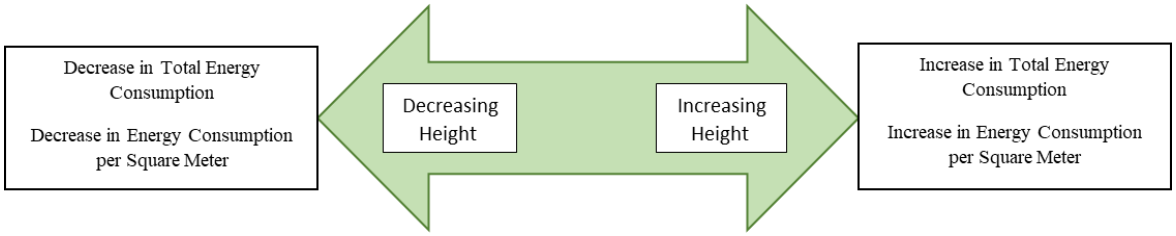

Figure 5-2. Analysis of the Impact of Space Height on Energy Performance Based on Results

Overall, the findings indicate that a north-south elongation of the floor area improves cooling demand per square meter. Conversely, an east-west elongation of the floor area enhances heating demand per square meter. Additionally, a length-to-width ratio close to one,

combined with limited east-west elongation, leads to an improvement in the Useful Daylight Illuminance (UDI) index (Figure 5-3).

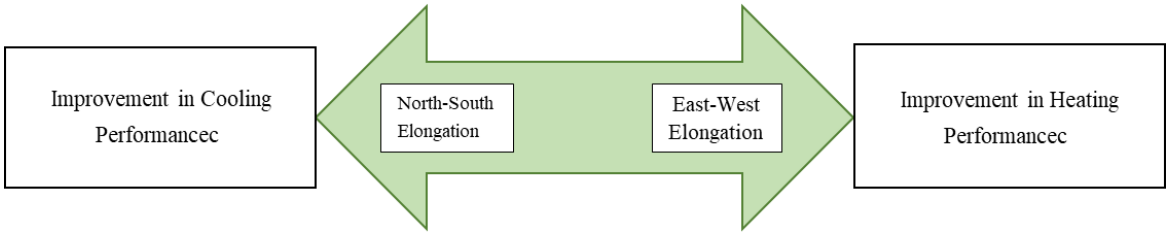

Figure 5-3. Analysis of the Impact of Elongation on Energy Performance Based on Results

Overall, the findings indicate that the orientation angle has a significant impact on energy performance. The results suggest that aligning the building's orientation closer to zero degrees (i.e., true north) generally leads to reduced energy consumption. Additionally, a positive orientation angle tends to improve daylight performance. This implies that carefully considering and optimizing the building's orientation can enhance both energy efficiency and daylight access (Figure 5-4).

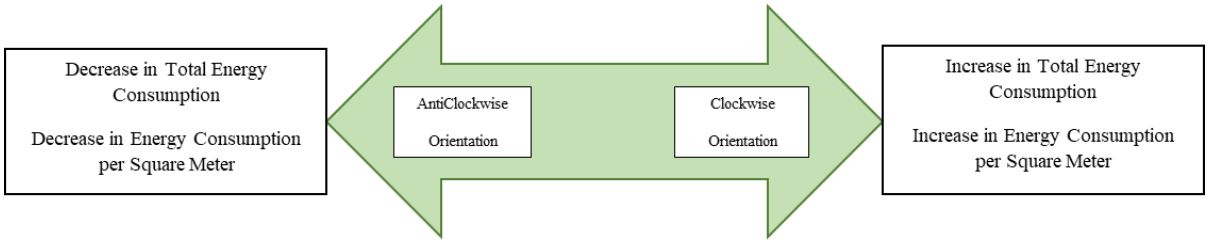

Figure 5-4. Analysis of the Impact of orientation on Energy Performance Based on Results

Therefore, in general, increasing the floor area while maintaining an orientation angle close to zero degrees, along with reducing the building height and achieving a length-to-width ratio close to one, with limited east-west elongation, can lead to optimized energy performance. This approach combines favorable factors to enhance overall energy efficiency and effectiveness.

The following is an examination of 2D diagrams between area, height, elongation, and orientation. These diagrams can provide good guidance for the design process. Based on the studies conducted, it is possible to define patterns of residential unit energy performance based on spatial configuration factors of single-story residential buildings. First, a diagram is presented based on the impact of two factors, building height and area, on residential unit energy consumption. This diagram defines four zones for the building, which are defined by the colors green (desirable) and red (undesirable).

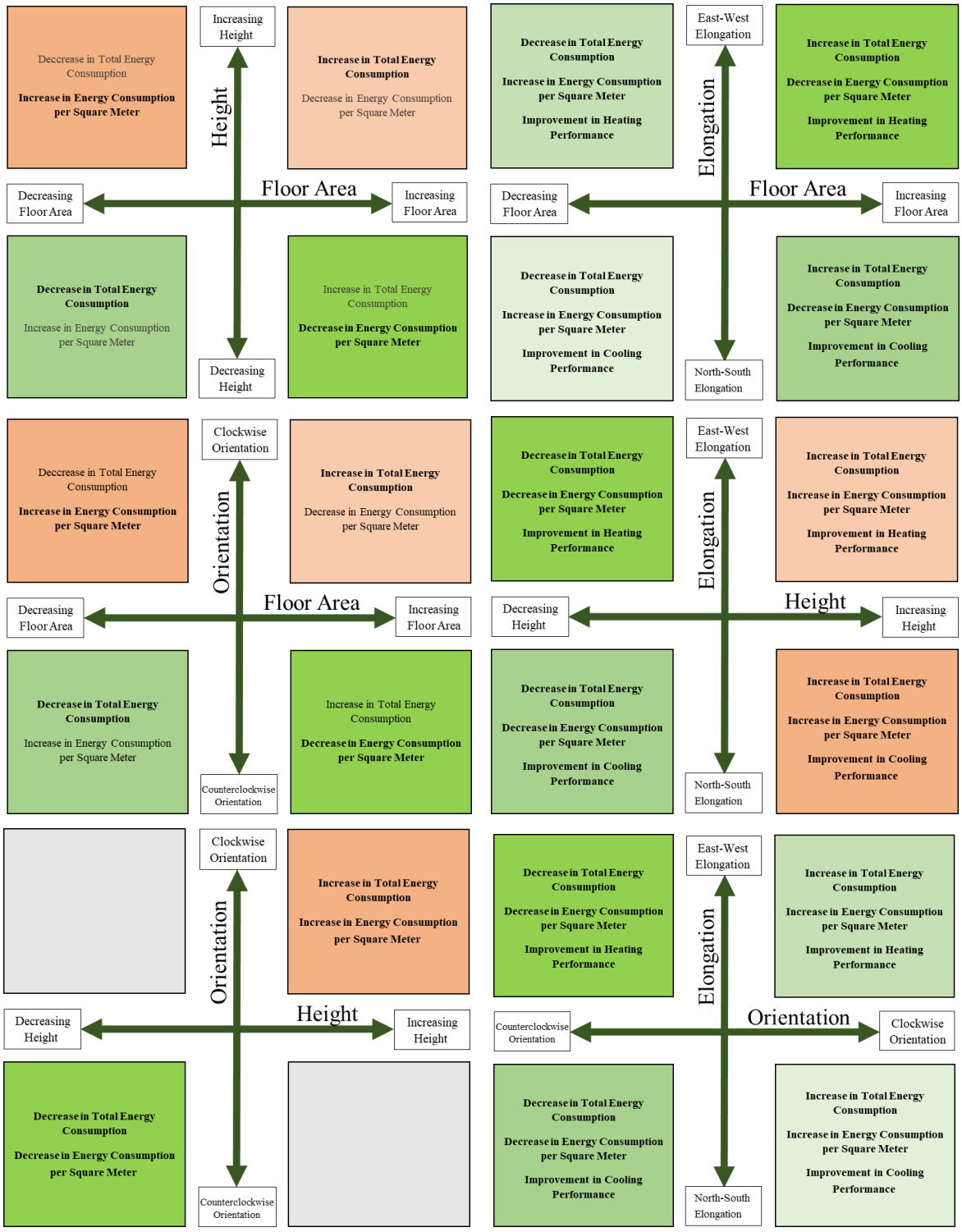

Figure 5-5. Analysis of the Impact of physical elements on Energy Performance Based on Results

Another diagram also considers the interaction between the building's area and elongation. This diagram provides a framework for the designer to explain his approach to environmental conditions. Next, the two-dimensional bivariate studies of orientation and area, elongation and height, orientation and height, and orientation and elongation are

outlined. Below, a diagram is presented based on the effect of two factors: the height of the interior spaces and the angle of orientation relative to the north-south axis of the building on the energy performance of the residential unit (Figure 5-6).

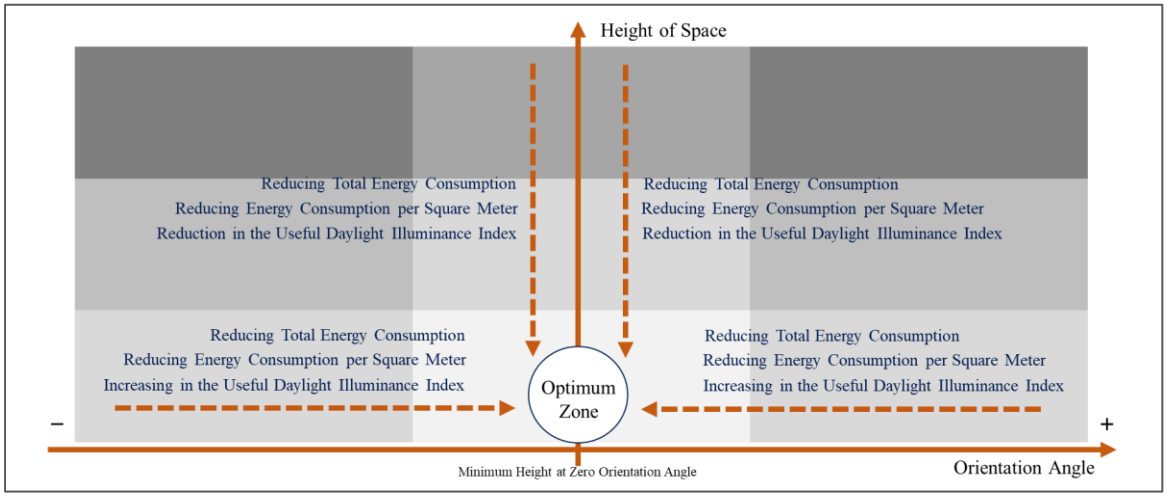

Figure 5-6. Analysis of the Impact of Height of Space and Orientation of Building on Energy and Daylighting Performance Based on Results

Therefore, the model, for any given area of the southern apartments, the inclination to a zero-degree angle relative to the north axis and the reduction of the height of the interior spaces leads to the optimization of energy performance based on total energy consumption, energy consumption per square meter, and the useful daylight index, and while improving daylight performance, reduces energy consumption.

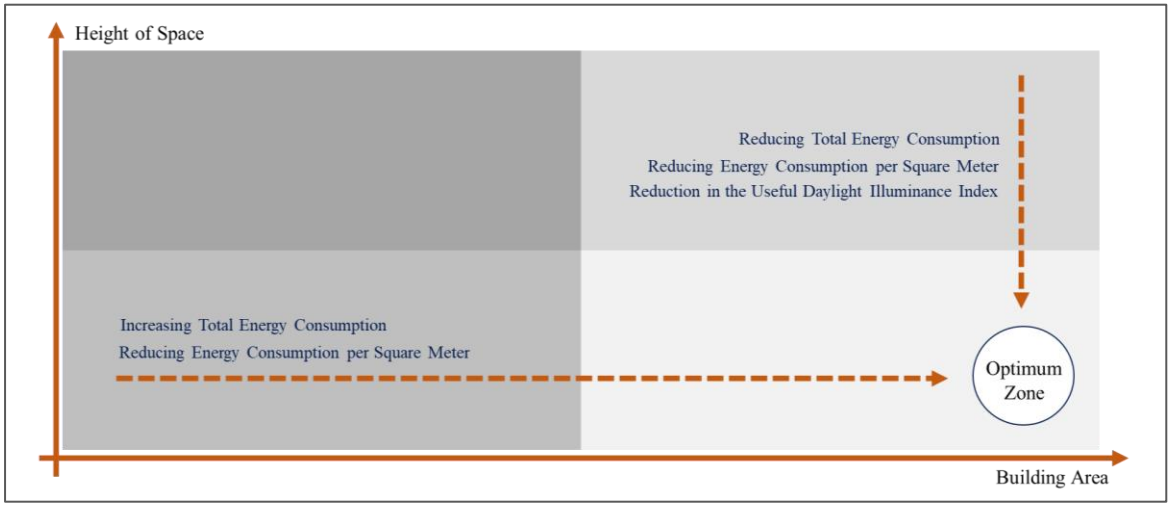

Figure 5-7. Analysis of the Impact of Height of Space and Area of Building on Energy and Daylighting Performance Based on Results

Also, a diagram is presented based on the effect of two factors: the height of the interior spaces and the area of the building's infrastructure on the energy consumption of the residential unit (Figure 5-7).

5-2-2- Analysis of the optimal WWR at each building orientation angle

In this section, a comparative analysis of the window-to-wall ratio (WWR) for buildings with varying floor areas, aspect ratios, and orientations is presented, with a focus on recommendations for the north-facing façade in Melbourne for orientation angles ranging from -15° to 15° (Figure 5-8).

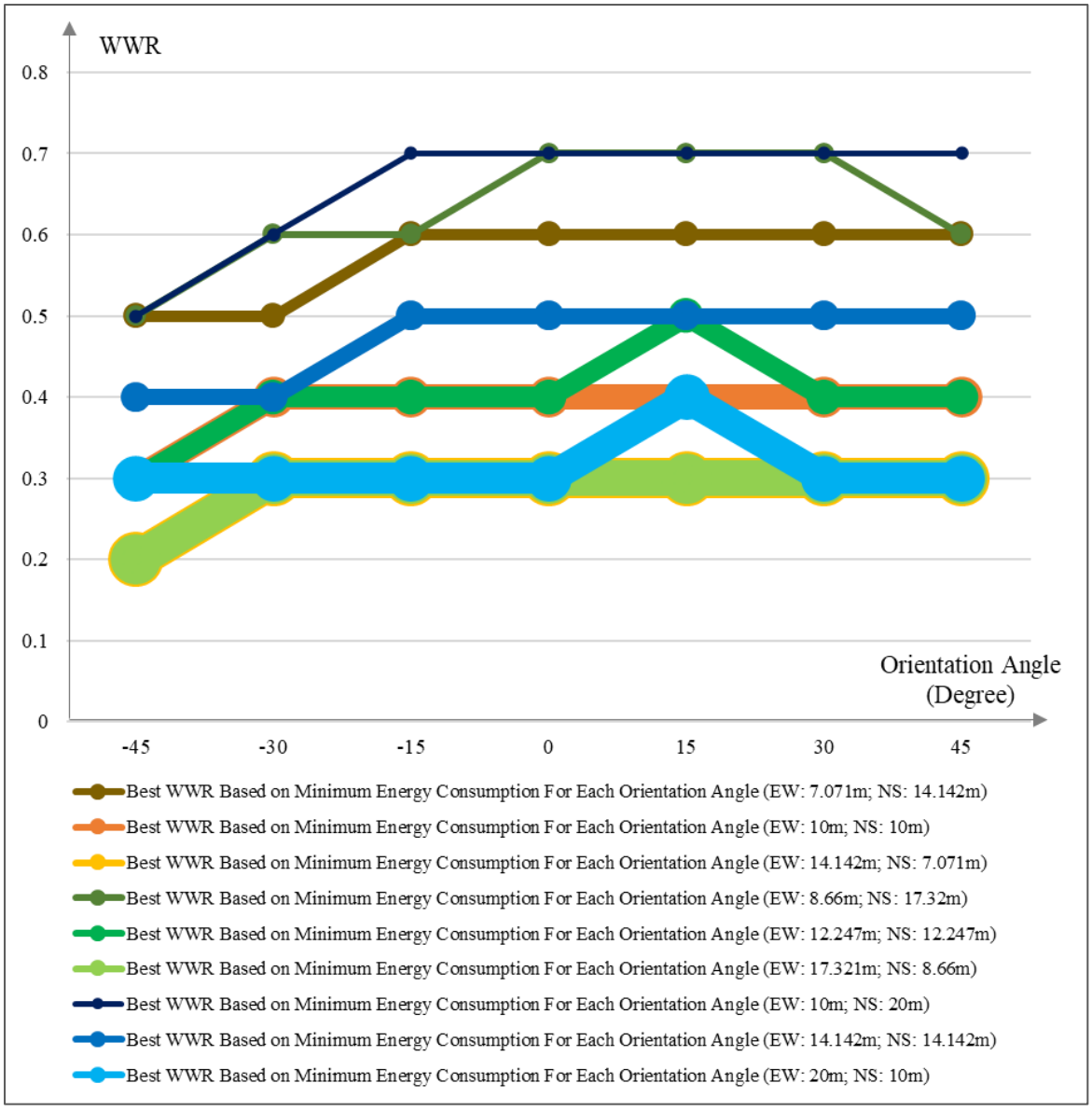

Figure 5-8. Comparative analysis Model of the optimal window-to-wall ratio

For a building with a floor area of 100 m², the analysis covers three aspect ratios. With an aspect ratio of 0.5 (east–west dimensions of 7.07 m, north–south dimensions of 14.142 m), a WWR of 0.6 is recommended. For a square building with an aspect ratio of 1 (10 m by 10 m), the recommended WWR is 0.4. For an aspect ratio of 2 (east–west dimensions of 14.142 m, north–south dimensions of 7.07 m), a WWR of 0.3 is suggested. For a building with a floor area of 150 m², three configurations were also analyzed. With an aspect ratio of 0.5 (8.66 m by 17.32 m), a WWR of 0.6 to 0.7 is recommended. For an aspect ratio of 1 (12.247 m by 12.247 m), the recommended WWR is also 0.6 to 0.7. For an aspect ratio of 2 (17.321 m by 8.66 m), the recommendation drops to a WWR of 0.3. For a building with a floor area of 200 m², the analysis continues. With an aspect ratio of 0.5 (10 m by 20 m), a WWR of 0.7 is recommended. For an aspect ratio of 1 (14.142 m by 14.142 m), a WWR of 0.5 is suggested. For an aspect ratio of 2 (20 m by 10 m), a WWR of 0.3 to 0.4 is recommended.

Overall, the results indicate a consistent trend: as the ratio of the east–west dimension to the north–south dimension (the aspect ratio) increases, the optimal window-to-wall ratio for reducing energy consumption decreases. This trend is observed across all floor areas analyzed, including 100 m², 150 m², and 200 m². Based on the presented findings, it is confirmed that the window-to-wall ratio of the north-facing façade in Melbourne has a significant impact on energy consumption. In general, the optimal window-to-wall ratio for the north-facing façade in Melbourne ranges from 0.3 to 0.7. Overall, the optimal window-to-wall ratio for the north-facing façade of buildings in Melbourne is defined across various building floor areas, aspect ratios, and energy consumption levels associated with each window-to-wall ratio. Based on the results of this section, guidelines can be developed to inform the national building regulations of Australia.

5-3- Discussion on Research Results

This section discusses the research findings and compares them with those from other studies. In this study, over 6000 simulations were conducted, which is considered substantial compared to similar research. For instance, Yi (2016), a notable study in this field, evaluated 936 models. Furthermore, Dino and Ucoluk (2017) assessed 7200 models, the highest number in existing studies. In this research, to enhance the accuracy of the results, more than 3000 models were simulated in the modelling phase alone, leading to a model accuracy of over 95%. Regarding the modelling process and the information derived from it, this study has been able to predict energy performance with an accuracy exceeding 95% based on a

precise equation. In corresponding studies, sufficient information about the models has not been provided; instead, they have focused on reporting total savings and performance improvements. Thus, comparison of the results of this study with existing research is not feasible in this section. Therefore, this section presents a report on model accuracy combined with validation results. The validation results indicate that this study achieved an average accuracy of approximately 96.9% relative to actual energy consumption results, and considering the model accuracy of over 95%, it can be stated that the models in this study can predict the actual energy consumption of typical single-story residential buildings in Melbourne, Australia, with an accuracy of over 93%, which is significant.

In terms of energy performance evaluation, it is worth noting that some studies have focused on using pre-configured designs in the optimization process (Ahmadi et al., 2023; Rodrigues et al., 2014), while others have optimized configuration generation parameters (Dino, 2017; Yi, 2016). In this study, both approaches were utilized within the framework of two generative algorithms. Additionally, in terms of objectives investigated, some studies have addressed only cooling and heating demands (Boonstra et al., 2018; Souza & Alsaadani, 2012), while others have also considered daylighting demands in addition to cooling and heating (Dino, 2017; Musau & Steemers, 2008). Furthermore, thermal comfort has been considered as a conflicting variable alongside these parameters in some studies (Yi, 2016). In this study, various sections were examined, including diverse energy performance objectives.

Based on the obtained results, modifying the spatial characteristics of buildings discussed in this study could lead to approximately 71 kWh per square meter and about a 34% change in annual total energy consumption, which is noteworthy compared to other studies. Musau and Steemers (2008) presented the highest improvement in energy performance, with an average of around 50%. Similarly, Poirazis et al. (2008) showed an average improvement of about 40%. Yi (2016) demonstrated a 10% improvement in energy performance. In the following sections, the energy performance of this study is compared with other studies, detailed by various aspects.

Moreover, changes in the spatial characteristics of the buildings in this study indicate a reduction of about 2 kWh per square meter and approximately a 9% improvement in cooling demands per square meter. Compared to the results of other studies, Poirazis et al. (2008) achieved about 57%, Dino (2017) achieved around 25%, and Souza and Alsaadani (2012)

achieved about 24% improvement in cooling demands. Additionally, Yi (2016) showed around 7.7% and Boonstra et al. (2018) about 10% improvement in energy performance. Changes in geometric factors of the buildings in this study could improve heating demands per square meter by up to about 70 kWh per square meter and approximately 86%. Among the studies, Musau and Steemers (2008) achieved the highest improvement, around 57%, Souza and Alsaadani (2012) achieved 52%, and Poirazis et al. (2008) achieved about 14% improvement in heating demands.

It is essential to examine the spatial layout factors influencing energy performance identified in this study in comparison with other research. The present study comprehensively investigates a range of configuration factors, including the dimensions of the building's footprint, footprint area, aspect ratio of the footprint, building orientation angle relative to the north-south axis, and the height of interior spaces. Among these, the footprint area has been identified as the most significant factor affecting energy performance. The study by Mukkavaara and Sandberg (2020) also demonstrated the impact of footprint area on cooling, heating, and lighting demands. Additionally, the aspect ratio has been recognized as one of the most critical configuration factors affecting energy performance in this research. In this regard, studies by Zhang and Wang (2021), Fattahi Tabasi et al. (2023), and Yi (2016) have similarly explained the impact of aspect ratio on energy consumption. However, the present study has conducted a systematic investigation of the effect of the aspect ratio on energy performance, including energy consumption, cooling demand, heating demand, and daylighting performance. The consideration of the aspect ratio based on north-south and east-west orientations is one of the innovative aspects of this research. This topic has generally been overlooked in other studies.

Moreover, the present study has examined the significant impact of interior space heights on the energy performance of residential buildings. Dino (2016) also addressed and confirmed this issue; however, a systematic analysis had not been conducted previously. Additionally, this study has shown that the impact of building orientation on energy performance is minimal compared to other factors of the external envelope configuration. This finding is in clear contradiction with the results of studies by Rodrigues et al. (2014) and Yi (2016). The reasons for this contradiction may lie in the differing climatic conditions of the regions studied. Nonetheless, the present research has performed a precise and

systematic analysis of the clockwise and counterclockwise variation in orientation angle, which has not been observed in the reviewed studies.

In summary, the discussions in this research are presented systematically, which is one of the innovative contributions of this study. Furthermore, the issues addressed in this research have not been previously explored in Australia, particularly in Melbourne. Therefore, this aspect can also be considered a novel contribution of the present study.

5-4- Examination of Research Hypotheses

This study investigates and optimizes the spatial layout of housing based on building energy performance using the Performative Computational Architecture (PCA) framework. Accordingly, in the first chapter, the research hypotheses were presented in two main and sub-sections aligned with the research objectives. In this section, after reviewing the results, it is necessary to examine the research hypotheses as follows:

Examination of the Main Hypothesis: The main hypothesis posited that the Predictive Model could significantly predict and optimize energy performance based on the geometric parameters of a typical single-story residential building in Melbourne. This study, based on two separate processes of modelling and optimizing energy performance and through over 6000 simulations, achieved approximately a 34% improvement in energy consumption based on changes in housing spatial layout. Therefore, the main hypothesis is confirmed.

Examination of the First Sub-Hypothesis: The first sub-hypothesis predicted that the study would identify the geometric parameters of residential buildings affecting energy performance and prioritize them based on energy performance. According to the regression and correlation results obtained from the modelling process, the geometric parameters of housing have been effectively prioritized. In this context, the floor area is identified as the most significant geometric factor affecting energy performance. Following this, building height and orientation angle are also important. Thus, the first sub-hypothesis is confirmed.

Examination of the Second Sub-Hypothesis: The second sub-hypothesis anticipated that the optimal specifications of geometric parameters for residential buildings based on building energy performance would be determined using the Performative Computational Architecture model. Based on the optimization process conducted within the framework of the Performative Computational Architecture model, the study has identified the optimal

geometric specifications for energy-efficient housing. Generally, increasing floor area, with an orientation angle close to zero degrees, along with reducing building height and a length-to-width ratio close to one with limited east-west elongation, can result in optimal energy performance. Consequently, this hypothesis is also confirmed.

Examination of the Third Sub-Hypothesis: The third sub-hypothesis projected that architectural solutions for the geometric parameters of typical single-story residential buildings in Melbourne would be determined to improve building energy performance based on the Performative Computational Architecture model. As previously mentioned, increasing floor area, favoring an orientation angle close to zero degrees, reducing building height, and aiming for a length-to-width ratio close to one with limited east-west elongation can enhance energy performance. Thus, this hypothesis is confirmed as well.

5-5-Innovations of the Research

Based on the research results, several innovations can be presented in various sections:

1. **Predictive Models for Energy Performance:** One of the key innovations of this research is the development of predictive models for energy performance using nonlinear regression methods. These models have demonstrated an accuracy of over 95% compared to simulated models and an average accuracy of 93% relative to actual energy consumption. To date, there has been no model in previous studies that offers such high precision through a defined mathematical equation. Therefore, the presentation of these predictive models is a notable innovation of this research.
2. **Generative Design Algorithm for Spatial Layouts:** Another significant innovation is the definition of a generative design algorithm for spatial layouts within the Grasshopper environment. This algorithm facilitates a comprehensive assessment by effectively exploring the design space and leading to the definition of practical configurations. This approach represents a novel contribution to the field by integrating advanced generative design techniques in a detailed analytical framework.

5-6-Strategic Approaches and Solutions

Based on the results obtained from performative computational architectural processes, strategies and solutions for optimizing energy performance in residential spatial layouts have been defined and elaborated. It is important to note that the proposed solutions are based on

the climatic data of Melbourne, and some adjustments may be necessary for different regions (Figure 5-9).

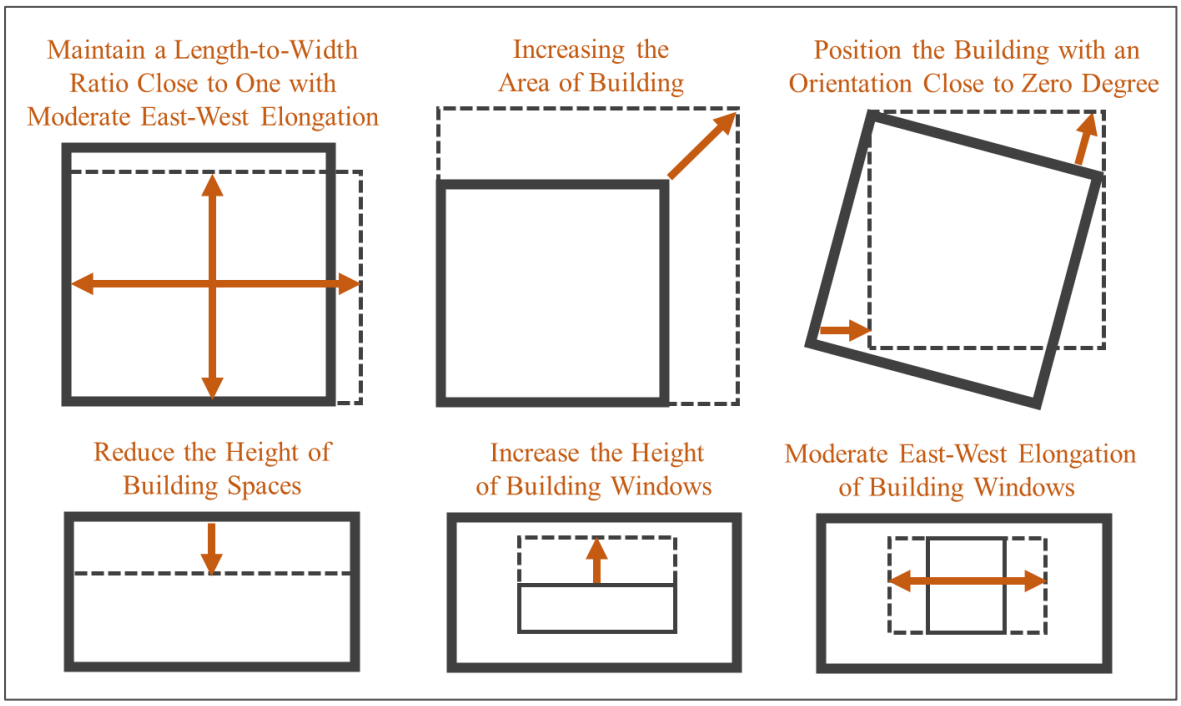

Figure 5-9. Classification of Strategic Approaches and Design Solutions

Nonetheless, some solutions are applicable across various climates. In general, increasing horizontal density leads to a reduction in energy consumption per square meter (Table 5-2).

Table 5-2: Classification of Strategic Approaches and Design Solutions

Design Strategies	Design Solutions
Increase Horizontal Density	- Increase the building's floor area
	- Maintain a length-to-width ratio close to one with moderate east-west elongation
Increase Vertical Density	- Reduce the height of building spaces
	- Increase the height of building windows
Optimize Solar Radiation Reception	- Position the building with an orientation close to zero degrees
	- Maintain a length-to-width ratio close to one
	- Moderate east-west elongation

While increasing the building's floor area results in a higher total energy consumption, it decreases energy consumption per square meter. Therefore, the use of compact building designs for small plots and the design of larger residential complexes are effective tools for reducing energy consumption.

Additional Design Insights:

- **Length-to-Width Ratio Optimization:** A length-to-width ratio of one for residential floor plans optimizes building energy performance. Specifically, increasing the east-west elongation of a single-story residential buildings's floor area, while keeping the total floor area constant, results in reduced heating demands and improved daylight performance. Conversely, increasing the north-south elongation while maintaining the floor area leads to reduced cooling demands and enhanced daylight performance. Thus, a length-to-width ratio of one with limited east-west elongation can provide a desirable balance in energy performance.
- **Vertical Density Increase:** Increasing the vertical density of a building is another strategy for optimizing energy performance. Reducing the height of internal spaces in a single-story residential building generally leads to lower energy consumption for residential buildings.
- **Building Orientation:** Changing the orientation of a building can significantly affect its solar radiation reception. Generally, positioning the building with an orientation close to zero degrees relative to the north-south axis results in reduced energy consumption.

These strategies highlight how specific design adjustments can improve energy efficiency and performance in residential buildings.

5-7-Final Conclusion

Conventional apartment housing is typically designed and constructed solely based on the experience of the designers. According to research findings, it is concluded that the geometric characteristics of housing significantly affect building energy consumption, and consequently, global energy consumption. Therefore, there is a pressing need for urban planning in the design and construction of single-story residential buildings, as well as the establishment of laws and regulations in this domain to reduce energy consumption at the national level. Based on the findings of this study, it is concluded that planning and legislation in the housing sector can lead to long-term energy savings of over 30% in

residential buildings in Melbourne. Considering that one-third of the world's energy consumption is related to the building sector, this translates to a substantial amount.

In this regard, given that based on the findings, floor area and the length-to-width ratio of the residential building's-built area are among the most significant physical factors influencing building energy consumption, it is concluded that incorporating these two factors in urban planning, municipal regulations, and construction permits can lead to a reduction in energy consumption at the national level in Melbourne. According to the findings, it is concluded that defining land plots in Melbourne in such a way that their built area has a 1:1 length-to-width ratio and an orientation of zero degrees relative to the north could be a highly effective step in optimizing building energy consumption in this region. Additionally, based on the findings, it is concluded that increasing horizontal density by using consolidated construction plans for smaller land plots and designing large residential complexes is an effective tool in reducing energy consumption in Melbourne.

Furthermore, increasing vertical density is important in reducing overall energy consumption per square meter. Incorporating both horizontal and vertical density increases into urban planning, while ensuring that the quality of residential life and the quality of solar radiation received by buildings are not compromised, could lead to reduced energy consumption in the residential building sector in Melbourne. Additionally, according to the findings, it is concluded that internal space height is another factor affecting energy consumption; reducing it results in lower energy consumption. Therefore, reducing the height of residential buildings to the extent that the quality of life in these spaces is not compromised could greatly contribute to optimizing energy consumption in Melbourne.

The findings also revealed that the energy performance models developed in the research can predict the actual energy consumption of residential buildings in Melbourne before construction with an average accuracy of 93% in less than a few seconds, without the need for specialized tools or expertise. This predictive accuracy is also influenced by the residents' lifestyle. Therefore, the use of these models is highly significant in urban and regional construction planning. Given the high correlation between the model's results and the actual energy consumption of buildings, the use of these models enables the prediction of energy consumption at the city level, which could be of great importance in the Ministry of Energy's planning. Moreover, it is concluded that the integration of artificial intelligence tools with these prediction models can provide essential assistance to policymakers, planners, and

designers at the macro level, enabling them to make decisions that optimize building energy consumption in a short period of time. Additionally, based on the accuracy of these prediction models, they can be utilized in high-speed optimization processes over a short timeframe. Regression-based prediction models, if achieving high accuracy, can be used by professionals in various building-related fields without requiring specialized knowledge of building energy performance.

5-8-Research Limitations

This study faced several limitations. The main limitation was related to hardware constraints in the building energy simulation calculations. Despite using a powerful system, it was not feasible to increase the number of cells or reduce the size of a cell due to the extended computation time and, in some cases, the system crashing during the process. Additionally, hardware and software limitations during the optimization process led to increased processing times, and it was not possible to increase the number of generations when necessary. Moreover, software limitations occasionally slowed access to several tools and features during the process (Table 5-3).

Table 5-3. Research Limitations

Number of floors	1 floor
East-west side dimensions	8 to 22 meters (east-west side dimensions)
North-south side dimensions	8 to 22 meters (north-south side dimensions)
Height of the residential building	2.6 to 4 meters (residential building height)
Orientation relative to the north-south axis	-45 to 45 degrees (orientation relative to the north-south axis)
Construction system	Timber frame structure
Window location	Windows only on the northern facade
Window-to-floor area ratio	10% window-to-floor area ratio
Roof type	Flat roof (no slope)
Glass type	Single-glazed

Another limitation of this study was the time constraint, particularly given the complexity of the topics related to spatial layout. Although this research focused on one optimization process, the results suggest that in some cases, further optimization tests or increasing the number of optimization generations were needed, which fell outside the scope and timeframe of this study. The research included some limitation to predict energy consumption in cooling, heating and lighting.

5-9-Research Novelty

This study provides a platform for examining the impact of residential building geometric characteristics on energy performance to support urban macro-planning in Melbourne. The

findings can significantly aid in decision-making regarding the range of geometric characteristics during the process, from defining the building's floor area to completing the design. The results highlight the relative importance of each geometric characteristic in influencing energy performance, enabling designers to optimize building proportions and orientation to reduce energy consumption.

Furthermore, based on these findings, it is possible to establish standards for the geometric characteristics of residential buildings in Melbourne's national building regulations. Additionally, buildings can be labelled before construction, and incentives can be allocated based on their labels.

To achieve this, the study employs parametric simulation, nonlinear regression modeling, and evolutionary algorithms. This combination not only predicts building energy consumption based on geometric characteristics but also identifies the optimal geometric parameters for residential buildings in terms of energy efficiency.

A review of relevant Australian studies indicates that no prior research has modeled energy consumption based on residential building geometric characteristics using a combination of nonlinear regression and evolutionary algorithms.

Based on the conducted tests, with a confidence level exceeding 95%, approximately 99.8% of the energy consumption per square meter of residential buildings has been accurately predicted. This level of precision surpasses that of comparable studies and is a notable achievement of this research. Additionally, with a confidence level exceeding 95%, 100% of the total energy consumption of residential buildings has been predicted, achieving a higher level of accuracy compared to other studies conducted globally.

Moreover, the tests demonstrate that, with a confidence level exceeding 95%, more than 96% of the variations in cooling demand, heating demand, and the average Useful Daylight Illuminance (UDI) index have been accurately predicted.

The energy performance prediction equations can determine the extent of variation in each energy performance parameter by altering the geometric characteristics of residential buildings. Consequently, the application of these equations in urban macro-planning, particularly in the design and construction of single-story residential buildings and the formulation of laws and regulations to reduce energy consumption at the national level, becomes essential (Figure 5-10).

The findings of this research conclude that strategic planning and regulation in the housing sector could, in the long term, reduce energy consumption in residential buildings by more than 50%. Considering that one-third of global energy consumption is attributed to the building sector, this represents a significantly high potential for energy savings.

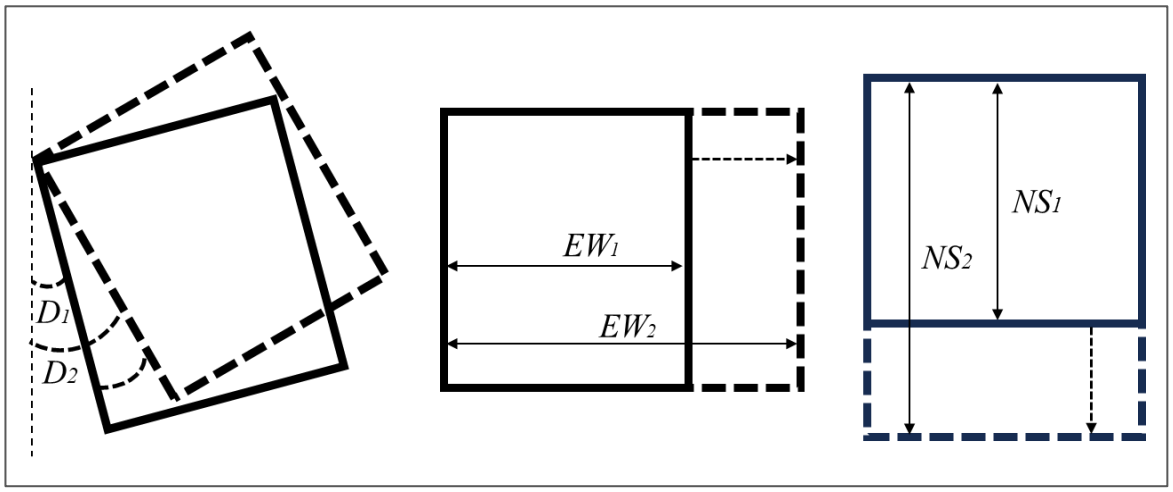

Figure 5-10. Variations in Geometric Characteristics of Residential buildings

It is essential to examine the spatial layout factors influencing energy performance identified in this study in comparison with another research. The present study comprehensively investigates a range of configuration factors, including the dimensions of the building's footprint, footprint area, aspect ratio of the footprint, building orientation angle relative to the north-south axis, and the height of interior spaces. Among these, the footprint area has been identified as the most significant factor affecting energy performance. The study by Mukkavaara and Sandberg (2020) also demonstrated the impact of footprint area on cooling, heating, and lighting demands.

Additionally, the aspect ratio has been recognized as one of the most critical configuration factors affecting energy performance in this research. In this regard, studies by Zhang and Wang (2021), Fattahi Tabasi et al. (2023), and Yi (2016) have similarly explained the impact of aspect ratio on energy consumption. However, the present study has conducted a systematic investigation of the effect of the aspect ratio on energy performance, including energy consumption, cooling demand, heating demand, and daylighting performance. The consideration of the aspect ratio based on north-south and east-west orientations is one of the innovative aspects of this research. This topic has generally been overlooked in other studies.

Moreover, the present study has examined the significant impact of interior space heights on the energy performance of residential buildings. Dino (2016) also addressed and confirmed this issue; however, a systematic analysis had not been conducted previously. Additionally, this study has shown that the impact of building orientation on energy performance is minimal compared to other factors of the external envelope configuration. This finding is in clear contradiction with the results of studies by Rodrigues et al. (2014) and Yi (2016). The reasons for this contradiction may lie in the differing climatic conditions of the regions studied. Nonetheless, the present research has performed a precise and systematic analysis of the clockwise and counterclockwise variation in orientation angle, which has not been observed in the reviewed studies.

In summary, the discussions in this research are presented systematically, which is one of the innovative contributions of this study. Furthermore, the issues addressed in this research have not been previously explored in Australia, particularly in Melbourne. Therefore, this aspect can also be considered a novel contribution of the present study.

5-10-Research Contributions

This research encompasses several key contributions, detailed as follows:

1. Development of a Predictive Model for Energy Efficiency

The study introduces a robust predictive model that quantifies the impact of geometric and spatial parameters of single-story residential buildings on energy performance. By leveraging computational simulation and predictive modeling, the thesis provides an analytical framework to evaluate energy consumption patterns, including heating, cooling, lighting, and ventilation requirements, tailored to Melbourne's climatic and geographical conditions.

2. Integration of Performative Computational Architecture (PCA)

By applying the Performative Computational Architecture framework, the thesis bridges the gap between parametric design and energy performance optimization. It effectively utilizes parametric tools like Grasshopper and Ladybug Plugins to automate the generation, simulation, and optimization of spatial layouts, enabling a seamless evaluation of energy efficiency across design iterations.

3. Optimization of Geometric Parameters in Housing Design

The research identifies and prioritizes geometric parameters that significantly influence the energy performance of residential buildings. It provides actionable guidelines for optimizing spatial layouts, enhancing energy efficiency while maintaining aesthetic and functional considerations in architectural design.

4. Adaptation of Simulation Tools for Early Design Phases

This thesis overcomes barriers associated with the complexity and limited usability of simulation tools in architectural design. By integrating user-friendly parametric tools and optimization algorithms, it enables energy performance assessments during the early design phases, where critical decisions have the most impact on energy efficiency.

5. Regional Contextualization for Australian Housing

Addressing a significant gap in region-specific studies, the thesis tailors its findings to Melbourne's climatic conditions and housing typologies. The proposed guidelines and models have direct applicability to Australia's residential sector, providing a foundation for localized sustainable design practices.

6. Generative Design of Spatial Layouts (GSL)

By implementing the Generative Design of Spatial Layouts framework, the research expands the design exploration process. It facilitates the generation and evaluation of multiple design solutions, ensuring optimal performance outcomes through Non-dominated Sorting Genetic Algorithm II (NSGA-II) optimization.

7. Contribution to Sustainable Energy Policies

The outcomes of this research inform sustainable energy policies by providing a decision-making framework for energy-efficient housing. The predictive models and optimization results offer policymakers and designers a scientific basis for advocating passive design strategies and sustainable residential development.

8. Advancement in Architectural Research Methodology

The thesis exemplifies the application of computational and statistical methods in architectural research. It employs nonlinear regression modeling, multi-objective optimization, and simulation-based analysis, setting a methodological benchmark for future studies in sustainable building design.

9. Comprehensive Framework for Design Practitioners

The study offers a systematic mechanism for practitioners to integrate energy performance simulations into the architectural workflow. This contribution enhances the capability of designers to create energy-efficient solutions without requiring advanced technical expertise in computational tools.

References

Abanda, F., & Byers, L. (2016). An investigation of the impact of building orientation on energy consumption in a domestic building using emerging BIM (Building Information Modelling). Energy, 97, 517-527.

Abdelmohsen, S. M. (2013, November). Reconfiguring architectural space using generative design and digital fabrication: a Project based course. In Proceedings of the 17th Conference of the Iberoamerican Society of Digital Graphics.

Adamski, M. (2007). Optimization of the form of a building on an oval base. Building and environment, 42(4), 1632-1643.

Adriaenssens, S., Block, P., Veenendaal, D., & Williams, C. (Eds.). (2014). Shell structures for architecture: form finding and optimization. Routledge.

Aeronautics, A. (1998). Astronautics, AIAA guide for the verification and validation of computational fluid dynamics simulations. American Institute of aeronautics and astronautics.

Afrazeh, A., Keivani, A., & Farahani, L. N. (2010). A new model for dynamic multi floor facility layout problem. Advanced Modeling and Optimization, 12(2), 249-256.

Afzal, S., Ziapour, B. M., Shokri, A., Shakibi, H., & Sobhani, B. (2023). Building energy consumption prediction using multilayer perceptron neural network-assisted models; comparison of different optimization algorithms. Energy, 282, 128446.

Aguirre, G., Al-Bender, F., & Van Brussel, H. (2010). A multiphysics model for optimizing the design of active aerostatic thrust bearings. Precision Engineering, 34(3), 507-515.

Ahmed, A. Z., & Nayar, C. (2008). Integrating sustainable energy in buildings: a case study in Malaysia. Paper presented at the FAU Conference, Copenhagen, Denmark.

Aksoy, U. T., & Inalli, M. (2006). Impacts of some building passive design parameters on heating demand for a cold region. Building and environment, 41(12), 1742-1754.

AlAnzi, A., Seo, D., & Krarti, M. (2009). Impact of building shape on thermal performance of office buildings in Kuwait. Energy Conversion and Management, 50(3), 822-828.

Alhawari, A., & Mukhopadhyaya, P. (2018). Thermal bridges in building envelopes–An overview of impacts and solutions. *International Review of Applied Sciences and Engineering*, *9*(1), 31-40.

Al-Khawaja, M. J. (2004). Determination and selecting the optimum thickness of insulation for buildings in hot countries by accounting for solar radiation. Applied Thermal Engineering, 24(17-18), 2601-2610.

Alsaqoor, T., & Krarti, M. (2017). Integration of Building Information Modeling and Building Energy Modeling: An Overview. Journal of Building Performance Simulation, 10(2), 101-116.

Amasyali, K., & El-Gohary, N. M. (2018). A review of data-driven building energy consumption prediction studies. Renewable and Sustainable Energy Reviews, 81, 1192-1205.

Amrhein, V., Greenland, S., & McShane, B. (2019). Comment: Retire statistical significance. Nature, 567, 305-307.

Amrhein, V., Greenland, S., & McShane, B. B. (2019). Statistical significance gives bias a free pass. European journal of clinical investigation, 49(12), e11976.

Andrade-Cabrera, C., Burke, D., Turner, W. J., & Finn, D. P. (2017). Ensemble Calibration of lumped parameter retrofit building models using Particle Swarm Optimization. Energy and buildings, 155, 513-532.

António, C. A. C., Monteiro, J. B., & Afonso, C. F. (2014). Optimal topology of urban buildings for maximization of annual solar irradiation availability using a genetic algorithm. Applied thermal engineering, 73(1), 424-437.

Ardehali, M. M., & Smith, T. F. (1996). Evaluation of variable volume and temperature HVAC system for commercial and residential buildings. Energy Conversion and Management, 37(9), 1469-1479.

Arjunan, T. V., & Athalye, A. (2019). Enhancing Building Performance Simulation for Predictive Modeling of Energy Consumption: A Case Study. Sustainable Cities and Society, 47, 101460.

Arsenovic, M., Lalic, Z., & Radojevic, Z. (2010). Clay brick walls thermal properties. International Journal of Modern Manufacturing Technologies, 2(1), 15-18.

Arvin, S. A., & House, D. H. (2002). Modeling architectural design objectives in physically based space planning. Automation in Construction, 11(2), 213-225.

Asadi, H., Mohamed, S., Lim, C. P., & Nahavandi, S. (2016). Robust optimal motion cueing algorithm based on the linear quadratic regulator method and a genetic algorithm. IEEE Transactions on Systems, Man, and Cybernetics: Systems, 47(2), 238-254.

Asadi, S., Fakhari, M., & Sendi, M. (2016). A study on the thermal behavior of traditional residential buildings: Rasoulian house case study. Journal of Building Engineering, 7, 334-342.

Asan, H. (2006). Numerical computation of time lags and decrement factors for different building materials. *building and environment*, *41*(5), 615-620.

Asdrubali, F., Baldinelli, G., & Bianchi, F. (2012). A quantitative methodology to evaluate thermal bridges in buildings. *Applied Energy*, *97*, 365-373.

Asdrubali, F., D'Alessandro, F., & Schiavoni, S. (2015). A review of unconventional sustainable building insulation materials. Sustainable Materials and Technologies, 4, 1-17.

Asdrubali, F., Schiavoni, S., & Horoshenkov, K. V. (2012). A review of sustainable materials for acoustic applications. Building Acoustics, 19(4), 283-311.

ASHRAE, A. (2002). Ashrae guideline 14: measurement of energy and demand savings. American Society of Heating, Refrigerating and Air-Conditioning Engineers, 35, 41-63.

Asli, A. (2019). Façade form-finding with swarm intelligence [J]. Automation in Construction, 99(3), 140-151.

Aste, N., Leonforte, F., Manfren, M., & Mazzon, M. (2015). Thermal inertia and energy efficiency–Parametric simulation assessment on a calibrated case study. *Applied Energy*, *145*, 111-123.

Ataman, C., & Dino, İ. G. (2022). Performative design processes in architectural practices in Turkey: architects' perception. Architectural Engineering and Design Management, 18(5), 690-704.

Attia, S., Hamdy, M., O'Brien, W., & Carlucci, S. (2013). Assessing gaps and needs for integrating building performance optimization tools in net zero energy buildings design. Energy and buildings, 60, 110-124.

Bademlioglu, A., Kaynakli, Ö., & Yamankaradeniz, N. (2018). The effect of water vapor diffusion resistance factor of insulation materials for outer walls on condensation. Isı Bilimi ve Tekniği Dergisi, 38(2), 15-23.

Bahrami, P., & Parnianpour, S. (2018). A study of the impact of building geometry on energy efficiency in residential buildings. Sustainable Cities and Society, 39, 354-362.

Bahrehmand, T. Batard, R. Marques, A. Evans, J. Blat, Optimizing layout using spatial quality metrics and user preferences, Graph. Model. 93 (2017) 25–38.

Bakar, N. N. A., Hassan, M. Y., Abdullah, H., Rahman, H. A., Abdullah, M. P., Hussin, F., & Bandi, M. (2015). Energy efficiency index as an indicator for measuring building energy performance: A review. Renewable and Sustainable Energy Reviews, 44, 1-11.

Bakhshi, S., Chenaghlou, M. R., Rahimian, F. P., Edwards, D. J., & Dawood, N. (2022). Integrated BIM and DfMA parametric and algorithmic design based collaboration for supporting client engagement within offsite construction. Automation in Construction, 133, 104015.

Banerjee, A., Quiroz, J. C., & Louis, S. J. (2008). A model of creative design using collaborative interactive genetic algorithms. In Design Computing and Cognition'08 (pp. 397-416): Springer.

Ban-Weiss, G. A., et al. (2015). Cooling the Cities: A Systematic Review of Urban Heat Mitigation Technologies. Energy and Buildings, 98, 154-185.

Barbieri, L., & Muzzupappa, M. (2022). Performance-driven engineering design approaches based on generative design and topology optimization tools: a comparative study. Applied Sciences, 12(4), 2106.

Barker, Roger (1968), Ecological Psychology: Concepts and Methods for Studying Human Behavior, Stanford, Ca.: Stanford University Press.

Baušys, I. Pankrašovaité, Optimization of architectural layout by the improved genetic algorithm, J. Civ. Eng. Manag. 11 (1) (2005) 13–21.

Baušys, R., & Pankrašovaite, I. (2005). Optimization of architectural layout by the improved genetic algorithm. Journal of Civil Engineering and Management, 11(1), 13-21.

Baybars, I. (1982). The generation of floor plans with circulation spaces. Environment and Planning B: Planning and Design, 9(4), 445-456.

Baybars, I., & Eastman, C. M. (1980). Enumerating architectural arrangements by generating their underlying graphs. Environment and Planning B: Planning and Design, 7(3), 289-310.

Baykan, Can A., and Mark S. Fox. "Spatial synthesis by disjunctive constraint satisfaction." AI EDAM 11, no. 4 (1997): 245-262.

Beasley, D., Bull, D. R., & Martin, R. R. (1993). An overview of genetic algorithms: Part 1, fundamentals. University computing, 15(2), 56-69.

Belzer, D. B., Scott, M. J., & Sands, R. D. (1996). Climate change impacts on US commercial building energy consumption: an analysis using sample survey data. Energy Sources, 18(2), 177-201.

Bentley, P. J., & Wakefield, J. P. (1998). Generic evolutionary design. In Soft computing in engineering design and manufacturing (pp. 289-298): Springer.

Bernal, M., Haymaker, J. R., & Eastman, C. (2015). On the role of computational support for designers in action. Design Studies, 41, 163-182.

Bian, Y., & Ma, Y. (2017). Analysis of daylight metrics of side-lit room in Canton, south China: A comparison between daylight autonomy and daylight factor. Energy and buildings, 138, 347-354.

Bleuler, S., Brack, M., Thiele, L., & Zitzler, E. (2001). Multiobjective genetic programming: Reducing bloat using SPEA2. Paper presented at the Proceedings of the 2001 Congress on Evolutionary Computation (IEEE Cat. No. 01TH8546).

Bloch, C. (1979). Catalogue of small rectangular plans. Environment and Planning B: Planning and Design, 6(2), 155-190.

Blum, C., & Li, X. (2008). Swarm intelligence in optimization. In Swarm intelligence. Springer, Berlin, Heidelberg. (43-85).

Bluyssen, P. (2009). The indoor environment handbook: how to make buildings healthy and comfortable: Routledge.

Bluyssen, P. M. (2013). The healthy indoor environment: How to assess occupants' wellbeing in buildings: Routledge.

Bohdanowicz, P., & Martinac, I. (2007). Determinants and benchmarking of resource consumption in hotels—Case study of Hilton International and Scandic in Europe. Energy and buildings, 39(1), 82-95.

Bolattürk, A. (2008). Optimum insulation thicknesses for building walls with respect to cooling and heating degree-hours in the warmest zone of Turkey. Building and environment, 43(6), 1055-1064.

Bonnaire, X., & Riff, M.-C. (2002). A self-adaptable distributed evolutionary algorithm to tackle space planning problems. Paper presented at the International Workshop on Applied Parallel Computing.

Boonstra, S., van der Blom, K., Hofmeyer, H., Emmerich, M. T., van Schijndel, J., & de Wilde, P. (2018). Toolbox for super-structured and super-structure free multi-disciplinary building spatial design optimisation. Advanced Engineering Informatics, 36, 86-100.

Bouchlaghem, N. (2000). Optimising the design of building envelopes for thermal performance. Automation in Construction, 10(1), 101-112.

Boyano, A., Hernandez, P., & Wolf, O. (2013). Energy consumptions and potential savings in European office buildings: Case studies based on EnergyPlus simulations. Energy and buildings, 65, 19-28.

Bozer, Y. A., Meller, R. D., & Erlebacher, S. J. (1994). An improvement-type layout algorithm for single and multiple-floor facilities. Management Science, 40(7), 918-932.

Brotchie, J., & Linzey, M. (1971). A model for integrated building design. Building Science, 6(3), 89-96.

Brown, Z., & Cole, R. J. (2009). Influence of occupants' knowledge on comfort expectations and behaviour. Building Research & Information, 37(3), 227-245.

Bukhari, F. A. (2011). A Hierarchical Evolutionary Algorithmic Design (HEAD) system for generating and evolving building design models (Doctoral dissertation, Queensland University of Technology).

Burt, William Henry (1943), Territoriality and Home Range Concepts as Applied to Mammals, Journal of Mammalogy, Vol. 24, No.3, pp. 346-352.

Cabeza, L. F., Castell, A., Medrano, M., Martorell, I., Pérez, G., & Fernández, I. (2010). Experimental study on the performance of insulation materials in Mediterranean construction. Energy and buildings, 42(5), 630-636.

Caetano, I., Santos, L., & Leitão, A. (2020). Computational design in architecture: Defining parametric, generative, and algorithmic design. Frontiers of Architectural Research, 9(2), 287-300.

Cagan, J., Degentesh, D., & Yin, S. (1998). A simulated annealing-based algorithm using hierarchical models for general three-dimensional component layout. Computer-aided design, 30(10), 781-790.

Cai, W., Wen, X., Li, C., Shao, J., & Xu, J. (2023). Predicting the energy consumption in buildings using the optimized support vector regression model. Energy, 273, 127188.

Caldas, L. (2008). Generation of energy-efficient architecture solutions applying GENE_ARCH: An evolution-based generative design system. Advanced Engineering Informatics, 22(1), 59-70.

Calixto, V., & Celani, G. (2015). A literature review for space planning optimization using an evolutionary algorithm approach: 1992-2014. Blucher Design Proceedings, 2(3), 662-671.

Cao, Q., Yang, D., & Lu, S. (2020). A Comprehensive Review of the Impact of Building Geometry on Energy Consumption. Energy and Buildings, 213, 109805.

Cao, Q., Yang, D., & Lu, S. (2020). A Comprehensive Review of the Impact of Building Geometry on Energy Consumption. Energy and Buildings, 213, 109805.

Cao, X., Dai, X., & Liu, J. (2016). Building energy-consumption status worldwide and the state-of-the-art technologies for zero-energy buildings during the past decade. Energy and buildings, 128, 198-213.

Capozzoli, A., Gorrino, A., & Corrado, V. (2013). A building thermal bridges sensitivity analysis. *Applied Energy*, *107*, 229-243.

Cardoso, C., Badke-Schaub, P., & Eris, O. (2016). Inflection moments in design discourse: How questions drive problem framing during idea generation. Design studies, 46, 59-78.

Carlon, E., Schwarz, M., Prada, A., Golicza, L., Verma, V. K., Baratieri, M., . . . Schmidl, C. (2016). On-site monitoring and dynamic simulation of a low energy house heated by a pellet boiler. Energy and buildings, 116, 296-306.

Catalina, T., Virgone, J., & Iordache, V. (2011). Study on the impact of the building form on the energy consumption. Paper presented at the Proceedings of building simulation.

Cha, M. Y., & Gero, J. S. (1998). Shape pattern recognition using a computable pattern representation. Paper presented at the Artificial intelligence in design'98.

Chaillou, S. (2019). AI+Architecture Towards New Approach, master Thesis Graduate School of Design, Harvard University, https://doi.org/10.9783/ 9781949057027-006.

Chang, J. R. (2018). HyperCell: A Bio-Inspired Design Framework for Real-time Interactive Architectures. A+ BE| Architecture and the Built Environment, (1), 1-250.

Chatzikonstantinou, I. (2014, September). A 3-dimensional architectural layout generation procedure for optimization applications: DC-RVD. In Proceedings of the 2014 eCAADe Conference (Vol. 1, pp. 287-296).

Chatzikonstantinou, I., & Sariyildiz, I. S. (2017). Addressing design preferences via auto-associative connectionist models: Application in sustainable architectural Façade design. Automation in Construction, 83, 108-120.

Chegari, B., Tabaa, M., Simeu, E., Moutaouakkil, F., & Medromi, H. (2021). Multi-objective optimization of building energy performance and indoor thermal comfort by combining artificial neural networks and metaheuristic algorithms. Energy and Buildings, 239, 110839.

Chen, X. et al. (2020). "Generative Design Algorithms for Energy-Efficient Building Geometry." Sustainable Design and Construction, 15(4), 345-362.

Chen, Y., & Wang, Y. (2018). Machine Learning Approaches in Predictive Modeling of Residential Building Energy Consumption. Automation in Construction, 87, 31-45.

Chen, Y., & Wang, Y. (2018). Machine Learning Approaches in Predictive Modeling of Residential Building Energy Consumption. Automation in Construction, 87, 31-45.

Chen, Y., Deng, Z., & Hong, T. (2020). Automatic and rapid calibration of urban building energy models by learning from energy performance database. Applied Energy, 277, 115584.

Cheng, W., Xie, B., Zhang, R., Xu, Z., & Xia, Y. (2015). Effect of thermal conductivities of shape stabilized PCM on under-floor heating system. Applied Energy, 144, 10-18.

Chong, A., Augenbroe, G., & Yan, D. (2021). Occupancy data at different spatial resolutions: Building energy performance and model calibration. Applied Energy, 286, 116492.

Chong, A., Gu, Y., & Jia, H. (2021). Calibrating building energy simulation models: A review of the basics to guide future work. Energy and buildings, 253, 111533.

Chwieduk, D., & Bogdanska, B. (2004). Some recommendations for inclinations and orientations of building elements under solar radiation in Polish conditions. Renewable Energy, 29(9), 1569-1581.

Clarke, J. A. (2007). Energy simulation in building design: Routledge.

Coakley, D., Raftery, P., & Keane, M. (2014). A review of methods to match building energy simulation models to measured data. Renewable and Sustainable Energy Reviews, 37, 123-141.

Coates, P., Healy, N., Lamb, C., & Voon, W. (1996). The use of Cellular Automata to explore bottom up architectonic rules.

Cobb, P., Confrey, J., DiSessa, A., Lehrer, R., & Schauble, L. (2003). Design experiments in educational research. Educational researcher, 32(1), 9-13.

Coffey, B. (2011). Using building simulation and optimization to calculate lookup tables for control. University of California, Berkeley.

Collins, M., & Curtis, J. (2018). Bunching of residential building energy performance certificates at threshold values. Applied Energy, 211, 662-676.

Çomaklı, K., & Yüksel, B. (2003). Optimum insulation thickness of external walls for energy saving. Applied Thermal Engineering, 23(4), 473-479.

Combes, L. (1976). Packing rectangles into rectangular arrangements. Environment and Planning B: Planning and Design, 3(1), 3-32.

Comerford, D. A., Lange, I., & Moro, M. (2018). Proof of concept that requiring energy labels for dwellings can induce retrofitting. Energy Economics, 69, 204-212.

Correia, R., Duarte, J., & Leitão, A. (2012). Gramatica a general 3d shape grammar interpreter targeting the mass customization of housing. In 30th International Conference on Education and research in Computer Aided Architectural Design in Europe, eCAADe 2012 (pp. 489-496). Education and research in Computer Aided Architectural Design in Europe.

Crawley, D. B., Hand, J. W., Kummert, M., & Griffith, B. T. (2008). Contrasting the capabilities of building energy performance simulation programs. Building and environment, 43(4), 661-673.

Cruz, C., Karakiewicz, J., & Kirley, M. (2016). Towards the implementation of a composite cellular automata model for the exploration of design space.

Damski, J. C., & Gero, J. S. (1997). An evolutionary approach to generating constraint-based space layout topologies. In CAAD futures 1997 (pp. 855-864): Springer.

Das, S., Day, C., Hauck, A., Haymaker, J., & Davis, D. (2016). Space plan generator: Rapid generationn & evaluation of floor plan design options to inform decision making. Proceedings of the ACADIA, Ann Arbor, MI, USA, 27-29.

Davis, D. (2013). Modelled on software engineering: Flexible parametric models in the practice of architecture. RMIT University,

De Rosa, M., Bianco, V., Scarpa, F., & Tagliafico, L. A. (2014). Heating and cooling building energy consumption evaluation; a simplified model and a modified degree days approach. Applied Energy, 128, 217-229.

De Souza, C. B., & Alsaadani, S. (2012). Thermal zoning in speculative office buildings: discussing the connections between space layout and inside temperature control. Paper presented at the Proceedings of the First Building Simulation and Optimization Conference, Loughborough, UK.

De Wit, S., & Augenbroe, G. (2002). Analysis of uncertainty in building design evaluations and its implications. Energy and buildings, 34(9), 951-958.

Deb, K., Pratap, A., Agarwal, S., & Meyarivan, T. (2002). A fast and elitist multiobjective genetic algorithm: NSGA-II. IEEE transactions on evolutionary computation, 6(2), 182-197.

Dehkordi, S. M., & Ma, Z. (2016). A Review of Building Energy Modeling for Heating, Ventilation, and Air Conditioning Systems. Energy and Buildings, 116, 277-288.

Depecker, P., Menezo, C., Virgone, J., & Lepers, S. (2001). Design of buildings shape and energetic consumption. Building and environment, 36(5), 627-635.

Ding, Z., Fan, Z., Tam, V. W., Bian, Y., Li, S., Illankoon, I. C. S., & Moon, S. (2018). Green building evaluation system implementation. Building and environment, 133, 32-40.

Dino, I. G. (2016). An evolutionary approach for 3D architectural space layout design exploration. Automation in construction, 69, 131-150.

Dino, I. G. (2016). An evolutionary approach for 3D architectural space layout design exploration. Automation in construction, 69, 131-150 .

Dino, I. G., & Üçoluk, G. (2017). Multiobjective design optimization of building space layout, energy, and daylighting performance. Journal of Computing in Civil Engineering, 31(5), 04017025.

Dong, B., Li, Z., Rahman, S. M., & Vega, R. (2016). A hybrid model approach for forecasting future residential electricity consumption. Energy and buildings, 117, 341-351.

Doulgerakis, A. (2007). Genetic programming+ unfolding embryology in automated layout planning. UCL (University College London),

Du, J., & Sharples, S. (2011). Assessing and predicting average daylight factors of adjoining spaces in atrium buildings under overcast sky. Building and environment, 46(11), 2142-2152.

Du, Q., Zhao, C., & Sun, Y. (2019). Predictive Modeling of Building Energy Consumption Using Artificial Neural Networks. Energy and Buildings, 186, 40-51.

Du, Q., Zhao, C., & Sun, Y. (2019). Predictive Modeling of Building Energy Consumption Using Artificial Neural Networks. Energy and Buildings, 186, 40-51.

Du, T., Turrin, M., Jansen, S., Van Den Dobbelsteen, A. A. J. F., & Biloria, N. (2018, February). A review on automatic generation of architectural space layouts with energy performance optimization. In Proceedings of the International Conference On Building Energy & Environment, COBEE.

Du, T., Turrin, M., Jansen, S., van den Dobbelsteen, A., & Fang, J. (2020). Gaps and requirements for automatic generation of space layouts with optimised energy performance. Automation in Construction, 116, 103132.

Du, X., Yao, X., Ni, Y., Minku, L. L., Ye, P., & Xiao, R. (2015). An evolutionary algorithm for performance optimization at software architecture level. Paper presented at the 2015 IEEE Congress on Evolutionary Computation (CEC).

Du, X., Zhang, Y., & Lv, Z. (2020). Investigations and analysis of indoor environment quality of green and conventional shopping mall buildings based on customers' perception. Building and environment, 177, 106851.

Dubois, M.-C. (2003). Shading devices and daylight quality: an evaluation based on simple performance indicators. Lighting Research & Technology, 35(1), 61-74.

Dunn, N. (2012). Digital fabrication in architecture: Laurence King Publishing. Building Energy Consumption. Journal of Sustainable Architecture and Urban Development, 5(2), 145-162.

Dutta, K., & Sarthak, S. (2011). Architectural space planning using evolutionary computing approaches: a review. Artificial Intelligence Review, 36(4), 311-321.

Dzeng, R. J., Lin, C. W., & Hsiao, F. Y. (2014). Application of RFID tracking to the optimization of function-space assignment in buildings. Automation in Construction, 40, 68-83.

Earl, C. F. (1977). A note on the generation of rectangular dissections. Environment and Planning B: Planning and Design, 4(2), 241-246.

Eberhart, R. (1942). James. Kennedy, Particle swarm optimization. Paper presented at the Proceedings of the IEEE international conference on neural networks, Australia.

Edwards, R. E., New, J., & Parker, L. E. (2012). Predicting future hourly residential electrical consumption: A machine learning case study. Energy and buildings, 49, 591-603.

Eisenhower, B., O'Neill, Z., Fonoberov, V. A., & Mezić, I. (2012). Uncertainty and sensitivity decomposition of building energy models. Journal of Building Performance Simulation, 5(3), 171-184.

Ekici, B., Cubukcuoglu, C., Turrin, M., & Sariyildiz, I. S. (2019). Performative computational architecture using swarm and evolutionary optimisation: A review. Building and Environment, 147, 356-371.

Elezkurtaj, T., & Franck, G. (2000). Geometry and Topology. A User-Interface to Artificial Evolution in Architectural Design.

Elezkurtaj, T., & Franck, G. (2002). Algorithmic support of creative architectural design. organization, 2, 16.

Evins, R. (2013). A review of computational optimisation methods applied to sustainable building design. Renewable and Sustainable Energy Reviews, 22, 230-245.

Fallahtafti, R., & Mahdavinejad, M. (2015). Optimisation of building shape and orientation for better energy efficient architecture. International Journal of Energy Sector Management, 9(4), 593-618.

Fan, L., Musialski, P., Liu, L., & Wonka, P. (2014). Structure completion for facade layouts. ACM Trans. Graph., 33(6), 210:211-210:211.

Fattahi Tabasi, S., Rafizadeh, H. R., Andaji Garmaroudi, A., & Banihashemi, S. (2023). Optimizing urban layouts through computational generative design: density distribution and shape optimization. *Architectural Engineering and Design Management*, 1-21.

Fernandez Bandera, C., & Ramos Ruiz, G. (2017). Towards a new generation of building envelope calibration. Energies, 10(12), 2102.

Ferrara, M., Lisciandrello, C., Messina, A., Berta, M., Zhang, Y., & Fabrizio, E. (2020). Optimizing the transition between design and operation of ZEBs: Lessons learnt from the Solar Decathlon China 2018 SCUTxPoliTo prototype. Energy and buildings, 213, 109824.

Fischer, A. J. (2015). Quelea: agent-based design for Grasshopper Agent-based design for Grasshopper.

Fischer, T., & Herr, C. M. (2001, December). Teaching generative design. In Proceedings of the 4th Conference on Generative Art (pp. 147-160). Milan: Politechnico di Milano University.

Flack, R. W., & Ross, B. J. (2011). Evolution of architectural floor plans. Paper presented at the European conference on the applications of evolutionary computation.

Flemming, U. (1978). Wall representations of rectangular dissections and their use in automated space allocation. Environment and Planning B: Planning and Design, 5(2), 215-232.

Florides, G. A., Tassou, S. A., Kalogirou, S. A., & Wrobel, L. (2002). Measures used to lower building energy consumption and their cost effectiveness. Applied Energy, 73(3-4), 299-328.

Fogel, L. J., & Owens, A. J. (1966). MJ Walsh Artificial intelligence through simulated evolution. In: New York, Wiley Pub.

Fossati, M., Scalco, V. A., Linczuk, V. C. C., & Lamberts, R. (2016). Building energy efficiency: An overview of the Brazilian residential labeling scheme. Renewable and Sustainable Energy Reviews, 65, 1216-1231.

Foucquier, A., Robert, S., Suard, F., Stéphan, L., & Jay, A. (2013). State of the art in building modelling and energy performances prediction: A review. Renewable and Sustainable Energy Reviews, 23, 272-288.

Frazer, J., Frazer, J., Liu, X., Tang, M., & Janssen, P. (2002). Generative and evolutionary techniques for building envelope design. In Generative Art 2002, 5th International Conference GA2002 (pp. 3-1). Generative Design Lab.

Galle, P. (1981). An algorithm for exhaustive generation of building floor plans. Communications of the ACM, 24(12), 813-825.

Galle, P. (1986). Abstraction as a tool of automated floor-plan design. Environment and Planning B: Planning and Design, 13(1), 21-46.

Gan, V. J. (2022). BIM-based graph data model for automatic generative design of modular buildings. Automation in Construction, 134, 104062.

Ganesan, Shankar; Othuman Mydin, Md Azree; Mohd Yunos, Mohd Yazid; Mohd Nawi, Mohd Nasrun (2015). Thermal Properties of Foamed Concrete with Various Densities and Additives at Ambient Temperature. Applied Mechanics and Materials, 747(), 230–233.

Gao, Y., Zhu, N., & Wang, J. (2021). Developing Predictive Models for Residential Building Energy Consumption Considering Climate and Urban Form. Energy and Buildings, 237, 110817.

Gao, Y., Zhu, N., & Wang, J. (2021). Developing Predictive Models for Residential Building Energy Consumption Considering Climate and Urban Form. Energy and Buildings, 237, 110817.

Garcia, R. et al. (2023). "Assessing Ecological Footprint in Residential Building Designs: A Comprehensive Approach." Journal of Environmental Impact Assessment, 30(2), 180-197.

Garg, N., Kumar, A., & Maji, S. (2014). Parametric sensitivity analysis of factors affecting sound transmission loss of multi-layered building elements using taguchi method. Archives of Acoustics, 39(2), 165-176.

Garrido, I., Lagüela, S., Arias, P., & Balado, J. (2018). Thermal-based analysis for the automatic detection and characterization of thermal bridges in buildings. *Energy and Buildings*, *158*, 1358-1367.

Garza, A., & Maher, M. (2001). GENCAD: A hybrid analogical/evolutionary model of creative design. Paper presented at the Proceedings of the 5th Intl. Conf. on Computational and Cognative Models of Creative Design, J. In Gero and M. Maher, eds.

Gaterell, M., & McEvoy, M. (2005). The impact of climate change uncertainties on the performance of energy efficiency measures applied to dwellings. Energy and buildings, 37(9), 982-995.

Gerber, D., & Pantazis, E. (2016). Design Exploring Complexity in Architectural Shells-Interactive form finding of reciprocal frames through a multi-agent system.

Gero, J. S. (1994). Towards a model of exploration in computer-aided design. Paper presented at the Formal design methods for CAD.

Gero, J. S., & Kazakov, V. A. (1997). Learning and re-using information in space layout planning problems using genetic engineering. Artificial Intelligence in engineering, 11(3), 329-334.

Gero, J. S., & Kazakov, V. A. (1998). Evolving design genes in space layout planning problems. Artificial Intelligence in engineering, 12(3), 163-176.

Ghaffarian, M., Fallah, R., & Jacob, C. (2018, June). Organic architectural spatial design driven by agent-based crowd simulation. In Proceedings of the Symposium on Simulation for Architecture and Urban Design (pp. 1-8).

Goetschalckx, M., & Irohara, T. (2007). Formulations and optimal solution algorithms for the multi-floor facility layout problem with elevators. Paper presented at the IIE Annual Conference. Proceedings.

Goldberg, D. E. (1989). Genetic algorithms in search, optimization, and machine learning. Addison. Reading.

Goldberg, D. E. (1991). Genetic algorithms as a computational theory of conceptual design. In Applications of Artificial Intelligence in Engineering VI (pp. 3-16): Springer.

Goldstein, R., Tessier, A., & Khan, A. (2011). Space layout in occupant behavior simulation. Paper presented at the Conference Proceedings: IBPSA-AIRAH Building Simulation Conference.

Gong, Y., Yang, S., Zhan, L., Ma, L., Vajtai, R., & Ajayan, P. M. (2014). A bottom-up approach to build 3D architectures from nanosheets for superior lithium storage. Advanced Functional Materials, 24(1), 125-130.

Gouveia, J. P., Fortes, P., & Seixas, J. (2012). Projections of energy services demand for residential buildings: Insights from a bottom-up methodology. Energy, 47(1), 430-442.

Gradišar, L., Klinc, R., Turk, Ž., & Dolenc, M. (2022). Generative design methodology and framework exploiting designer-algorithm synergies. *Buildings*, *12*(12), 2194.

Guo, J., Wu, J., & Wang, R. (2011). A new approach to energy consumption prediction of domestic heat pump water heater based on grey system theory. Energy and buildings, 43(6), 1273-1279.

Guo, Z., & Li, B. (2017). Evolutionary approach for spatial architecture layout design enhanced by an agent-based topology finding system. Frontiers of Architectural Research, 6(1), 53-62.

Gupta, R., & Ralegaonkar, R. (2004). Estimation of beam radiation for optimal orientation and shape decision of buildings in India. Architectural Journal of Institution of Engineers India, 85, 27-32.

Gürsel Dino, İ. (2012). Creative design exploration by parametric generative systems in architecture. METU Journal of Faculty of Architecture 29(1). 207-224.

Haberl, J. S., & Cho, S. (2004). Literature Review of Uncertainty of Analysis Methods,(DOE-2 Program), Report to the Texas Commission on Environmental Quality.

Harada, M., Witkin, A., & Baraff, D. (1995). Interactive physically-based manipulation of discrete/continuous models. Paper presented at the Proceedings of the 22nd annual conference on Computer graphics and interactive techniques.

Hassan, S. R., Megahed, N. A., Eleinen, O. M. A., & Hassan, A. M. (2022). Toward a national life cycle assessment tool: Generative design for early decision support. Energy and Buildings, 267, 112144.

Hassanli, S., Chauhan, K., Zhao, M., & Kwok, K. C. (2019). Application of through-building openings for wind energy harvesting in built environment. Journal of Wind Engineering and Industrial Aerodynamics, 184, 445-455.

Hensen, J. L., & Lamberts, R. (2019). Building performance simulation–challenges and opportunities. Building performance simulation for design and operation, 1-10.

Hill, C., Norton, A., & Dibdiakova, J. (2018). A comparison of the environmental impacts of different categories of insulation materials. Energy and Buildings, 162, 12-20.

Holland, J. H. (1992). Adaptation in natural and artificial systems: an introductory analysis with applications to biology, control, and artificial intelligence: MIT press.

Holland, T. (1975). Transportable solar laboratory test results and utilization study for Miami, Florida. Retrieved from

Homayouni, H. (2007). A genetic algorithm approach to space layout planning optimization. Citeseer,

Hooke, R. T. A. JEEVES,“. Direct search” sohtaon of numerical and statistical problems, 212-229.

Hua, H. (2016). Irregular architectural layout synthesis with graphical inputs. Automation in construction, 72, 388-396.

Huang, M., Gaj, K., & El-Ghazawi, T. (2010). New hardware architectures for Montgomery modular multiplication algorithm. IEEE Transactions on computers, 60(7), 923-936.

Huang, W., & Zheng, H. (2018, October). Architectural drawings recognition and generation through machine learning. In Proceedings of the 38th annual conference of the association for computer aided design in architecture, Mexico City, Mexico (pp. 18-20).

Huang, X., Liu, G., Guo, W., Niu, Y., & Chen, G. (2015). Obstacle-avoiding algorithm in X-architecture based on discrete particle swarm optimization for VLSI design. ACM Transactions on Design Automation of Electronic Systems (TODAES), 20(2), 1-28.

Huang, Y., & Niu, J. L. (2016). Optimal building envelope design based on simulated performance: History, current status and new potentials. Energy and Buildings, 117, 387-398.

Hubka, V., & Eder, W. E. (1987). A scientific approach to engineering design. Design studies, 8(3), 123-137.

Humppi, H., & Österlund, T. (2016). Algorithm-aided BIM. In Complexity & simplicity–Proceedings of the 34th eCAADe conference (pp. 601-609).

Hybs, I., & Gero, J. S. (1992). An evolutionary process model of design. Design studies, 13(3), 273-290.

Ibrahim, M., Ghaddar, N., & Ghali, K. (2012). Optimal location and thickness of insulation layers for minimizing building energy consumption. Journal of Building Performance Simulation, 5(6), 384-398.

Inoue, M., & Takagi, H. (2008). Layout algorithm for an EC-based room layout planning support system. Paper presented at the 2008 IEEE Conference on Soft Computing in Industrial Applications.

Inoue, M., & Takagi, H. (2009). EMO-based architectural room floor planning. Paper presented at the 2009 IEEE international conference on systems, man and cybernetics.

Ito, T. (1999). A genetic algorithm approach to piping route path planning. Journal of Intelligent Manufacturing, 10(1), 103-114.

J., Maddahi, S. M., & Mirzaei, R. (2023). Generative Design of Housing Spatial Layout Based on Rectangular Spaces. Advances in Civil Engineering, 2023(1), 1142371.

Jabi, W. (2013). Parametric design for architecture. Hachette UK.

Jabi, W., Soe, S., Theobald, P., Aish, R., & Lannon, S. (2017). Enhancing parametric design through non-manifold topology. Design Studies, 52, 96-114.

Jackson, H. (2002). Toward a symbiotic coevolutionary approach to architecture. In Creative evolutionary systems (pp. 299-313): Elsevier.

Jackson, J. (2002). Data mining; a conceptual overview. Communications of the Association for Information Systems, 8(1), 19.

Jagielski, R., & Gero, J. S. (1997). A genetic programming approach to the space layout planning problem. In CAAD futures 1997 (pp. 875-884): Springer.

Jain, M., Sanyal, A., Goyal, S., Chattopadhyay, C., & Bhatnagar, G. (2018). Automatic rendering of building floor plan images from textual descriptions in English. arXiv preprint arXiv:1811.11938.

Jamaludin, A. A., Inangda, N., Ariffin, A. R. M., & Hussein, H. (2011). Energy performance: A comparison of four different multi-residential building designs and forms in the equatorial region. Paper presented at the 2011 IEEE Conference on Clean Energy and Technology (CET).

Janda, K. B. (2009). Worldwide status of energy standards for buildings: a 2009 update. Proceedings of the European Council for an Energy Efficient Economy (ECEEE) Summer Study, 1-6.

Janssen, P., & Stouffs, R. (2015). Types of parametric modelling. In: Proceedings of the 20th International Conference of Association for Computer-Aided Architectural Design Research in Asia CAADRIA 2015, pp. 157e166.

Jazizadeh, F., Levermore, G., & Virk, G. S. (2017). Impact of Urban Geometry on Building Energy Use: A Review. Renewable and Sustainable Energy Reviews, 73, 810-824

Jeremy, M., Ruchi, C., & Panos, P. (2002). Architectural layout design optimization. Engineering optimization, 34(5), 461-484.

Jin, S., Xu, N., & Li, Y. (2020). Application of Machine Learning Algorithms in Predictive Modeling of Building Energy Performance: A Case Study. Automation in Construction, 114, 103212.

Jin, S., Xu, N., & Li, Y. (2020). Application of Machine Learning Algorithms in Predictive Modeling of Building Energy Performance: A Case Study. Automation in Construction, 114, 103212.

Jo, J. H., & Gero, J. S. (1995). A genetic search approach to space layout planning. Architectural Science Review, 38(1), 37-46.

Jo, J. H., & Gero, J. S. (1998). Space layout planning using an evolutionary approach. Artificial intelligence in Engineering, 12(3), 149-162.

Jo, J. H., & Gero, J. S. (1998). Space layout planning using an evolutionary approach. Artificial Intelligence in engineering, 12(3), 149-162.

Johnson, D. H. (1982). The application of spectral estimation methods to bearing estimation problems. Proceedings of the IEEE, 70(9), 1018-1028.

Kahng, A. B. (2000). Classical floorplanning harmful? Paper presented at the Proceedings of the 2000 international symposium on Physical design.

Kalay, Y. E. (1989). Modeling objects and environments. (Principles of Computer Aided Design) Wiley-Academy, New York.

Kalay, Y. E. (1989). The hybrid edge: a topological data structure for vertically integrated geometric modelling. Computer-aided design, 21(3), 130-140.

Kalay, Y. E. (2004). Architecture's new media: Principles, theories, and methods of computer-aided design: MIT press.

Kallioras, N. A., & Lagaros, N. D. (2020). DzAIN: Deep learning based generative design. Procedia Manufacturing, 44, 591-598.

Kämpf, J. H., & Robinson, D. (2012). Integration of Urban and Building Simulation Models. Energy and Buildings, 45, 15-25.

Kanters, J., Horvat, M., & Dubois, M.-C. (2014). Tools and methods used by architects for solar design. Energy and buildings, 68, 721-731.

Kapp, S., Choi, J. K., & Hong, T. (2023). Predicting industrial building energy consumption with statistical and machine-learning models informed by physical system parameters. Renewable and Sustainable Energy Reviews, 172, 113045.

Karatas, A., & El-Rayes, K. (2015). Optimizing tradeoffs among housing sustainability objectives. Automation in construction, 53, 83-94.

Kavousian, A., Rajagopal, R., & Fischer, M. (2013). Determinants of residential electricity consumption: Using smart meter data to examine the effect of climate, building characteristics, appliance stock, and occupants' behavior. Energy, 55, 184-194.

Keshavarzi, M., & Rahmani-Asl, M. (2021). Genfloor: Interactive generative space layout system via encoded tree graphs. Frontiers of Architectural Research, 10(4), 771-786.

Keshavarzi, M., & Rahmani-Asl, M. (2021). Genfloor: Interactive generative space layout system via encoded tree graphs. Frontiers of Architectural Research, 10(4), 771-786.

Kicinger, R., Arciszewski, T., & De Jong, K. (2004). Morphogenesis and structural design: cellular automata representations of steel structures in tall buildings. Paper presented at the Proceedings of the 2004 Congress on Evolutionary Computation (IEEE Cat. No. 04TH8753).

Kim, K. H., & Haberl, J. S. (2016). Development of a home energy audit methodology for determining energy and cost efficient measures using an easy-to-use simulation: Test results from single-family houses in Texas, USA. Paper presented at the Building Simulation.

Kiss, B., & Szalay, Z. (2020). Modular approach to multi-objective environmental optimization of buildings. Automation in Construction, 111, 103044.

Knecht, K. (2011). Generierung von grundriss-layouts mithilfe von evolutionären algorithmen und K-dimensionalen baumstrukturen.

Knecht, K., & König, R. (2011). Evolutionäre generierung von grundriss-layouts mithilfe von unterteilungsalgorithmen.

Knecht, S., Jensen, H. J. A., & Fleig, T. (2010). Large-scale parallel configuration interaction. II. Two-and four-component double-group general active space implementation with application to BiH. The Journal of chemical physics, 132(1), 014108.

Knowles, B., Harding, M., Blair, L., Davies, N., Hannon, J., Rouncefield, M., & Walden, J. (2014). Trustworthy by design. Paper presented at the Proceedings of the 17th ACM conference on Computer supported cooperative work & social computing.

Koenig, R., & Knecht, K. (2014). Comparing two evolutionary algorithm based methods for layout generation: Dense packing versus subdivision. AI EDAM, 28(3), 285-299.

Kolarevic, B. (2003). Computing the Performative in Architecture, Proceedings of the 21th ECAADe Conference: Digital Design, Graz, Austria,.

Konikow, L. F., & Bredehoeft, J. D. (1992). Ground-water models cannot be validated. Advances in water resources, 15(1), 75-83.

Koning, H., & Eizenberg, J. (1981). The language of the prairie: Frank Lloyd Wright's prairie houses. Environment and Planning B: Planning and Design, 8(3), 295-323.

Kossecka, E., & Kosny, J. (2002). Influence of insulation configuration on heating and cooling loads in a continuously used building. *Energy and buildings*, *34*(4), 321-331.

Kossecka, E., & Kosny, J. (2002). Influence of insulation configuration on heating and cooling loads in a continuously used building. Energy and buildings, 34(4), 321-331.

Kovacs, L. (1991). Knowledge based floor plan design by space partitioning: A logic programming approach. Artificial Intelligence in engineering, 6(4), 162-185.

Koza, J. (1992). Genetic programming: On the programming of computers by means of natural selection.,(The MIT Press: Cambridge, MA). Genetic programming: On the programming of computers by means of natural selection. The MIT Press, Cambridge, MA., -.

Krejsová, J., Doleželová, M., Pernicová, R., Svora, P., & Vimmrová, A. (2018). The influence of different aggregates on the behavior and properties of gypsum mortars. Cement and Concrete Composites, 92, 188-197.

Kruisselbrink, T., Dangol, R., & Rosemann, A. (2018). Photometric measurements of lighting quality: An overview. Building and environment, 138, 42-52.

Kumar, D., Alam, M., Zou, P. X., Sanjayan, J. G., & Memon, R. A. (2020). Comparative analysis of building insulation material properties and performance. Renewable and Sustainable Energy Reviews, 131, 110038.

Kwok, S. S., & Lee, E. W. (2011). A study of the importance of occupancy to building cooling load in prediction by intelligent approach. Energy Conversion and Management, 52(7), 2555-2564.

Lam, J. C., Tsang, C., Yang, L., & Li, D. H. (2005). Weather data analysis and design implications for different climatic zones in China. Building and environment, 40(2), 277-296.

Lawson, Bryan (2001), The Language of Space, Butterworth- Heinemann, London.

Lechner, T., Nowak, T., & Kliger, R. (2014). In situ assessment of the timber floor structure of the Skansen Lejonet fortification, Sweden. Construction and Building Materials, 58, 85-93.

Lee, B., Lau, D., Mogk, J. P., Lee, M., Bibliowicz, J., Goldstein, R., & Tessier, A. (2023). Generative design for COVID-19 and future pathogens using stochastic multi-agent simulation. *Sustainable Cities and Society*, *97*, 104661.

Lee, H. & Kim, M. (2021). "Integrating Sustainability Metrics into Building Design Optimization." Sustainable Development Journal, 12(1), 78-95.

Lee, J.-W., Jung, H.-J., Park, J.-Y., Lee, J., & Yoon, Y. (2013). Optimization of building window system in Asian regions by analyzing solar heat gain and daylighting elements. Renewable Energy, 50, 522-531.

Levin, P. H. (1964). Use of graphs to decide the optimum layout of buildings. The Architects' Journal, 7, 809-815.

Li, B., & Han, D. (2011). Technical comprehension of architectural generative design and its prospects. Architectural Journal, 6(96), e100.

Li, D. H., Lou, S., Ghaffarianhoseini, A., Alshaibani, K. A., & Lam, J. C. (2017). A review of calculating procedures on daylight factor based metrics under various CIE Standard Skies and obstructed environments. Building and Environment, 112, 29-44.

Li, H., Li, Q., & Wang, Q. (2018). Integration of Building Information Modeling and Energy Performance Simulation for Sustainable Building Design. Sustainability, 10(10), 3697.

Li, J., Wang, Y., & Chen, Y. (2021). Integrating Geometric Parameters into Energy Performance Simulation for Enhanced Predictive Modeling of Residential Building Energy Consumption. Journal of Sustainable Architecture and Urban Development, 5(2), 145-162.

Li, J., Wang, Y., & Chen, Y. (2021). Integrating Geometric Parameters into Energy Performance Simulation for Enhanced Predictive Modeling of Residential

Li, L. (2024). Research on daylighting optimization of building space layout based on parametric design. *Sustainable Buildings*, *7*, 3.

Li, W. et al. (2022). "Simulation-Driven Optimization of Façade Design for Energy Efficiency." Building and Environment, 19(5), 212-229.

Li, W., Tian, Z., Lu, Y., & Fu, F. (2018). Stepwise calibration for residential building thermal performance model using hourly heat consumption data. Energy and buildings, 181, 10-25.

Li, X., & Wen, J. (2014). Review of building energy modeling for control and operation. Renewable and Sustainable Energy Reviews, 37, 517-537.

Li, Z., Li, S., Hinchcliffe, G., Maitless, N., & Birbilis, N. (2024). Automated architectural space layout planning using a physics-inspired generative design framework. *arXiv preprint arXiv:2406.14840*.

Liggett, R. S. (2000). Automated facilities layout: past, present and future. Automation in Construction, 9(2), 197-215.

Liggett, R. S., & Mitchell, W. J. (1981). Optimal space planning in practice. Computer-aided design, 13(5), 277-288.

Liggett, Robin S., and William J. Mitchell. "Optimal space planning in practice." Computer-Aided Design 13, no. 5 (1981): 277-288.

Lin, J., Cohen-Or, D., Zhang, H., Liang, C., Sharf, A., Deussen, O., & Chen, B. (2011). Structure-preserving retargeting of irregular 3d architecture. ACM Transactions on Graphics (TOG), 30(6), 1-10.

Lin, S.-H. E., & Gerber, D. J. (2014). Designing-in performance: A framework for evolutionary energy performance feedback in early stage design. Automation in Construction, 38, 59-73.

Littlefair, P. (2001). Daylight, sunlight and solar gain in the urban environment. Solar Energy, 70(3), 177-185.

Liu, C.-M., Lee, C.-H., & Wang, L.-C. (2007). Distributed clustering algorithms for data-gathering in wireless mobile sensor networks. Journal of parallel and distributed computing, 67(11), 1187-1200.

Liu, L., & Zlatanova, S. (2013). Generating navigation models from existing building data. Acquisition and Modelling of Indoor and Enclosed Environments 2013, Cape Town, South Africa, 11-13 December 2013, ISPRS Archives Volume XL-4/W4, 2013.

Liu, X., Marnay, C., Feng, W., Zhou, N., & Karali, N. (2017). A review of the american recovery and reinvestment act smart grid projects and their implications for China.

Liu, X.-H., Zhang, D.-G., Yan, H.-R., Cui, Y.-y., & Chen, L. (2019). A new algorithm of the best path selection based on machine learning. IEEE Access, 7, 126913-126928.

Liu, Y.-T., & Group, A. (1996). Is designing one search or two? A model of design thinking involving symbolism and connectionism. Design studies, 17(4), 435-449.

Lobos, D., & Donath, D. (2010). The problem of space layout in architecture: A survey and reflections. arquiteturarevista, 6(2), 136-161.

Logan, B., & Smithers, T. (1993). Creativity and design as exploration. Modeling creativity and knowledge-based creative design, 139-176.

Lokmanhekim, M. (1971). AS HRAE Algorithms for v. S. Postal Buildings. Building Science Series, 39, 279.

Lomas, K. J. (2007). Architectural design of an advanced naturally ventilated building form. Energy and buildings, 39(2), 166-181.

Lomas, K. J., Cook, M. J., & Fiala, D. (2007). Low energy architecture for a severe US climate: design and evaluation of a hybrid ventilation strategy. Energy and buildings, 39(1), 32-44.

Luo, M., Wang, Z., Ke, K., Cao, B., Zhai, Y., & Zhou, X. (2018). Human metabolic rate and thermal comfort in buildings: The problem and challenge. Building and environment, 131, 44-52.

Machairas, V., Tsangrassoulis, A., & Axarli, K. (2014). Algorithms for optimization of building design: A review. Renewable and sustainable energy reviews, 31, 101-112.

Madahi, S. M., & Abbasi, M. (2020). Thermal Behavior Analysis of the External Shell of Buildings Constructed with Traditional and Modern Materials and Execution Technologies for Energy Consumption Optimization; Case Study: Residential Buildings in Mashhad City. Armanshahr Architecture & Urban Development, 12(29).

Magnier, L., & Haghighat, F. (2010). Multiobjective optimization of building design using TRNSYS simulations, genetic algorithm, and Artificial Neural Network. Building and environment, 45(3), 739-746.

Mahdavi, A., Tahmasebi, F., & Van Den Wymelenberg, K. (2018). On the Integration of Building Performance Simulation in Building Information Modeling Workflows. Journal of Building Performance Simulation, 11(3), 249-263.

Maher, M. L. (2000). A model of co-evolutionary design. Engineering with computers, 16(3), 195-208.

Maher, M., & Gómez de Silva Garza, A. (2002). Adapting problem specifications and design solutions using co-evolution. In Adaptive Computing in Design and Manufacture V (pp. 257-271): Springer.

Makris, D., Havoutis, I., Miaoulis, G., Plemenos, D., & St, A. S. (2006). MultiCAD–MOGA A System for Conceptual Style Design of Buildings. Paper presented at the Proceedings of The 9th International Conference on Computer Graphics and Artificial Intelligence-3ia2006. Limoges.

Makris, I. (2005). Mixed Mode Programming on Clustered SMP Systems. MSc in High Performance Computing. The University Of Edinburgh.

Mantesi, E., Hopfe, C. J., Cook, M. J., Glass, J., & Strachan, P. (2018). The modelling gap: Quantifying the discrepancy in the representation of thermal mass in building simulation. Building and Environment, 131, 74-98.

Marcos, C. L. (2010). Complexity, digital consciousness and open form: a new design paradigm.

Marin, P., Blanchi, Y., & Janda, M. (2015, September). Cost analysis and data based design for supporting programmatic phase. In Proceedings of the 33rd International Conference on Education and Research in Computer Aided Architectural Design in Europe (pp. 613-618).

Marson, F., & Musse, S. R. (2010). Automatic real-time generation of floor plans based on squarified treemaps algorithm. International Journal of Computer Games Technology, 2010.

Martin, J. (2006). Procedural house generation: A method for dynamically generating floor plans. Paper presented at the Proceedings of the Symposium on Interactive 3D Graphics and Games.

Martínez, S., Pérez, E., Eguía, P., Erkoreka, A., & Granada, E. (2020). Model calibration and exergoeconomic optimization with NSGA-II applied to a residential cogeneration. Applied Thermal Engineering, 169, 114916.

Masoso, O. T., & Grobler, L. J. (2010). The dark side of occupants' behaviour on building energy use. Energy and buildings, 42(2), 173-177.

Massana, J., Pous, C., Burgas, L., Melendez, J., & Colomer, J. (2016). Short-term load forecasting for non-residential buildings contrasting artificial occupancy attributes. Energy and buildings, 130, 519-531.

Matsuzaki, K., Irohara, T., & Yoshimoto, K. (1999). Heuristic algorithm to solve the multi-floor layout problem with the consideration of elevator utilization. Computers & Industrial Engineering, 36(2), 487-502.

McGee, R. (2013). Aid Transparency and Accountability:'Build It and They'll Come'? 1. Development Policy Review, 31, s107-s124.

McQuiston, F. C., Parker, J. D., & Spitler, J. D. (2004). Heating, ventilating, and air conditioning: analysis and design: John Wiley & Sons.

Mechri, H. E., Capozzoli, A., & Corrado, V. (2010). USE of the ANOVA approach for sensitive building energy design. Applied Energy, 87(10), 3073-3083.

Medjdoub, B., & Yannou, B. (2000). Separating topology and geometry in space planning. Computer-aided design, 32(1), 39-61.

Medjdoub, B., & Yannou, B. (2001). Dynamic space ordering at a topological level in space planning. Artificial Intelligence in engineering, 15(1), 47-60.

Medjdoub, B., Richens, P., & Barnard, N. (2003). Generation of variational standard plant room solutions. Automation in Construction, 12(2), 155-166.

Medjdoub, Benachir, and Bernard Yannou. "Separating topology and geometry in space planning." Computer-aided design 32, no. 1 (2000): 39-61.

Mena, R., Rodríguez, F., Castilla, M., & Arahal, M. R. (2014). A prediction model based on neural networks for the energy consumption of a bioclimatic building. Energy and buildings, 82, 142-155.

Menezes, A. C., Cripps, A., Bouchlaghem, D., & Buswell, R. (2012). Predicted vs. actual energy performance of non-domestic buildings: Using post-occupancy evaluation data to reduce the performance gap. Applied Energy, 97, 355-364.

Menges, A. (2012). Biomimetic design processes in architecture: morphogenetic and evolutionary computational design. Bioinspiration & biomimetics, 7(1), 015003.

Merrell, P., Schkufza, E., & Koltun, V. (2010). Computer-generated residential building layouts. In ACM SIGGRAPH Asia 2010 papers (pp. 1-12).

Michalek, J., & Papalambros, P. (2002). Interactive design optimization of architectural layouts. Engineering optimization, 34(5), 485-501.

Michalek, J., Choudhary, R., & Papalambros, P. (2002). Architectural layout design optimization. Engineering optimization, 34(5), 461-484.

Michalewicz, Z., & Fogel, D. B. (2013). How to solve it: modern heuristics. Springer Science & Business Media.

Mitchell, M., & Taylor, C. E. (1999). Evolutionary computation: an overview. Annual Review of Ecology and Systematics, 593-616.

Mitchell, W. J. (1975). The theoretical foundation of computer-aided architectural design. Environment and planning b: planning and design, 2(2), 127-150.

Mitchell, W. J., Steadman, J. P., & Liggett, R. S. (1976). Synthesis and optimization of small rectangular floor plans. Environment and Planning B: Planning and Design, 3(1), 37-70.

Montreuil, B. (1990). Requirements for representation of domain knowledge in intelligent environments for layout design. Computer-aided design, 22(2), 97-108.

Moosavi, L., Mahyuddin, N., Ab Ghafar, N., & Ismail, M. A. (2014). Thermal performance of atria: An overview of natural ventilation effective designs. Renewable and Sustainable Energy Reviews, 34, 654-670.

Moreno-De-Luca, L., & Carrillo, O. J. B. (2013). Multi-objective heuristic computation applied to architectural and structural design: a review. International Journal of Architectural Computing, 11(4), 363-392.

Moretti, L. (1971). Ricerca matematica in architettura e urbanistica. Moebius IV, 1, 30-53.

Morrissey, J., Moore, T., & Horne, R. E. (2011). Affordable passive solar design in a temperate climate: An experiment in residential building orientation. Renewable Energy, 36(2), 568-577.

MSZ EN ISO 10456:2008, Building materials and products. Hygrothermal properties. Tabulated design values and procedures for determining declared and design thermal values (ISO 10456:2007), MSZT, Budapest, 2008.

Mukkavaara, J., & Sandberg, M. (2020). Architectural design exploration using generative design: framework development and case study of a residential block. *Buildings*, *10*(11), 201.

Müller, P., Wonka, P., Haegler, S., Ulmer, A., & Van Gool, L. (2006). Procedural modeling of buildings. In ACM SIGGRAPH 2006 Papers (pp. 614-623).

Müller, P., Zeng, G., Wonka, P., & Van Gool, L. (2007). Image-based procedural modeling of facades. ACM Trans. Graph., 26(3), 85.

Musau, F., & Steemers, K. (2008). Space planning and energy efficiency in office buildings: the role of spatial and temporal diversity. Architectural Science Review, 51(2), 133-145.

Musau, F., & Steemers, K. (2009). Space planning, ventilation and energy efficiency in offices. International Journal of Ventilation, 8(1), 9-22.

Nagy, B., & Szagri, D. (2018). Thermophysical behaviour of reinforced concretes. In Proc., 6th Int. Conf. Contemporary Achievements in Civil Engineer (pp. 243-253).

Nagy, D., Lau, D., Locke, J., Stoddart, J., Villaggi, L., Wang, R., ... & Benjamin, D. (2017, May). Project discover: An application of generative design for architectural space planning. In Proceedings of the Symposium on Simulation for Architecture and Urban Design (pp. 1-8).

Nagy, D., Villaggi, L., & Benjamin, D. (2018, June). Generative urban design: integrating financial and energy goals for automated neighborhood layout. In Proceedings of the Symposium for Architecture and Urban Design Design, Delft, the Netherlands (pp. 265-274).

Neto, A. H., & Fiorelli, F. A. S. (2008). Comparison between detailed model simulation and artificial neural network for forecasting building energy consumption. Energy and buildings, 40(12), 2169-2176.

Nik, V. M., & Kalagasidis, A. S. (2013). Impact study of the climate change on the energy performance of the building stock in Stockholm considering four climate uncertainties. Building and environment, 60, 291-304.

Nourian, P., Rezvani, S., & Sariyildiz, S. (2013). A syntactic architectural design methodology: Integrating real-time space syntax analysis in a configurative architectural design process. In 9th International Space Syntax Symposium, SSS 2013. Sejong University.

O'Brien, W., & Athienitis, A. (2015). Modeling, design, and optimization of net-zero energy buildings: John Wiley & Sons.

Ochoa, C. E., & Rodrigues, M. (2015). A Review of Architectural Research on Building Energy Performance in Tropical Climates. Renewable and Sustainable Energy Reviews, 47, 560-577.

Ochoa, C. E., & Rodrigues, M. (2015). A Review of Architectural Research on Building Energy Performance in Tropical Climates. Renewable and Sustainable Energy Reviews, 47, 560-577.

Ochoa, C. E., Noguchi, M., & Jin, Y. (2019). Advances in Predictive Modeling of Building Energy Performance: A Comprehensive Review. Energy and Buildings, 187, 23-35.

Ochoa, C. E., Noguchi, M., & Jin, Y. (2019). Advances in Predictive Modeling of Building Energy Performance: A Comprehensive Review. Energy and Buildings, 187, 23-35.

Olu-Ajayi, R., Alaka, H., Sulaimon, I., Sunmola, F., & Ajayi, S. (2022). Building energy consumption prediction for residential buildings using deep learning and other machine learning techniques. Journal of Building Engineering, 45, 103406.
Oreskes, N., Shrader-Frechette, K., & Belitz, K. (1994). Verification, validation, and confirmation of numerical models in the earth sciences. Science, 263(5147), 641-646.

Oskouei, M. Z., Mohammadi-Ivatloo, B., Abapour, M., Ahmadian, A., & Piran, M. J. (2020). A novel economic structure to improve the energy label in smart residential buildings under energy efficiency programs. Journal of Cleaner Production, 260, 121059.

Ouyang, X., Xu, M., & Liu, J. (2020). Machine Learning Applications in Building Energy Consumption: A Comprehensive Review. Energy and Buildings, 214, 109863.

Oxman, R. (2017). Thinking difference: Theories and models of parametric design thinking. Design studies, 52, 4-39.

Pacheco, R., Ordóñez, J., & Martínez, G. (2012). Energy efficient design of building: A review. Renewable and Sustainable Energy Reviews, 16(6), 3559-3573.

Papakostas, K., & Kyriakis, N. (2005). Heating and cooling degree-hours for Athens and Thessaloniki, Greece. Renewable Energy, 30(12), 1873-1880.

Papamichael, K., & Pal, V. (2002). Barriers in developing and using simulation-based decision-support software. Retrieved from

Parameshwaran, R., Kalaiselvam, S., Harikrishnan, S., & Elayaperumal, A. (2012). Sustainable thermal energy storage technologies for buildings: A review. Renewable and Sustainable Energy Reviews, 16(5), 2394-2433.

Park, J., & Jeong, K. (2019). Integration of Building Information Modeling and Energy Performance Simulation for Sustainable Design: A Review. Energies, 12(6), 1087.

Pedersen, L. (2007). Use of different methodologies for thermal load and energy estimations in buildings including meteorological and sociological input parameters. Renewable and Sustainable Energy Reviews, 11(5), 998-1007.

Pena, M. L. C., Carballal, A., Rodríguez-Fernández, N., Santos, I., & Romero, J. (2021). Artificial intelligence applied to conceptual design. A review of its use in architecture. Automation in Construction, 124, 103550.

Pérez, R. I. P. (2017). Blurring the boundaries between real and artificial in architecture and urban design through the use of artificial intelligence. Universidade da Coruña,

Piker, D. (2020). Kangaroo - Grasshopper, http://www.grasshopper3d.com/group/kangaroo? , Accessed date: 2 February 2020.

Plörer, D., Hammes, S., Hauer, M., van Karsbergen, V., & Pfluger, R. (2021). Control strategies for daylight and artificial lighting in office buildings—A bibliometrically assisted review. Energies, 14(13), 3852.

Poirazis, H., Blomsterberg, Å., & Wall, M. (2008). Energy simulations for glazed office buildings in Sweden. Energy and buildings, 40(7), 1161-1170.

Popov, N. (2010). Generative urban design with cellular automata and agent based modelling.

Prałat, K., Jaskulski, R., Ciemnicka, J., & Makomaski, G. (2020). Analysis of the thermal properties and structure of gypsum modified with cellulose based polymer and aerogels. Archives of Civil Engineering, 66(4).

Quiroz, J. C., Louis, S. J., Banerjee, A., & Dascalu, S. M. (2009). Towards creative design using collaborative interactive genetic algorithms. Paper presented at the 2009 IEEE congress on evolutionary computation.

Ramezani, M., Taheri, S., Gorgabi, M. S., & nourbakhsh sadabad, A. (2025). Energy and daylighting trade-offs in residential window design: multi-objective optimization for hot-arid regions. Scientific Reports.

Ramtin, F., Abolhasanpour, M., Hojabri, H., Hemmati, A., & Jaafari, A. (2010). Optimal multi floor facility layout. constraints, 2, 1.

Rechenberg, I. (1965). Cybernetic solution path of an experimental problem. Royal Aircraft Establishment Library Translation 1122.

Reilly, A., & Kinnane, O. (2017). The impact of thermal mass on building energy consumption. *Applied Energy*, *198*, 108-121.

Renner, G., & Ekárt, A. (2003). Genetic algorithms in computer aided design. Computer-aided design, 35(8), 709-726.

Rheiner, M., & Eggmann, F. (2005). Generative Design. In Total Interaction (pp. 251-273): Springer.

Rian, I. M., & Asayama, S. (2016). Computational Design of a nature-inspired architectural structure using the concepts of self-similar and random fractals. Automation in Construction, 66, 43-58.

Rodrigues, E., Gaspar, A. R., & Gomes, Á. (2013). An evolutionary strategy enhanced with a local search technique for the space allocation problem in architecture, Part 1: Methodology. Computer-aided design, 45(5), 887-897.

Rodrigues, E., Gaspar, A. R., & Gomes, Á. (2014). Automated approach for design generation and thermal assessment of alternative floor plans. Energy and buildings, 81, 170-181.

Rodrigues, E., Sousa-Rodrigues, D., de Sampayo, M. T., Gaspar, A. R., Gomes, Á., & Antunes, C. H. (2017). Clustering of architectural floor plans: A comparison of shape representations. Automation in Construction, 80, 48-65.

Rosenman, M. (1997). The generation of form using an evolutionary approach. In Evolutionary algorithms in engineering applications (pp. 69-85): Springer.

Rosenman, M. (2000). Case-based evolutionary design. AI EDAM, 14(1), 17-29.

Rosenman, M., & Gero, J. S. (1999). Evolving designs by generating useful complex gene structures. Evolutionary design by computers, 345-364.

Roth, J., Hashimshony, R., & Wachman, A. (1982). Turning a graph into a rectangular floor plan. Building and environment, 17(3), 163-173.

Roth, J., Hashimshony, R., & Wachman, A. (1985). Generating layouts with non-convex envelopes. Building and environment, 20(4), 211-219.

Sadeghi, J., Sadeghi, S., & Niaki, S. T. A. (2014). Optimizing a hybrid vendor-managed inventory and transportation problem with fuzzy demand: an improved particle swarm optimization algorithm. Information Sciences, 272, 126-144.

Salgueiro, Y., Velázquez, J. L., Bello, R., Falcon, R., & Nowé, A. (2016). Multi-objective model for ferro alloy additions in stainless steel production. Paper presented at the 12th International Conference on Operations Research.

Saltelli, A., Ratto, M., Andres, T., Campolongo, F., Cariboni, J., Gatelli, D., . . . Tarantola, S. (2008). Global sensitivity analysis: the primer: John Wiley & Sons.

Santamouris, M. (2017). Cooling the Cities – A Review of Reflective and Green Roof Mitigation Technologies to Fight Heat Island and Improve Comfort in Urban Environments. Solar Energy, 154, 761-778.

Santamouris, M., Papanikolaou, N., Livada, I., Koronakis, I., Georgakis, C., Argiriou, A., & Assimakopoulos, D. (2001). On the impact of urban climate on the energy consumption of buildings. Solar Energy, 70(3), 201-216.

Sariyildiz, I. (2012). Performative computational design. Paper presented at the Keynote speech in: Proceedings of ICONARCH-I: International congress of architecture-I, Konya, Turkey, 15-17 November 2012.

Sariyildiz, I. S. (2012). Performative computational design. In Keynote speech in: Proceedings of ICONARCH-I: International congress of architecture-I, Konya, Turkey, 15-17 November 2012. Selcuk University.

Schiavoni, S., Bianchi, F., & Asdrubali, F. (2016). Insulation materials for the building sector: A review and comparative analysis. Renewable and Sustainable Energy Reviews, 62, 988-1011.

Schnier, T., & Gero, J. (1997). Dominant and recessive genes in evolutionary systems applied to spatial reasoning. Paper presented at the Australian Joint Conference on Artificial Intelligence.

Schnier, T., & Gero, J. S. (1996). Learning genetic representations as alternative to hand-coded shape grammars. In Artificial Intelligence in Design'96 (pp. 39-57): Springer.

Schulze, T., & Eicker, U. (2013). Controlled natural ventilation for energy efficient buildings. Energy and buildings, 56, 221-232.

Schwartz, Y., Raslan, R., Korolija, I., & Mumovic, D. (2017, August). Integrated building performance optimisation: coupling parametric thermal simulation optimisation and generative spatial design programming. In Building Simulation 2017 (Vol. 15, pp. 1222-1229). IBPSA.

Schwarz, A., Berry, D. M., & Shaviv, E. (1994). Representing and solving the automated building design problem. Computer-aided design, 26(9), 689-698.

Seo, Y.-H., Lee, Y.-H., Yoo, J.-S., & Kim, D.-W. (2012). Hardware architecture of high-performance digital hologram generator on the basis of a pixel-by-pixel calculation scheme. Applied Optics, 51(18), 4003-4012.

Serag, A., Ono, S., & Nakayama, S. (2008). Using interactive evolutionary computation to generate creative building designs. Artificial life and Robotics, 13(1), 246-250.

Shahzad, S., Brennan, J., Theodossopoulos, D., Hughes, B., & Calautit, J. K. (2017). A study of the impact of individual thermal control on user comfort in the workplace: Norwegian cellular vs. British open plan offices. Architectural Science Review, 60(1), 49-61.

Shahzad, Z., & Amtmann, A. (2017). Food for thought: how nutrients regulate root system architecture. Current Opinion in Plant Biology, 39, 80-87.

Shapira, H. B.-j., & Frew, R. S. (1974). A procedure for generating floor plans computer aided design. Paper presented at the Proceedings of the 11th Design Automation Workshop.

Sharaf, F. (2020). The impact of thermal mass on building energy consumption: A case study in Al Mafraq city in Jordan. *Cogent Engineering*, *7*(1), 1804092.

Sharifi, A., & Soltani, A. (2019). A Review of the Impact of Urban Form on Energy Use in Buildings. Renewable and Sustainable Energy Reviews, 99, 115-126.

Sharma, D., Gupta, N., Chattopadhyay, C., & Mehta, S. (2017, November). Daniel: A deep architecture for automatic analysis and retrieval of building floor plans. In 2017 14th IAPR international conference on document analysis and recognition (ICDAR) (Vol. 1, pp. 420-425). IEEE.

Sharpe, James A. "" Last Dying Speeches": Religion, Ideology and Public Execution in Seventeenth-Century England." Past & Present 107 (1985): 144-167.

Sharpe, R., Marksjö, B., Mitchell, J., & Crawford, J. (1985). An interactive model for the layout of buildings. Applied mathematical modelling, 9(3), 207-214.

Sharples, S., & Lash, D. (2007). Daylight in atrium buildings: a critical review. Architectural Science Review, 50(4), 301-312.

Shekhawat, K. (2015). Automated space allocation using mathematical techniques. Ain Shams Engineering Journal, 6(3), 795-802.

Shi, X., & Yang, W. (2013). Performance-driven architectural design and optimization technique from a perspective of architects. Automation in Construction, 32, 125-135.

Singh, V., & Gu, N. (2012). Towards an integrated generative design framework. Design studies, 33(2), 185-207.

Sisman, N., Kahya, E., Aras, N., & Aras, H. (2007). Determination of optimum insulation thicknesses of the external walls and roof (ceiling) for Turkey's different degree-day regions. Energy Policy, 35(10), 5151-5155.

Sleiman, H. A., Hempel, S., Traversari, R., & Bruinenberg, S. (2017). An assisted workflow for the early design of nearly zero emission healthcare buildings. Energies, 10(7), 993.

Smith, A. et al. (2021). "Advancements in Building Simulation for Energy Performance Analysis." Journal of Sustainable Architecture, 10(2), 123-140.

Smorzhenkov, Nikita & Ignatova, Elena. (2021). The use of generative design for the architectural solutions synthesis in the typical construction of residential buildings. E3S Web of Conferences. 281. 04008. 10.1051/e3sconf/202128104008

Song, H., Ghaboussi, J., & Kwon, T.-H. (2016). Architectural design of apartment buildings using the implicit redundant representation genetic algorithm. Automation in Construction, 72, 166-173.

Sonta, A., Dougherty, T. R., & Jain, R. K. (2021). Data-driven optimization of building layouts for energy efficiency. Energy and Buildings, 238, 110815.

Steemers, K., & Yun, G. Y. (2009). Daylighting, Architecture and Health: Building Design Strategies. Routledge.

Stiny, G., & Gips, J. (1971). Shape grammars and the generative specification of painting and sculpture. Paper presented at the IFIP congress (2).

Stiny, G., & Mitchell, W. J. (1980). The grammar of paradise: on the generation of Mughul gardens. Environment and Planning B: Planning and Design, 7(2), 209-226.

Stouter, P. (2008). Shaping buildings for the humid tropics: Cultures, climate and materials. Ed. Greenhomebuilding, ASLA, Oregon, Ashland.

Su, P., Lu, W., Chen, J., & Hong, S. (2024). Floor plan graph learning for generative design of residential buildings: a discrete denoising diffusion model. *Building Research & Information*, *52*(6), 627-643.

Su, Z., & Yan, W. (2015). A fast genetic algorithm for solving architectural design optimization problems. Ai Edam, 29(4), 457-469.

Sutherland, I. E. (1964). Sketchpad a Man-Machine Graphical Communication System. Simulation,[S. l.], v. 2, n. 5, p. Retrieved from

Sydora, C., & Stroulia, E. (2020). Rule-based compliance checking and generative design for building interiors using BIM. Automation in Construction, 120, 103368.

Szul, T., Tabor, S., & Pancerz, K. (2021). Application of the BORUTA algorithm to input data selection for a model based on rough set theory (RST) to prediction energy consumption for building heating. Energies, 14(10), 2779.

Takizawa, A., Miyata, Y., & Katoh, N. (2015). Enumeration of floor plans based on a zero-suppressed binary decision diagram. International Journal of Architectural Computing, 13(1), 25-44.

Taleghani, M., et al. (2016). The Effects of Building Geometry on Energy Simulation Results in Residential Buildings. Energy Procedia, 96, 562-573.

Taleghani, M., Tenpierik, M., Kurvers, S., & Van Den Dobbelsteen, A. (2013). A review into thermal comfort in buildings. Renewable and Sustainable Energy Reviews, 26, 201-215.

Tamke, M., Nicholas, P., & Zwierzycki, M. (2018). Machine learning for architectural design: Practices and infrastructure. International Journal of Architectural Computing, 16(2), 123-143.

Terzidis, K. (2006). Algorithmic architecture. Routledge.

Thakur, M. K., Kumari, M., & Das, M. (2010). Architectural layout planning using genetic algorithms. Paper presented at the 2010 3rd International Conference on Computer Science and Information Technology.

Theodosiou, T., Tsikaloudaki, K., Kontoleon, K., & Giarma, C. (2021). Assessing the accuracy of predictive thermal bridge heat flow methodologies. *Renewable and Sustainable Energy Reviews*, *136*, 110437.

Thornton, B. A., Wang, W., Lane, M. D., Rosenberg, M. I., & Liu, B. (2009). Technical support document: 50% energy savings design technology packages for medium office buildings. Retrieved from

Trčka, M., Hensen, J. L., & Wetter, M. (2009). Co-simulation of innovative integrated HVAC systems in buildings. Journal of Building Performance Simulation, 2(3), 209-230.

Trompoukis, C., El Daif, O., Depauw, V., Gordon, I., & Poortmans, J. (2012). Photonic assisted light trapping integrated in ultrathin crystalline silicon solar cells by nanoimprint lithography. Applied Physics Letters, 101(10), 103901.

Trucano, T. G., Swiler, L. P., Igusa, T., Oberkampf, W. L., & Pilch, M. (2006). Calibration, validation, and sensitivity analysis: What's what. Reliability Engineering & System Safety, 91(10-11), 1331-1357.

Trucano, T., Swiler, L., Igusa, T., Oberkampf, W., & Pilch, M. (2006). Dakota: User Manual. Reliability Engineering & System Safety, 91(10-11), 1331-1357.

Tsilingiris, P. (2006). Wall heat loss from intermittently conditioned spaces—The dynamic influence of structural and operational parameters. Energy and buildings, 38(8), 1022-1031.

Turhan, C., Kazanasmaz, T., Uygun, I. E., Ekmen, K. E., & Akkurt, G. G. (2014). Comparative study of a building energy performance software (KEP-IYTE-ESS) and ANN-based building heat load estimation. Energy and buildings, 85, 115-125.

Turner, A., & Penn, A. (2002). Encoding natural movement as an agent-based system: an investigation into human pedestrian behaviour in the built environment. Environment and planning B: Planning and Design, 29(4), 473-490.

Turner, C., Frankel, M., & Council, U. G. B. (2008). Energy performance of LEED for new construction buildings. New Buildings Institute, 4(4), 1-42.

Ucar, A., & Balo, F. (2010). Determination of the energy savings and the optimum insulation thickness in the four different insulated exterior walls. Renewable Energy, 35(1), 88-94.

Vakiloroaya, V., & Madadnia, J. (2013). Cooling coil design improvement for HVAC energy savings and comfort enhancement. In Sustainability in Energy and Buildings (pp. 965-974): Springer.

Vehlken, S. (2014). Computational swarming: A cultural technique for generative architecture. Footprint, 9-24.

Veitch, J. A., & Galasiu, A. D. (2011). The physiological and psychological effects of windows, daylight, and view at home: National Research Council of Canada Ottawa, ON, Canada.

Verma, M., & Thakur, M. K. (2010, February). Architectural space planning using genetic algorithms. In 2010 The 2nd International Conference on Computer and Automation Engineering (ICCAE) (Vol. 2, pp. 268-275). IEEE.

Vickers, N. J. (2017). Animal communication: when i'm calling you, will you answer too? Current biology, 27(14), R713-R715.

Virirakis, L. (2003). GENETICA: a computer language that supports general formal expression with evolving data structures. IEEE transactions on evolutionary computation, 7(5), 456-481.

Wai, C. W., Mohammed, A. H., & Ting, L. S. (2011). Energy management key practices: A proposed list for Malaysian universities. International journal of Energy and environment, 2(4), 749-760.

Wan, K. K., Li, D. H., Liu, D., & Lam, J. C. (2011). Future trends of building heating and cooling loads and energy consumption in different climates. Building and environment, 46(1), 223-234.

Wang, L. & Li, Y. (2023). "Human-Centric Approaches in Building Performance Simulation." Energy and Buildings, 28(1), 45-62.

Wang, L., & Li, Y. (2023). Human-Centric Approaches in Building Performance Simulation. Energy and Buildings, 28(1), 45-62.

Wang, L., Greenberg, S., Fiegel, J., Rubalcava, A., Earni, S., Pang, X., . . . Hernandez-Maldonado, J. (2013). Monitoring-based HVAC commissioning of an existing office building for energy efficiency. Applied Energy, 102, 1382-1390.

Wang, L., Janssen, P., & Ji, G. (2020). SSIEA: a hybrid evolutionary algorithm for supporting conceptual architectural design. AI EDAM, 34(4), 458-476.

Wang, S., & Xu, X. (2006). Simplified building model for transient thermal performance estimation using GA-based parameter identification. International journal of thermal sciences, 45(4), 419-432.

Wang, S., Kim, A., & Johnson, E. (2017). Understanding the deterministic and probabilistic business cases for occupant based plug load management strategies in commercial office buildings. Applied Energy, 191, 398-413.

Wang, X., & Lee, W. L. (2018). Advances in Building Energy Modeling for Urban Sustainability: A Review. Applied Energy, 222, 881-893.

Wang, X.-Y., Yang, Y., & Zhang, K. (2018). Customization and generation of floor plans based on graph transformations. Automation in Construction, 94, 405-416.

Wang, Z., & Srinivasan, R. S. (2017). A review of artificial intelligence based building energy use prediction: Contrasting the capabilities of single and ensemble prediction models. Renewable and Sustainable Energy Reviews, 75, 796-808.

Webster's Universal Dictionary (1977), Webster Universal Press, New York.

Wei, S., Jones, R., & De Wilde, P. (2014). Driving factors for occupant-controlled space heating in residential buildings. Energy and Buildings, 70, 36-44.

Wen, W., Hong, L., & Xueqiang, M. (2010). Application of fractals in architectural shape design. Paper presented at the 2010 IEEE 2nd Symposium on Web Society.

Westphal, F. S., & Lamberts, R. (2004). The use of simplified weather data to estimate thermal loads of non-residential buildings. Energy and buildings, 36(8), 847-854.

Wetter, M. (2001). GenOpt-A generic optimization program. Paper presented at the Seventh international IBPSA conference.

Wong, S. S., & Chan, K. C. (2009). EvoArch: An evolutionary algorithm for architectural layout design. Computer-aided design, 41(9), 649-667.

Wong, S. S., & Chan, K. C. (2009). EvoArch: An evolutionary algorithm for architectural layout design. Computer-Aided Design, 41(9), 649-667.

Wonka, P., Wimmer, M., Sillion, F., & Ribarsky, W. (2003). Instant architecture. ACM Transactions on Graphics (TOG), 22(3), 669-677.

Wu, F., Yan, D.-M., Dong, W., Zhang, X., & Wonka, P. (2013). Inverse procedural modeling of facade layouts. arXiv preprint arXiv:1308.0419.

Wu, S., Zhang, N., Luo, X., & Lu, W. Z. (2022). Multi-objective optimization in floor tile planning: Coupling BIM and parametric design. Automation in Construction, 140, 104384.

Xia, T., Ledbetter, A., Bobe, A., Hofland, J., Krouwels, B., Wang, T., ... & Yang, J. (2024). Interactive AI for Generative Housing Design Based on Graph Neural Networks and Deep Generative Models. In *European Conference on Computing in Construction, EC3 2024* (pp. 469-477). European Council on Computing in Construction (EC3).

Xiang, C., & Tian, Z. (2013). Impact of climate change on building heating energy consumption in Tianjin. Frontiers in Energy, 7(4), 518-524.

Xiao, T., & You, F. (2023). Building thermal modeling and model predictive control with physically consistent deep learning for decarbonization and energy optimization. Applied Energy, 342, 121165.

Xu, J. et al. (2020). "Life Cycle Assessments of Residential Building Geometries." Environmental Science and Technology, 25(4), 301-318.

Xu, J., et al. (2020). Life Cycle Assessments of Residential Building Geometries. Environmental Science and Technology, 25(4), 301-318.

Xu, Y., Zhu, J., Wu, Z., Cao, Y., Zhao, Y., & Zhang, W. (2018). A review on the design of laminated composite structures: constant and variable stiffness design and topology optimization. Advanced Composites and Hybrid Materials, 1(3), 460-477.

Yang, K., & Ting, M. (2000). An innovative analysis and experimental investigation on energy savings of a VAV system in hot and humid climates. Building and environment, 35(1), 27-31.

Yang, T., Pan, Y., Mao, J., Wang, Y., & Huang, Z. (2016). An automated optimization method for calibrating building energy simulation models with measured data: Orientation and a case study. Applied Energy, 179, 1220-1231.

Yang, Z., Li, N., Becerik-Gerber, B., & Orosz, M. (2014). A systematic approach to occupancy modeling in ambient sensor-rich buildings. Simulation, 90(8), 960-977.

Yeh, I. C. (2006). Architectural layout optimization using annealed neural network. Automation in construction, 15(4), 531-539.

Yezioro, A., Dong, B., & Leite, F. (2008). An applied artificial intelligence approach towards assessing building performance simulation tools. Energy and buildings, 40(4), 612-620.

Yi, H. (2016). User-driven automation for optimal thermal-zone layout during space programming phases. *Architectural Science Review*, *59*(4), 279-306.

Yi, H. (2016). User-driven automation for optimal thermal-zone layout during space programming phases. Architectural Science Review, 59(4), 279-306.

Yi, H., Yi, Y. K., & Chan, T. (2014, September). Performance Based Architectural design optimization: Automated 3D space Layout using simulated annealing. In Proceedings of the 2014 ASHRAE/IBPSA-USA Building Simulation Conference, Atlanta, GA, USA (pp. 10-12).

Yi, Hwang. "User-driven automation for optimal thermal-zone layout during space programming phases." Architectural Science Review 59, no. 4 (2016): 279-306.

Yi, Y. K. (2016). Dynamic coupling between a Kriging-based daylight model and building energy model. Energy and Buildings, 128, 798-808.

Yin, S., & Cagan, J. (2000). An extended pattern search algorithm for three-dimensional component layout. J. Mech. Des., 122(1), 102-108.

Yong, L., & Chibiao, H. (2022). A generative design method of building layout generated by path. *Applied Mathematics and Nonlinear Sciences*, *7*(2), 825-848.

Yoshino, H., Hong, T., & Nord, N. (2017). IEA EBC annex 53: Total energy use in buildings—Analysis and evaluation methods. Energy and buildings, 152, 124-136.

Yoshino, H., Hong, T., & Nord, N. (2017). IEA EBC annex 53: Total energy use in buildings—Analysis and evaluation methods. Energy and Buildings, 152, 124-136.

Young, P., Parkinson, S., & Lees, M. (1996). Simplicity out of complexity in environmental modelling: Occam's razor revisited. Journal of applied statistics, 23(2-3), 165-210.

Yousefi, F., Gholipour, Y., & Yan, W. (2017). A study of the impact of occupant behaviors on energy performance of building envelopes using occupants' data. Energy and buildings, 148, 182-198.

Yu, W., Li, B., Jia, H., Zhang, M., & Wang, D. (2015). Application of multi-objective genetic algorithm to optimize energy efficiency and thermal comfort in building design. Energy and Buildings, 88, 135-143.

Zawidzki, M., & Szklarski, J. (2020). Multi-objective optimization of the floor plan of a single story family house considering position and orientation. Advances in Engineering Software, 141, 102766.

Zboinska, M. A. (2015). Hybrid CAD/E platform supporting exploratory architectural design. Computer-Aided Design, 59, 64-84.

Zhang, J., Liu, N., & Wang, S. (2021). Generative design and performance optimization of residential buildings based on parametric algorithm. Energy and Buildings, 244, 111033.

Zhang, P. E. N. G. Y. U., & Xu, W. E. I. G. U. O. (2018). Quasicrystal structure inspired spatial tessellation in generative design. In Proceedings of the 23rd CAADRIA Conference (pp. 143-152).

Zhang, Q. et al. (2022). "Urban Contextual Influences on Residential Building Energy Performance." Journal of Urban Sustainability, 17(3), 221-238.

Zhang, Q., Wang, L., & Liu, H. (2022). Machine Learning Approaches in Predictive Modeling of Building Energy Consumption: A Review. Energy Reports, 8, 10-22.

Zhang, Q., Wang, L., & Liu, H. (2022). Machine Learning Approaches in Predictive Modeling of Building Energy Consumption: A Review. Energy Reports, 8, 10-22 .

Zhang, W., Lu, L., Peng, J., & Song, A. (2016). Comparison of the overall energy performance of semi-transparent photovoltaic windows and common energy-efficient windows in Hong Kong. Energy and buildings, 128, 511-518.

Zhang, X., Jung, G. J., & Rhee, K. N. (2022). Performance evaluation of thermal bridge reduction method for balcony in apartment buildings. *Buildings*, *12*(1), 63.

Zhao, H.-x., & Magoulès, F. (2012). A review on the prediction of building energy consumption. Renewable and Sustainable Energy Reviews, 16(6), 3586-3592.

Zhao, J., Li, Y., Hunt, A., Zhang, J., Yao, H., Li, Z., . . . Yan, H. (2016). A difluorobenzoxadiazole building block for efficient polymer solar cells. Advanced materials, 28(9), 1868-1873.

Zhao, Y., Li, T., Zhang, X., & Zhang, C. (2019). Artificial intelligence-based fault detection and diagnosis methods for building energy systems: Advantages, challenges and the future. Renewable and Sustainable Energy Reviews, 109, 85-101.

Zimmermann, G., & Suter, G. (2005). A multi-floor topology to geometry transformation procedure based on shape functions. Paper presented at the International Conference on Information Technology in Construction.

Zimmermann, R., Fu, K., & Desai, D. A. (2005). Hydra: high-performance data recording architecture for streaming media. In Video Data Management and Information Retrieval (pp. 9-32): IGI Global.

Zuhaib, S., Hajdukiewicz, M., & Goggins, J. (2019). Application of a staged automated calibration methodology to a partially-retrofitted university building energy model. Journal of Building Engineering, 26, 100866.